Biosynthèse et remodelage des polysaccharides pariétaux au cours de la croissance cellulaire :modèles tube pollinique et racine

Arnaud Lehner

Mémoire présenté en vue de l'obtention de

L'HABILITATION à DIRIGER DES RECHERCHES

Biosynthèse et remodelage des polysaccharides pariétaux au cours de la croissance cellulaire : modèles tube pollinique et racine

par

Arnaud LEHNER

Mémoire soutenu le 24 novembre 2017 devant le jury composé de

Dr. Marie-Christine **Ralet**, Directrice de Recherche, INRA Nantes	Rapporteur
Pr. Jean-Christophe **Avice**, Professeur, Université de Caen Normandie	Rapporteur
Dr. Aurélien **Boisson-Dernier**, Chargé de Recherche, University of Cologne	Rapporteur
Pr. Hayat **El Maarouf-Bouteau**, Professeur, Université Pierre et Marie Curie	Examinateur
Pr. Patrice **Lerouge**, Professeur, Université de Rouen Normandie	Examinateur
Pr. Jean-Claude **Mollet**, Professeur, Université de Rouen Normandie	Directeur

à Yasmine, Ainis
et Nawal

Remerciements

Je tiens, tout d'abord, à adresser mes sincères remerciements à Marie-Christine Ralet, Aurélien Boisson-Dernier et Jean-Christophe Avice qui ont bien voulu accepter la tâche d'examiner ce travail, malgré leurs nombreuses obligations.

Ce mémoire fait la synthèse des activités scientifiques et administratives dont j'ai eu la charge depuis ma thèse. Je tiens donc à remercier l'ensemble des personnes avec qui j'ai partagé mon temps entre bureau, réunions et paillasse…avec une pensée particulière pour mes collègues qui m'ont transmis leur rigueur, leur honneteté scientifique et leur esprit critique. Parmi eux, Christophe Bailly, Françoise Corbineau, Jill Farrant, François Bouteau, Hayat El-Maarouf Bouteau, Azeddine Driouich, Muriel Bardor, Patrice Lerouge et Jean-Claude Mollet. J'ai aussi une pensée émue pour Daniel Côme qui m'a fait découvrir le monde de la recherche.

Merci également à ma famille et surtout MERCI à Nawal, Ainis et Yasmine qui me supportent au quotidien…

Sommaire

Curriculum vitae

Activités de recherche

Liste des Abréviations

·OH·, radical hydroxyl

2F-Ara, 2-fluoro-Arabinose

2F-Fuc, 2-désoxy 2-fluoro L-fucose

2F-Gal, 2-fluoro-Galactose

Ace, acide acérique

AGP, ArabinoGalactane Protéine

Api, Apiose

BGAL, β-galactosidases

CALS, callose synthases

CAZy, Carbohydrate Enzyme

Calmodulines, CALcium MODULated proteINS

CCRC-M1, Complex Carbohydrate Research Center Monoclonal1, XyG fragments fucosylés

CE, Carbohydrate Esterase

CERMN, Centre d'Etudes et de Recherche sur le Médicament de Normandie

CM-H2DCFDA, 5-(and-6)-chloromethyl-2',7'-dichlorodihydrofluorescein diacetate, acetyl ester

cPTIO, 2-(4-Carboxyphenyl)-4,4,5,5-tetramethylimidazoline-1-oxyl-3-oxide

CRIB4, Cdc42/Rac-inter-active binding 4

Dha, acide 3-déoxy-D-lyso-heptulosarique

DMSO, DiMethylSulfOxyde

DPI, Diphenylene iodonium

EXP, Expansine

FITC, Fluorescéine Isothiocyanate

FUT, α1-2 galactoside fucosyltranferase

GalA, acide galacturonique

GDP, guanosine diphosphate

GH, Glycoside hydrolase

GME, GDP-d-mannose 3, 5-epimérase

GPI, glycosylphosphatidylinositol

H_2O_2, peroxyde d'hydrogène

HG, homogalacturonane

HRGP, HydroxyProline-Rich GlycoProteins

HSP, Heat Shock protein

JIM5, John Innes Monoclonal5, épitopes associés aux HG faiblement méthylés

JIM7, John Innes Monoclonal7, épitopes associés aux HG fortement méthylés

JIM20, John Innes Monoclonal20, épitopes associés aux extensines

Kdo, acide 3-déoxy-D-manno-octulosonique

KDSA, KDO-8-P SYNTHASE

LaCl, Chlorure de Lanthane

LM2, Leeds Monoclonal2, épitopes associés aux AGPs

LM6, Leeds Monoclonal6, épitopes associés aux arabinanes

LM8, Leeds Monoclonal8, épitopes associés aux xylogalacturonanes

LM13, Leeds Monoclonal13, épitopes associés aux arabinanes

LM15, Leeds Monoclonal15 épitopes associés aux XyG non fucosylés

LM19, Leeds Monoclonal19, épitopes associés aux HG faiblement méthylés

LM20, Leeds Monoclonal20, épitopes associés aux HG fortement méthylés

LM25, Leeds Monoclonal25, épitopes associés aux XyG galactosylés

MGP, MALE GAMETOPHYTE DEFECTIVE

MV, méthylviologène

NPG1, No Pollen Germination 1

NO, oxyde nitrique

RNS, Espèces actives de l'Azote

$O_2^{\cdot -}$, anion superoxyde

PEX1, Pollen EXtensine-like 1

PGases, polygalacturonases

PL, Pectine/Pectate lyase

pLAT52, promoteur LAT52 (Anther specific LAT52), spécifique du pollen

PLL, pectine lyase-like

PME, Pectine MéthylEstérase

PMEI, Inhibiteur de Pectine MéthylEstérase

PPME1, Pollen Pectin methylesterase 1

PRP, protéines riches en proline

RbOH, Respiratory burst Oxidase Homologs

RG-I, rhamnogalacturonane-I

RG-II, rhamnogalacturonane-II

RGP, Reversibly Glycosylated Peptide

RIC4, Rop-Interactive CRIB motif–containing proteins 4

RSL, Roothair Defective Six-Like

ROP, Rho-Related GTPase from Plants

ROS, Espèces actives de l'Oxygène

ROS, Reactive Oxygen Species

SETH1 et SETH2, gènes impliqués dans la biosynthèsee de l'ancre GPI

SIA2, sialyltransferase-like2

XG, Xylogalacturonane

XTH, xyloglucane *endo*-transglucosylase hydrolase

XyG, xyloglucane

WAK, Wall Associated Kinase

Curriculum vitae

1. Curriculum Vitae

Arnaud LEHNER

Maître de Conférences - Physiologie Végétale
Section CNU 66
Normandie Univ, UNIROUEN, Glyco-MEV*, 76000 ROUEN
* Glyco-MEV, EA 4358 Laboratoire de Glycobiologie et Matrice Extracellulaire Végétale
Université de Rouen Normandie, 76821 Mont Saint Aignan CEDEX-France.

Tél : 02 35 14 66 90 email : arnaud.lehner@univ-rouen.fr

1.1. Déroulement de carrière

Depuis Septembre 2008 : Maître de Conférences, Université de Rouen Normandie.

Enseignement : Physiologie végétale ; Biologie cellulaire et moléculaire végétale. UFR des Sciences et Techniques, Département de Biologie.

Recherche : Génomique fonctionnelle, Physiologie végétale, biologie cellulaire et imagerie. Laboratoire Glyco-MEV, EA 4358.
Les thèmes de recherche développés au sein du laboratoire Glyco-MEV ont pour sujet la biosynthèse, le remodelage des composés pariétaux et leurs implications dans la croissance cellulaire végétale. Plus spécifiquement, ils portent sur (1) l'implication du remodelage des pectines dans la croissance cellulaire et (2) l'implication des polysaccharides pariétaux dans l'adhésion et la croissance du tube pollinique.

Septembre 2007-Septembre 2008 : Attaché Temporaire d'Enseignement et de Recherche, Université Paris Diderot, Paris 7.

Enseignement : Physiologie végétale ; Biologie cellulaire et moléculaire végétale. UFR des Sciences et Techniques, Département de Biologie.

Recherche : Electrophysiologie cellulaire. Laboratoire d'Electrophysiologie des Membranes, EA 3514.
Thème de recherche développé sous la direction du Pr JP. Rona et du Dr F. Bouteau : « Implication des canaux ioniques dans la transduction du signal de mort cellulaire chez *Arabidopsis thaliana* ».

Janvier 2007-aout 2007 : Contrat Post-doctoral, Université Pierre et Marie Curie, Paris 6.

Recherche : Physiologie des semences. Laboratoire de Physiologie Végétale Appliquée, EA 2388.
Thème de recherche développé sous la direction du Pr. F. Corbineau : « Projet ANR MALTECO : Maltage d'orge brassicole à faible humidité pour réduire la consommation d'énergie et préserver l'environnement ».

Janvier 2006-décembre 2006 : Contrat Post-doctoral, University of Cape Town, Cape Town, Afrique du Sud.

Recherche : Biologie cellulaire et moléculaire. Department of Molecular and Cell Biology.
Thème de recherche développé sous la direction du Pr. J.M. Farrant : 1) Etude moléculaire du gène codant une myo-inositol 1-phosphate synthase dans la résistance à la dessiccation chez *Xerophyta viscosa* et 2) évolution des systèmes antioxydants au cours de la déshydratation de la fougère *Mohria caffrorum*.

1.2. Titres et Diplômes Universitaires

2005 Doctorat de Physiologie Végétale

Thèse préparée à l'Université Pierre et Marie Curie, Paris 6 et obtenue le 13/12/2005 avec la mention très honorable et les félicitations du jury.
Financement Syngenta-Agro.

Laboratoire de Physiologie Végétale Appliquée, EA2388. Directeur de thèse : Pr. F. Corbineau. « Recherche d'indicateurs physiologiques et biochimiques de la qualité germinative et de l'aptitude à la conservation des semences de blé (*Triticum aestivum* L.) ».

2002 DEA Science des Agro-ressources

Université de Toulouse, Ecole Nationale Supérieure d'Agronomie de Toulouse, Institut National Polytechnique de Toulouse.

Stage réalisé au Laboratoire de Physiologie Végétale Appliquée, EA2388 sous la direction du Pr. F. Corbineau et du Dr. C. Bailly. « Recherche, au cours du développement et de la levée de dormance des semences de tournesol, d'indicateurs biochimiques et biophysiques de leur aptitude à la germination ».

2001 DES Diplôme d'Etude Supérieure en Sciences Naturelles

Université Pierre et Marie Curie, Paris 6, Laboratoire de Physiologie Végétale Appliquée, EA2388. Directeur du DES: Dr. C. Bailly. « Recherche de facteurs associés à l'élaboration de la qualité germinative des semences de tournesol au cours de leur développment ».

2000 Maitrise Biologie Cellulaire et Physiologie, Université Pierre et Marie Curie, Paris 6

1999 Licence Biologie Cellulaire et Physiologie, Université Pierre et Marie Curie, Paris 6

1998 DEUG B, Université Pierre et Marie Curie, Paris 6

1.3. Domaines de compétences techniques

- ***Biochimie*** : Electrophorèse SDS-PAGE ; western blot. Extraction et dosage de sucres solubles (HPLC) ; dosage calcium (système apo-aéquorine, luminomètre) ; extraction de polysaccharides pariétaux ; extraction et analyse du RG-II par PAGE ; dosages enzymatiques en spectrophotométrie.

- ***Biologie moléculaire*** : Extraction d'ADN et d'ARN ; Southern et northern blot, clonage de gènes, PCR.

- ***Electrophysiologie*** : Voltage imposé à électrode (voltage clamp).

- ***Culture in vitro*** : Culture de cals et de cellules en suspension ; transformation par *Agrobacterium*, Culture de tubes polliniques.

- ***Microscopie*** : microscopie optique (transmise, épi-fluorescence) ; Microscopie électronique à balayage, analyse histo-cytochimique (calcofluor, aniline bleue, carmino-vert) ; immunocytochimie ; coloration GUS.

- ***Biophysique*** : Microcalorimétrie différentielle à balayage (DSC) ; isotherme de sorption.

- ***Physiologie*** : Criblage de mutants ; germination en milieu contrôlé (graine, pollen) ; traitements de vieillissement accéléré et de détérioration contrôlée ; viabilité cellulaire (rouge neutre, bleu Evans, FDA).

- ***Informatique*** : Design d'amorce PCR ; analyses et traitements d'images : Image J, IrfanView, Photoshop ; création site web : Dreamweaver, FileZilla ; Webmaster du site web du Glyco-MEV : http://www.univ-rouen.fr/Glyco-MEV/

1.4. Prix et distinctions

- Bénéficiaire d'une bourse de la Claude Leon Foundation pour une année de recherche post-doctorale menée à l'Université de Cape Town, Afrique du Sud.
- Bénéficiaire de la PES (2012-2016)
- Bénéficiaire de la PEDR (2016-2020)

2. Activités pédagogiques

2.1. Activités d'enseignement

- ***Depuis 2008*** : Maître de conférences à l'Université de Rouen Normandie

Licence 1 Cours magistraux : Anatomie de la conduction ; transport de la sève brute et de la sève élaborée ; évapo-transpiration.
Travaux dirigés : cellules procaryotes, eucaryotes et organites cellulaires
Travaux pratiques : microscopie ; biologie cellulaire ; mitose et méiose; extraction et séparation de pigments végétaux.

Licence 2 Cours magistraux : le sol : composition, notion d'eau libre et d'eau liée, potentiel hydrique ; nutrition hydrique et minérale ; les éléments minéraux essentiels: rôle et détail des mécanismes d'absorption ; les stomates, structure, fonction, mécanismes de régulation de l'évapotranspiration.
Travaux dirigés : nutrition minérale ; potentiel hydrique
Travaux pratiques : effets de carence et de toxicité minérale sur le développement de plantules de trèfle ; extraction et dosage de pigments photosynthétiques.

Licence 3 Travaux pratiques : culture *in vitro* : balance auxine/cytokinine et organogénèse ; Effet des gibbérellines sur la germination d'orge et sur l'activité amylasique.

Master 1 et 2 Cours magistraux : nutrition minérale et fertilisation ; symbiose plantes-rhizobiums ; mise en place des réserves : oléagineux, protéagineux, amylacées ; dormance et qualité des semences ; rôle et fonction des pectines méthylestérases.
Travaux pratiques : étude du pollen et du tube pollinique d'*Arabidopsis thaliana* sauvage et mutant. GUS, immunolocalisation, coloration aniline bleue.

- ***2007 - 2008*** : ATER, Université Diderot, Paris 7

Licence 2 Travaux dirigés : hormones végétales et croissance des plantes.
Travaux pratiques : effet d'hormones végétales sur la croissance et le développment.

Licence 3 Travaux pratiques : approche génétique du développement d'*Arabidopsis thaliana*.

- ***2006*** : Post-doctorat, University of Cape Town, Afrique du Sud

Licence 3 Cours magistraux : seed development and dormancy

- ***2003 - 2005*** : Université Pierre et Marie Curie-Paris 6

Licence 3 Travaux pratiques : biochimie végétale, dosage de sucres solubles.

Master 2 Travaux pratiques : extraction de protéine et SDS-PAGE.

Formation permanente
Travaux pratiques : germination, dormances et qualité des semences.

2.2. Responsabilités pédagogiques et administratives

- Responsable pédagogique de la Licence 1 SVT-Chimie, 2012-2013
- Co-Responsable pédagogique du Master ECOBIOVALO (ECOproduction, BIOtechnologie végétale et bioVALOrisation), depuis 2016
- Co-Responsable de l'UE « Nutrition végétale » de Licence 2 SVT (depuis 2012)
- Co-Responsable de l'UE « Méthodologie en sciences du végétal », Master ECOBIOVALO
- Membre du jury de Licence 1 SVT, 2012-2013
- Membre du jury de Licence 2 SVT, depuis 2012
- Membre du Jury de Master 1 ECOBIOVALO depuis 2016
- Membre du jury de Master 1 MEEF (Métiers de l'Enseignement, de l'Éducation et de la Formation) de 2010-2014
- Membre du comité de perfectionnement du Master MEEF, 2012-2016
- Membre du comité de sélection M1 et M2 ECOBIOVALO, depuis 2014
- Membre élu de la CCSE restreinte, section 66 (2012-2014 et depuis 2016)
- Membre du conseil de laboratoire de l'UPRES EA 4358, depuis 2010
- Tuteur de monitorat d'Aline Voxeur, doctorante au laboratoire Glyco-MEV (2008-2011)
- Correspondant informatique du Glyco-MEV, depuis 2009

3. Encadrement

3.1. Encadrement doctoral

2006 : Claire Whitaker, thèse préparée à l'Université du Kwazulu-Natal. Encadrement de courte durée, 4 mois. Formation aux techniques d'extraction et d'analyse de heat shock protéines dans les graines de *Welwitschia mirabilis*.

2011-2015 : Co-Encadrant de Christelle Leroux. Thèse préparée au Glyco-MEV, Université de Rouen Normandie et soutenue le 7 septembre 2015. « Implication des pectines méthyl-estérases (PMEs) et de leurs inhibiteurs (PMEIs) au cours de la germination du grain de pollen et de la croissance polarisée du tube pollinique chez *Arabidopsis thaliana*. »

Depuis 2013 : Co-Encadrant de Ferdousse Laggoun. Thèse préparée au Glyco-MEV, Université de Rouen Normandie. « Utilisation de génétique chimique pour étudier l'adhésion et la croissance polarisée des tubes polliniques. »

Depuis 2016 : Co-Encadrant de Jeremy Dehors. Thèse préparée au Glyco-MEV, Université de Rouen Normandie. « Implication des espèces actives de l'oxygène et du calcium dans la croissance polarisée des tubes polliniques d'*Arabidopsis thaliana*. »

3.2. Encadrement d'ingénieurs et de diplômés de master

2004 : Alexandre David, Ingénieur d'étude. Université Pierre et Marie Curie, Paris 6. 2 mois. « Mise au point d'un kit de dosage de l'activité catalase dans les semences de blé ».

2013 : Valentin Lemaistre, titulaire M2. Université de Rouen Normandie. 6 mois. « Etude de l'effet d'extraits naturels sur le pourcentage et la vitesse de germination du pollen d'espèces cultivées ». Co-encadrant

2014 : Romain Castilleux, titulaire M2. Université de Rouen Normandie. 6 mois. « Effet d'extraits naturels sur l'induction des mécanismes de défense chez *Solanum lycopersicum* (tomate) et *Arabidopsis thaliana »*. Co-encadrant

2016 : Romain Menival, titulaire M2. Université de Rouen Normandie. 5 mois. « Effet d'extraits naturels sur la germination et la croissance des tubes polliniques chez *Solanum lycopersicum* (tomate) en conditions de stress thermique ». Co-encadrant

3.3. Encadrement d'étudiants ingénieurs et master

2004 : Benjamin Bouancheau, M1. Université Pierre et Marie Curie, Paris 6. 1 mois. « Comparaison de la précision d'un dosage des sucres solubles des grains de blé par HPLC ou par un kit commercial ».

2005 : Norbert Mamadou, M2. Université Pierre et Marie Curie, Paris 6. 6 mois. « Evolution des systèmes de détoxication cellulaire au cours du vieillissement des grains de blé ».

2005 : Hughes Boulland, M1. Université Pierre et Marie Curie-Paris 6. 2 mois. « Evolution des sucres solubles dans les semences de blé au cours de leur conservation ».

2006 : Vundli Ramokolo, M1. University of Cape Town. 5 mois. « Antioxidant enzyme assays in *Xerophyta humilis* and *Craterostigma wilmsii* leaves subjected to dehydration, dry storage and rehydration ».

2007 : Mélanie Jonnard, M1. Université Pierre et Marie Curie, Paris 6. 3 mois. « Germination de grains d'orge à faible teneur en eau : évolution des enzymes impliquées dans l'hydrolyse de l'amidon et dosage des sucres solubles ».

2008 : Julien Frescura, M1. Université Pierre et Marie Curie, Paris 6. 4 mois. « Implication de l'éthylène dans la signalisation de mort cellulaire induite par l'acide oxalique chez *Arabidopsis thaliana* ».

2008 : Laure Barthelemy, M1. Université Pierre et Marie Curie, Paris 6. 4 mois. « Implication du calcium dans la mort cellulaire programmée en réponse des stress hyper-osmotiques chez les cellules de tabac ».

2010 : Florian Païola, M1. Université de Rouen Normandie. 5 mois. « Localisation des polymères pariétaux dans les tubes polliniques de plantes mutantes d'*Arabidopsis thaliana* : implication des PME dans la croissance des tubes polliniques ».

2011 : Christelle Leroux, M2. Université de Rouen Normandie. 6 mois. « Implication des PME dans la croissance des tubes polliniques d'*Arabidopsis thaliana* ».

2012 : Maxime Grare, M2. Université de Rouen Normandie. 6 mois. « Analyse biochimique des xyloglucanes de tube pollinique de tomate ». Co-encadrant

2016 : Flavien Macquart, M1. Université de Rouen Normandie. 2 mois. « Détermination de l'activité PME dans l'exudat de cellules bordantes chez *Arabidopsis thaliana* ».

2016 : Juliette Havel, 2ème année école Ingénieur ESITECH. Université de Rouen Normandie. 2 mois. « Etude de l'effet de différents fluoro-sucres sur la croissance de la racine et de l'hypocotyle d'*Arabidopsis thaliana* ».

2017 : Sabine Tourneur, M2, Université de Rouen Normandie. 5 mois. « Effet de produits naturels sur la germination et la croissance des tubes polliniques de tomate en conditions de stress thermique : recherche de marqueurs moléculaires de croissance et de stress ». Co-encadrant

2017 : Marie Bourgeais, 1ere année école Ingénieur ESITECH. Université de Rouen Normandie. 1 mois. « Etude de l'effet du 2F-Gal et du 2F-Ara sur la croissance et la composition pariétale de la paroi de racine d'*Arabidopsis thaliana* ».

3.4. Encadrement d'étudiants en licence ou BTS

2004 : Charlotte Mesre, L3. Université Pierre et Marie Curie, Paris 6. 1 mois. « Evolution des sucres solubles dans les semences de blé après différentes durées de vieillissement accéléré ».

2009 : Alexandre Allard, BTS. 3 mois. « Mise au point d'un test de criblage primaire d'une chimiothèque : étude de la sécretion du mucilage, de la germination et de la croissance des plantules d'*Arabidopsis thaliana* ».

2010 : Valentin Lemaistre, L3. Université de Rouen Normandie. 2 mois. « Effets d'une chimiothèque sur la germination, la croissance et le développement de plantules d'*Arabidopsis thaliana* ».

2016 : Sophie Guinant, L3. Université de Rouen Normandie. 2 mois. « Etude de l'effet de polygalacturonase exogène sur la croissance du tube pollinique d'Amaryllis ».

4. Valorisation et financement de la recherche

4.1. Participation à des comités et jurys de thèse

- Membre du comité de thèse d'Elissa NAIM. Thèse en cours à l'Université Pierre et Marie Curie, Paris 6. Directrice de thèse: Pr. H. Bouteau. « Oxidative modification of macromolecules and their impact on the quality of sunflower seed »

- Membre invité du Jury de thèse de Marie Dumont. Thèse effectuée et soutenue à l'Université de Rouen Normandie le 10 juillet 2015. Directeurs de thèse : Pr. P. Lerouge et Pr. J-C. Mollet. « Rôle du rhamnogalacturonane de type II dans l'élongation cellulaire »

- Membre du Jury de thèse de Christelle Leroux en qualité de co-encadrant. Thèse effectuée et soutenue à l'Université de Rouen Normandie le 7 septembre 2015. Directeur de thèse : Pr. J-C. Mollet ; co-encadrant : Dr. A. Lehner. « Implication des pectines méthyl-estérases (PMEs) et de leurs Inhibiteurs (PMEIs) au cours de la germination du grain de pollen et de la croissance polarisée du tube pollinique chez *Arabidopsis thaliana* »

- Membre du jury de thèse de Ludivine Hocq en qualité d'examinateur. Thèse effectuée et soutenue le 4 décembre 2015 à L'Université de Picardie Jules Verne. Directeur de thèse : Pr. J. Pelloux ; co encadrante : Dr. V. Lefebvre. « Les pectine-méthylestérases (PME) et leurs inhibiteurs (PMEI) : rôles dans la croissance de la racine et de l'hypocotyle chez *Arabidopsis thaliana*-caractérisation de leur interaction »

4.2. Responsabilités scientifiques

- Responsable scientifique de l'axe « Implication des pectine-methylestérases dans la croissance cellulaire » au sein du Glyco-MEV (2011-2016).

- Co-Responsable scientifique de l'axe « polysaccharides pariétaux et croissance cellulaire » au sein du Glyco-MEV (depuis 2017).

- Référent sectoriel du Carnot I2C, secteur Agroalimentaire et Agroressources

4.3. Recherche de financements

La liste présentée ci-dessous reprend les projets, financés ou non, dans lesquels ma participation dans la conception du projet, la réalisation du projet ou la direction du projet est détaillée. Les projets **en**

gras correspondent aux projets où j'interviens comme **Responsable scientifique (rédaction et réalisation du projet).**

- GRR VATA: Alternatives agronomiques pour la qualité des sols et la protection des cultures 2010-2013: 148 000 €. Participation à la conception du projet de recherche et encadrement des travaux sur le criblage de chimiothèque en vue de trouver des nouveaux éliciteurs capables d'induire la défense des plantes.

- **ANR Jeune chercheur 2012 : 221 650 €, dépôt janvier 2012. Non financée.** Responsable scientifique du projet sur le rôle des pectine-méthylesterases et de leurs inhibiteurs dans la germination et la croissance polarisée des tubes polliniques d'*Arabidopsis thaliana*.

- ANR-DFG SUBWALL, Cell wall targets of subtilisin-like serine proteases during cell elongation in Arabidopsis: 198 900 € dépot 2014. Non financée. Co-reponsable du work package WP2c et WP4 sur le phénotypage de mutant et la colocalisation subcellulaire et cellulaire des subtilases et des pectines methyl esterases.

- Projet Interreg IVA « Trans Channel Wallnet » 2012-2015 : 272 000 €. Co-encadrement d'une partie des travaux de thèse de Marie Dumont sur le phénotypage de pollen mutant d'*Arabidopsis thaliana* et sur l'analyse du RG-II dans des lignées RNAi de tomates en collaboration avec l'INRA de Bordeaux.

- ANR-DFG SUBWALL, Cell wall targets of subtilisin-like serine proteases during cell elongation in Arabidopsis: 186 300 € dépot 2015. Non financée. Co-reponsable du work package WP2c et WP4 sur le phénotypage de mutant et la colocalisation subcellulaire et cellulaire des subtilases et des pectines methyl-esterases.

- **Contrat de Recherche Glyco-MEV-TIMAC AGRO INTERNATIONAL (groupe Roullier) 2013 : 23 375 €.** Co-responsable scientifique d'une étude sur les effets d'extraits naturels sur le pourcentage et la vitesse de germination du pollen d'espèces cultivées.

- **ANR PreGERM pollen transcriptomic remodelling: 260 500 €, dépot 2014. Non financée.** Responsable scientifique du projet consistant à dresser une carte de l'expression de l'ensemble des gènes impliqués dans le remodelage des pectines au cours de la germination du grain de pollen.

- **Contrat de Recherche Glyco-MEV- TIMAC AGRO INTERNATIONAL (groupe Roullier) 2014 : 31 571 €.** Co-responsable scientifique d'une étude sur l'effet d'extraits naturels sur l'induction des mécanismes de défense chez *Solanum lycopersicum* (tomate) et *Arabidopsis thaliana*.

- **ANR GAPWARM Research of adaptative mechanisms involved in pollen germination and seed production in a context of global warming: 297 500 € dépot 2015. Non financée.** Responsable scientifique d'un projet visant à trouver des marqueurs moléculaires liés à l'adaptabilité du pollen aux températures élevées.

- GRR VASI LIPS Lutte Intégrée pour la Protection et la qualité Sanitaire des plantes (LIPS). 2015-2018 : 280 000 €. Participation à la conception du projet et implication scientifique dans le volet 1 : Suivi des interactions plantes / pathogènes *in vitro* et identification de nouvelles molécules et d'agents de biocontrôle.

- **BQR 2016 : projet transcriptome remodelage pectine paroi : 12 688 €.** Responsable du projet, financement de l'achat d'un FastPrep, utilisé pour l'extraction d'ADN et d'ARN végétaux.

- **Contrat de Recherche Glyco-MEV- CMI (groupe Roullier) 2016 : 21 342 €.** Co-responsable scientifique d'une étude sur l'Effet d'extraits naturels sur la germination et la croissance des tubes polliniques chez *Solanum lycopersicum* (tomate) en conditions de stress thermique.

- ANR ERA-CAPS MECHAGROWTIP Deciphering the effect of ROS, RNS, calcium, and cell wall integrity sensing on mechanical and growth properties of Arabidopsis pollen tubes: Dépôt 2016. Non financée. Co-responsable du work package concernant l'approche pharmacologique et les analyses biochimiques sur le modèle tube pollinique.

- ANR IP-DIP Imaging of Polymer Dynamics In Plants. 150 000 €. Dépôt 2016. Non financée. Participation à la conception du projet et implication scientifique dans la partie click-chemistry *in planta*.

- **Contrat de Recherche Glyco-MEV- CMI (groupe Roullier) 2017 : 20 832 €.** Co-responsable scientifique d'une étude sur les « effets d'extraits naturels sur la germination et la croissance des tubes polliniques de tomate en conditions de stress thermique : Recherche de marqueurs moléculaires de stress et de croissance ».

4.4. Collaborations scientifiques

Nationales

Dr. Sophie Bouton, Université de Picardie Jules Verne, Amiens (2012-2014) : Analyse de l'expression des gènes codant pour des PME dans des grains de pollen secs, hydratés et germés.

Dr. Valérie Lefebvre, Université de Picardie Jules Verne, Amiens (2016-2017) : Effet de l'application exogène de polygacturonases produites en système hétérologue sur la paroi de tubes polliniques d'Amarillys.

Pr. Jérome Pelloux, Université de Picardie Jules Verne, Amiens (2015-2016) : Inhibition pH dépendante de PME à l'aide de PMEI produits en système hétérologue. Effet sur l'activité PME et le phénotype des tubes polliniques d'*Arabidopsis thaliana*.

Pr. Hayat Bouteau, Université Pierre et Marie Curie, Paris 6 (depuis 2015) : Analyse des xyloglucanes de graines de tournesol dormantes et non dormantes.

Dr Pierre Baldet, INRA Bordeaux (2013-2015) : Analyse du Rhamnogalacturonane de type 2 par gel d'électrophorèse dans des fruits de tomates sauvages et RNAi pour une GDP-D-mannose epimérase (SlGME1, SlGME2).

Dr Denis Falconet, Université Joseph Fourier, Grenoble (depuis 2012): Impact de la galvestine sur la croissance polarisée des tubes polliniques de tabac et d'*Arabidopsis thaliana*.

Dr Jean Claude Yvin, Timac-Agro, Groupe Roullier, Saint-Malo (2013-2014) : Etude de l'effet d'extraits naturels sur le pourcentage et la vitesse de germination du pollen d'espèces cultivées. Effet d'extraits naturels sur l'induction des mécanismes de défense chez *Solanum lycopersicum* (tomate) et *Arabidopsis thaliana*.

Dr Eric NGuema-Ona, CMI, groupe Roullier, Saint-Malo (depuis 2016) : Effet d'extraits naturels sur la germination et la croissance des tubes polliniques chez *Solanum lycopersicum* (tomate) en conditions de stress thermique.

Internationales

Pr. Christophe Ringli, University of Zurich, Zurich, Suisse. 2013 : préparation et cryo-fixation de tubes polliniques mutants (*xxt1/xxt2* ; *xeg113* ; *xxt1/xxt2/xeg113*). 2014 : Analyse des propriétés mécaniques de la plasticité de la paroi de tubes polliniques sauvages et mutants (*pme48*) par microscopie à force cellulaire.

Pr. Ariel Orellana, Universidad Andres Belo, Santiago, Chili (2015) : extraction et analyse de la paroi de tubes polliniques de plantes déficientes en un transporteur d'UDP-glucuronic acid (*uuat1*).

Dr. Mark Johnson, Brown University, Providence, USA (2011) : Etude phénotypique et immunolocalisation de composés pariétaux (AGP, galactan, xyloglucan) sur des tubes polliniques sauvages et mutants (*gal11*, *gal13*).

L'ensemble de ces collaborations scientifiques a donné lieu à :

7 publications :

ACL-17 Dumont et al., 2014 ***Annals of Botany*** 114, 1177-1188.
ACL-19 Leroux et al., 2015 ***Plant Physiology*** 167, 367-380.
ACL-21 Dumont et al., 2015 ***Bio-Protocol*** 5, e1502.
ACL-25 Gilbert-Mounet et al., 2016 ***Journal of Experimental Botany*** 67, 4767-77.
ACL-26 Saez-Aguayo et al., 2017 ***The Plant Cell*** 29,129-163.
ACL-27 Hocq et al., 2017 ***Plant Physiology*** 173, 1075-1093.
ACL-28 Guénin et al., 2017 ***Journal of Experimental Botany*****,** 68, 1083-1095.

4 communications orales: ACTI-09, ACTI-11, ACTI-12, ACTN-07
11 communications par affiches: AFF-12, AFF-14, AFF-15, AFF-17, AFF-19, AFF-22, AFF-24, AFF-25, AFF-26, AFF-27, AFF-30

4.5. Organisations de congrès (ORG)

ORG-01 Driouich A, Vicré-Gibouin M, **Lehner A.** "From Dry Kalahari in South Africa to Wet Normandy": Joint international meeting on revival plants in the era of global warming. University of Cape Town and University of Rouen. Espace Sciences H_2O-Rouen. February 3-4th 2011. 90 participants.

ORG-02 Mancuso S, Baluška F, **Lehner A**, Van Volkenburgh L, Kawano T, Yokawa K, Thuleau P, Meimoun P, Errakhi R, Chedly A, Frachisse JM, Gakière B, Mithoefer A, Limami A, Bhatla S, Herbert E, Ninkovic V, Bouteau F. International Symposium on Plant Signaling and Behavior, Paris, France, June 29th - July 2rd 2015. 200 participants.

4.6. Activité de reviewing

Au cours de ces dernères années, plusieurs missions de reviewing m'ont été confiées par différents journaux scientifiques :

- **Plant Growth Regulation,**
- **Planta**
- **Annals of Botany**
- **Journal of Experimental Botany**
- **Scientific Reports**

4.7. Diffusion scientifique au grand public (INF)

INF-01 Vivré-Gibouin M, **Lehner A**, Driouich A. Les plantes reviviscentes : une solution au réchauffement climatique ? 17ème édition de la fête de la science, Rouen, France. November 14th-23rd 2008.

INF-02 Lehner A, Dardelle F, Mollet JC. De la fleur à la graine : le fabuleux destin du pollen. 17ème édition de la fête de la science, Rouen, France. November 14th-23rd 2008.

INF-03 Lehner A, Vicré-Gibouin M, Farrant JM, Driouich A. 2010. Les plantes reviviscentes. ***Biofutur***, 311, 50-55.

INF-04 Lehner A, Dardelle F, Mollet JC. De la fleur à la graine : le fabuleux destin du pollen. 21ème édition de la fête de la science, Rouen, France. October 10-14th 2012.

INF-05 **Lehner A**, Dardelle F, Mollet JC. De la fleur à la graine : le fabuleux destin du pollen. 22ème édition de la fête de la science, Rouen, France. November 10-12th 2013.

INF-06 Leroux C, Bouton S, Kiefer-Meyer MC, Morvan C, Pelloux J, Driouich A, Lerouge P, **Lehner A**, Mollet JC. Involvement of pectin methylesterase during imbibition and germination of Arabidopsis pollen grain. «Research Worth Spreading », Mock Conference, Rouen, France. March 21st 2014.

INF-07 Laggoun F, Driouich A, Lerouge P**, Lehner A**, Mollet JC. Small molecules interfere with the tip-polarized growth of Arabidopsis and tomato pollen tube. «Research Worth Spreading », Mock Conference, Rouen, France. June 5th 2015.

5. Production scientifique

5.1. Articles dans des revues à comité de lecture (ACL)

ACL-01 Bailly C, Leymarie J, **Lehner A**, Rousseau S, Côme D, Corbineau F. 2004. Catalase activity and expression in developing sunflower seeds as related to drying. ***Journal of Experimental Botany*** 55, 1-9. (IF_{2004} 3.36)

ACL-02 Lehner A, Bailly C, Flechel B, Poels P, Côme D, Corbineau F. 2006. Changes in wheat seed germination ability, soluble carbohydrate and antioxidant enzyme activities in the embryo during the desiccation phase of maturation. ***Journal of Cereal Science***, 43, 175-182. (IF_{2006} 2.05)

ACL-03 Lehner A, Corbineau F, Bailly C. 2006. Changes in lipid status and glass properties in cotyledons of developing sunflower seeds. ***Plant and Cell Physiology***, 47, 818-828. (IF_{2006} 3.32)

ACL-04 Lehner A, Chopera DR, Peters SW, Bohnert HJ, Mundree SG, Thomson JA, Farrant JM. 2008. Protection mechanisms in the resurrection plant *Xerophyta viscosa* (Baker): Cloning, expression, characterization and role of *XvINO1*, a gene coding for a *myo*-inositol 1-phosphate synthase. ***Functional Plant Biology***, 35, 26-39. (IF_{2008} 2.25)

ACL-05 Lehner A, Mamadou N, Côme D, Bailly C, Corbineau F. 2008. Changes in soluble carbohydrates, lipid peroxidation and antioxidant enzyme activities in the embryo during ageing in wheat grains. ***Journal of Cereal Science***, 47, 555-565. (IF_{2008} 3.03)

ACL-06 Errakhi R, Meimoun P, **Lehner A**, Vidal G, Briand J, Corbineau F, Rona JP, Bouteau F. 2008. Anion channel activity is necessary to induce ethylene synthesis and programmed cell death in response to oxalic acid. ***Journal of Experimental Botany***, 59, 3121-3129. (IF_{2008} 4.01)

ACL-07 Lehner A, Meimoun P, Errakhi R, Madiona K, Barakate M, Bouteau F. 2008. Toxic and signalling effects of oxalic acid. Oxalic acid: natural born killer or natural born protector? ***Plant Signaling and Behavior***, 3, 746-748.

ACL-08 Errakhi R, Dauphin A, Meimoun P, **Lehner A**, Reboutier D, Vatsa P, Briand J, Madiona K, Rona JP, Barakate M, Wendehenne D, Beaulieu C, Bouteau F. 2008. An early Ca^{2+} influx is a prerequisite to Thaxtomin A-induced cell death in *Arabidopsis thaliana* cells. ***Journal of Experimental Botany***, 59, 4259-4270. (IF_{2008} 4.01)

ACL-09 Farrant JM, **Lehner A**, Cooper K, Wiswedel S. 2009. Desiccation tolerance in the vegetative tissues of the fern *Mohria caffrorum* is seasonally regulated. ***The Plant Journal***, 57, 65-79. (IF_{2009} 6.95)

ACL-10 Meimoun P, Tran D, Baz M, Errakhi R, Dauphin A, **Lehner A**, Briand J, Biligui B, Madiona K, Beaulieu C, Bouteau F. 2009. Two different signaling pathways for thaxtomin A-induced cell death in Arabidopsis and tobacco BY2. ***Plant Signaling and Behavior***, 4, 142-144.

ACL-11 Meimoun P, Vidal G, Bohrer AS, **Lehner A**, Bouteau F, Rona JP. 2009. Intracellular Ca^{2+} stores could participate to abscisic acid-induced depolarization and stomatal closure in Arabidopsis thaliana. ***Plant Signaling and Behavior*****,** 4, 830-835.

ACL-12 Dardelle F, **Lehner A**, Ramdani Y, Bardor M, Lerouge P, Driouich A, Mollet JC. 2010. Biochemical and immunocytological characterizations of Arabidopsis thaliana pollen tube cell wall. ***Plant Physiology***, 153, 1563-1576. (IF_{2010} 6.45)

ACL-13 Lehner A, Dardelle F, Soret-Morvan O, Lerouge P, Driouich A, Mollet JC. 2010. Pectins in the cell wall of *Arabidospis thaliana* pollen tube and pistil. ***Plant Signaling and Behavior*****,** 10, 1-4.

ACL-14 Gribaa A, Dardelle F, **Lehner A**, Rihouey C, Burel C, Ferchichi A, Driouich A, Mollet JC. 2013. Effect of water deficit on the cell wall of the date palm (Phoenix dactylifera 'Deglet nour', Arecales) fruit during development. ***Plant Cell & Environment,*** 36, 1056-1070. (IF_{2013} 5.91).

ACL-15 Mollet JC, Leroux C, Dardelle F, **Lehner A**. 2013. Cell wall composition, biosynthesis and remodeling during pollen tube growth. ***Plants,*** 2, 107-147. Revue sur invitation

ACL-16 Paynel F, Leroux C, Surcouf O, Schaumann A, Pelloux J, Driouich A, Mollet JC, Lerouge P, **Lehner A***, Mareck A*. 2014. Kiwi fruit PMEI inhibits PME activity, modulates root elongation and induces pollen tube burst in Arabidopsis thaliana. ***Plant Growth Regulation,*** 74, 285-297. *Equal contribution of the senior authors. (IF_{2014} 1.67).

ACL-17 Dumont M, **Lehner A**, Bouton S, Kiefer-Meyer MC, Voxeur A, Pelloux J, Lerouge P, Mollet JC. 2014. The cell wall pectic polymer rhamnogalacturonan-II is required for proper pollen tube elongation: implication of a putative sialyltransferase-like protein. ***Annals of Botany***, 114, 1177-1188. (IF_{2014} 3.65).

ACL-18 Dardelle F, Le Mauff F, **Lehner A**, Bourrhis-Loutellier C, Bardor M, Rihouey C, Causse M, Lerouge P, Driouich A, Mollet JC. 2015. Pollen tube cell walls of wild and domesticated tomatoes contain arabinosylated and fucosylated xyloglucan. ***Annals of Botany,*** 115, 55-66. (IF_{2015} 3.98).

ACL-19 Leroux C, Bouton S, Kiefer-Meyer MC, Tohnyui Ndinyanka F, Mareck A, Guénin S, Fournet F, Ringli C, Pelloux J, Driouich A, Lerouge P, **Lehner A***, Mollet JC*. 2015. PECTIN METHYLESTERASE48 is involved in Arabidopsis pollen grain germination. ***Plant Physiology***, 167, 367-380. (IF_{2015} 6.28). * Equal contribution of the senior authors.

ACL-20 Lehner A, Menu-bouaouiche L, Dardelle F, Le Mauff F, Driouich A, Lerouge P, Mollet JC. 2015. In silico prediction of proteins related to xyloglucan fucosyltransferases in solanaceae genomes. ***Plant Signaling and Behavior,*** 10, e1026023.

ACL-21 Dumont M, Cataye C, **Lehner A**, Maréchal E, Lerouge P, Falconet D, Mollet JC. 2015. A Simple Protocol for the Immunolabelling of Arabidopsis Pollen Tube Membranes and Cell Wall Polymers. ***Bio-protocol*** 5(12): e1502.

ACL-22 Dumont M, **Lehner A**, Loutelier-Bourhis C, Mollet JC, Lerouge P.2015. Analysis of Sugar Component of a Hot Water Extract from Arabidopsis thaliana Pollen Tubes Using GC-EI-MS. ***Bio-protocol*** 5(12): e1503.

ACL-23 Dumont M, **Lehner A**, Bardor M, Burel C, Vauzeilles B, Lerouxel O, Anderson CT, Mollet JC, Lerouge P. 2015. Inhibition of fucosylation of cell wall components by 2-fluoro 2-deoxy-L-fucose induces defects in root cell elongation. ***Plant Journal***, 84, 1137-1151. (IF_{2015} 5.47).

ACL-24 Dumont M, **Lehner A**, Vauzeilles B, Malassis J, Marchant A, Smyth K, Linclau B, Baron A, Mas Pons J, Anderson CT, Schapman D, Galas L, Mollet JC, Lerouge P.2016. Plant cell wall imaging by metabolic click-mediated labelling of rhamnogalacturonan II using azido 3-deoxy-D-manno-oct-2-ulosonic acid. ***Plant Journal***, 85, 437-447. (IF_{2016} 5.90).

ACL-25 Gilbert-Mounet L, Dumont M, Ferrand C, Bournonville C, Monier A, Jorly J, Mori K, Lemaire-Chamley M, Atienza I, Hernould M, Stevens R, **Lehner A**, Mollet JC, Rothan C, Lerouge P, Baldet P.2016. Tomato GDP-D-mannose epimerase SlGME1 and SlGME2 play specific roles in cell wall biosynthesis during plant growth but show redundancy in terms of ascorbate synthesis. ***Journal of Experimental Botany***, 67, 4767-4777. (IF_{2016} 5.83).

ACL-26 Saez-Aguayo S, Rautengarten C, Temple H, Sanhueza D, Ejsmentewicz T, Sandoval-Ibañez O, Doñas D, Parra-Rojas JP, Ebert B, **Lehner A**, Mollet JC, Dupree P, Scheller HV, Heazlewood JL, Reyes FC, Orellana A. 2017. UUAT1, a Golgi-localized UDP-uronic acid transporter, plays a role defining the polysaccharide composition of Arabidopsis seed mucilage. ***The Plant Cell***, 29, 129-143. (IF_{2016} 8.69).

ACL-27 Hocq L, Sénéchal F, Lefebvre V, **Lehner A**, Domon JM, Mollet JC, Dehors J, Pageau K, Marcelo P, Guérineau F, Kolšek K, Mercadante D, Pelloux J. 2017. Combined experimental and computational approaches reveal distinct pH-controlled inhibiting capacities of Arabidopsis Pectin Methylesterase Inhibitors (PMEIs). ***Plant Physiology***, 173, 1075-1093. (IF_{2016} 6.45).

ACL-28 Guénin S, Hardouin J, Paynel F, Müller K, Mongelard G, Driouich A, Lerouge P, Kermode A, **Lehner A**, Mollet JC, Pelloux J, Gutierrez L, Mareck A. AtPME3, a ubiquitous cell wall pectin methylesterase of Arabidopsis thaliana, alters the metabolism of cruciferin seed storage

proteins during post-germinative growth of seedlings. ***Journal of Experimental Botany***, 68, 1083-1095. (IF_{2016} 5.83).

ACL-29 Zahid A, Jaber R, Laggoun F, **Lehner A**, Remy-Jouet I, Pamlard O, Beaupierre S, Leprince J, Follet-Gueye ML, Vicré-Gibouin M, Latour X, Richard V, Guillou C, Lerouge P, Driouich A*, Mollet JC*. Holaphyllamine, a steroid, is able to induce defense responses in Arabidopsis thaliana and increases resistance against bacterial infection. ***Planta***, DOI 10.1007/s00425-017-2755-z. * Equal contribution of the senior authors. (IF_{2016} 3.36)

5.2. Communications dans des congrès nationaux et internationaux

5.2.1. Conférences données sur invitation du comité d'organisation dans un congrès national ou international (INV) **Le nom de l'orateur est souligné**

INV-01 Corbineau F, **Lehner A**, Côme D. Recherche de critères physiologiques et biochimiques de la qualité des grains de blé. 23ème congrès du GETIS (Groupement des Experts des Technologies Industrielles des Semences), Deauville, France. March 27-28th 2003.

INV-02 Corbineau F, **Lehner A**, Côme D. Facteurs d'altération de la qualité des semences de céréales. 24ème congrès du GETIS, Le Touquet, France. May 30-31st 2004.

INV-03 **Lehner A**, Côme D, Corbineau F. Appréciation de la qualité des semences à la récolte et au cours de leur conservation. 25ème congrès du GETIS, Paris, France. March 29-30th 2005.

INV-04 Dardelle F, **Lehner A**, Ramdani Y, Bardor M, Lerouge P, Driouich A, Mollet J-C. Characterization of *Arabidopsis thaliana* pollen tube cell wall. Minisymposium Pollen Biology, ASPB-CSPP Annual Plant Biology Meeting, Montreal, Canada. July 31st - august 4th 2010.

INV-05 Driouich A, Cannesan M-A, Durand C, Dardelle F, Bernard S, Percoco G, Plancot B, **Lehner A**, Follet-Gueye M-L, Moore J, Hadrami I, Farrant J, Lerouge P, Vicré-Gibouin M. La matrice extracellulaire végétale: propriétés fonctionnelles en lien avec les stress biotique et abiotique. XIIème congrès de l'AUF-BIOVEG Cluj-Napoca, Roumania. September 26-29th 2010.

INV-06 Leroux C, Driouich A, Lerouge P, Mollet JC, **Lehner A.** Pectin methylesterases, calcium and cell wall remodeling during pollen grain germination in *Arabidopsis thaliana*. Plant Cell Signalling 2014, Paris, France. June 13th 2014.

INV-07 Leroux C, Dumont M, Driouich A, Lerouge P, Mollet JC, **Lehner A**. Biosynthesis and remodelling of pollen tube cell wall. 1ere journée scientifiques Université Cadi Ayyad-Université de Rouen, Marrakech, Morocco. April 22-24th 2014.

INV-08 Dardelle F, Le Mauff F, Loutelier-Bourhis C, Bardor M, Rihouey C, Causse M, Lerouge P, Driouich A, Mollet JC, **Lehner A**. Solanaceae pollen tubes and vegetative organs have

structurally divergent cell wall xyloglucan. International Symposium on Plant Signaling and Behavior. Paris, France. June 29th-July 2nd 2015.

5.2.2. Communications avec actes dans un congrès international (ACTI)

ACTI-01 Farrant JM, Wiswedel S, Stowell C, **Lehner A**. Desiccation is switched on and off in the fern *Mohria caffrorum*. 5th International Workshop on Desiccation Sensitivity and -Tolerance in Seeds and Vegetative Plant Tissues, Drakensberg, South Africa. January 14-21st 2007.

ACTI-02 Errakhi R, Bouteau F, **Lehner A**, Meimoun P, Barakate M. Rôle de l'acide oxalique, facteur de pathogénie de différents champignons nécrotrophes dans l'induction de réponses de défense chez *Arabidopsis thaliana*. 2nd édition du congrès national amélioration de la production agricole, Setta, Morocco. April 3-4th 2008.

ACTI-03 Vidal G, madiona K, Meimoun P, **Lehner A**, Briand J, Kawano T, Bouteau F, Rona JP. Abscisic acid-induced anion currents activation mediated by ADP-ribose/ryanodine receptor (RyR) in *Arabidopsis thaliana* suspensions cells. 4th International Symposium on Plant Neurobiology, Fukuoka, Japan. June 6-9th 2008.

ACTI-04 Errakhi R, Meimoun P, **Lehner A**, Vidal G, Briand J, Corbineau F, Rona JP, Bouteau F. Anion channel activity is necessary to induce ethylene synthesis and programmed cell death in response to oxalic acid. 4th International Symposium on Plant Neurobiology, Fukuoka, Japan. June 6-9th 2008.

ACTI-05 Errakhi R, Dauphin A, Meimoun P, **Lehner A**, Reboutier D, Vatsa P, Briand J, Madiona K, Rona JP, Wendehenne D, Beaulieu C, Bouteau F. Thaxtomin A-induced defense responses in Arabidopsis thaliana cells require an early Ca2+ influx. 4th International Symposium on Plant Neurobiology, Fukuoka, Japan. June 6-9th 2008.

ACTI-06 Rona JP, Vidal G, Meimoun P, **Lehner A**, Bouteau F. Estrés. (ABA) y señalización Ca^{2+} en las plantas. Colloque « Calcio y células vegetales » Universidad Nacional de La Pampa, Santa Rosa, Argentina. December 2-4th 2008.

ACTI-07 Rona JP, Meimoun P, Vidal G, Bohrer AS, **Lehner A**, Tran D, Kadono T, Bouteau F. Biotic and abiotic stress-induced anion currents activation mediated by CICR channels (Ca^{2+}-induced Ca^{2+} release) in plant cells. Colloque « Calcio y células vegetales » Universidad Nacional de La Pampa, Santa Rosa, Argentina. December 2-4th 2008.

ACTI-08 Lehner A, Bailly C, Corbineau F. Changes in embryo soluble carbohydrates and antioxydant system during ageing of wheat (Triticum aestivum L.) grains. Seed Longevity Workshop of the International Society for Seed Science, Wernigerode, Germany. July 5-8th 2015.

ACTI-09 Gilbert L, Dumont M, Ferrand C, Bournonville C, Monier A, Jorly J, Atienza I, Hernould M, Stevens R, **Lehner A**, Mollet JC, Rothan C, Lerouge P, Baldet P. Vitamin C and Cell Wall Metabolisms in Tomato: GDP-D-mannose epimerase (GME) a key actor of these interrelated pathways. The 12th Solanaceae Conference, Bordeaux, France. October 25-29th 2015.

ACTI-10 Anderson C, McClosky D, Wang B, Dumont M, Zhu C, Chen G, Dixit R, **Lehner A**, Mollet JC, Lerouge P. Turning on the light: using click chemistry to probe polysaccharide delivery, assembly, and dynamics in plant cell walls. XIV Cell Wall Meeting, Chania, Greece. June 14-17th 2016.

ACTI-11 Hocq L, Sénéchal F, Lefebvre V, **Lehner A**, Domon JM, Mollet JC, Pageau K, Marcelo P, Guérineau F, Kolšek K, Mercadante D, Pelloux J. Combined experimental and computational approaches reveal distinct pH-controlled inhibiting capacities of Arabidopsis pectin methylesterase inhibitors (PMEIs). XIV Cell Wall Meeting, Chania, Greece. June 14-17th 2016.

ACTI-12 Saez-Aguayo S, Temple H, Rautengarten C, Sanhueza D, Ejsmentewicz T, Sandoval-Ibañez O, Doñas D, Parra J.P, Ebert B, **Lehner A**, Mollet JC, Dupree P, Scheller H.V, Heazlewood J.L, Reyes F.C, Orellana A. UDP-Uronic acid transporters are important providing galacturonic acid and arabinose, but not xylose, into the cell wall. XIV Cell Wall Meeting, Chania, Greece. June 14-17th 2016.

ACTI-13 Zahid A, Laggoun F, Vicré M, **Lehner A**, Remy-Jouet I, Pamlard O, Beaupierre S, Leprince J, Latour X, Richard V, Guillou C, Lerouge P, Driouich A, Mollet JC. Chemical sScreen of natural small molecules identified a steroidal alkaloid, Holaphyllamine, able to induce defense responses in *Arabidopsis thaliana* and increase resistance against *Pseudomonas syringae*. Plant Bioprotech, 1st International Symposium on Plant Bioprotection Sciences & Technologies. Reims, France. June 27th – 30th 2017.

5.2.3. Communications avec actes dans un congrès national (ACTN)

ACTN-01 Dardelle F, N'Gouala Finassi R, **Lehner A**, Bardor M, Follet-Gueye ML, Driouich A, Mollet JC. Extracellular matrix characterization of *in vitro* grown *Arabidopsis thaliana* pollen tubes. 8th national meeting of the SFPV, Strasbourg, France. July 8-10th 2009.

ACTN-02 Dardelle F, **Lehner A**, Lerouge P, Driouich A, and Mollet JC. The pollen tube cell wall: a microscopic and biochemical characterization. 13èmes Journées Ecole Doctorale Normande Biologie Intégrative, Santé, Environnement. Deauville, France. May 11-12th 2010.

ACTN-03 Dardelle F, **Lehner A**, Ramdani Y, Soret-Morvan O, Bardor M, Lerouge P, Driouich A, Mollet JC. Sexual reproduction in plants: role of the cell wall in adhesion. 2ème Journée GRR VATA, Mont-Saint-Aignan, France. October 15th 2010.

ACTN-04 Dardelle F, **Lehner A**, Rihouey C, Bardor M, Lerouge P, Driouich A, and Mollet JC. Structural characterization of pollen tube xyloglucan of *Nicotiana tabacum*. 9ème Journées du Réseau Français des Parois. Lille, France. June 6-8th 2011.

ACTN-05 Zahid A, **Lehner A**, Lerouge P, Vicré-Gibouin M, Driouich A, and Mollet JC. Bioprotection des plantes : criblage de molécules naturelles capables d'induire les défenses des plantes. 3ème Journée GRR VATA, Mont-Saint-Aignan, October 14th 2011.

ACTN-06 Zahid A, Laggoun F, Plancot B, Leprince J, **Lehner A**, Vicré-Gibouin M, Driouich A, Mollet JC. Immunité végétale : Criblage et évaluation de nouveaux éliciteurs naturels dans

l'induction des mécanismes de défense chez A. thaliana. 4ème Journée GRR VASI, Mont-Saint-Aignan, October 12th 2012.

ACTN-07 Leroux C, Bouton S, Kiefer-Meyer MC, Pelloux J, Driouich A, Lerouge P, Lehner A, Mollet JC. 10-11 Avril 2014 lors des journées de l'EdN BISE au Havre, France. Involvement of pectin methylesterase during imbibition and germination of Arabidopsis pollen grain. 17èmes journées de l'EdNBISE. Le Havre, France. April 10-11th 2014.

ACTN-08 Dumont M, Bardor M, **Lehner A**, Mollet JC and Lerouge P. Fucosyltransferase inhibitor: a tool to study plant cell wall biosynhtesis. 17èmes journées de l'EdNBISE. Le Havre, France. April 10-11th 2014.

ACTN-09 Dumont M, Bardor M, **Lehner A**, Mollet JC and Lerouge P. Fucosyltransferase inhibitor: a tool to study plant cell wall biosynhtesis. 10ème Journées du Réseau Français des Parois, Amiens, France. July 7-9th 2014.

ACTN-10 Laggoun F, Dardelle F, Driouich A, Lerouge P, **Lehner A,** Mollet JC. Characterization of Arabidopsis pollen tube adhesion matrix using an enzymatic approach. 11ème Journées du Réseau Français des Parois, Orléans, France. June 27-29th 2017.

5.2.4. Communications par affiche dans un congrès international ou national (AFF)

AFF-01 **Lehner A**, Bailly C, Leymarie J, Rousseau S, Côme D, Corbineau F. Evolution des systèmes de détoxication au cours du développement des semences de tournesol. 10èmes Journées des Sciences de la Vie de l'Université Pierre et Marie Curie, Paris, France. July 4-5th 2001.

AFF-02 Bailly C, Leymarie J, **Lehner A**, Rousseau S, Côme D, Corbineau F. Changes in free radical scavenging during sunflower seed development. 5th Meeting on Oxygen, free Radicals and Oxidative Stress in Plants, Nice, France. November 19-21st 2001.

AFF-03 Bailly C, **Lehner A**, Rousseau S, Côme D, Corbineau F. Composition and thermal properties of reserve lipids of developing sunflower seeds. 7th International Workshop on Seeds, Salamanqua, Spain. May 12-16th 2002.

AFF-04 Bailly C, **Lehner A**, Rousseau S, Côme D, Corbineau F. Variation de la composition et des propriétés thermodynamiques des lipides de réserve des semences de tournesol au cours de leur développement. 11èmes journées des Sciences de la Vie de l'Université Pierre et Marie Curie, Paris, France. January 7-8th 2003.

AFF-05 **Lehner A**, Bailly C, Côme D, Corbineau F. Activité catalase : un moyen d'apprécier l'aptitude à la conservation des semences de blé. 25ème congrès du GETIS, Paris, France. March 29-30th 2005.

AFF-06 **Lehner A**, Côme D, Corbineau F. Teneur en sucres solubles : mise en évidence d'un début de germination sur pied pendant la culture. 25ème congrès du GETIS, Paris, France. March 29-30th 2005.

AFF-07 Lehner A, Côme D, Corbineau F. Oligosaccharide metabolism in wheat embryo as possible indicator of sprouting susceptibility. 8th International Workshop on Seeds, Brisbane, Australia. May 8-13th 2005.

AFF-08 Lehner A, Mamadou N, Côme D, Bailly C, Corbineau F. Wheat ageing : Two (or more) ways to die. 1er colloque du Reseau Français de Biologie des Graines, Angers, France. June 7-8th 2007.

AFF-09 Dardelle F, N'Gouala Finassi R, **Lehner A**, Bardor M, Follet-Gueye ML, Driouich A, Mollet JC. Extracellular matrix characterization of *in vitro* grown *Arabidopsis thaliana* pollen tubes. 15ème journée de l'IFRMP23, Mont-Saint Aignan, France. June 5th 2009.

AFF-10 Dardelle F, N'Gouala Finassi R, **Lehner A**, Bardor M, Follet-Gueye ML, Driouich A, Mollet JC. Extracellular matrix characterization of *in vitro* grown *Arabidopsis thaliana* pollen tubes. 8th national meeting of the SFPV, Strasbourg, France. July 8-10th 2009.

AFF-11 Dardelle F, **Lehner A**, Ramdani Y, Bardor M, Lerouge P, Driouich A, Mollet J-C. Characterization of *Arabidopsis thaliana* pollen tube cell wall. ASPB-CSPP Annual Plant Biology Meeting, Montreal, Canada. July 31st - august 4th 2010.

AFF-12 Lehner A, Païola F, Louvet R, Pelloux J, Driouich A, Lerouge P, Mollet J-C. Pectin methylesterases and Arabidopsis pollen tube growth. ASPB-CSPP Annual Plant Biology Meeting, Montreal, Canada. July 31st - august 4th 2010.

AFF-13 Dardelle F, **Lehner A**, Ramdani Y, Bardor M, Lerouge P, Driouich A, Mollet JC. The pollen tube cell wall: a microscopic and biochemical characterization. XIIth Cell Wall Meeting, Porto, Portugal. July 25-30th 2010.

AFF-14 Leroux C, **Lehner A**, Fournet F, Guénin S, Kiefer-Meyer MC, Pelloux J, Driouich A, Lerouge P, Mollet JC. Involvement of two Pectin methylesterases AtPPME1 and AtPME48 during Arabidopsis pollen germination. 9ème Journées du Réseau Français des Parois, Lille, France. June 6-8th 2011.

AFF-15 Leroux C, **Lehner A**, Kiefer-Meyer MC, Pelloux J, Driouich A, Lerouge P, Mollet JC. Involvement of pectin methylesterases during pollen imbibition and germination. Journée Ecole Doctorale Normande Biologie Intégrative, Santé, Environnement. Mont-saint-Aignan, France. March 23rd 2012.

AFF-16 Dardelle F, Grare M, **Lehner A**, Rihouey C, Bardor M, Lerouge P, Driouich A, Mollet JC (2012). Characterization of pollen tube xyloglucan from tobacco and tomato (Solanaceae) 24èmes Journées du Groupe Français des Glycosciences, Le Val Joly, France. May 21-25th 2012.

AFF-17 Leroux C, **Lehner A**, Kiefer-Meyer MC, Pelloux J, Driouich A, Lerouge P, Mollet JC. Involvement of Pectin methylesterases in Arabidopsis pollen imbibitions and germination. 1ere journée de scientifique de l'IRIB, Rouen, France. June 1th 2012.

AFF-18 Dardelle F., Grare M., **Lehner A**., Rihouey C., Bardor M., Lerouge P., Driouich A. and Mollet J-C. (2012). Characterization of pollen tube xyloglucan from tobacco and tomato

(Solanaceae). Symposium - Everything you want to know about Plant Sex but were afraid to ask. Porto, Portugal. July 9-11th 2012.

AFF-19 Leroux C, **Lehner A**, Kiefer-Meyer MC, Pelloux J, Driouich A, Lerouge P, Mollet JC. A new model depicting the role of PME during dehydration and germination of the pollen grain. Colloque Grands Réseaux de Recherche, Rouen, France. November 29-30th 2012.

AFF-20 Dumont M, Voxeur A, **Lehner A,** Mollet JC, Lerouge P. Role of Rhamnogalacturonan type II in pollen tube elongation. 2nd Journée de l'IRIB, Rouen. June 21st 2013.

AFF-21 Dumont M, Voxeur A, **Lehner A,** Mollet JC Lerouge P. Role of Rhamnogalacturonan type II in pollen tube elongation. XIIIth Cell Wall Meeting, Nantes, France. July 7-12th 2013.

AFF-22 Lehner A, Leroux C, Guénin S, Fournet F, Kiefer-Meyer MC, Pelloux J, Driouich A, Lerouge P, Mollet JC. AtPME48 encodes a pectin methylesterase involved in Arabidopsis pollen grain germination. XIIIth Cell Wall Meeting, Nantes, France. July 7-12th 2013.

AFF-23 Dardelle F, **Lehner A**, Bardor M, Rihouey C, Causse M, Lerouge P, Driouich A, Mollet JC. The cell wall of tobacco and tomato pollen tubes contains fucosylated xyloglucan not found in somatic cells. XIIIth Cell Wall Meeting, Nantes, France. July 7-12th 2013.

AFF-24 Laggoun F, Dardelle F, Falconet D, Lesnard A, Rault S, Driouich A, Lerouge P, **Lehner A**, Mollet JC. Small molecules interfere with the tip-polarized growth of Arabidopsis and tomato pollen. 17èmes journées de l'EdNBISE, Le Havre, France. April 10-11th 2014.

AFF-25 Laggoun F, Dardelle F, Falconet D, Lesnard A, Rault S, Driouich A, Lerouge P, **Lehner A**, Mollet JC. Small molecules interfere with the tip-polarized growth of Arabidopsis and tomato pollen. 23rd ICSPR, Porto, Portugal. July 13-18th 2014.

AFF-26 Leroux C, Bouton S, Morvan C, Fournet F, Guénin S, Kiefer-Meyer MC, Mareck A, Pelloux J, Driouich A, Lerouge P, **Lehner A,** Mollet JC. Decrease in PME48 activity leads to abnormal pollen germination. 23rd ICSPR, Porto, Portugal. July 13-18th 2014.

AFF-27 Dumont M, **Lehner A**, Bouton S, Kiefer-Meyer MC, Voxeur A, Pelloux J, Lerouge P, Mollet JC. The cell wall pectic polymer rhamnogalacturonan-II is required for proper pollen tube elongation: implication of a putative sialyltransferase-like protein. 23rd ICSPR, Porto, Portugal. July 13-18th 2014.

AFF-28 Dumont M, **Lehner A**, Marchant A, Vauzeilles B, Anderson CT, Mollet JC, Lerouge P. Plant cell wall imaging using metabolic click-mediated labelling. 4ème Journée de l'IRIB, Rouen, France. June 5th 2015.

AFF-29 Laggoun F, Dardelle F, Driouich A, Lerouge P, **Lehner A**, Mollet J-C. Arabidopsis pollen tube growth and adhesion using an enzymatic approach. 24th International Congress on Sexual Plant Reproduction, ICSPR, Tucson, Arizona, USA. March 18-23th 2016.

AFF-30 Naim E, Meimoun P, **Lehner A**, Gugi B, Laggoun F, Bailly C, tabcheh M, Haddarah A, El-Maarouf-Bouteau H. Cell wall Changes induced by ROS and ethylene in sunflower seed

dormancy alleviation. 11ème Journées du Réseau Français des Parois, Orléans. June 27-29th 2017.

AFF-31 Dehors J, Laggoun F, Gügi B, Mareck A, Leouge P, **Lehner A**, Mollet JC. Deciphering the links between ROS, Ca^{2+} and cell wall remodeling during *Arabidopsis thaliana* pollen tube growth. 1ère journée de la SFR Normandie Végétal, Rouen. July 11th 2017.

AFF-32 Laggoun F, Dardelle F, Driouich A, Lerouge P, **Lehner A**, Mollet J-C. Arabidopsis pollen tube growth and adhesion using an enzymatic approach. 1ère journée de la SFR Normandie Végétal, Rouen. July 11th 2017.

AFF-33 Zahid A, Laggoun F, Vicré M, **Lehner A**, Remy-Jouet I, Pamlard O, Beaupierre S, Leprince J, Latour X, Richard V, Guillou C, Lerouge P, Driouich A, Mollet JC. Chemical Screen of Natural Small Molecules Identified a steroidal alkaloid, Holaphyllamine, Able to Induce Defense Responses in *Arabidopsis thaliana* and Increase Resistance against *Pseudomonas syringae*. 12th European Fondation for Plant Pathology (EFPP) & 10th French Socity for Plant Pathology (SFP) congress. 29th may- 2nd june 2017.

Activité de recherche

Préambule

La partie scientifique de ce mémoire d'Habilitation à Diriger des Recherches est divisée en plusieurs sous châpitres correspondant aux thématiques de recherche qui m'ont été confiées, depuis mon doctorat jusqu'au poste de maître de conférences que j'occupe actuellement à l'Université de Rouen Normandie. Cela permet aux rapporteurs, qui doivent juger de mon aptitude à diriger des recherches d'avoir une vue de l'ensemble des travaux de recherche effectués. Chacun de ces sous chapitres est conclu par la synthèse des productions scientifiques du sujet décrit. La partie la plus conséquente correspond à mon activité depuis ma nomination à l'Université de Rouen Normandie. Les travaux qui y sont présentés ne représentent que les sujets dans lesquels je me suis investi en tant que responsable, co-responsable, ou expérimentateur et dans lesquels mon implication a été très forte. La transdisciplinarité qui existe au sein des différents axes de recherche du Glyco-MEV m'a aussi permis de participer à de nombreux sujets, que je ne considère pas comme secondaires, mais où mon implication scientifique et technique a été moins importante. Les productions scientifiques issues de ces travaux (click chemistry, screening d'éliciteurs, PME3) apparaissent dans la partie production scientifique (chapitre 5, p. 13). Enfin, la synthèse des travaux de recherche se poursuit par une 7ème partie correspondant aux sujets de recherche que je développerai au cours des prochaines années au Glyco-MEV.

6. Synthèse des travaux de recherche

6.1. Doctorat, Laboratoire de Physiologie Végétale Appliquée

Thème de recherche développé au cours du Doctorat (2002-2005) au laboratoire de Physiologie Végétale Appliquée (Université Paris 6) sous la direction du Pr. F. Corbineau : « Recherche d'indicateurs biochimiques de la qualité germinative au cours de la maturation et de la conservation des semences de blé ».

Le travail que j'ai effectué pour obtenir mon doctorat *es* sciences était partagé entre des travaux appliqués et des recherches plus fondamentales.

La partie appliquée de ce travail consistait à rechercher des indicateurs biochimiques permettant aux semenciers de mieux gérer leurs lots de semences dès la récolte et pendant la conservation. Deux thèmes principaux ont particulièrement été étudiés pour essayer de répondre aux problèmes rencontrés par les semenciers :

- La mise au point d'un kit colorimétrique du dosage de l'activité de la catalase permettant de déterminer la viabilité des semences au cours de leur conservation. L'activité catalase semble en effet être un bon indicateur de la viabilité des semences de blé.
- La mise au point d'un kit de dosage des sucres solubles (raffinose, saccharose et glucose) permettant de déterminer si les semences ont subi un début de germination sur pied avant la récolte. Ces travaux s'orientent, en particulier, vers la recherche d'une

relation entre la teneur en sucres solubles (raffinose et saccharose) des semences dès leur récolte et leur aptitude à la conservation. Un début de germination sur pied, même invisible à la récolte, entraîne une diminution du rapport raffinose/saccharose. En outre, les semences qui ont subi un début de germination sur pied sont particulièrement sensibles au vieillissement.

L'ensemble des résultats de ces travaux sont confidentiels et appartiennent à la société Syngenta-Agro.

Outre ce volet de recherche appliquée, mes travaux de thèse comportaient aussi une partie de recherche fondamentale, axée sur deux thématiques :

- l'évolution des systèmes de détoxication cellulaire au cours du développement des embryons sur la plante et après séchage. L'activité des principales enzymes intervenant dans l'élimination des formes actives de l'oxygène a été dosée (catalase, glutathion réductase, superoxyde dismutase). Les quantités d'H_2O_2 et de malondialdéhyde ont été mesurées. Par ailleurs, la teneur en sucres solubles des embryons a été suivie, par HPLC, au cours de la maturation des grains. Cette étude biochimique a été couplée à une étude physiologique des propriétés des semences au cours de leur développement (teneur en eau, vigueur et viabilité) afin de relier l'acquisition de la qualité germinative et la capacité des semences à se conserver à d'éventuels marqueurs biochimiques.
- l'étude du métabolisme des sucres solubles au cours de la ré-imbibition des semences suivie ou non d'un début de germination. Cette étude a été menée avec des semences dormantes et non dormantes dans des conditions favorisant ou défavorisant leur germination. L'objectif principal de ce travail était de déterminer si l'aptitude à la germination des semences de blé est corrélée au métabolisme des sucres solubles.

D'un point de vue fondamental, les travaux menés au cours de ces trois années de recherche ont permis d'apporter des précisions sur les mécanismes d'acquisition de la qualité des semences au cours de leur maturation sur la plante mère et au cours de leur conservation. La qualité des grains s'acquiert progressivement au cours de la maturation. Depuis la fin du remplissage jusqu'à la récolte, les activités des principales enzymes impliquées dans les mécanismes de détoxication cellulaire évoluent peu. La phase de maturation est associée à une synthèse de sucres solubles dans l'embryon ainsi qu'à une augmentation du rapport (raffinose/saccharose). En revanche, lors de la germination des grains, la teneur en raffinose des embryons diminue rapidement et elle est associée à une forte expression des gènes codant pour l'invertase et l'α-galactosidase. La diminution du raffinose n'est ni liée à la croissance de la radicule ni à la tolérance à la déshydratation des grains. L'accumulation du saccharose lors de la déshydratation des grains préalablement imbibés semble confirmer les nombreux travaux effectués sur les mécanismes mis en jeu dans la tolérance à la dessiccation.

Au cours de leur conservation, simulée par les traitements de vieillissement accéléré, les semences perdent progressivement leur aptitude à la germination. La résistance au vieillissement est variable d'un cultivar à un autre et dépend du génotype, de l'état physiologique des semences au moment de leur prélèvement, des conditions de conservations et du stade de germination lorsque le processus de germination sur pied se produit. La perte

de vigueur puis de viabilité des semences au cours des traitements de vieillissement accéléré est associée à une diminution de l'activité catalase et une baisse de la valeur du rapport (raffinose/saccharose). Sur le plan appliqué, il semble difficile de lier directement la diminution d'activité catalase à la perte de viabilité des grains puisqu'elle est dépendante des conditions de vieillissement accéléré testées. En revanche, si une activité catalase dosable ne prouve pas que les grains soient viables, il a été clairement montré que les semences dont l'activité catalase est nulle ne sont plus capables de germer. La teneur en sucre soluble est un bon critère pour évaluer le démarrage des processus de germination sur pied et par conséquent de l'augmentation de la sensibilité des grains à la conservation.

D'un point de vue appliqué, la transposition des travaux fondamentaux effectués sur les embryons à des mesures sur les grains entiers a permis de mettre au point deux outils de mesure simples et utilisables en routine au sein d'une entreprise. La mise au point de ces outils ainsi que leurs protocoles d'utilisation sont à l'usage exclusif de Syngenta-Agro.

La valeur du rapport (raffinose/saccharose) est un excellent indicateur (beaucoup plus précoce que le test de Hagberg habituellement utilisé) d'un début de germination sur pied. La diminution du rapport (raffinose/saccharose) observée dans les embryons est mesurable en travaillant sur le grain entier, et un dosage des sucres solubles à la récolte permettra désormais de pouvoir écarter les lots à risque au plus tôt après la récolte. En outre, le dosage de la catalase permet de suivre, à la récolte et au cours de la conservation des lots de report l'altération progressive de la viabilité des grains. Ces outils ont été utilisés de façon expérimentale au cours de la récolte 2005 dans les locaux de Syngenta-Agro et ont permis d'éliminer des lots qui avaient subi un épisode de germination sur pied et d'autres lots dont l'activité catalase était nulle.

L'ensemble de ces travaux de recherche a donné lieu à :

2 publications : **ACL-02** Lehner et al., 2006 ***Journal of Cereal Science*** 43, 175-182.
ACL-05 Lehner et al., 2008 ***Journal of Cereal Science*** 47, 555-565.

4 communications orales: INV-01, INV-02, INV-03, ACTI-08
4 communications par affiche: AFF-05, AFF-06, AFF-07, AFF-08

6.2. Post-Doctorat, Department of Molecular and Cell Biology

Thème de recherche développé au cours du Post Doctorat (2006, 1 an) au sein du Department of Molecular and Cell Biology, University of Cape Town, sous la direction du Pr. J.M. Farrant.

Le travail effectué a consisté à étudier la régulation de certains gènes candidats surexprimés lors de divers stress abiotiques, en particulier lors des stress hydriques et salins. La plante modèle utilisée dans le cadre de cette étude a été une monocotylédone nommée *Xerophyta viscosa*. Cette plante possède la particularité de survivre à une déshydratation très poussée alors que sa teneur en eau n'est plus que de l'ordre de 5%, de rester plusieurs mois à l'état sec et de retrouver la totalité de ses activités biochimiques et physiologiques au cours de la réhydratation (80 h). Cette plante constitue donc un excellent réservoir de gènes

potentiellement impliqués dans la résistance aux stress hydriques. Le but de ces recherches est d'identifier les principaux mécanismes impliqués dans la résistance à la déshydratation afin d'améliorer la résistance des plantes de grandes cultures aux périodes de sécheresse qui surviennent dans les régions semi-arides. L'analyse d'une banque d'ADNc générée à partir de plantes soumises à un stress hydrique a permis d'isoler plusieurs gènes surexprimés lors de la déshydratation. Le travail a consisté à i) cloner, ii) séquencer, et iii) étudier l'expression d'un de ces gènes et de sa protéine lors de différents stress (hydriques et salins) ou sous l'influence d'acide abscissique. Le gène isolé code pour une *myo*-inositol 1-phosphate synthase, enzyme clé impliquée dans la formation du myo-inositol. Ce gène ainsi que sa protéine sont surexprimés lors de stress salins, hydriques et sous l'influence d'acide abscissique. L'activité de l'enzyme a été déterminée de façon indirecte en dosant les sucres impliqués dans la voie métabolique de cette enzyme (saccharose, glucose, fructose, galactose, galactinol, inositol, raffinose et stachyose). Ces résultats ont mis en évidence une forte participation de cette enzyme lors de stress salins ou hydriques.

Mes travaux de recherches ont aussi porté sur l'étude d'une fougère, *Morhia Caffrorum*, qui présente la particularité d'être à la fois tolérante et intolérante à la déshydratation. Au cours de l'été, cette plante est tolérante à la déshydratation, tolérance qu'elle perd au cours des mois d'hiver lors de sa période de reproduction. L'étude anatomique, physiologique et biochimique a été menée sur des fougères prélevées dans un état tolérant et intolérant et ont consisté en 1) une analyse des protéines de type Heat Shock (HSP), 2) des dosages des principales enzymes impliquées dans les systèmes de détoxication cellulaire (catalase, glutathion réductase, superoxyde dismutase), 3) des dosages des sucres solubles.

L'ensemble de ces travaux de recherche a donné lieu à :

2 publications : **ACL-04** Lehner et al., 2008 ***Functional Plant Biology*** 35, 26-39.
ACL-09 Lehner et al., 2009 ***The Plant Journal*** 57, 65-79.

1 communication orale : ACTI-01

6.3. ATER, Laboratoire d'Electrophysiologie des Membranes

Thème de recherche développé au sein du laboratoire d'Electrophysiologie des Membranes (Université Diderot-Paris 7) sous la direction du Pr. J-P. Rona et du Dr. F. Bouteau : « Implication des canaux ioniques dans la transduction du signal de mort cellulaire chez Arabidopsis thaliana ».

Les travaux de recherche effectués avaient pour objectif de préciser le rôle des canaux ioniques dans la transduction du signal de mort cellulaire chez deux plantes modèles *Arabidopsis thaliana* et le tabac. Différents stress biotiques (phytotoxines) et abiotiques (stress salin, stress hyper osmotique) impliqués dans l'induction de la mort cellulaire ont été étudiés. L'implication des canaux ioniques a été étudiée par la technique de voltage imposé à électrode. Cette technique d'électrophysiologie permet de suivre au cours des stress l'évolution des courants ioniques au travers des membranes des cellules entières. Ces études

d'électrophysiologie ont été complétées par l'étude, en luminométrie, de la mort cellulaire et des variations en calcium cytosolique des cellules grâce à l'utilisation de cellules d'*Arabidopsis thaliana* et de tabac sur-exprimant un gène codant pour une aequorine.

Deux thématiques ont été étudiées et concernent 1) le rôle du calcium en tant que messager secondaire. Différents stocks de calcium (apoplastique, vacuolaire…) peuvent être impliqués dans la régulation de la concentration en calcium cytosolique en réponse à différents stress (biotiques et abiotiques) participant aux voies de signalisation amenant à des processus de mort cellulaire programmée. Les travaux ont consisté à étudier, lors de stress salin (NaCl) et non salin (mannitol), ainsi qu'à l'aide d'inhibiteurs sélectifs des canaux calciques (plasmalemme et tonoplaste) le degré et l'importance de la mobilisation du calcium dans la cellule dans l'induction de la mort cellulaire. Ces travaux ont été menés sur des cultures cellulaires de tabac aequorine. 2) des travaux portant sur une phytotoxine : l'acide oxalique. Cet acide, produit par de nombreux champignons nécrotrophes, induit la mort cellulaire des cellules d'*Arabidopsis thaliana*. Ces travaux ont mis en évidence le rôle des canaux anioniques, du pore de transition mitochondrial et de l'éthylène dans la transduction du signal de mort cellulaire en présence d'acide oxalique. Le but des recherches était de préciser l'implication d'un signal éthylène- ou mitochondrie- dépendant dans la mort cellulaire lors de l'infection des plantes par des champignons nécrotrophes.

L'ensemble de ces travaux de recherche a donné lieu à :

5 publications :

ACL-06 Errakhi et al., 2008 ***Journal of Experimental Botany*** 59, 3121-29.
ACL-07 Lehner et al., 2008 ***Plant Signaling and Behavior*** 3, 746-748.
ACL-08 Errakhi et al., 2008 ***Journal of Experimental Botany*** 59, 4259-70.
ACL-10 Meimoun et al., 2009 ***Plant Signaling and Behavior*** 4, 142-144.
ACL-11 Meimoun et al., 2009 ***Plant Signaling and Behavior*** 4, 830-835.

6 communications orales : ACTI-02, ACTI-03, ACTI-04, ACTI-05, ACTI-06, ACTI-07

6.4. Maître de conférences, Laboratoire de Glycobiologie et Matrice Extracellulaire Végétale

Les travaux présentés dans ce mémoire d'Habilitation à Diriger des Recherches concernent les projets développés au cours des doctorats de Flavien Dardelle et Marie Dumont au cours desquels je suis intervenu comme expérimentateur et les travaux de doctorats de Christelle Leroux, Ferdousse Laggoun et Jeremy dehors, au cours desquels j'ai été ou je suis directement impliqué comme responsable scientifique, encadrant ou co-encadrant. Les sujets de recherche présentés traitent principalement de la paroi du tube pollinique, de sa biosynthèe, sa composition et de son remodelage au cours de la croissance cellulaire Le modèle utilisé est le tube pollinique, cellule unique, dont la croissance rapide et polarisée en fait un excellent modèle expérimental.

La reproduction sexuée chez les plantes supérieures a une importance économique considérable puisqu'elle permet la production de graines. Ce processus commence lorsque le grain de pollen tombe sur le stigmate, se réhydrate et germe en formant un tube pollinique qui va croitre à travers le tissu de transmission femelle et transporter les gamètes à l'ovule et permettre la double fécondation et la production de graines. Le tube pollinique présente une croissance polarisée rapide qui nécessite la synthèse et la mise en place d'une grande quantité de membrane plasmique et de paroi. Ce transport massif de vésicules chargées de composés membranaires et pariétaux est entretenu par un cytosquelette dynamique. Le tube pollinique a également la capacité de percevoir divers signaux émis par le tissu de transmission femelle et les ovules qui permettent son guidage spatio-temporel à travers la matrice extracellulaire. Cette matrice extracellulaire est principalement constituée de pectines dont le rôle est de permettre aux tubes polliniques d'adhérer (Mollet et al., 2000). Les particularités de cette cellule unique, à croissance rapide et polarisée en font l'un des meilleurs modèles cellulaires pour l'étude de la biosynthèse, de la mise en place, du remodelage et de la capacité de la cellule à percevoir des signaux de guidage et d'adhésion. Les travaux présentés ci-dessous ont été réalisés depuis mon arrivée au Glyco-MEV, en septembre 2008. Ils sont la synthèse des travaux de thèse de Flavien Dardelle, Marie Dumont et Christelle Leroux. Ces travaux ont permis de caractériser la composition biochimique de la paroi des tubes polliniques ainsi que de préciser le role des pectines et de leurs modifications dans la croissance et la germination du pollen.

6.4.1. Biosynthèse, localisation, caractérisation biochimique et remodelage des polysaccharides de la paroi du tube pollinique

6.4.1.1. La paroi végétale

Les cellules végétales sont entourées d'une matrice extracellulaire appelée paroi. Lors des mitoses, les cellules sont séparées par une lamelle moyenne riche en polysaccharides pectiques puis chaque cellule va synthétiser une paroi dite primaire qui constituera l'unique enveloppe durant toute la croissance cellulaire. Cette paroi confère à la cellule de multiples fonctions tant physiques que biologiques. Ainsi, outre sa capacité à maintenir la turgescence cellulaire (Ray et al., 1972) et la transduction de signaux (Shibuya et Minami, 2001 ; Roberts, 2001), notamment pour la défense des plantes (Silipo et al., 2010), la paroi est également impliquée dans l'adhésion cellulaire (Durand et al., 2009) ou encore dans la communication avec les cellules environnantes (Brownlee, 2002). Une fois la croissance cellulaire terminée, certains tissus synthétiseront une paroi dite secondaire pour consolider la paroi primaire, conférant ainsi aux tissus une plus forte rigidité.

La biosynthèse et la mise en place de la paroi présentent un coût énergétique élevé pour la plante. On estime que 10% du génome code pour des gènes impliqués dans le métabolisme de la paroi chez *Arabidopsis thaliana*, regroupant la biosynthèse, le transport et le remodelage des molécules pariétales ainsi que la régulation de tous ces processus (McCann

et Carpita, 2008). De manière générale, la paroi primaire est de nature polysaccharidique et protéique. Trois familles de polysaccharides sont représentées : la cellulose, les hémicelluloses et les pectines ainsi que les protéines structurales et enzymes pouvant être glycosylées et qui résident dans cette matrice (Gibeaut et Carpita, 1994). Parmi ces protéines structurales de la paroi on trouve les glycoprotéines riches en hydroxyproline (HRGP : Arabinogalactane protéines, AGP et extensines) et les protéines riches en proline (PRP).

Malgré l'importance de la germination des grains de pollen et la croissance des tubes polliniques pour assurer la double fécondation, peu de données sont disponibles concernant la biosynthèse et le remodelage de la paroi du tube pollinique au cours de sa croissance. Les travaux de thèse de Flavien Dardelle consistaient à déterminer la composition et la localisation des composés pariétaux de la paroi des tubes polliniques, en particulier celle de la plante modèle *Arabidopsis thaliana* (Fig. 1A).

6.4.1.2. La paroi végétale du tube pollinique

6.4.1.2.1. les β-glucanes

Parmi les trois types de β-glucanes mis en évidence, seulement deux sont retrouvés dans la paroi du tube pollinique d'*Arabidopsis thaliana* : la cellulose et la callose (Fig. 1B, C). La dernière famille, les "Mixed-Linked Glucans" spécifique de certaines monocotylédones dont les Poaceae (Sørensen et al., 2008) et assimilée à la famille des hémicelluloses du fait de leur biosynthèse complexe dans l'appareil de Golgi ne sont pas retrouvées dans la paroi du tube pollinique d'*Arabidopsis thaliana*.

Malgré sa faible abondance (Schlüpmann et al., 1994), la cellulose est présente le long de la paroi des tubes polliniques et joue un rôle important dans la stabilisation de la paroi spécialement dans la zone de transition entre la zone apicale et le reste du tube (Geitmann, 2010). Les microfibrilles de cellulose sont orientées de façon oblique le long de la paroi des tubes polliniques du pin (Derksen et al., 1999) contre une orientation plus longitudinale observée chez le lys, *Solanum chacoense* et *Arabidopsis thaliana* suggérant que les microfibrilles de cellulose ne sont pas les seuls composants jouant un rôle contre la pression de turgescence (Aouar et al., 2010 ; Lehner et al., 2010 ; Chebli et al., 2012 ; Cai et al., 2015 ; Hepler et Winship, 2015).

La biosynthèse de la callose est peu étudiée car elle est en général constitutivement peu abondante dans la paroi des plantes non stressées. En revanche, la biosynthèse et la mise en place de la callose dans les parois est très souvent associée à des stress biotiques ou abiotiques (Fujita et al., 2006). Néanmoins, certaines cellules contiennent naturellement de la callose ; c'est le cas des tubes criblés du phloème (Xie et al., 2011), du pollen et des tubes polliniques (Parre et Geitmann, 2005a). Enfin, la callose est présente dans la plaque cellulaire lors des divisions (Chen et Kim, 2009).

La callose est un polysaccharide formé d'un enchaînement de résidus glucoses reliés par des liaisons en β-(1-3). Certains résidus glucosyles liés en β-(1-6) peuvent aussi être trouvés (Chen et Kim, 2009). Cette longue chaîne se conforme sous la forme d'une hélice, laquelle est capable de s'associer avec une, voire deux autres chaînes de même nature. La biosynthèse de la callose est effectuée au niveau de la membrane plasmique par les callose

synthases (CALS) (Hong et al., 2001 ; Verma et Hong, 2001). Parmi les 12 CALS, CALS5 est impliquée dans le dépôt de callose dans les grains de pollen et participe également à la formation de l'exine du grain de pollen (Nishikawa et al., 2005 ; Dong et al., 2005). La callose n'est pas répartie uniformément dans la paroi des tubes polliniques (Fig. 1B). En effet, comme nous l'avons montré pour *Arabidopsis thaliana* (Dardelle et al., 2010) et comme il avait précedemment été montré pour les tubes polliniques d'autres espèces (Li et al., 1995 ; Roy et al., 1997 ; Ferguson et al., 1998 ; Lennon et Lord, 2000 ; Derksen et al., 2002 ; Bove et al., 2008 ; Moscatelli et Idilli, 2009) la paroi des tubes est constituée de deux couches en arrière de la zone apicale, une interne enrichie en callose et une externe fibrillaire (Fig. 1D, E). A l'inverse, dans la région apicale, une seule couche est présente et ne contient pas, en condition normale, de callose.

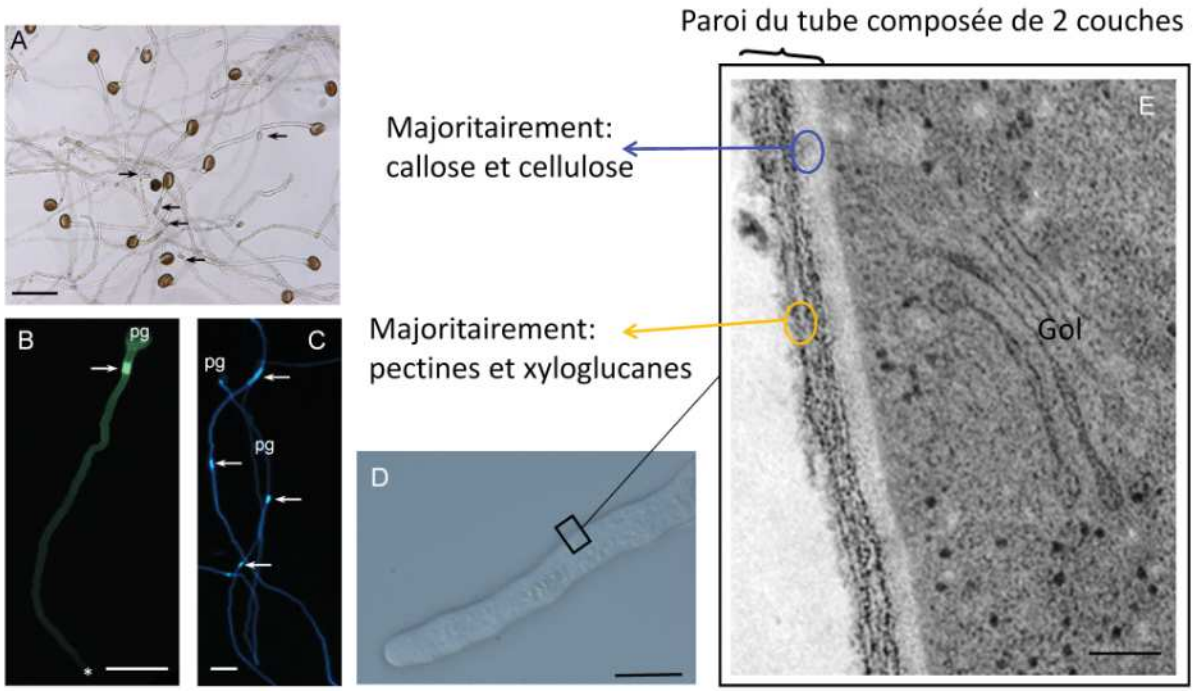

Figure 1. Tubes polliniques d'*Arabidopsis thaliana*, Coloration des β-glucanes et détail de la paroi du tube observé en microscopie électronique. **A**, tubes polliniques après 16 h de culture en milieu liquide. Les flèches indiquent les bouchons de callose. **B**, Coloration cytochimique des β-glucanes (callose) à l'aniline bleue. La flèche indique la présence d'un bouchon de callose. Noter l'absence de marquage dans la zone apicale (*). **C.** Coloration cytochimique au calcofluor blanc montrant les bouchons de callose et la localisation des β-glucanes (callose et cellulose) dans la paroi. D, E, partie apicale et sub apicale d'un tube pollinique d'*Arabidopsis thaliana* (D) et observation de la paroi de la partie subapicale en microscopie electronique à transmission montrant les deux couches pariétales (E). pg, grain de pollen. échelle = 50 µm (A-C), 10 µm (D) et 0,1 µm (E). Dardelle et al. 2010

6.4.1.2.2. Les hémicelluloses

On comptabilise à ce jour de nombreux polymères appartenant à cette famille de polysaccharides. Parmi les plus abondants, on retrouve les xylanes, arabinoxylanes, les mannanes, les glucomannanes, les β-(1-3,1-4)-glucanes (mixed-linkage glucans) ainsi que les

xyloglucanes (XyGs) (Scheller et Ulvskov, 2010). Les polymères hémicellulosiques s'associent à la cellulose par des liaisons non covalentes et permettent ainsi aux microfibrilles cellulosiques d'être indirectement, mais solidement reliées les unes aux autres (McCann et al., 1990 ; Scheller et Ulvskov, 2010). Ces polymères peuvent également établir des liaisons covalentes avec les pectines acides (Thompson et Fry, 2000).

Lors de l'étude de la composition de la paroi du tube pollinique d'*Arabidopsis thaliana*, nous nous sommes particulièrement intéressés aux hémicelluloses de type xyloglucanes, les hémicelluloses les plus abondantes de la paroi primaire. Ce polymère est constitué d'une chaine principale β-D-Glc*p* liés en (1-4) pouvant être ramifiée en 0-6, par des chaines latérales de natures diverses (Fig. 2) contenant des résidus xylose, galactose et fucose chez la majorité des angiospermes (fucogalactoxyloglucanes) à l'exception des Lamiids (Solanacées) où le fucose n'est pas présent et est remplacé par l'arabinose branché sur le xylose (Fry, 2011). On parle alors d'arabinoxyloglucanes. Afin d'aider à la description des différentes structures, Fry et collaborateurs (1993) ont développé une nomenclature avec une lettre correspondant aux structures suivantes : G = β-D-Glc*p* non substitué ; X = α-D-Xyl*p*-(1-6)-β-D-Glc*p* ; S = X substitué par un α-L-Ara*f*-(1-2) et L = X substitué par un β-D-Gal*p*-(1-2) et F = L substitué par un α-L-Fuc*p* (Fig. 2). Certains oses peuvent être *O*-acétylés et les motifs sont alors soulignés.

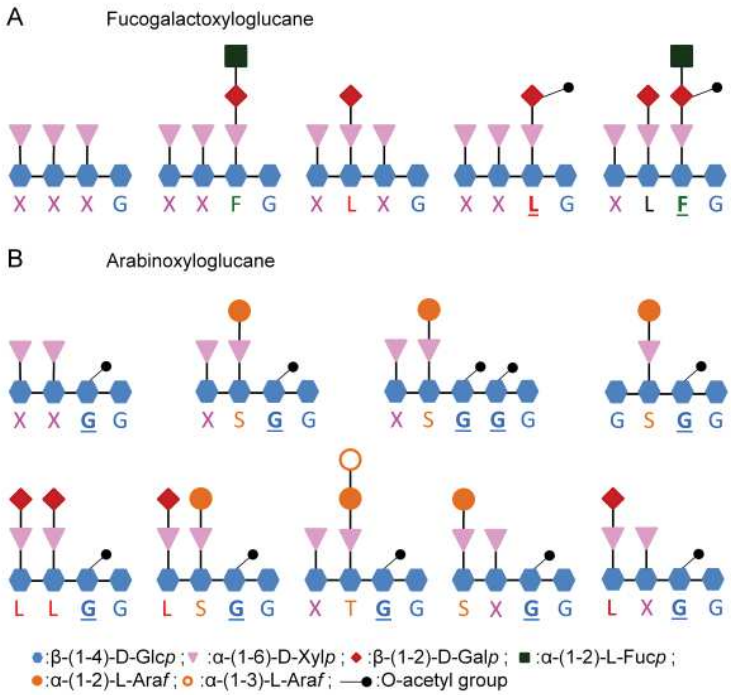

Figure 2. Représentation schématique des principaux motifs de XyGs et leurs nomenclatures (Dardelle et al., 2015).

Les épitopes associés aux XyGs sont détectés tout le long du tube pollinique d'*Arabidopsis thaliana* (Fig. 3A, B) et principalement dans la paroi externe fibrillaire (Fig. 1E). L'analyse biochimique par spectrométrie de masse MALDI-TOF des XyGs après traitement par une *endo*-glucanase de la paroi cellulaire des tubes polliniques a révélé deux

oligosaccharides dominants mono *O*-acétylés (XLXG / XXLG et XXFG) qui représentent plus de 68% des ions totaux (Fig. 3C). Ces résultats démontrent que la paroi du tube pollinique d'*Arabidopsis thaliana* a ses propres caractéristiques en comparaison avec d'autres types de cellules du sporophyte d'*Arabidopsis thaliana* (Dardelle et al., 2010). En effet, les principaux fragments de XyG libérés après un traitement à l'*endo*-glucanase de la paroi cellulaire des organes végétatifs d'*Arabidopsis thaliana* sont généralement XXXG, XXLG / XLXG, XXFG, et XLFG (Zablackis et al., 1995 ; Lerouxel et al., 2002 ; Nguema- Ona et al., 2006 ; Obel et al., 2009).

La singularité de la composition en XyG de la paroi du tube pollinique d'*Arabidopsis thaliana* nous a amené à étudier la composition des XyGs dans les tubes polliniques de tomate, *Solanum lycopersicum*, espèce dont les parties végétatives sont dépourvues de fragments fucosylés, mais qui contiennent des fragments arabinosylés (Fig. 2). Ces recherches ont été entreprises afin de déterminer si la présence en abondance de fragments fucosylés dans le tube pollinique était une caractéristique générale liée aux particularités mécaniques et adhésives de la paroi des tubes polliniques.

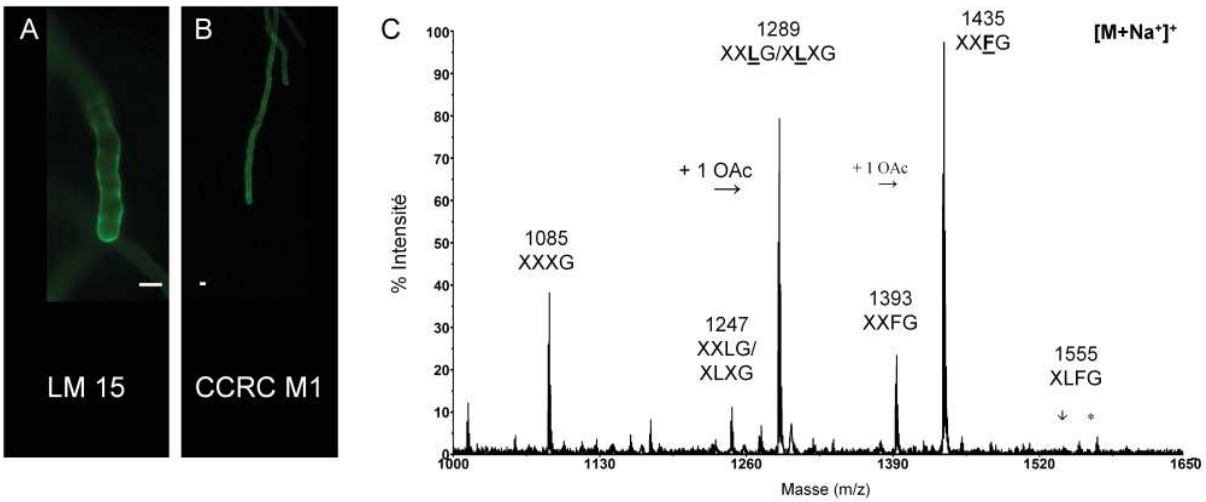

Figure 3. Analyse des xyloglucanes du tube pollinique d'*Arabidopsis thaliana*. A, B, Immunomarquages des épitopes associés aux XyGs non fucosylés et fucosylés avec les anticorps LM15 (A) and CCRC-M1 (B), respectivement. C, Spectre MALDI-TOF des fragments de xyloglucanes obtenus après digestion à l'*endo*-glucanase. Les différents fragments et leurs masses respectives sont indiqués. Les lettres en gras soulignés indiquent une *O*-acétylation (OAc). Echelle en A et B, 5 µm.

Nos travaux ont porté sur l'étude des tubes polliniques de plusieurs espèces de tomates *Solanum peruvianum*, *Solanum pimpinellifollium*, *Solanum lycopersycum* var. *Saint Pierre* et *Solanum lycopersicum* var. wva106 et sur des cultures cellulaires de *Solanum lycopersicum* cv. Dombito (Fig. 4A, D, G, J M). Nos résultats, analyses biochimiques et immunolocalisation à l'aide des anticorps LM15 et CCRC M1 montrent bien la présence de fragments fucosylés dans la paroi des tubes polliniques (Fig. 4). Les épitopes correspondant aux fragments fucosylés ne sont pas reconnus par CCRC M1 dans les cultures cellulaires de

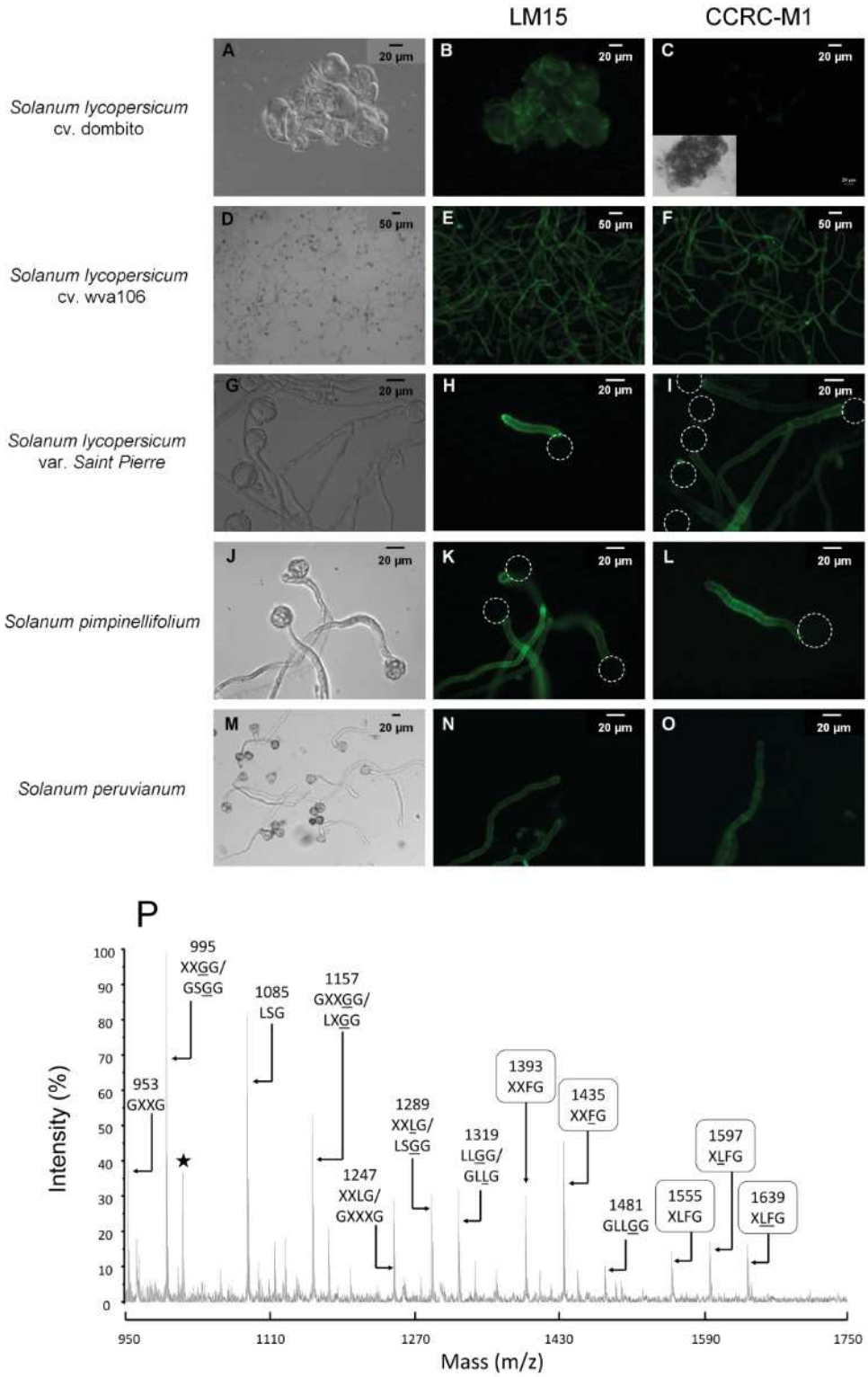

Figure 4. Immunolocalisation fragments fucosylés (CCRC-M1) et non fucosylés (LM15) de xyloglucan dans des tissus végétatifs (A, B, C) et dans les tubes polliniques de différentes espèces de tomates de (D à O). P, Analyse MaldiTOF des fragments de XyG après digestion.

Solanum lycopersicum cv. Dombito alors que la totalité des tubes polliniques des 4 autres espèces est clairement marquée par l'anticorps CCRC-M1 (Fig. 4C, F, I, L et O). Les

fragments non fucosylés sont retrouvés à la fois dans les cultures cellulaires et dans les tubes polliniques (Fig. 4B, E, H, K et N). Les analyses biochimiques des fragments libérés après digestion à l'*endo*-glucanase ont confirmé l'absence de fragments fucosylés dans les parties végétatives et leur présence dans les tubes polliniques (Dardelle et al., 2015). Plus surprenant, l'abondance des fragments fucosylés semble être le résultat de la pression de sélection puisque les proportions les plus importantes de fragments fucosylés sont retrouvées chez les espèces sauvages (Fig. 4P, *Solanum peruvianum*), les deux espèces cultivées *Solanum lycopersycum* var. *Saint Pierre* et *Solanum lycopersicum* var. wva106 étant celles dont les parois contenaient les proportions de fucose les plus faibles. Une autre étude a démontré la présence de XyGs fucosylés dans les tubes polliniques de *Nicotiana alata* (Lampugnani et al., 2013). L'analyse bio-informatique réalisée au laboratoire (Lehner et al., 2015) a permis de mettre en évidence dans plusieurs espèces de solanacées l'existence de gènes codant des protéines possédant une forte similarité avec les deux α1-2 galactoside fucosyltranferase (FUT) décrites à ce jour, AtFUT1 et PsFUT1 (Perrin et al., 1999 ; Faik et al., 2000) et possédant les motifs protéiques indispensables à l'activité de ces α1-2 galactoside fucosyltranférases. Trois gènes ont été trouvés chez *Solanum lycopersicum* (*Solyc07g047920.1*, *Solyc06g061210.2*, *Solyc03g115830.1*), deux chez *Solanum tuberosum* (*PGSC0003DMG400033900*, *PGSC0003DMG400003781*), deux chez *Solanum melongena* (*Sme2.5_14353.1_g00002.1*, *Sme2.5_00136.1_g00018.1*) deux chez *Nicotiana benthamiana* (*NbS00022797g0009.1*, *NbS00026070g0016.1*), trois chez *Nicotiana tabacum* (*mRNA_11650_cds*, *mRNA_55231_cds*, *mRNA_67630_cds*, mRNA_120465_cds) et enfin deux chez *Capsicum annuum* (*Ca03g29900 et Ca06g13300*). Ces observations semblent indiquer que la fucosylation des XyGs dans la paroi des tubes polliniques aurait un rôle important qui reste à ce jour encore non élucidé.

6.4.1.2.3. Les pectines

Les pectines sont avec les XyGs, les polysaccharides complexes les plus abondants de la paroi primaire. Elles constituent 40% de la paroi primaire chez *Arabidopsis thaliana* (Liepman et al., 2010). Les pectines sont majoritairement retrouvées dans la lamelle moyenne, assurant ainsi la cohésion entre les cellules végétales, et dans la paroi primaire. Parmi les pectines on retrouve les homogalacturonanes (HG), les rhamnogalacturonanes de type I et II (respectivement RG-I et RG-II) (Zablackis et al., 1995), le xylogalacturonane (XG) (Zandleven et al., 2007). D'autres pectines comme l'apiogalacturonane chez la lentille d'eau ont été caractérisées (Schols et al., 1995 ; Hart et Kindel, 1970).

- Le xylogalacturonane :

Le xylogalacturonane possède une chaine principale du type HG où des résidus xyloses sont substitués en position C-3 de certains acides galacturoniques. Au cours des travaux de doctorat de Flavien Dardelle, nous avons mis en évidence la présence des épitopes associés aux xylogalacturonanes à l'aide de l'anticorps LM8 (Willats et al., 2004) dans les tubes polliniques d'*Arabidopsis thaliana* (Dardelle et al., 2010). Très peu de travaux existent à l'heure actuelle sur le rôle des XG dans la croissance cellulaire. Il semble que le gène

At5g33290 soit impliqué dans la synthèse du XG, mais puisque le mutant *xgd1* (*xylogalacturonan deficient 1*) ne présente aucun phénotype visible au niveau de son grain de pollen ou de ses tubes polliniques (Jensen et al., 2008) tout laisse à croire que d'autres gènes sont impliqués dans la biosynthèse du XG dans le pollen. A ce jour, ils n'ont pas été caractérisés.

- Le rhamnogalacturonane de type I (RG-I) :

Le RG-I consiste en une chaîne principale du motif répété [α-(1-4)GalA-α-(1-2)-Rha] sur laquelle des ramifications de chaînes α-(1-5)-arabinanes, β-(1-4)-galactanes et/ou arabinogalactanes de type I peuvent être trouvées en position C-4 des résidus rhamnoses (Harholt et al., 2010). Le RG-I semble participer à la rigidification de la paroi puisqu'une paroi riche en chaînes galactanes sera deux fois plus rigide qu'une paroi dépourvue de ces chaines (McCartney et al., 2000).

Au cours de nos études sur la composition et la localisation des polymères pariétaux des tubes polliniques d'*Arabidopsis thaliana*, nous avons mis en évidence la présence du RG-I (Fig. 5A-D) à l'aide des anticorps LM6 et LM13, reconnaissant des épitopes associés aux arabinanes (Willats et al., 1998). La fluorescence est répartie uniformément le long de l'ensemble du tube pollinique chez *Arabidopsis thaliana* (Fig. 5A-D), *Actinidia deliciosa* (Abreu et Oliveira, 2004) et chez *Picea wilsonii* (Chen et al., 2008) avec néanmoins une intensité de fluorescence plus importante à l'apex du tube (Fig. 5B, D). Depuis cette étude menée au laboratoire par Flavien Dardelle, deux autres anticorps monoclonaux (INRA-RU1 et RU2-INRA) ont été mis en évidence comme étant spécifiques de la chaine principale du RG-I (Ralet et al., 2010) et un troisième anticorps, LM6-M, dérivé du LM6, possederait aussi une affinité plus grande pour les chaines de α-1,5-L-arabinan du RG-I (Cornuault et al., 2017). Ces anticorps n'ont pas été testés sur le tube pollinique. En revanche, nos travaux de microscopie électronique ont permis de déterminer que les arabinanes sont principalement détectés dans la couche externe de la paroi cellulaire chez *Arabidopsis thaliana* (Dardelle et al., 2010). En outre, l'analyse biochimique de la paroi cellulaire des tubes polliniques d'*Arabidopsis thaliana* a révélé une teneur importante en résidus arabinose (43%) provenant essentiellement des α-(1-5)-L-arabinanes des RG-I. D'autres études sur la paroi des tubes polliniques de *Nicotiana alata* (Lampugnani et al., 2013) ont confirmé la richesse de ces polymères dans la paroi des tubes polliniques.

La raison de l'abondance des arabinanes dans la paroi des tubes polliniques n'est pas connue. Cependant, chez *Arabidopsis thaliana*, un double mutant KO (knock-out) pour deux *RGPs* (*REVERSIBLY GLYCOSYLATED PEPTIDEs*) (*RGP1* et *RGP2*) présente une forte altération de l'intine et une létalité du pollen (Drakakaki et al., 2006). Ces RGPs présentent une forte homologie (~80%) avec la séquence protéique d'une UDP-arabinopyranose mutase chez le riz impliquée dans l'interconversion de l'UDP-Ara*p* et de l'UDP-Ara*f* (Konishi et al., 2007 ; Rautengarten et al., 2011). Bien que l'analyse de la paroi des grains de pollen n'ait pas été entreprise afin de vérifier que les arabinanes des RG-I étaient affectés, les résultats suggèrent que RGP1 et RGP2 agissent de façon redondante durant le développement du pollen et pourraient être impliquées dans la synthèse des arabinanes lors de la maturation du pollen (Drakakaki et al., 2006).

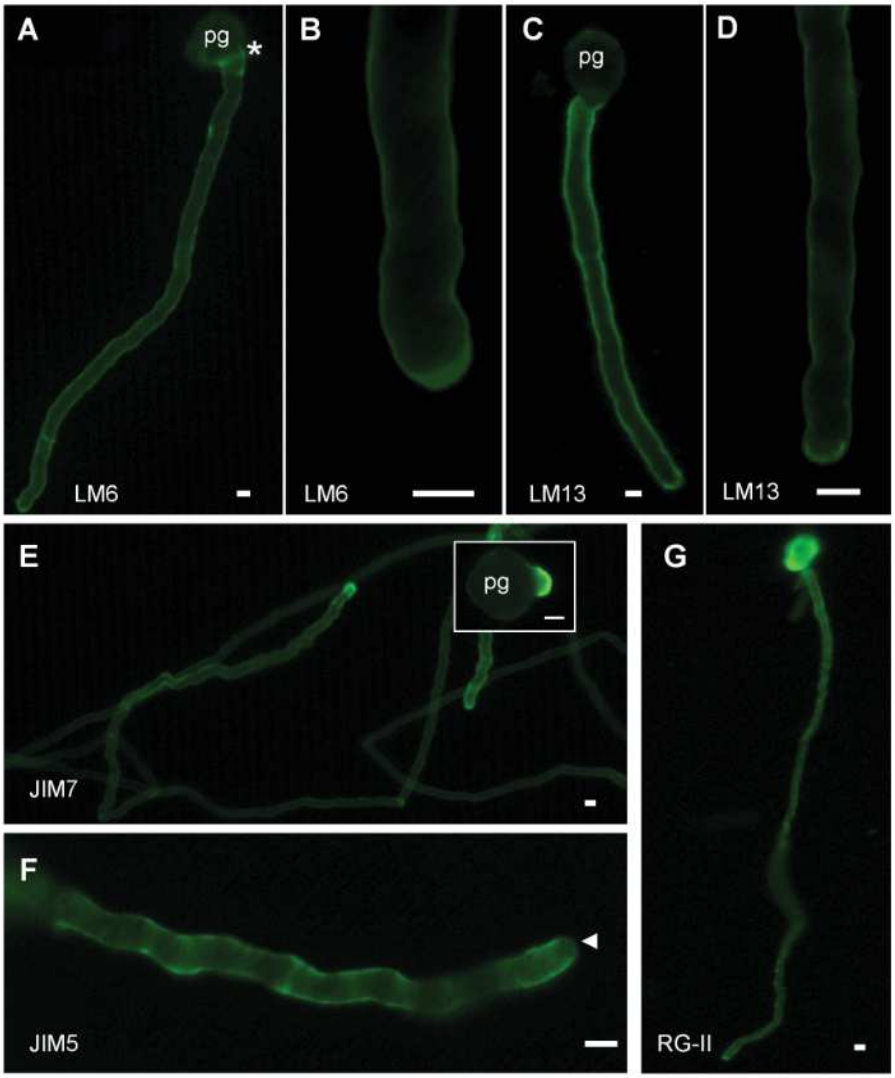

Figure 5. Immunolocalisation des pectines dans les tubes polliniques d'*Arabidopsis thaliana*. A-D, Immunolocalisation des épitopes associés aux RG-I à l'aide des anticorps LM6 et LM13. E, F, Immunolocalisation des HG fortement (E) et faiblement methylestérifiés (F) à l'aide des anticorps JIM7 et JIM5 respectivement. G, Immunolocalisation des épitopes associés au RG-II à l'aide de l'anticorps décrit par Matoh et al. 1998. Pg, grain de pollen ; la flèche indique l'apex d'un tube. *, anneau de fluorescence observé avec LM6 au niveau de la zone d'émergence du tube pollinique. Les barres d'échelle représentent 5 µm.

- Les homogalacturonanes (HG):

Les HG se composent de chaines d'acides galacturoniques (GalA) liés en α-(1-4). Cette famille est la plus abondante car elle représente environ 65% des pectines totales. Ce polymère peut être méthyl-estérifié sur le carbone 6 et *O*-acétylé en position 0-2 et 0-3. D'ailleurs, c'est sous la forme fortement méthyl-estérifiée que les HGs sont synthétisés dans l'appareil de Golgi, où seraient localisées des protéines possédant un domaine méthyltransférase putatif (Mouille et al., 2007). Dans la paroi, ces groupements méthyles

peuvent être éliminés sous l'action de pectines méthyl-estérases (PMEs) pour aboutir à la formation de groupements carboxyliques sur le C-6. Selon les conditions de pH et la régulation ionique, les pectines vont subir, soit une dé-méthyl-estérification partielle et aléatoire, soit en bloc. Dans le premier cas, les HGs seraient alors sensibles aux *endo*-polygalacturonases, favorisant un relâchement de la paroi. Dans le second cas, les charges négatives contigües établies par les groupements carboxyles (COO^-) pourront interagir avec des ions Ca^{2+} (Ralet et al., 2008) permettant l'association de plusieurs chaines de HG. Cette association établit la structure dite "boîte à œuf" (Jarvis et al., 2003 ; Micheli, 2001 ; Pelloux et al., 2007). En établissant des structures "boîte à œuf", les HGs se lient entre eux et rigidifient la paroi (Micheli, 2001 ; Pelloux et al., 2007). Ce modèle est cependant en parti remis en question puisque les travaux sur le développement des primordia foliaires montrent que la déméthylestérification des HG est couplée à une augmentation de l'élasticité de la paroi, et ce même en présence de calcium (Peaucelle et al., 2011).

Des études d'immunomarquages réalisées au laboratoire sur les tubes polliniques avec des anticorps monoclonaux reconnaissant des épitopes associés aux HGs faiblement méthyl-estérifiés (JIM5) ou fortement méthyl-estérifiés (JIM7) montrent que ces pectines ont une distribution spatiale caractéristique chez de nombreuses espèces avec les HGs fortement méthyl-estérifiés localisés principalement dans la zone apicale (lieu de sécrétion des HGs, Fig. 5E) et les HGs faiblement méthyl-estérifiés en arrière (Fig. 5F) suggérant l'action de PMEs (Bosch et Hepler, 2005 ; Dardelle et al., 2010 ; Lehner et al., 2010, Chebli et al., 2012 ; Mollet et al., 2013). Le remodelage des pectines, et particulièrement des HG au cours de la croissance apicale des tubes polliniques est détaillé dans le chapitre résumant les travaux effectués sur le remodelage des pectines de la paroi par les PME et les PMEI.

- Le rhamnogalacturonane de type II (RG-II).

Le RG-II est constitué d'un squelette d'acide galacturonique sur lequel viennent se substituer cinq chaînes latérales notées A à D. Ces oligosaccharides sont composés de 12 monosaccharides différents dont certains sont rares tels que l'apiose (Api), l'acide 3-déoxy-D-lyso-heptulosarique (Dha), l'acide 3-déoxy-D-manno-octulosonique (Kdo) ou encore l'acide acérique (Ace) (Whitcombe et al., 1995 ; Pérez et al., 2003 ; Dumont et al., 2014). L'un de ces monosaccharides, l'apiose de la chaine A, permet au RG-II de former des dimères par l'intermédiaire d'un pont diester de borate (Kobayashi et al., 1996 ; O'Neill et al., 1996 ; Vidal et al., 2001; Matsunaga et al., 2004) qui contribuerait à la rigidification de la paroi. Chez le mutant *mur1-1* et *gme* (GDP-d-mannose 3, 5-epimérase), l'absence respective de fucose ou de L-galactose provoque une diminution de cette dimérisation et induit un phénotype nain (O'Neill et al., 1996, 2001 ; Voxeur et al., 2011). Dans les deux cas, la complémentation de ces mutants avec du bore restaure le phénotype sauvage suggérant que le développement de la plante dépend de l'organisation du réseau pectique et de la dimérisation du RG-II (O'Neill et al., 2001 ; Voxeur et al., 2011). De même, l'absence d'acide glucuronique sur la chaîne A du RG-II altère la dimérisation et entraine une perte d'adhésion des cellules en suspension chez le tabac (Iwai et al., 2002).

Au cours de la thèse de Marie Dumont, nous avons été amenés à étudier le rôle du RG-II dans le développement et la germination du pollen. Les immunomarquages effectués en utilisant un anticorps reconnaissant les formes monomérique et dimérique du RG-II semblent indiquer que le RG-II est présent dans la paroi des tubes polliniques du lys (Matoh et al., 1998), de la tomate, du tabac (Dumont et al., 2014) et d'*Arabidopsis thaliana* (Fig. 5G ; Fig. 6D). La détection par GC-MS d'un des sucres à 8 carbones spécifiques du RG-II, le Kdo, dans un extrait pariétal de tubes polliniques d'*Arabidopsis thaliana* a été la première preuve biochimique de la présence de ce motif pectique dans la paroi des tubes polliniques (Dumont et al., 2014). Cependant, aucune évidence ne permet de déterminer s'il se trouve sous forme monomérique ou dimérique.

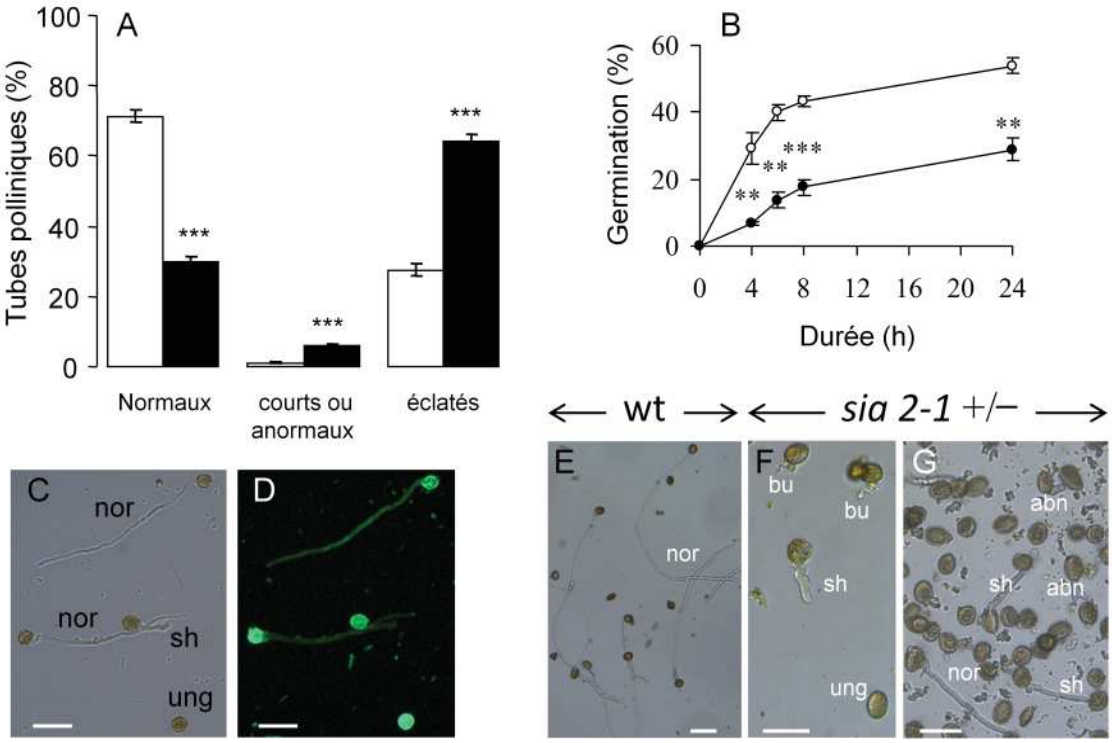

Figure 6. Etude phénotypique du mutant *sia2*+/-. A, pourcentage de tubes dont les tubes présentent un phénotype normal, anormal ou éclatés chez le mutant héterozygote *sia2*+/- (noir) par rapport à des plantes sauvages (blanc). B, cinétique de germination du pollen sauvage (blanc) et mutant *sia2*+/- (noir). C, D, Immunolocalisation des des épitopes associés aux RG-II à l'aide de l'anticorps décrit par Matoh et al. (1998) chez les tubes polliniques du mutant heterozygote (*sia2*+/-). E-G, Phénotypes observés chez les tubes sia2+/- (F, G) par rapport au pollen sauvage (E). abn, anormaux ; bu, éclaté ; nor, normaux ; sh, court ; ung, non germés, wt, sauvage ; Les barres d'échelle représentent 50 µm. Analyse statistique : Student's t-test, **P<0.01 et ***P<0.001.

Chez *Arabidopsis thaliana*, 5 gènes impliqués dans la biosynthèse du RG-II ont permis de démontrer que ce motif était important pour l'élongation du tube pollinique. Les *KDO-8-P SYNTHASEs* (*AtKDSA1* et *AtKDSA2*) seraient impliqués dans la synthèse du Kdo. Le double mutant *Atkdsa1* et *Atkdsa2* présente des grains de pollen incapables d'avoir une élongation convenable de leurs tubes polliniques et sont stériles (Delmas et al., 2008). L'étude du mutant dont le gène coderait pour la CTP:3-deoxy-D-manno-2-octulosonate

cytidylyltransferase (CMP-KDO synthetase, *CKS*) mitochondriale, responsable de l'activation du Kdo comme un sucre nucléotidique avant son incorporation dans le RG-II, n'a pas permis d'obtenir des lignées homozygotes (Kobayashi et al., 2011). Chez le mutant hétérozygote, l'élongation des tubes est anormale et les plantes stériles (Kobayashi et al., 2011). L'étude de deux mutants *mgp* (*male gametophyte defective*) et nos travaux sur le mutant *sia2* (*sialyltransferase-like2*) a permis de conforter l'idée que l'altération de la biosynthèse du RG-II dans le pollen impacte la croissance du tube pollinique. En effet, *mgp4*, mutant KO pour une xylosyltransferase du RG-II (Liu et al., 2011) ainsi que *mgp2*, mutant KO pour une sialyltransferase-like 1 (Deng et al., 2010) et *sia2+/-* (Fig. 6) présentent des phénotypes similaires : nombreux tubes déformés et/ou éclatés (Fig. 6A, E-G) avec une forte inhibition de la germination du pollen ainsi qu'un retard de croissance des tubes polliniques *in-vitro* et *in-vivo* comparé au sauvage (Fig. 6B).

Notre étude a permis par ailleurs de montrer que les tubes sauvages, présentant un phénotype normal, parmi la population de mutant héterozygotes *sia2+/-* étaient correctement marqué par l'anticorps reconnaissant le RG-II (Fig. 6C, D) confortant l'hypothèse que l'absence de RG-II chez les mutants est à l'origine des phénotypes anormaux observés (Fig. 6E-G). L'ensemble de ces données semble indiquer que le RG-II joue un rôle primordial dans la croissance du tube pollinique. Néanmoins, il est à noter, dans ces études, l'absence d'analyse biochimique montrant que la structure du RG-II était affectée.

6.4.1.2.4. Les protéines pariétales structurelles

Si les travaux menés au Glyco-MEV au cours de ces dernières années se sont focalisés sur les polysaccharides pariétaux, la paroi primaire est aussi composée de protéines structurales qui peuvent être, ou non, glycosylées. Parmi ces protéines, les ArabinoGalactane Protéines (AGP) et les extensines ont été les plus étudiées. Ces glycoprotéines appartiennent à la famille des HRGP (Hydroxyproline-Rich GlycoProteins), et se caracterisent par une ossature polypeptidique riche en hydroxyprolines (Hyp) sur laquelle de larges fragments glycaniques sont insérés par *O*-glycosylation (Showalter, 1993).

Les AGPs sont ubiquistes et constituées d'un squelette protéique représentant 1 à 10% de la masse totale. Cette partie protéique est riche en Hyp/Pro, Ser, Thr et Ala. Le séquençage du génome d'*Arabidopsis thaliana* (AGI, 2000), et l'analyse des données bioinformatiques ont permis la prédiction de 47 gènes codants des AGPs. Les AGPs sont classées en quatre catégories : les AGPs classiques, les AGPs riches en lysines (Lys-rich AGP), les AGs peptides et les fasciclin-like AGPs (Schultz et al., 2002). Une ancre glycosylphosphatidylinositol (GPI) membranaire est prédite sur la plupart des séquences de gènes codant les AGPs (Ellis et al., 2010). Cette ancre a été caractérisée chez le poirier (Oxley et Bacic, 1999) et la rose (Svetek et al., 1999) et pourrait être clivée sous l'action des phospholipases C ou D et ainsi libérer le protéoglycane dans la matrice extracellulaire. La partie polysaccharidique représente 90 à 99% du protéoglycane et est majoritairement composée d'arabinogalactanes de type II (AG II), c'est à dire, une chaine principale de β-(1→3)-galactane décorée de courtes ramifications de galactanes liées en β-(1→6) terminées par des résidus arabinosyles liés en α-(1→3). Toutefois, les motifs retrouvés peuvent être

différents selon les espèces, les tissus et le stade de développement (Seifert et Roberts, 2007, Tryfona et al., 2010).

Les extensines ont également un corps protéique riche en hydroxyproline puisqu' environ 40% de la masse molaire provient de cet acide aminé. Ces protéines sont caractérisées par un motif Ser-Hyp4 avec une chaine oligosaccharidique de trois ou quatre arabinosyles sur chacun des Hyp. Ces extensines auraient la faculté de se dimériser de façon non covalente à la condition que le motif Val-Tyr-Lys ne soit pas retrouvé dans la séquence protéique (Kieliszewski et Lamport, 1994; Lamport et al., 2011). Enfin, les PRP (Proline Rich Protein), représentent une classe de HRGP faiblement glycosylées caractérisée par la présence du motif pentamérique répétitif $(Pro\text{-}Hyp\text{-}Val\text{-}Tyr\text{-}Lys)_n$ ou ses variantes (Cassab, 1998). Peu de données sur leurs glycosylations et leurs rôles sont disponibles dans la littérature.

Des études immunocytochimiques ont dévoilé la présence des AGPs dans les tubes polliniques de nombreuses espèces (Jauh et Lord, 1996 ; Mollet et al., 2002 ; Pereira et al., 2006 ; Qin et al., 2007 ; Chen et al., 2008 ; Dardelle et al., 2010 ; Coimbra et Pereira, 2012 ; Nguema-Ona et al., 2012). Des marquages de surface sur des tubes polliniques de lys ont montré la présence d'AGPs à l'apex mais aussi tout le long du tube pollinique après un traitement enzymatique avec une pectinase (Jauh et Lord, 1996). Les AGPs ont la particularité de se lier de façon réversible à un antigène synthétique : le β-D-glycosyl de Yariv (Yariv et al., 1962 ; 1967). Les tubes polliniques de lys traités au Yariv phénylglucoside ont une croissance inhibée sans que la sécrétion des nouveaux composés pariétaux soit stoppée (Roy et al., 1998). Ce phénomène est réversible et si l'on enlève le Yariv du milieu de culture un nouveau tube émerge alors en arrière de la zone apicale (Mollet et al., 2002). Le nouveau site d'émergence peut alors être prédit par la sécrétion localisée de nouveaux AGPs ce qui suggère que les AGPs ont un rôle dans la croissance polarisée (Cheung et Wu, 1999 ; Mollet et al., 2002). Chez *Arabidopsis thaliana*, l'anticorps LM2 utilisé a également localisé les épitopes spécifiques des AGPs dans l'apex ainsi que dans la zone d'émergence du tube pollinique (Pereira et al., 2006 ; Dardelle et al., 2010) (Fig. 7A, B).

Des travaux ont aussi mis en évidence le rôle de certaines AGPs dans la maturation du pollen. En effet, lorsque les gènes *AGP6* et *AGP11*, spécifiquement exprimés dans le pollen d'*Arabidopsis thaliana* (Pereira et al., 2006) sont mutés, le double mutant *agp6*/*agp11* présente de nombreux grains de pollen avortés (Coimbra et al., 2009). Le taux de germination des grains de pollen est réduit de 80 %, les grains de pollen avortent ou dans certains cas germent précocement dans les anthères (Coimbra et al., 2009, Coimbra et al., 2010).

L'ancre GPI qui permet l'attachement des AGPs à la membrane plasmique peut être clivée par les phospholipases C ou D (Svetek et al., 1999 ; Takos et al., 2000 ; Gaspar et al., 2001 ; Testerink et Munnik, 2011). Les AGPs sont alors libérées dans l'apoplasme. Parmi les protéines prédites avec une ancre GPI, 11 seraient spécifiquement exprimées dans le pollen et possiblement associées à la membrane plasmique (Lalanne et al., 2004). Les gènes *SETH1* et *SETH2* (Lalanne et al., 2004) ainsi que *PNT1* (Gillmor et al., 2005) sont impliqués dans les premières étapes de la biosynthèse des ancres GPI. La mutation de ces gènes affecte la germination du pollen et la croissance des tubes polliniques (Lalanne et al., 2004 ; Gillmor et al., 2005) ce qui confirme l'importance de ces glycoprotéines dans le développement des tubes polliniques. D'autre part, Les AGPs solubilisées après le clivage de l'ancre GPI pourraient servir d'intermédiaires à la transduction de signaux cellulaires. En effet, et malgré

la rareté des preuves expérimentales, la combinaison des caractéristiques principales des AGPs : i) localisation à la surface cellulaire, ii) présence probable dans les radeaux lipidiques, iii) libération contrôlée de la membrane plasmique par des stimuli et iv) complexité structurale des chaînes osidiques, fait des AGPs, ou des fragments d'AGPs, des candidats susceptibles d'exercer des fonctions de signalisation chez les plantes et dans les processus de reproduction des plantes (Coimbra et Pereira, 2012).

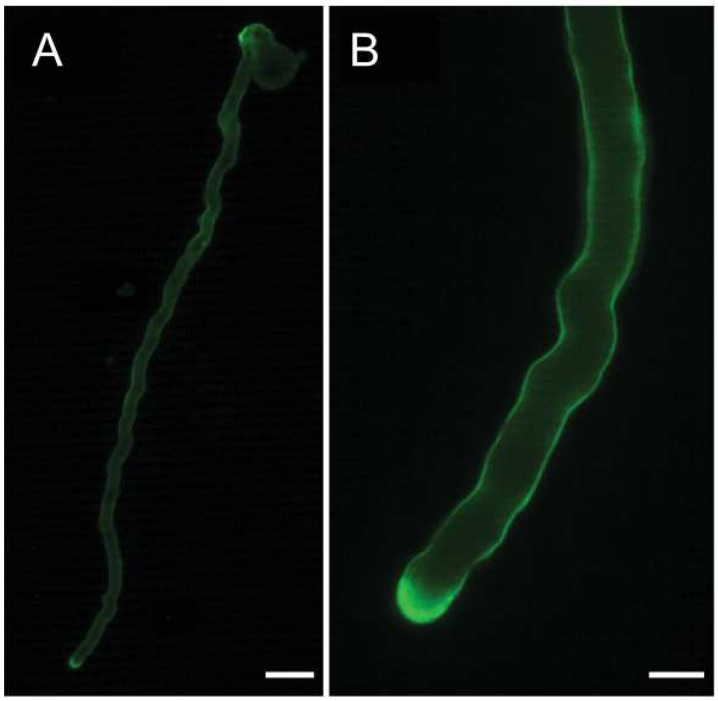

Figure 7. Immunolocalisation des épitopes associés aux AGPs dans les tubes polliniques d'*Arabidopsis thaliana* (A, B) à l'aide de l'anticorps LM2. Les barres d'échelle représentent 20 et 5 µm respectivement pour les figures A et B.

Leur abondance dans les tissus femelles principalement dans les exsudats du stigmate et dans le tissu de transmission du style chez de nombreuses espèces (Cheung et al., 1995 ; Wu et al., 1995 ; Jauh et Lord, 1996 ; Coimbra et Salema, 1997 ; Coimbra et Duarte, 2003 ; Coimbra et al., 2008) renforce l'idée d'une implication dans le guidage des tubes polliniques (Cheung et al., 1995 ; Wu et al., 1995 ; Coimbra et al., 2007 ; Coimbra et al., 2008 ; Pereira et al., 2014) et lors de l'incompatibilité gamétophytique (Nguema-Ona et al., 2012 ; Costa et al., 2013).

Les extensines sont aussi présentes dans la paroi des tubes polliniques (Rubinstein et al., 1995 ; Sommer-Knudsen et al., 1997). Le gène *PEX1* (*POLLEN EXTENSIN-LIKE 1*) est spécifiquement exprimé dans le pollen de maïs et code une protéine riche en motifs (Ser-Hyp_4) (Rubinstein et al., 1995). Cette protéine est retrouvée dans la paroi interne du tube pollinique avec la callose. Les épitopes spécifiques des extensines reconnus par l'anticorps JIM20 (Smallwood et al., 1994) ont été abondamment retrouvés *in-vivo* dans les tubes polliniques et dans le tissu de transmission de *Nicotiana tabacum* (Zhang et al., 2014). Par ailleurs, l'ajout d'un inhibiteur de la synthèse de l'hydroxyproline (3,4-déhydro-L proline) entraîne une diminution du contenu en hydroxyproline couplée à une diminution de la vitesse de croissance du tube pollinique et raccourci la longueur du style (Zhang et al., 2014).

L'ensemble de ces travaux de recherche a donné lieu à :

5 publications :
ACL-12 Dardelle et al., 2010 ***Plant Physiology*** 153, 1563-76.
ACL-13 Lehner et al., 2010 ***Plant Signaling and Behavior*** 10, 1-4.
ACL-17 Dumont et al., 2014 ***Annals of Botany*** 114, 1177-88.
ACL-18 Dardelle et al., 2015 ***Annals of Botany*** 115, 55-66.
ACL-20 Lehner et al., 2015 ***Plant Signaling and Behavior*** 10, e1026023.

5 communications orales : INV-04, INV-08, ACTN-01, ACTN-02, ACTN-04

10 communications par affiche: AFF-09, AFF-10, AFF-11, AFF-13, AFF-16, AFF-18, AFF-20, AFF-21, AFF-23, AFF-27

6.4.2. Le remodelage des pectines de la paroi du tube pollinique au cours de la germination et de la croissance polarisée.

Dans le cadre de la thèse de Christelle Leroux, nous nous sommes intéressés au remodelage des pectines au cours de la germination et de la croissance polarisé des tubes polliniques. Les résultats principaux de ce travail de doctorat sont présentés ci-dessous après la présentation des principaux systèmes de remodelage de la paroi.

6.4.2.1. Le remodelage de la paroi

La croissance cellulaire nécessite une biosynthèse et une sécrétion massive de composés pariétaux afin d'assurer l'élongation nécessaire à la paroi végétale. La croissance, anisotropique (zone d'élongation de la racine, hypocotyle) ou polarisée (poil absorbant, tube pollinique) requiert aussi une action essentielle des enzymes de remodelage des composés pariétaux afin d'assurer la souplesse nécessaire à l'expansion des cellules tout en contrôlant la rigidité pariétale afin de contenir la pression de turgescence. En outre, ces enzymes permettent de contrôler la forme propre à chaque type cellulaire (rectangulaire dans le cas de l'hypocotyle ou de la zone d'élongation de la racine ou cylindrique dans le cas du poil absorbant ou du tube pollinique). Du fait de sa croissance très rapide et polarisée à l'apex, le tube pollinique a rapidement été adopté comme modèle d'étude des systèmes de remodelage de la paroi en lien avec la croissance. De nombreux systèmes enzymatiques interviennent pour modifier les propriétés de la paroi végétale (Fig. 8). Ainsi, on peut noter les protéines impliquées dans le remodelage du réseau cellulose/XyG comme les expansines (EXPs) et les XyG endo-transglucosylase hydrolases (XTHs), celles impliquées dans la dégradation des polysaccharides appartenant à la famille des glycosides hydrolases (GHs) comme les glucanases, glucosidases, galactosidases, xylosidases, arabinosidases… et finalement, celles impliquées dans le remodelage des HGs comme les pectate lyases (PLs), polygalacturonases (PGases) et pectines méthylestérases (PMEs). Ces protéines de remodelage peuvent être produites par le pollen lui-même mais dans un contexte *in-vivo* peuvent aussi émaner des tissus femelles facilitant ainsi la progression des tubes polliniques (Fig. 8).

6.4.2.2. Le remodelage des β-glucanes et des pectines de la paroi

Les pectines, et en particulier les HG sont impliquées dans la modification de la plasticité pariétale, essentielle à la régulation de l'élongation des cellules. Les travaux menés au laboratoire visent à comprendre l'implication des enzymes de remodelage des pectines dans les processus d'élongation cellulaire. Les différents systèmes enzymatiques impliqués dans ce remodelage sont présentés ci-dessous.

6.4.2.2.1. Les pectines lyases

Les gènes codant des PLs (pectine lyases) et les PLLs (pectine lyases-like) sont fortement exprimés dans le pollen de tomate, de tabac, de luzerne et d'*Arabidopsis thaliana* (Wing et al., 1989 ; Kulikauskas et McCormick, 1997). Plusieurs allergènes de pollen possèdent des activités PLLs (Marin-Rodriguez et al., 2002).

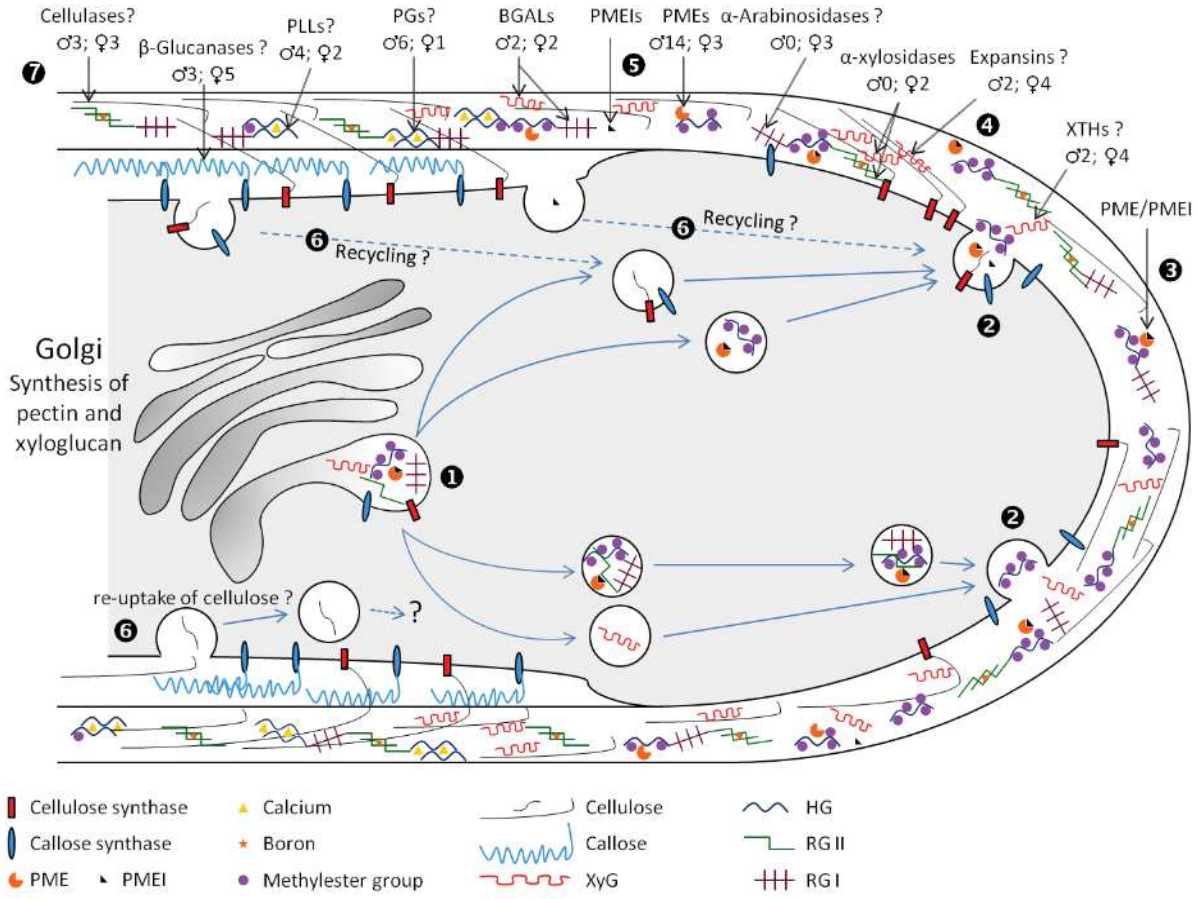

Figure 8. Modèle représentant la mise en place des principaux polysaccharides pariétaux ainsi que les enzymes capables de les remodeler ou de les dégrader. (❶) Les callose et cellulose synthases ainsi que les XyG et les pectines (RG-II, RG-1, HG) sont transportés dans des vésicules Golgiennes. Les HG sont synthétisés sous une forme fortement méthylestérifiée et pourraient être transportés en présence de complexes PME/PMEI. (❷) Les vésicules sont acheminées à la membrane plasmique, où elles fusionnent avant de relarguer leurs contenus (polysaccharide et/ou enzymes de remodelage) dans la matrice extracellulaire. Les XyG sont exocytés sous leur forme mature, fucosylée. Les callose et cellulose synthases restent dans la membrane plasmique alors que les complexes PME/PMEI et les autres enzymes de remodelage sont relargués dans l'apoplasme (❸). (❹), Le XyG et les microfibrilles de cellulose interviennent probablement dans le relâchement pariétal, facilité par les XTH et

les expansines. (❺) Les PME sont activées après leur séparation des PMEIs. Les PMEs deméthylestérifient les HG, favorisant la fixation des ions calcium et la formation de complexes entre chaines parallèles d'HG. La rigidité du tube est ainsi renforcée. Les PMEs pourraient rester dans l'apoplasme tandis que les PMEI seraient dégradés par des protéases ou recyclés par endocytose (❻). De la même manière, l'excès de cellulose et de callose synthases pourrait être recyclé par endocytose. Les microfibrilles de cellulose pourraient aussi être endocytées après action des cellulases. (❼) Des processus similaires pourraient exister avec la dégradation de la callose par des β-glucanases. Les principaux types d'enzymes (cellulases, β-glucanases, PLLs, PGs, PMEs, BGALs, α-xylosidases and α-arabinosidases, expansins et XTHs) qui pourraient être impliqués dans le remodelage ou la dégradation de la paroi du tube pollinique sont indiqués. Le chiffre associé aux enzymes correpond au nombre de gènes fortement exprimés dans le pistil (♀) ou dans le tube pollinique (♂) d'*Arabidospis thaliana*. BGALs, β-galactosidases; PGs, polygalacturonases; PLLs, pectate lyase-like; PMEs, pectine méthylestérases; PMEIs, Inhibiteurs de pectine méthylestérases; RG-I, rhamnogalacturonane-I; RG-II, rhamnogalacturonane-II; XTHs, xyloglucane *endo*-transglucosylase hydrolases; XyG, xyloglucane (Mollet *et al.,* 2013).

Chez *Arabidopsis thaliana*, parmi les 26 gènes codant pour des PLLs, 14 sont exprimés dans le pollen (Palusa et al., 2007). Aucun de ces 14 gènes n'est cependant spécifiquement dédié au gamétophyte mâle, mais 4 d'entre eux sont fortement exprimés dans les grains de pollen (Fig. 8) (Mollet et al., 2013). De nombreuses activités promotrices des gènes de PLLs sont similaires à celles présentées par des PGases (Sun et Van Nocker, 2010). Ceci pourrait impliquer une association fonctionnelle étroite entre les PLLs et les PGases, en particulier dans la digestion de la paroi cellulaire des grains de pollen, avant la germination, et pendant la croissance du tube pollinique (Fig. 8) (Dai et al., 2007 ; Sun et Van Nocker, 2010 ; Jiang et al., 2014).

6.4.2.2.2. Les glycosides hydrolases

Les glycosides hydrolases (GHs) sont des enzymes qui catalysent l'hydrolyse des liaisons glycosidiques entre deux ou plusieurs glycosides ou entre un hydrate de carbone et une fraction non glucidique. Celles impliquées dans le remodelage de la paroi cellulaire du tube pollinique appartiennent au GH3, 9, 10, 17, 28, 35, 43 et 51 (Mollet et al., 2013).

Les *endo*-(1-4)-β-glucanases et les *endo*-(1-3)-β-glucosidases sont membres de la famille GH17 et GH9, respectivement (Mollet et al., 2013). Chez *Arabidopsis thaliana*, 25 gènes codent pour des GH9 et 49 pour des GH17. Parmi les 25 CELLULASES putatives, deux sont fortement exprimées dans les grains de pollen et trois dans les tubes polliniques cultivés in-vitro (Mollet et al., 2013). Il a été montré que la cellulose, malgré sa faible abondance dans la paroi cellulaire du tube pollinique, jouerait un rôle essentiel en agissant sur le diamètre des tubes polliniques cultivés *in-vitro* (Aouar et al., 2010). Comme décrit précédemment, la paroi cellulaire des tubes polliniques est enrichie en callose (Fig. 1 et 8) et plusieurs études ont montré que des traitements modérés avec des β-(1-3)-glucanases sont capables de stimuler la germination des grains de pollen (Roggen et Stanley, 1969 ; Parre et Geitmann, 2005a, 2005b). En outre, il a été signalé que des *exo*-β-glucanases pourraient jouer un rôle important dans la régulation de l'allongement du tube pollinique chez le lys (Takeda et al., 2004). A l'inverse, des traitements avec des inhibiteurs de glucosidases inhibent sévèrement la croissance des tubes polliniques (Kotake et al., 2000). Il a été émis l'hypothèse que les propriétés mécaniques de la callose et plus précisément la résistance à la déformation latérale du tube seraient régulées par les glucanases (Parre et Geitmann, 2005a).

Les polygalacturonases (PGases) sont impliquées dans la dégradation des HGs. Six gènes codant pour des PGases sont fortement exprimés dans les tubes polliniques et un est exprimé dans le pistil (Fig. 8) suggérant un remodelage important des pectines, notamment des HGs au cours de la croissance du tube pollinique. Les PGases sont impliquées, au cours de la maturation du pollen de *Brassica campestris*, dans la formation de l'intine et/ou de l'exine (Huang et al., 2009a, 2009b) et chez *Turnera subulata*, les PGases ont été impliquées dans l'auto-incompatibilité (Tamari et Shore, 2006). Des PGases sont libérées lors de la réhydratation de grains de pollen chez *Triticum* (Zaidi et al., 2012) et sont également détectées à l'extrémité des tubes polliniques chez *Brassica napus* lors de la pénétration du tube pollinique dans les papilles du stigmate (Dearnaley et Daggard, 2001) suggérant que certaines PGases sont plutôt impliquées dans le relâchement de la paroi cellulaire des tissus femelles.

Deux gènes codant pour des β-galactosidases (βGALs) qui peuvent agir sur différents substrats dont les AGPs, des galactolipides, le RG-I, le RG-II et le XyG (Dey et Del Campillo, 1984) sont fortement exprimés dans les grains de pollen matures et 2 autres sont fortement exprimées dans le pistil (Fig. 8). D'autre part, 1 gène codant pour une β-xylosidase (Hruba et al., 2005) ainsi que deux gènes codant des α-xylosidases sont exprimés dans le pistil (Mollet et al., 2013).

6.4.2.2.3 Les pectines méthylestérases

Les PMEs représentent une large famille multigénique de pectinases (Micheli et al., 1998 ; Sénéchal et al., 2014) et appartiennent à la famille CAZy des carbohydrates estérases de la famille 8 (CE8 ; E.C.3.1.1.11 ; http://www.cazy.org) qui comporte 66 gènes chez *Arabidopsis thaliana* (AGI, 2000). Ces enzymes sont fortement impliquées dans le remodelage de la paroi au cours de la croissance cellulaire.

Plus précisement, dans le cas de la croissance polarisée du tube pollinique, les HGs sont synthétisés dans l'appareil de Golgi et déposés à l'extrémité de tube en expansion sous une forme hautement méthyl-estérifiée (Zhang et Staehelin, 1992) (Fig. 8). Les HGs méthyl-estérifiés dans la zone apicale pourraient fournir une plasticité suffisante pour soutenir la croissance du tube pollinique (Cheung et Wu, 2008). La dé-méthylestérification des HGs méthyl-estérifiés par les PMEs à l'extrémité du tube est accompagnée d'une libération de protons assurant une modification locale du pH dans la paroi cellulaire du tube pollinique (Micheli, 2001 ; Bosch et Hepler, 2005). En effet, dans les tubes en croissance, des oscillations d'influx (acidification apicale) et d'efflux (bande alcaline) de protons (H+) (Feijó et al., 1999) ont été observées. Ceci suggère qu'une variation du pH régulerait l'activité des PMEs (Feijó et al., 1999). Ainsi, la croissance des tubes polliniques pourrait être associée à une régulation des PMEs permettant de maintenir une zone apicale lâche et à l'inverse de rigidifier l'arrière du tube (Bosch et Hepler, 2005). L'influx oscillatoire des H+ et du Ca^{2+}, qui maintiennent respectivement un pH acide et un gradient de Ca^{2+} à l'apex du tube pollinique, influencerait l'activité des PMEs. De même, l'efflux de H+ qui maintient la présence d'une bande alcaline en amont de l'apex durant la croissance du tube pollinique pourrait réguler différemment l'activité des PMEs et activer des PGases. Ces influx

oscillatoires pourraient agir directement sur la formation des complexes PMEI-PME pH-dépendant. Finalement, l'activation des PGases pourrait contrôler le relâchement de la paroi cellulaire du tube pollinique en arrière de la pointe et promouvoir l'impulsion de la croissance propre du tube (Mollet et al., 2013) en contrôlant les propriétés mécaniques de la paroi cellulaire.

Parmi les 66 gènes codant des PMEs putatives dans le génome d'*Arabidopsis thaliana*, 14 seraient spécifiques du pollen (Pina et al., 2005 ; Qin et al., 2009 ; Wolf et al., 2009 ; Mollet et al., 2013). On retrouve les 14 isoformes dans le zymogramme présenté dans la figure 9. De plus, le génome d'*Arabidopsis thaliana* contient 76 gènes codant des PMEIs/inhibiteurs d'invertases putatifs. Des données de transcriptomique ont révélé que ces PMEIs/inhibiteurs d'invertases sont très exprimés dans le pollen d'*Arabidopsis thaliana* comparé aux autres tissus (Wolf et al., 2003 ; Raiola et al., 2004). Des approches protéomiques ont aussi permis l'identification de plusieurs PMEs : 2 PMEs putatives dans le pollen germé de maïs (Zhu et al., 2011), une dans le pollen de riz (Dai et al., 2006) et une dans les tubes polliniques d'*Arabidopsis thaliana* (Ge et al., 2011). Chez les tubes polliniques du tabac, des analyses biochimiques ont montré la présence de 7 isoformes ayant le même pI (point isoélectrique) (Li et al., 2002). Deux de ces isoformes sont co-localisées avec les HGs méthyl-estérifiés dans la paroi et dans les vésicules de sécrétion provenant du Golgi, suggérant que ces PMEs sont transportées jusqu'à l'apex du tube pollinique sous leur forme inactive (Li et al., 2002).

La première caractérisation fonctionnelle de gènes PMEs et leurs rôles cruciaux dans la croissance des tubes polliniques a été obtenue à partir de deux lignées mutantes : *vanguard1* et *ppme1* (Jiang et al., 2005; Tian et al., 2006). Le mutant *vanguard1* (*vdg1*), dont le gène *At2g47040* codant une PME pollen spécifique est inactivé, présente des tubes polliniques instables *in-vitro* et dont la croissance est fortement ralentie *in-vivo* (Jiang et al., 2005). L'étude d'un autre mutant, *ppme1*, dont *PPME1*, code une autre PME pollen spécifique, présente des anomalies au niveau de la forme des grains de pollen, ainsi qu'au niveau du taux de la germination, indiquant que *PPME1* est nécessaire pour l'intégrité de la paroi et pour la croissance polarisée (Tian et al., 2006).

Plusieurs études ont aussi montré l'importance des PMEIs dans la croissance des tubes polliniques. En effet, un apport exogène du PMEI de maïs purifié (ZmPMEI1) sur des tubes polliniques de cette même espèce, altère sa croissance en déstabilisant la paroi dans la zone subapicale du tube pollinique (Woriedh et al., 2013). Les travaux menés au laboratoire ont aussi mis en évidence l'interaction entre le PMEI de kiwi et la PME3 d'*Arabidopsis thaliana*, ainsi que l'effet du PMEI de kiwi sur la déstabilisation de la paroi des tubes polliniques (Paynel et al., 2014). Récemment, une étude de transcriptomique sur le pollen du lys a mis en évidence des gènes surexprimés dans le gamétophyte mâle par rapport aux organes végétatif, et parmi ceux-ci, on retrouve une PME ainsi qu'une PMEI (Lang et al., 2015).

Au cours de la préparation du doctorat de Christelle Leroux, nous avons mis en évidence le rôle d'une PME pollen spécifique lors de la germination du grain de pollen. La caractérisation d'une lignée mutante pour le gène *PME48* (*pme48-/-*) montre clairement le rôle de PME48 lors de la germination du grain puisque les mutants présentent une

germination très retardée *in vitro* (Fig. 9A) et *in vivo* (Leroux et al., 2015). Cette germination est accompagnée d'un phénotype particulier avec un début de germination, suivi d'un arrêt total de croissance, puis une seconde germination, en général à l'opposé de la première (Fig. 9A). Ce second tube est capable de pousser, ce qui explique que le nombre de graine des mutants ne soit pas différent des plantes sauvages. Ce phénotype est observé pour 18% des grains de pollen mutants alors qu'il n'est observé que dans 3% des grains sauvages (Leroux et al., 2015). En outre, les tubes polliniques mutants sont plus fragiles puisque le pourcentage de tube éclaté est largement supérieur dans le mutant comparé au sauvage (Leroux et al., 2015). Nous avons relié le phénotype observé à un défaut d'imbibition de grain et à une diminution de l'activité PME dans les grains de pollen du mutant (Fig. 9B-D). En effet, les grains mutants s'imbibent moins vite que ceux du sauvage (Fig. 9B), et l'activité PME mesurée dans le pollen mutant est plus faible que celle mesurée dans le pollen sauvage (Fig. 9D). La diminution de cette activité correspond à la diminution de l'activité d'une PME dont le pI correspond à celle de la PME48 (Fig. 9C). En outre, l'intine des grains mutants contient des HG plus fortement méthylestérifiés que celle du sauvage révélant que l'absence de PME48 a un impact direct sur le degré de méthylestérification des HGs (Leroux et al., 2015). Finalement, nous avons pu réverser le phénotype des plantes mutantes en ajoutant du calcium au milieu de germination (Leroux et al., 2015).

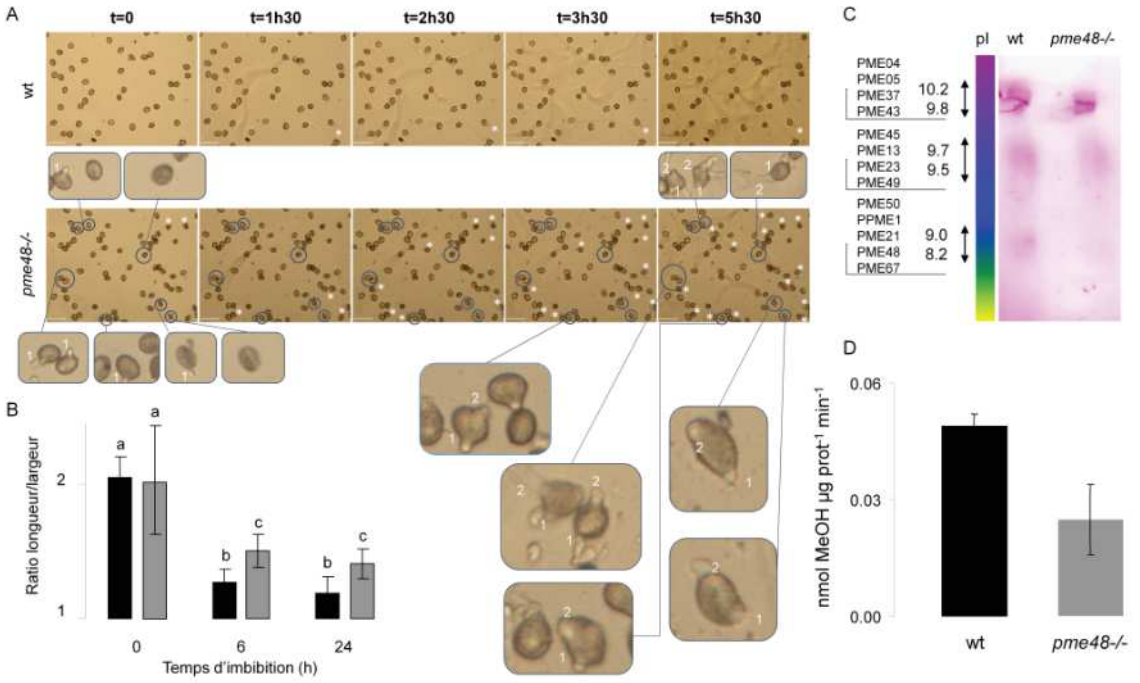

Figure 9. Caractérisation du mutant *pme48-/-*. A, phénotype observé lors de la germination *in vitro* du pollen *pme48-/-* et du sauvage. On distingue nettement un retard de germination ainsi que le phénotype de double germination présent chez le mutant. B, Estimation de la vitesse d'imbibition des grains mutants par rapport aux sauvages en estimant le ratio longueur/largeur des grains. C, Zymogramme présentant la répartition des activités des différentes isoformes de PME présentent dans le pollen sauvage et *pme48-/-*. La bande d'activité plus faible au pI situé entre 8.2 et 9 correspond au pI attendu de la PME48. D, Dosage de l'activité PME totale dans les grains de pollen sauvage et *pme48-/-*, exprimée en nmol de methanol libérées par µg de protéine et par minute.

L'ensemble de ces résultats a permis de mettre en évidence le rôle d'une PME dans la germination du pollen d'*Arabidopsis thaliana*. Un modèle schématisant la fonction supposée de cette PME48 est présenté dans la Figure 10. Il est fort probable que certaines PMEs, dont la PME48, agissent au cours de la déshydratation et démethylestérifient les HGs de l'intine permettant ainsi la formation des complexes entre les HGs et les ions Ca^{2+} (Fig. 10❶). Au cours de l'imbibition (Fig. 10❷), le calcium est libéré et permet en partie, de créer le gradient de calcium nécessaire à la germination du grain de pollen (Fig. 10❸). Les HGs libérés du Ca^{2+} peuvent alors être dégradés par l'action de PGases et de PLL (Fig. 10❹a) mais il est aussi possible que la fragilisation des HGs libérés de Ca^{2+} permette au tube en croissance de traverser l'intine à la faveur de la pression de turgescence (Fig. 10❹b). L'ensemble de ces processus cellulaires permet la germination du pollen (Fig. 10❺).

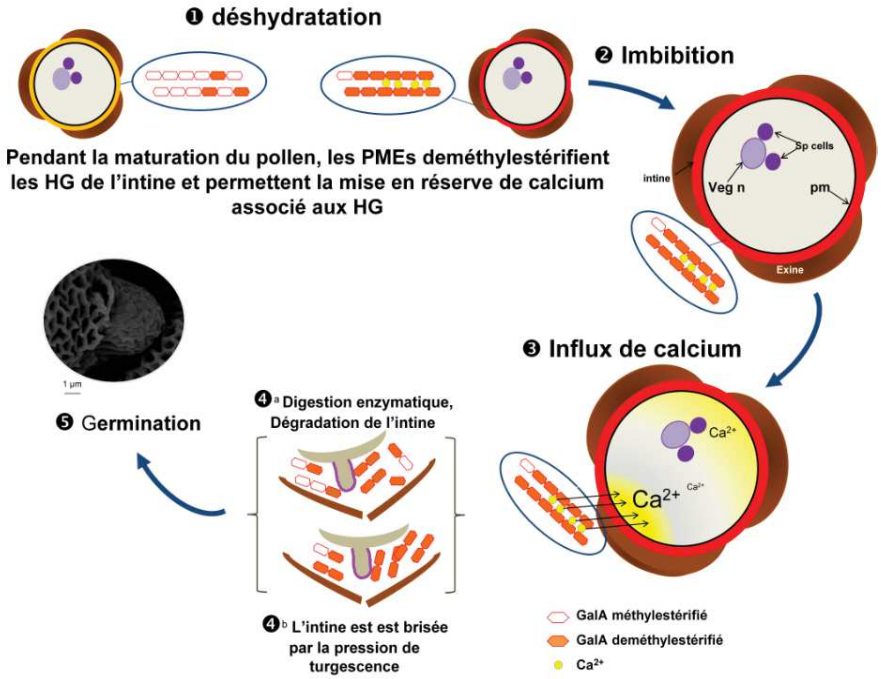

Figure 10. Modèle théorique présentant le rôle des PMEs au cours de la maturation des grains de pollen et l'impact sur la mobilisation des ions calcium au cours de l'imbibition et de la germination (Leroux et al., 2015).

6.4.2.2.4. Les inhibiteurs de pectine méthylestérases

Les PMEs peuvent être inhibées par des inhibiteurs, nommés PMEIs. L'axe de recherche que je dirige « étude de la régulation de la croissance cellulaire par les PMEs » s'intéresse aussi au rôle que peuvent jouer les PMEIs dans les mécanismes d'élongation cellulaire. Pour cela, le Dr. A. Mareck et moi-même, en étroite collaboration avec les Dr. V. Lefebvre et Pr. J. Pelloux de l'Université Picardie Jule Vernes, nous nous intéressons à la régulation de l'activité PME par les PMEIs et à son incidence dans la croissance des cellules.

Plusieurs études ont montré l'importance des PMEIs dans la croissance des tubes polliniques. Ainsi, comme précédement évoqué, un apport exogène du PMEI de maïs purifié (ZmPMEI1) sur des tubes polliniques de cette même espèce, altère sa croissance en déstabilisant la paroi dans la zone sub-apicale du tube pollinique (Woriedh et al., 2013). Récemment, une étude de transcriptomique sur le pollen du lys a mis en évidence des gènes surexprimés dans le gamétophyte mâle par rapport aux organes végétatifs, et parmi ceux-ci, on retrouve une PME ainsi qu'un PMEI (Lang et al., 2015).

Nos travaux menés dans le cadre de cette étude sont assez récents, mais très prometteurs puisqu'ils ont déjà permis de mettre en évidence que le PMEI de kiwi est capable de se fixer et de former un complexe (1/1) à la PME3 d'*Arabidopsis thaliana* (Paynel et al., 2014). D'autre part, le PMEI de kiwi entraîne une fragilisation de la paroi du tube pollinique d'*Arabidopsis thaliana* (Paynel et al., 2014) qui aboutit à la rupture et à l'éclatement du tube. Très récemment, nous avons montré, *in vivo*, en collaboration avec le Pr. J. Pelloux de l'Université de Picardie Jules Verne, et en utilisant le tube pollinique comme modèle cellulaire, que l'activité inhibitrice des PMEIs était bien pH dépendante (Hocq et al., 2017).

L'ensemble de ces travaux de recherche a donné lieu à :

4 publications :
ACL-15 Mollet et al., 2013 ***Plants*** 2, 107-147.
ACL-16 Paynel et al., 2014 ***Plant Growth Regulation*** 74, 285-297.
ACL-19 Leroux et al., 2015 ***Plant Physiology*** 167, 367-380.
ACL-27 Hocq et al., 2017 ***Plant Physiology*** 173, 1075-1093.

4 communications orales: INV-06, INV-07, ACTN-07, ACTI-11
7 communications par affiche: AFF-12, AFF-14, AFF-15, AFF-17, AFF-19, AFF-22, AFF-26

6.4.3. Génétique chimique : criblage de chimiothèque et utilisation de petites molécules capables de perturber l'adhésion et la croissance polarisée des tubes polliniques.

Les travaux présentés ci-dessous résultent pour part des travaux des thèses de Flavien Dardelle et de Ferdousse Laggoun. Ces travaux consistent à caractériser des mécanismes moléculaires impliqués dans l'adhésion des tubes polliniques et dans la croissance polarisée des cellules végétales. Le développement de cet axe de recherche dans les projets futurs du laboratoire Glyco-MEV a été initié au cours de ces dernières années en se focalisant sur le développement des outils moléculaires nécessaires à leur réalisation. Pratiquement, nous avons mis au point une matrice d'adhésion sur laquelle les tubes polliniques peuvent adhérer et croitre. En outre, afin d'étudier les mécanismes d'adhésion et de croissance polarisée, nous avons criblé une chimiothèque et isolé plusieurs molécules capables de perturber l'adhesion et/ou la croissance polarisée. Ces travaux sont présentés ci-dessous.

6.4.3.1. Rôle des pectines dans l'adhésion cellulaire

L'adhésion et la séparation cellulaire sont des phénomènes très largement observés au cours du développement des plantes et jouent un rôle capital dans de nombreux mécanismes physiologiques, en particulier lors de la reproduction des plantes (Mollet et al., 2007). Dans la majorité de ces cas, la paroi cellulaire et plus particulièrement les pectines, ont été impliquées dans les mécanismes d'adhésion cellulaire (Mollet et al., 2000). La dégradation, la modification ou la réduction de la quantité de pectines dans la paroi de mutants dont les voies de biosynthèse sont perturbées, sont corrélées avec une séparation cellulaire ou une adhésion cellulaire anormale (Bouton et al., 2002). Cette étude consiste à étudier l'adhésion des tubes polliniques *in vitro* sur une matrice d'adhésion. Plus précisément, de caractériser, à l'aide d'une matrice extracellulaire pectique extraite à partir de feuilles, les motifs pectiques minimums permettant l'adhésion des tubes polliniques par des traitements enzymatiques. Des travaux antérieurs réalisés par Flavien Dardelle (Dardelle, 2011) ont montré que les pectines extraites de fleurs ou de feuilles d'*Arabidopsis thaliana* permettaient l'adhésion des tubes.

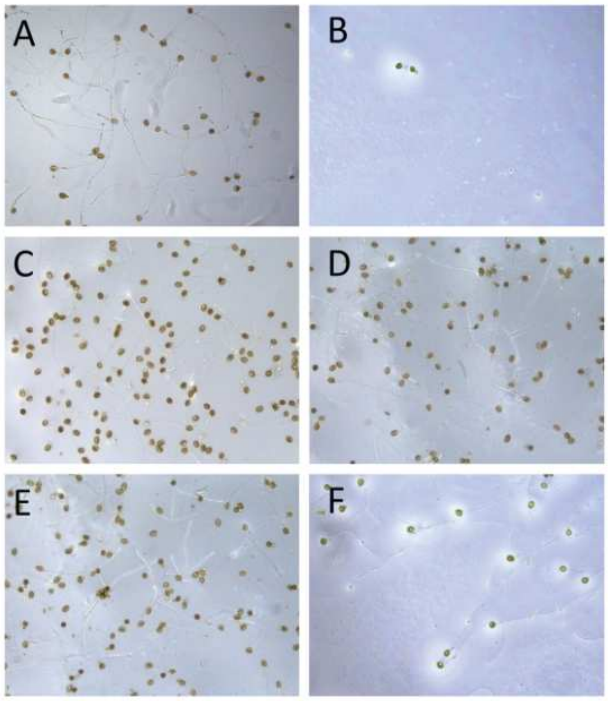

Figure 11. Test d'adhésion des tubes polliniques en présence de la matrice pectique de feuilles *d'Arabidopsis thaliana* non digérée (A) ou digérée à la PGase (B), ou issue de pectines commerciales de citron présentant des degrés de méthylestérification différents 85% (C), 62% (D), 8,6% (E), et 85% traitées à la PGase (F).

Afin d'étudier les mécanismes d'adhésion des tubes polliniques, un test d'adhésion *in vitro* a été mis au point sur le modèle développé chez le lys (Mollet et al., 2000). Ce test consiste à faire germer les grains de pollen en milieu liquide sur une matrice d'adhésion déposée dans le fond de plaques 96 puits. Après 6 h de culture, la plaque est observée avant et après rinçage. Le taux d'adhésion représente le nombre de tubes polliniques restant après le rinçage par rapport au nombre total de tubes présents avant rinçage, exprimé en pourcentage. Plusieurs matrices ont été testées. Des matrices constituées de pectines extraites de fleurs ou

de feuilles d'*Arabidopsis thaliana* ou des pectines commerciales de citron présentant différents degrés de méthylestérification ou des pectines digérées avec différentes enzymes commerciales ont été testées.

L'adhésion des tubes polliniques sur la matrice composée de pectines de feuilles est de l'ordre de 40% alors qu'elle est supérieure à 90% avec les pectines de citron (Fig. 11A, C, D, E). La digestion des pectines de feuilles et de citron par une *endo*-polygalacturonase empêche totalement l'adhésion avec les pectines de feuille (Fig. 11B) et la réduit avec les pectines de citron (Fig. 11F). Cela suggère que la structure des HGs est impliquée dans l'adhésion. L'analyse monosaccharidique des différents types de pectines indique que les pectines de citron sont constituées majoritairement d'HGs. En revanche, les pectines de feuille d'*Arabidopsis thaliana* sont composées d'un mélange d'HG et de RG-I ramifiés par des arabinanes, des galactanes et/ou des arabinogalactanes.

Il est intéressant de noter qu'un traitement des pectines de feuilles à l'*endo*-arabinanase induit une perte des épitopes associés aux chaines d'arabinane du RG-I mais n'induit pas de changement significatif du taux d'adhésion (42,9% à 51,2%). En revanche, lorsque les chaines de galactanes sont digérées par une *endo*-galactanase, l'adhésion est significativement perturbée. Enfin, lorsque la matrice utilisée est composée de pectines extraites du mucilage de graines d'*Arabidopsis thaliana*, composées à 97,7% de chaines principales de RG-I (Macquet et al., 2007), aucune adhésion n'est observée. Il semble donc que la chaîne principale du RG-I seule ainsi que les chaines latérales arabinanes du RG-I ne soient pas importantes pour l'adhésion des tubes polliniques. En revanche, les chaînes galactanes sembleraient jouer un rôle important. Des travaux complémentaires sont en cours afin de préciser les motifs pectiques impliqués dans l'adhésion des tubes.

6.4.3.2. Génétique chimique : perturbation de la croissance polarisée

Le tube pollinique représente certainement le meilleur modèle cellulaire pour étudier les mécanismes de signalisation, de biosynthèse, de mise en place et de remodellage de la paroi au cours de la morphogénèse cellulaire. Bien sûr, les poils absorbants possèdent aussi une croissance polarisée, mais elle est plus lente que celle des tubes polliniques et surtout leur longueur est régulée par des facteurs de transcription de type ROOTHAIR DEFECTIVE SIX-LIKE (RSL) (Honkanen and Dolan, 2016). En outre, la vitesse de croissance des tubes polliniques est plus rapide que celle des poils absorbants et peut atteindre 4 $\mu m\ s^{-1}$ (Michard et al., 2017). Mis à part ces différences, la croissance apicale polarisée des poils absorbants et des tubes polliniques est caractérisée par la biosynthèse, l'exocytose et le remodellage de composés pariétaux, par des gradients ioniques dans la zone apicale et par une dynamique importante du réseau d'actine qui supporte l'élongation cellulaire (Gu and Nielsen, 2013 ; Ketelaar, 2013 ; Mendrinna and Persson, 2015 ; Mangano et al., 2016). Cependant, l'utilisation des techniques de génomique fonctionnelle n'est pas toujours possible puisque certaines mutations entrainent l'infertilité des lignées sélectionnées, et donc l'absence ou la lethalité de graines homozygotes. Par conséquent, nous avons développé des outils moléculaires capables de perturber la croissance polarisée des tubes polliniques afin de pouvoir étudier les mécanismes impliqués dans la régulation de la croissance apicale. Pour

cela, un accord de transfert de matériel a été signé entre le Glyco-MEV et le CERMN (Centre d'Etudes et de Recherche sur le Médicament de Normandie) UPRES EA3915 et une chimiothèque comptant 11234 composés (représentant 250 familles de molécules) a été mise à notre disposition. Le criblage des chefs de famille de cette chimiothèque a permis de sélectionner 2 composés qui perturbent la croissance du tube pollinique, les molécules 42 et 146 dont les structures sont données dans la Figure 12.

Afin de préciser le rôle de ces molécules dans la desorganisation de la croissance apicale, les dynamiques des filaments d'actine et des vésicules d'exocytose ont été suivies par microscopie confocale. La visualisation des filaments d'actine a été suivie à l'aide d'une lignée d'*Arabidopsis thaliana* exprimant une construction *pLAT52::LifeAct-mEGFP* (Vidali et al., 2009). Ces plantes expriment, à l'aide d'un promoteur pollen spécifique (*LAT52*) une sonde spécifique de l'actine et couplée à la GFP. Cette construction n'affecte pas le développement du pollen et permet de visualiser spécifiquement les filaments d'actine et de suivre leur évolution au cours de la croissance des tubes (Vidali et al., 2009).

La dynamique de l'exocytose a été suivie par microscopie confocale à l'aide d'une lignée d'*Arabidopsis thaliana* contenant la construction *pCL::CRIB4-GFP* (Rong et al., 2016). Cette construction contient le domaine CRIB4 (Cdc42/Rac-inter-active binding 4) de la proteine RIC4 (Rop-interactive CRIB motif–containing proteins 4), exprimé sous le contrôle du promoteur pollen spécifique *LAT52*. Les domaines CRIB interragissent avec les protéines ROP (Rho-Related GTPase from Plants), membres de la famille des Rho GTPase, régulateurs essentiels de la croissance apicale et de la croissance polarisée de plusieurs types cellulaire (Kost et al., 1999; Li et al., 1999; Molendijk et al., 2001; Fu et al., 2002; Jones et al., 2002). En particulier, ROP1, a été impliquée dans la croissance apicale des tubes polliniques (Kost et al., 1999; Li et al., 1999). Les ROPs sont activées sur la membrane plasmique des tubes polliniques (Hwang et al., 2005) et sont les principaux régulateurs de sa croissance puisqu'elles sont impliquées dans l'établissement du gradient de calcium et la dynamique des filaments d'actine qui sont indispensables à l'exocytose des vésicules dans la zone apicale du tube (Lin et al., 1996; Lin and Yang, 1997; Li et al., 1999; Fu et al., 2001; Gu et al., 2005; Hwang et al., 2008; Chang et al., 2013). L'utilisation de cette lignée transgénique permet donc de suivre la localisation de l'exocytose dans les tubes polliniques.

Après 6 h de germination, les tubes polliniques témoins continuent à croître et présentent une forme cylindrique régulière et une zone apicale semi-circulaire caractéristique (Fig. 12B). L'actine n'est pas répartie uniformément, mais forme un collier, l'actine fringe, juste en arrière de l'apex du tube (Fig. 12A) et est absente de l'apex. Les phénotypes observés après 6 h de culture en présence des molécules 42 et 146 sont différents. La molécule 42 induit une déformation : un boursoufflement de la partie apicale (Fig. 12D) associé à la présence d'une grande vacuole. Les tubes cessent de croitre après 2 h et l'actine fringe n'est plus présente dans la zone apicale (Fig. 12C). On note l'apparition d'anneaux d'actine en arrière de la région subapicale (Fig. 12C). Ces anneaux, déjà observés dans le grain de pollen lors de la germination (Vogler et Sprunck., 2015, Vogler et al., 2015) pourraient servir de réserve d'actine, rapidement mobilisable au cours de la germination (Vogler et Sprunck., 2015). Dans notre cas, nous n'avons pas d'explication à la présence de ces structures. Les traitements effectués avec la molécule 146 modifient aussi la répartition de l'actine dans le

tube pollinique. On trouve en effet une accumulation d'actine au niveau de l'apex du tube (Fig. 12E, G) et une actine fringe moins marquée ou absente (Fig. 12E, G).

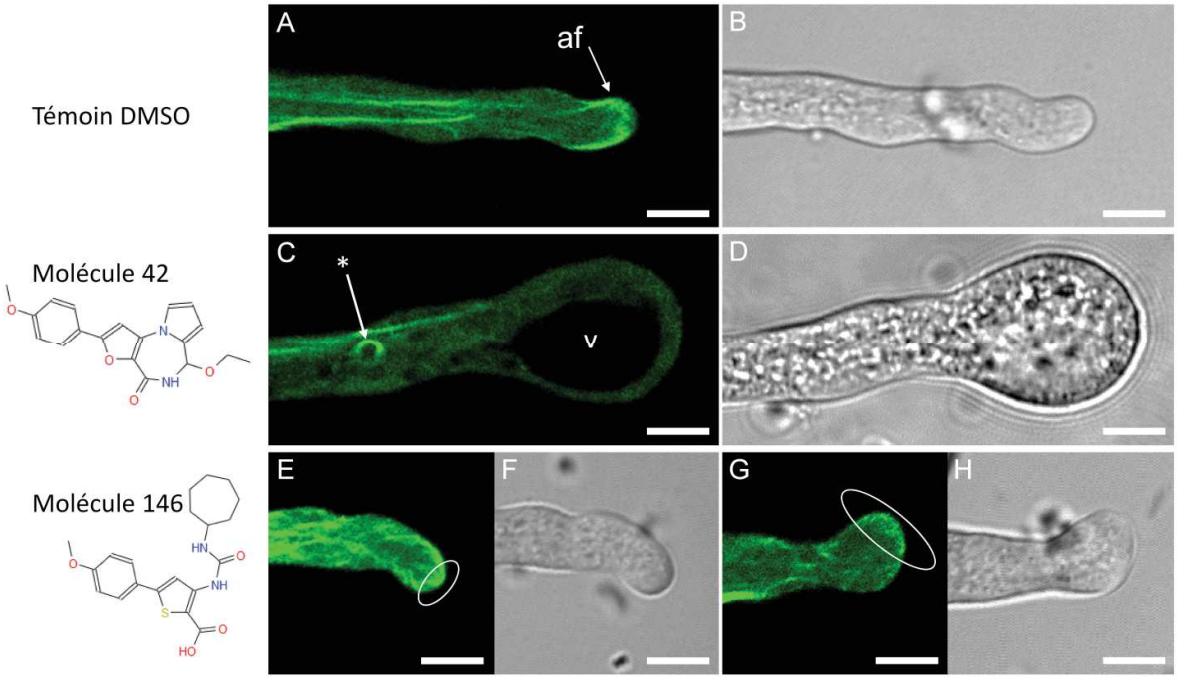

Figure 12. Structure des molécules perturbant la croissance apicale et effets sur l'organisation du réseau de filament d'actine après 6 h de culture. La lignée d'*Arabidopsis thaliana* contenant la construction *pLAT52::lifeact-mEGFP* a été utilisée afin de visualiser l'actine en microscopie confocale. Les images en lumière transmise correspondantes apparaissent en niveau de gris. A-B, témoin ; C-D, tubes traités avec la molécule 42 ; E-H, tubes traités avec la molécule 146. Af, Actine Fringe ; v, Vacuole ; *, Actine en anneau. Les parties cerclées indiquent l'accumulation anormale d'actine à l'apex du tube. Les barres d'échelles représentent 5 µm.

La répartition de ROP1, visualisée à l'aide de la construction *pCL::CRIB4-GFP* est caractéristique de celle décrite dans la littérature (Hwang et al., 2005) et est localisée uniquement à l'apex (Fig. 13B, C). Les traitements avec les molécules 42 et 146 perturbent l'exocytose puisque la localisation de ROP1 est affectée dans les tubes traités. ROP1 n'est plus marquée par CRIB4 sur la partie apicale des tubes traités avec la molécule 42 (Fig. 13E, F) et est anormalement repartie sur les parties sub-apicales lors de traitements avec la molécule 146 (Fig. 13H, I). D'autre part, l'oscillation de ROP1 qui serait à l'origine des oscillations calciques dans la zone apicale (Hwang et al., 2005) n'est plus visible sur les tubes traités avec la molécule 146. En revanche, on observe un déplacement de la fluorescence sur la membrane plasmique des tubes au cours du temps (Fig. 14). On distingue nettement sur la Figure 14 que ROP1, plutôt localisée sur la partie haute de la zone apicale (Fig. 14, 0 s), se déplace vers la partie basse (Fig. 14, 27 et 36 s) avant d'occuper toute la zone apicale (Fig. 14, 57 s) puis de se relocaliser vers la partie basse (Fig. 14, 90 s) avant de se déplacer à nouveau vers la partie haute (Fig. 14, 114 s). Pendant ce temps, le tube ne croît plus et la croissance apicale reprend à nouveau après 168 s (Fig. 14). Ces changements de localisation de ROP1, et

donc de perturbation de l'exocytose induisent une croissance saccadée et multi-directionnelle en « zig-zag » (Fig. 13 G), contrairement au tube témoin dont la croissance uni-directionnelle lui permet de conserver sa forme cylindrique (Fig. 13A).

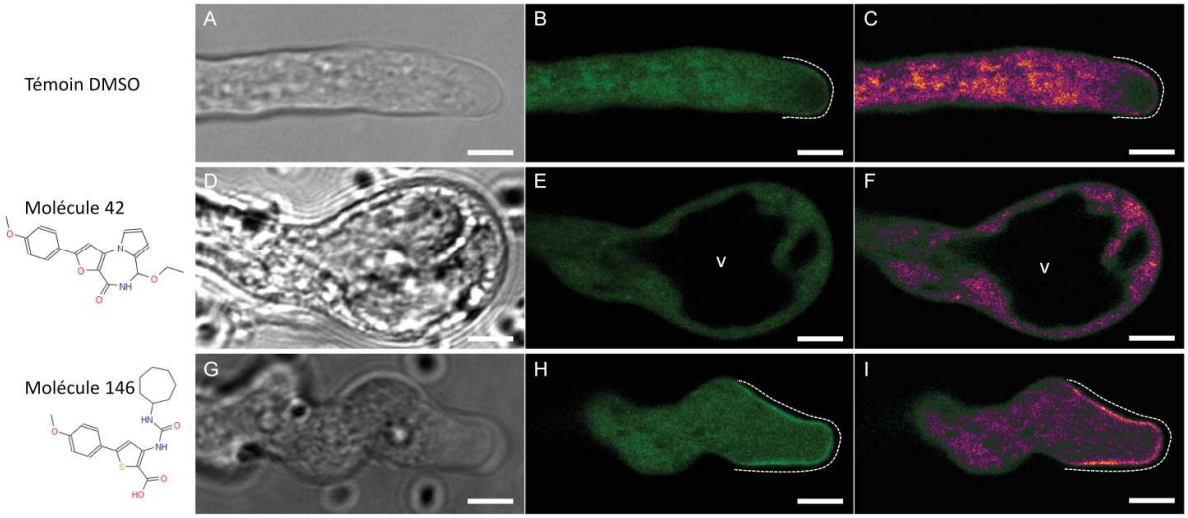

Figure 13. Effets des molécules sur la répartition de ROP1 dans la membrane plasmique des tubes polliniques après 6 h de culture. La lignée d'*Arabidopsis thaliana* contenant la construction *pCL::CRIB4-GFP* a été utilisée afin de visualiser ROP1 en microscopie confocale. A, D, G, Images en lumière transmise ; (B, E, H) images de microscopie confocale (filtre FITC) ; C, F, I, images recolorées à l'aide du filtre Blue Orange icb (Image J, Abramoff et al., 2004). A-C témoin ; D-F, tubes traités avec la molécule 42 ; G-I, tubes traités avec la molécule 146. v, Vacuole ; Les parties surlignées en pointillés indiquent la repartition de ROP1. Les barres d'échelles représentent 5 µm.

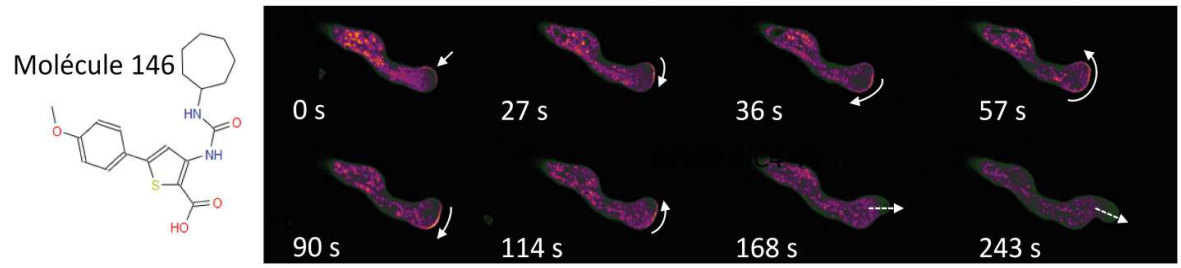

Figure 14. Evolution de la localisation de ROP1 sur un tube pollinique traité avec la molécule 146 pendant 6 h. La lignée d'*Arabidopsis thaliana* contenant la construction *pCL::CRIB4-GFP* a été utilisée afin de visualiser ROP1 en microscopie confocale. Les images sont recolorées à l'aide du filtre Blue Orange icb afin de mieux visualiser la localisation de ROP1 (Image J, Abramoff et al., 2004).

Outre la modification du déroulemement de l'exocytose et la répartition du réseau d'actine, les perturbations engendrées par l'action de ces molécules ont pour effet de modifier la distribution des composés de la paroi des tubes polliniques. En effet, la callose, absente de l'apex des tubes chez le témoin (Fig. 15A), est accumlée dans zone apicale des tubes polliniques traités avec les molécules 42 et 146 (Fig. 15B-E). D'autre part, l'immunolocalisation des épitopes associés aux HG faiblement méthylestérifiés à l'aide de l'anticorps LM19 met en évidence un remodelage de la paroi des tubes polliniques sous l'effet des traitements avec les molécules.

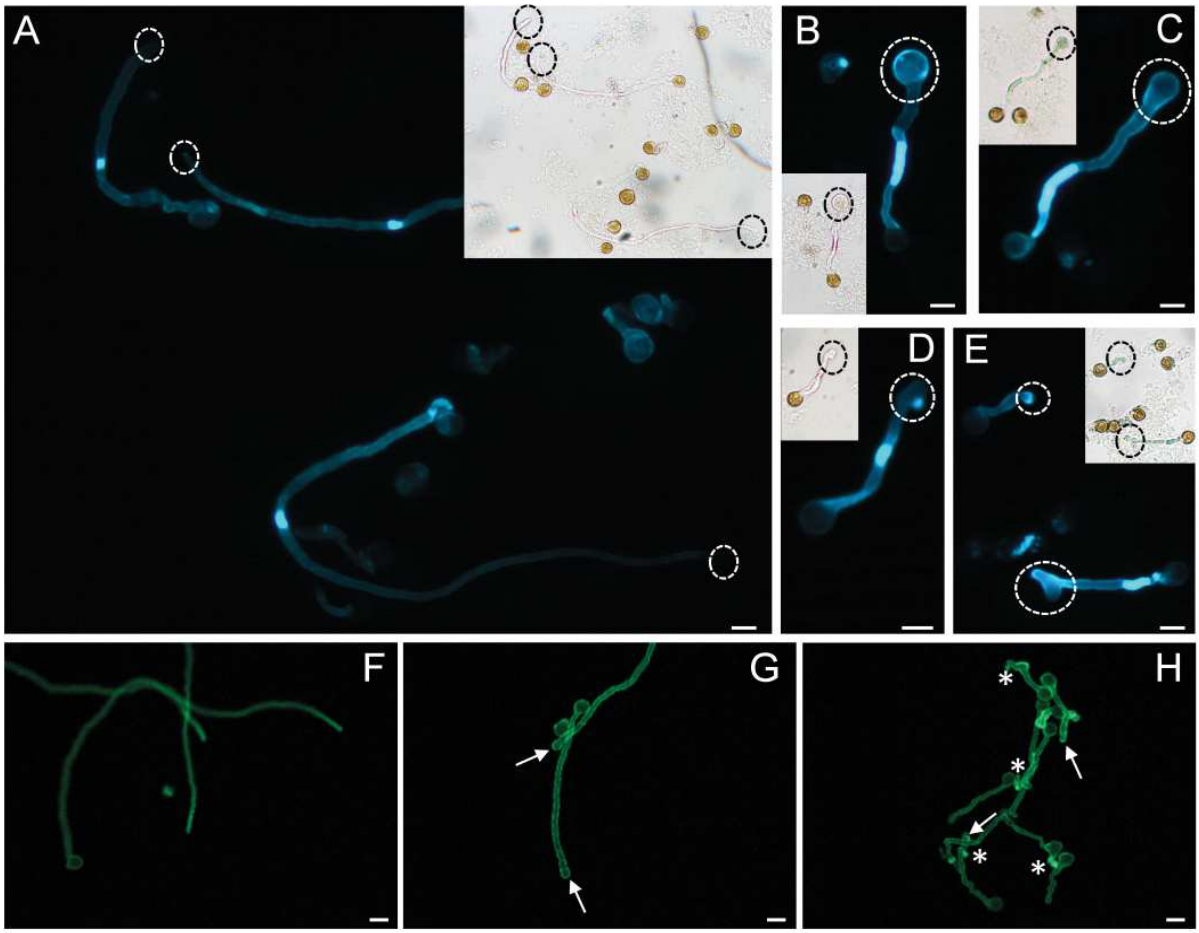

Figure 15. Observation de la callose et des épitopes associés aux homogalacturonanes HGs faiblement méthylestérifiés. La callose est colorée à l'aniline bleue sur des tubes polliniques traités ou non avec les molécules. A, tubes témoins ; B, C, tubes traités avec la molécule 42 ; D, E, tubes traités avec la molecule 146. Les HGs faiblement méthylesterifiés sont marqués par l'anticorps LM19 sur des tubes témoins (F) ou traités respectivement par la molécule 42 (G) et 146 (H). Les cercles en pointillés indiquent l'apex des tubes polliniques. Les flèches montrent la présence d'HG faiblement méthylesterifiés à l'apex des tubes. Les * indiquent l'éclatement des tubes. Les barres d'échelles représentent 10 µm.

Lorsque des tubes polliniques croissent dans un milieu de germination témoin, la répartition des HGs dans la paroi du tube pollinique est répartie en deux zones (Fig. 5). A l'apex du tube, les HGs sont exocytés sous une forme méthylée et sont déméthylés en arrière de la zone apicale. Ces changements sont associés à une réorganisation structurale de la paroi qui lui confère la plasticité et la résistance nécessaires pour maintenir la forme cylindrique du tube et la croissance apicale. Dans les tubes polliniques témoins, le marquage des HGs faiblement méthylés est faible, voire absent de la zone apicale (Fig. 15F). En revanche, les tubes traités ont un marquage assez intense dans la zone apicale, ce qui traduit la présence de HGs faiblement méthylés (Fig. 15 G, H) à l'apex. Ce remodelage de la paroi consécutif à la desorganisation de l'excrétion des vésicules pourrait expliquer l'arrêt de la croissance des tubes traités avec la molécule 42 ainsi que l'appartion d'une extrémité boursoufflée. Dans le cas des traitements avec la molécule 146, on note la présence de fuite de cytoplasme (marqués par des * sur la figure 15H) ainsi qu'une répartition anormale des HGs faiblement méthylés.

Les HGs faiblement méthylés sont en effet présents au niveau apical et sont répartis de façon hétérogène le long du tube, avec un marquage plus intense dans les zones où le tube change de direction (Fig. 15H).

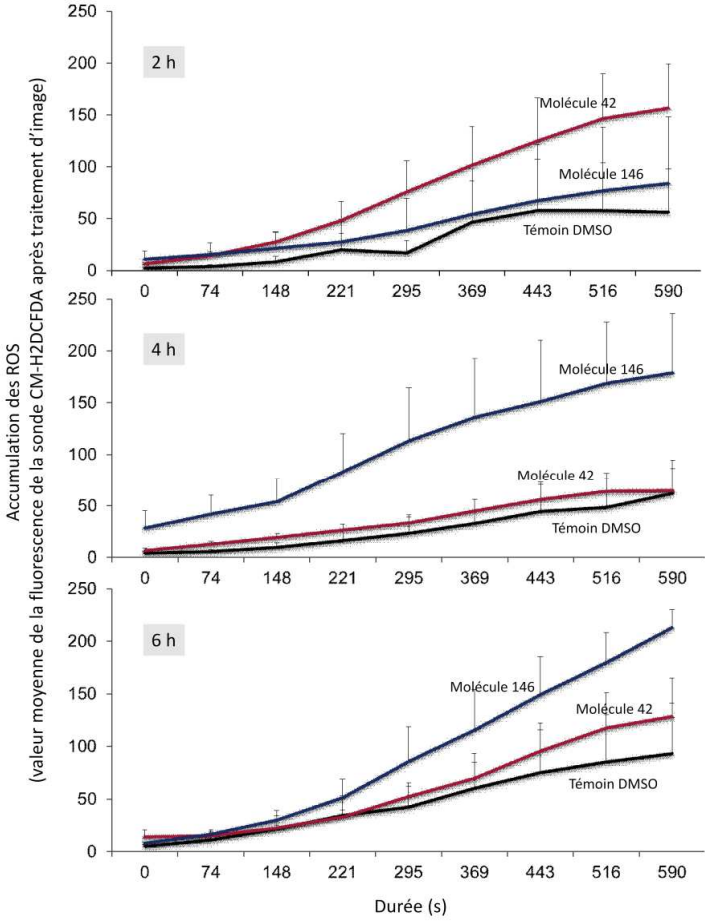

Figure 16. Quantification de l'accumulation des ROS par la mesure de la fluorescence de la sonde CM-H2DCFDA. Les images obtenues au microscope confocal (exitation 488 nm, emission 500-535 nm) sont traitées en niveau de gris à l'aide du logiciel Image J afin de déterminer la valeur moyenne d'intensité des pixels sur une surface de tube donnée. Les acquisitions sont effectuées pendant 10 minutes, après 3 durées de traitement (2, 4 et 6 h) avec les molécules 42 et 146 ou à l'aide du DMSO (témoin).

Le suivi de l'accumulation des ROS après traitements avec les molécules 42 et 146, sur des tubes cultivés pendant 2, 4 ou 6 h montre une augmentation rapide des ROS avec la molécule 42 (Fig. 16), dès 2 h de traitement, puis un niveau de ROS stable et proche du témoin. Ce résultat semble logique puisqu'après 2 h de traitement, les tubes cessent de croitre en présence de la molécule 42 (Fig. 12). En revanche, le traitement avec la molécule 146 s'accompagne d'une accumulation de ROS plus tardive, visible après 4 h de traitement, et maintenue à un niveau élevé après 6 h de traitement (Fig. 16).

L'ensemble de ces travaux de recherche a donné lieu à :

2 communications orales : ACTN-10, INF-07
4 communications par affiches: AFF-24, AFF-26, AFF-29, AFF-32

Les résultats obtenus avec ces inhibiteurs de la croissance polarisée du tube pollinique suggèrent l'existence d'un lien direct entre la production de ROS, les modifications de la paroi, l'exocytose et la croissance polarisée. Plusieurs travaux ont démontré que les ROS et le Ca^{2+} avaient un rôle prépondérant lors de la germination du grain de pollen (Speranza et al., 2012), la croissance du tube pollinique (Potocky et al., 2007, Boisson-Dernier et al., 2013) et au cours du stade final de la reproduction, lorsque les tubes polliniques explosent dans les synergides permettant la libération des gamètes (Duan et al, 2014). Au cours du doctorat de Christelle Leroux nous avons mis en évidence le lien entre la germination du grain de pollen, le remodelage de la paroi et le calcium. En effet, les grains de pollen *pme48* cultivés *in vitro* présentent un retard considérable de germination (moins de 10% après 24 h de culture contre 90% chez le sauvage). Ce défaut de germination peut être restauré si le milieu de culture est supplémenté par du calcium, suggérant un rôle important de cet élément dans la signalisation. Le remodelage de la paroi du grain de pollen, au cours de sa maturation, par la PME48 permettrait donc de séquestrer le calcium *via* les HGs faiblement méthylestérifiés qui sera nécessaire lors de la germination du grain de pollen (Leroux et al., 2015). D'ailleurs, un autre lien entre le calcium, la germination du pollen et la croissance du tube pollinique a été mis en évidence par l'étude du mutant *npg1* (*no pollen germination1*) (Golovkin & Reddy, 2003). Le gène *NPG1* code une « calmodulin-binding protein » spécifique du pollen. Les calmodulines (CALcium MODULated proteINS) sont capables de fixer le calcium et de moduler les signaux calciques. Plus récemment, ces mêmes auteurs ont montré que cette NPG1 pourrait interagir dans la paroi des grains de pollen et des tubes polliniques avec 4 PLLs, impliquées dans le remodelage des HGs associés au calcium (Shin et al., 2014). Cependant, à ce jour, la relation précise entre les ROS, le calcium et le remodelage de la paroi du grain de pollen en germination et la croissance du tube pollinique est peu connue.

De ce fait, et afin de mettre en évidence les liens qui peuvent exister entre ces différents acteurs, nous développons au laboratoire une stratégie d'étude ciblée sur les flux de calcium, les ROS et la composition de la paroi ainsi que la mise au point de nouveaux inhibiteurs de la biosynthèse des composés pariétaux.

7. Approche ciblée de l'étude du remodelage de la paroi au cours de l'élongation cellulaire

Ces approches ont pour objectifs 1) de modifier la transduction des signaux calciques, la production de ROS et 2) d'inhiber le fonctionnement des enzymes impliquées dans la synthèse des polysaccharides pariétaux : les glycosyltransférases. Le développement de ces méthodes d'inhibitions ciblées devrait, en complément des techniques de microscopie (immunocytochimie, actine, ROP1), de transcriptomique et de biochimie (chromatographie gazeuse), nous permettre de mieux comprendre les mécanismes impliqués dans la biosynthèse et la remodelage de la paroi végétale au cours de la croissance cellulaire.

7.1. Approche pharmacologique : Implication du Calcium et des ROS dans le remodelage de la paroi au cours de la croissance cellulaire

Plusieurs équipes s'intéressent à la régulation de la plasticité pariétale par des systèmes non enzymatiques, en particulier les ROS. Parmi ces ROS, le peroxyde d'hydrogène (H_2O_2), le radical hydroxyl ($^{\cdot}OH$) et l'anion superoxyde ($O2^{-}$) participent à la régulation des propriétés mécaniques des parois (Carol et Dolan, 2006 ; Liszkay et al., 2004 ; Lindsay et Fry, 2008). Il a été mis en évidence qu'en condition de stress biotiques et abiotiques, les ROS produites en quantité importante associées au Ca^{2+} pourraient (1) modifier directement les propriétés mécaniques de la paroi et (2) induire l'expression de gènes codant pour des protéines de remodelage des composés pariétaux (Dangl et Jones, 2001 ; Tenhaken, 2014). En effet, il a été montré que $^{\cdot}OH$ pouvait cliver localement des polysaccharides de la paroi (Schopfer et al., 2001). Inversement, le H_2O_2 en présence de péroxydases peut participer au renforcement de la paroi en favorisant des liaisons entre les tyrosines des protéines pariétales ou entre des groupements phénoliques (Wolf et Höfte, 2014). D'autre part, il a été montré que certaines péroxydases pouvaient se fixer aux HGs associés au Ca^{2+} (Carpin et al., 2001) participant probablement à la régulation des ROS dans l'apoplaste. Il existe donc un système de régulation de la plasticité pariétale associant le Ca^{2+}, les enzymes de remodelage de la paroi et les ROS. Des travaux récents ont montré que le Ca^{2+} extracellulaire pouvait activer, lors de son entrée dans la cellule, une voie de signalisation générée par les ROS *via* les RbOHs (Respiratory burst Oxidase Homologs) et en particulier par RbohH et RbohJ chez Arabidopsis (Kaya et al., 2014). En outre, RbohH et RbohJ sont indispensables à une croissance normale du tube pollinique (Kaya et al., 2014). D'autres études ont montré que les ROS et le Ca^{2+} avaient un rôle prépondérant lors de la germination du grain de pollen (Speranza et al., 2012), la croissance du tube pollinique (Potocký et al., 2007 ; Boisson-Dernier et al., 2013) et au cours du stade final de la reproduction lorsque les tubes polliniques explosent dans les synergides, permettant la libération des gamètes (Duan et al., 2014). D'autres radicaux libres de l'azote (RNS) comme le NO (oxyde nitrique) sont aussi produits par les grains de pollen et pourraient aussi jouer un rôle important dans la signalisation cellulaire (Bright et al., 2009) mais leurs fonctions exactes ne sont pas connues. Il a été suggéré que le NO pourrait servir à la réorientation spatiale des tubes polliniques au cours de leur croissance dans les tissus femelles (Prado et al., 2004), affecterait le ciblage des ovules par le tube pollinique au niveau du micropyle et modulerait la signalisation dépendante du Ca^{2+} (Prado et al., 2008).

Afin de mieux comprendre les relations qui existent entre les modifications de la paroi, les ROS et le calcium au cours de la croissance polarisée, nous développons des approches (1) pharmacologiques, (2) d'imagerie en utilisant des sondes spécifiques (détection des ROS, du calcium et des polymères de la paroi) visualisables par microscopie confocale, (3) des approches transcriptomiques pour le suivi de l'expression des gènes de remodelage de la paroi et (4) biochimiques (analyse de la composition de la paroi) en utilisant le modèle tube pollinique comme modèle de cellule à croissance polarisée. Ces travaux seront complétés par

une approche plus classique de génomique fonctionnelle (mutants paroi, signalisation calcium, detoxification (catalase, superoxyde dismutase).

Tableau I : Pharmacothèque utilisée pour l'étude des liens entre les espèces actives de l'oxygène, les flux calciques et la croissance polarisée des tubes polliniques.

Methylviologène (MV)	Inducteur de ROS
Diphenyleneionodium (DPI)	Inhibiteur des NADPH oxydase
Nitroarginine	Inhibiteur de NOS
Benzoate de Sodium	Piègeur de ROS
Chlorure de Lanthane (LaCl)	Inhibiteur de canaux calcium
EGTA	Chelateur du calcium
Nitroprusside de sodium	Inducteur de NO
2-(4-Carboxyphenyl)-4,4,5,5-tetramethylimidazoline-1-oxyl-3-oxide (cPTIO)	Inhibiteur de NO

Pour le moment, plusieurs molécules ont été utilisées afin de tester leurs effets sur la croissance du tube pollinique (Tableau I). Les travaux les plus avancés concernent les traitements au chlorure de lanthane (LaCl) et au diphenylene ionodium (DPI) (Fig. 17). Le DPI, inhibiteur de NADPH oxydases, induit un éclatement des tubes (Fig. 17B), dose dépendant, qui se traduit par une diminution de la longueur des tubes et de leur viabilité (Fig. 17D et E). Un traitement des tubes avec le LaCl n'induit pas d'explosion des tubes (Fig. 17C), mais une diminution de leur longueur significativement différente par rapport au témoin à partir de 20 µM (Fig. 17 F). Les immunomarquages réalisés à l'aide d'anticorps dirigés contre les HGs fortement et faiblement méthylestérifiés, respectivement LM20 et LM19 ainsi que contre des épitopes de fragments galactosylés des XyG (LM25) sont présentés dans la Figure 17G-J. Ces immunomarquages de surface sont un bon indicateur des modifications discrètes qui peuvent intervenir au cours du remodelage de la paroi suite à un stress. Dans notre cas, on note l'abondance du marquage avec LM20 à l'apex du tube dans la condition témoin (Fig. 17G). Cette accumulation de HG fortement méthylestérifié à l'apex du tube d'*Arabidopsis thaliana* est caractéristique de la structure pariétale du tube pollinique (Dardelle et al., 2010). Lors d'un traitement au DPI 25 µM, l'anticorps LM20 ne marque plus l'apex des tubes (Fig. 17H) suggérant un remodelage anormal par déméthylestérification des HGs au niveau de l'apex qui pourrait expliquer la forte proportion de tubes éclatés (Fig. 17E). Après un traitement au LaCl, on observe un marquage moins dense des anticorps LM19 et LM25 sur les tubes polliniques par rapport aux tubes témoins (Fig. 17I-L). La répartition des anticorps ne semble pas modifiée à la surface du tube, ni à l'apex, ni en amont de la zone apicale. En revanche, dans les deux cas, on observe des fragments de paroi marqués à la fois par LM19 et LM25 qui desquament des tubes polliniques. L'apparition de ces fragments de paroi dans le milieu de culture indique que la structure de la paroi a été modifiée par le traitement au LaCl. Il est intéressant de noter que cette modification de la paroi est associée, lors d'un traitement au LaCl, à une augmentation du diamètre des tubes qui ont, malgrè leur taille réduite, une surface 2 fois supérieure à celle des tubes témoins (Fig. 17M). Ces résultats suggèrent que la modification des flux calciques agit sur la structure de la paroi qui perd alors son intégrité physique. Consécutivement, la pression de turgescence exercée par le cytoplasme sur la membrane plasmique n'est plus contenue par la paroi et le diamètre des tubes augmente alors

que la croissance s'arrête. Lors d'un double traitement des tubes avec le DPI et le LaCl, l'augmentation de diamètre des tubes n'est plus observée (Fig. 17 M), il n'y a plus de phénomène d'éclatement des tubes, mais leur croissance reste ralentie.

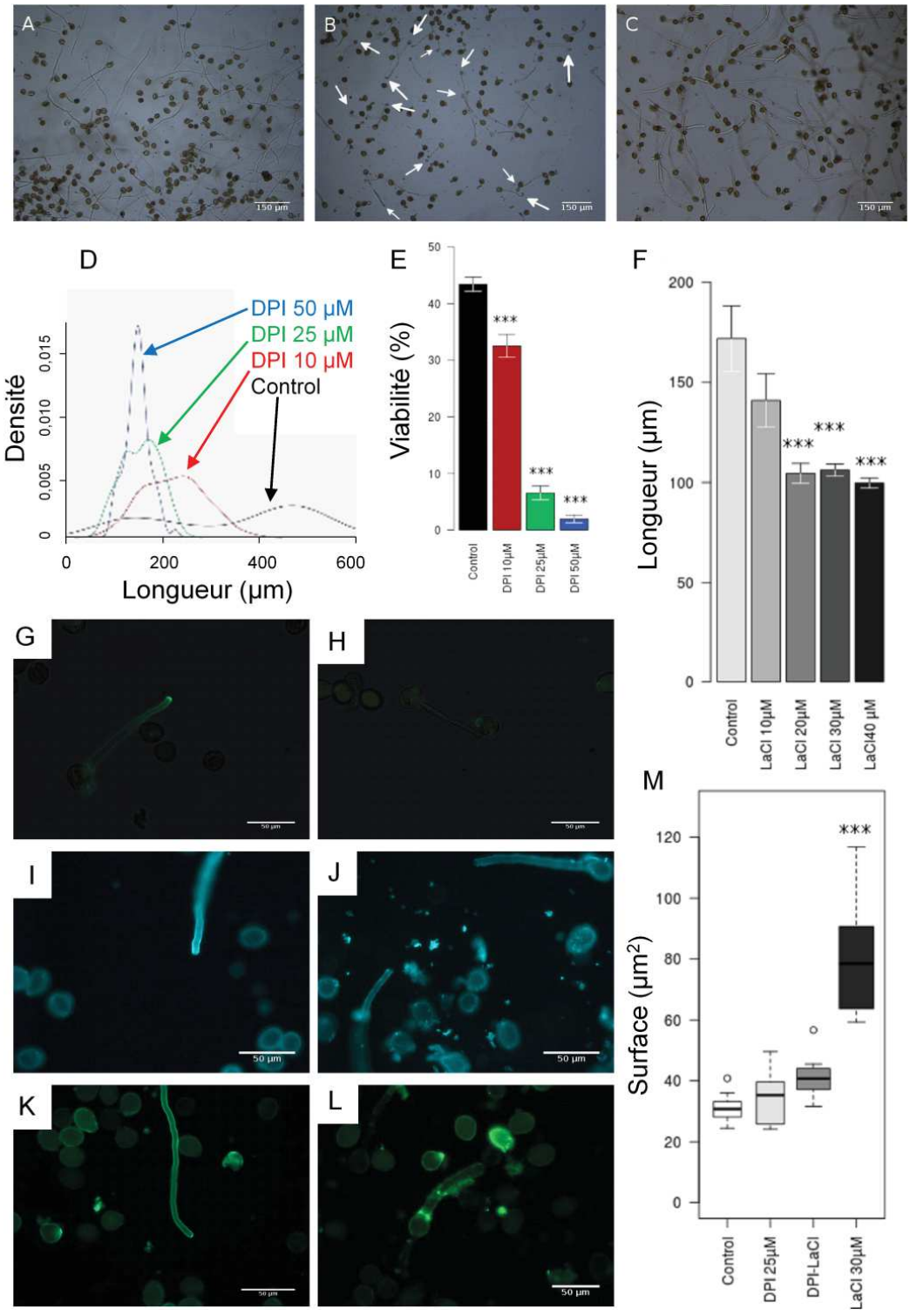

Figure 17. Effets du DPI et du LaCl sur la croissance du tube pollinique. A-C, phénotype des tubes témoins (A) et traités au DPI 25 µM (B) ou au LaCl 50 µM (C). D, E, courbe de densité de la longueur des tubes traités au DPI 25 µM (D) et pourcentage de viabilité (tubes germés et non éclatés) après 6 h en condition témoin ou traités au DPI 10, 25 et 50 µM (E). F, longueur moyenne des tubes traités pendant 3 h avec des doses croissantes de

LaCl. G-L, immunolocalisation d'épitopes associés à des polysaccharides pariétaux. G, H, immunolocalisation des épitopes associés aux HGs fortement méthylestérifiés (LM20) sur des tubes témoins (G) ou traités au DPI 25 µM (H). I, J, immunolocalisation des épitopes associés aux HGs faiblement méthylestérifiés (LM19) sur des tubes témoins (I) ou traités au LaCl 30 µM (J). K, L, immunolocalisation des épitopes associés au XyG avec l'anticorps LM25 dirigé contre les motifs galactosylés sur des tubes témoins (K) ou traités au LaCl 30 µM (L). M, détermination de la surface des tubes pollinique. Les barres d'échelle représentent 150 µm (A-C) ou 50 µm (G-L). Les flèches blanches indiquent les tubes éclatés.

Ces résultats préliminaires confirment que des liens entre les signalisations ROS et calcium existent au cours de la croissance polarisée et posent plusieurs questions sur cette cascade d'évènements : quels signaux sont situés en amont ? Quels sont les liens entre défaut de signalisation et strucure de la paroi ? Quelles sont les enzymes impliqués dans le remodelage de la paroi en réponse aux signaux calciques et ROS ? Quels sont les liens entre le remodelage des pectines et les Wall Associated Kinase (WAK), senseur de la paroi, connus pour intéragir avec les pectines lors de l'elongation cellulaire (Kohorn et Kohorn, 2012) ? Pour répondre à ces questions, nous continuons à analyser l'effet de molécules capables de piéger les ROS (benzoate de sodium, Tableau I) ou au contraire des générateurs de ROS comme le méthylviologène. Les modifications des voies de signalisation des RNS sont aussi en cours (Tableau I) et devraient permettre d'intégrer à nos modèles le calcium, les ROS et les RNS. Les chaînes de transduction de ces signaux oxydatifs ou ioniques seront étudiées en faisant varier les concentrations, les mélanges, et l'ordre des traitements afin d'augmenter, ou de reverser les phénotypes observés et d'ordonner ainsi le rôle des différents signaux. Ces études seront complétées par des approches 1) d'immunocytochimie des épitopes pariétaux en surface sur la paroi des tubes, et sur des extraits pariétaux (dot-blot) ; 2) d'analyse transciptomique, en qRT-PCR, des variations d'expression de l'ensemble des gènes de remodelage des pectines ; 3) d'analyse de la composition et de l'activité enzymatique pariétale, en particulier l'activité PME 4) l'utilisation de plantes mutantes dans les voies de signalisations (RBOH, WAK) ou dans le remodelage des HGs (PME).

7.2. Criblage et développement d'inhibiteurs des voies glucidiques

La seconde aproche que je contribue à développer au Glyco-MEV consiste à caractériser de nouveaux inhibiteurs des voies glucidiques, en particulier des inhibiteurs des glycosyltransférases. En effet, même si les approches de génomique fonctionnelle menées sur des espèces modèles (*Arabidopis thaliana*, riz, tomate …) ont largement contribué à une meilleure compréhension de nombreux processus physiologiques, elles restent longues à mettre en œuvre (sélection de mutants homozygotes) et se heurtent dans certains cas à la létalité des lignées mutantes. Lors des travaux de thèse de Marie Dumont, puis des stages d'étudiants ingénieurs (Juliette Havel et Marie Bourgeais) en 2016 et 2017, nous avons démontré que des monosaccharides fluorés sont d'excellents inhibiteurs de glycosyltransférases végétales. En particulier, le 2-désoxy 2-fluoro L-fucose a été démontré

comme capable, à faible dose, d'inhiber les fucosyltransférases végétales et ainsi de perturber la fucosylation des polysaccharides de la paroi primaire (Dumont *et al*., 2015). L'approche pharmacologique entreprise avec les analogues fluorés a montré que le remplacement d'un groupement hydroxyl par un atome de fluor dans la structure de glucides pouvait être un outil puissant pour perturber le métabolisme de la plante. Ainsi, le 2F-Fuc est capable d'inhiber plusieurs fucosyltransférases *via* son activation présumée sous forme GDP. Il en résulte un phénotype racinaire fortement altérée avec un défaut d'élongation cellulaire de la racine principale. La fucosylation du XyG et des N-glycannes est inhibée et la synthèse du RG-II fortement perturbée. Sur le profil électrophorétique du RG-II extrait de plantes traitées au 2F-Fuc, l'altération de la dimérisation du RG-II et la présence d'oligosaccharides de poids moléculaire plus faible que le monomère de RG-II est nette (Dumont et al., 2015). Ces résultats montrent l'intérêt des sucres fluorés dans l'étude de la synthèse et la fonction de la paroi végétale puisqu'ils offrent l'avantage de permettre d'obtenir des phénotypes dose-dépendants, au cas où l'inhibition soit létale, et de contrôler le stade de développement ou le tissu à cibler, ce qui est difficilement réalisable par une approche de génétique fonctionnelle classique.

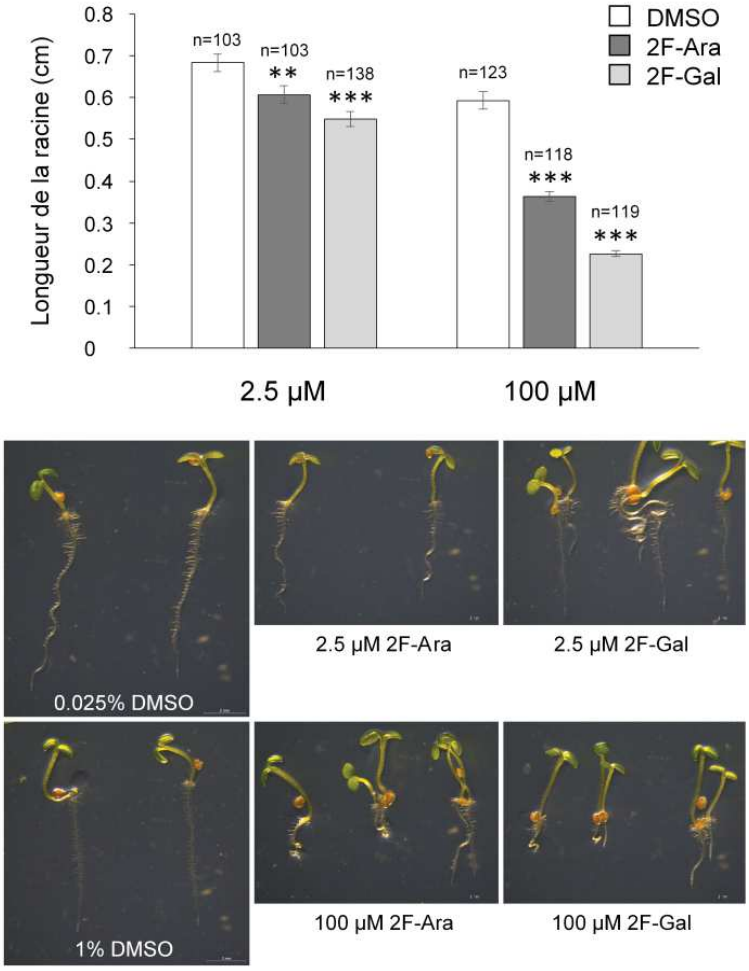

Figure 18. Etude de l'effet de sucres fluorés, le 2-fluoro-Arabinose (2F-Ara) et le 2-fluoro-Galactose (2F-Gal) sur la croissance de la racine d'*Arabidopsis thaliana*. Le DMSO 0.025 et 1% représente le contôle pour les concentrations respectives de 2,5 et 100 µM.

Ce projet de recherche consistera dans un premier temps à développer puis à tester de nouveaux fluorosucres sur le développement des zones en croissance d'*Arabidopsis thaliana* (zone d'élongation de la racine) afin de trouver de nouveau inhibiteurs capables de perturber la biosynthèse de composés pariétaux. La racine d'Arabidopsis est reconnue depuis longtemps comme un modèle intéressant pour étudier la croissance cellulaire. Son ontogenèse est peu variable et l'organisation cellulaire y est très contrôlée. La fonction de nombreux gènes a ainsi pu être déterminée grâce à des criblages de mutants présentant des défauts de croissance racinaire (Benfey *et al.*, 1993), qu'il s'agisse de mutant affecté dans le cycle cellulaire (Nezames *et al.*, 2012), dans la perception d'hormones ou dans la synthèse de composés pariétaux (Desnos *et al.*, 1996 ; Fagard *et al.*, 2000). Cette étude a déjà débuté, au printemps 2016 avec le test de plusieurs fluoro sucres : 2,3-F_2-Glucose, 3,4-F_4-Glucose, 2,3-F_2-Galactose, 2-F-Arabinose (2F-Ara) et 2-F-Galactose (2F-Gal). Ces travaux, poursuivis en 2017, donnent des résultats très encourageants, en particulier avec le 2F-Ara et 2F-Gal (Fig. 18) qui présentent un effet dose sur l'élongation de la racine dès la concentration de 2,5 µM jusqu'à 100 µM (Fig. 18). Ces expériences préliminaires, seront poursuivies, avec le 2-F-Xylose avec le modèle racine. La caractérisation biochimique de l'effet de ces fluorosucres sur la biosynthèse des composés pariétaux ainsi que l'utilisation des approches d'imageries cellulaires permettront de caractériser les voies bloquées par ces fluoro sucres et de mieux comprendre le rôle de certains polysaccharides pectiques dans l'élongation cellulaire.

Cette mise en place de nouveaux outils d'étude devrait aussi se poursuivre sur le tube pollinique, afin de compléter les outils nécessaires à l'étude de la biosynthèse pariétale et du remodellage de la paroi dans la croissance cellulaire sur un modèle original et parfaitement maîtrisé au laboratoire. Des études avaient été engagées dans ce sens au laboratoire à l'aide du 2F-Fuc, qui s'avérait, à des concentrations de 20 µM capable de désorganiser la paroi des tubes polliniques (Dumont, 2015).

8. Conclusion

Les travaux de recherche menés par le Glyco-MEV ont permis de mieux caractériser la composition en polysaccharides et leur répartition dans la paroi au cours de la croissance cellulaire. Nous avons aussi mis en évidence que les enzymes de remodelage de la paroi et/ou leurs inhibiteurs jouent un rôle crucial dans le contrôle des mécanismes de croissance polarisée. Notre maîtrise des techniques de culture du pollen et la mise au point de nouvelles techniques d'imagerie (click-chemistry) ainsi que l'utilisation de la génétique chimique et le criblage des inhibiteurs de glycosyltransférases nous permettent aujourd'hui de songer à développer des approches plus ciblées afin de préciser le rôle et la localisation des polysaccharides pariétaux au cours de leur synthèse, de leur mise en place et de leur remodelage dans la paroi. Puisque le tube pollinique se révèle être un excellent modèle cellulaire, je propose de continuer à développer au cours des prochaines années la mise au point d'outils d'analyse du remodelage pariétal sur ce modèle d'étude. Les résultats que nous

avons obtenus avec les inhibiteurs de glycosyltransferase et d'enzymes de remodelage de la paroi (2F-fuc, PMEI) sont très encourageants (Dumont et al., 2015 ; Paynel et al., 2014, Hocq et al., 2017). Les travaux en cours avec des polygalacturonases valident notre modèle d'étude (Lehner et al., non publié). Ainsi, et puisque nous disposons d'outils permettant une approche pharmacologique d'étude de la signalisation calcique et ROS, j'envisage de coupler les traitements pharmacologiques, l'inhibition de la synthèse ou du remodelage pariétal et l'imagerie cellulaire. Cette approche intégrative devrait nous permettre de mieux comprendre les mécanismes cellulaires, moléculaires et biochimiques qui gouvernent la mise en place et le remodelage de la paroi végétale au cours de la croissance.

9. Bibliographie

Abràmoff MD, Magalhães PJ, Ram SJ. Image processing with ImageJ. *Biophotonic Intern*. **2004. 11 :** 36-42.

Abreu I, Oliveira M. Immunolocalisation of arabinogalactan proteins and pectins in *Actinidia deliciosa* pollen. *Protoplasma.* **2004. 224 :** 123-128.

AGI Arabidopsis Genome Initiative. Analysis of the genome sequence of the flowering plant *Arabidopsis thaliana*. *Nature.* **2000. 408 :** 796-815.

Aouar L, Chebli Y, Geitmann A. Morphogenesis of complex plant cell shapes : The mechanical role of crystalline cellulose in growing pollen tubes. *Sex Plant Reprod*. **2010. 23 :** 15-27.

Benfey PN, Linstead PJ, Roberts K, Schiefelbein JW, Hauser MT, Aeschbacher RA. Root development in *Arabidopsis*: four mutants with dramatically altered root morphogenesis. *Development.* **1993. 119 :** 57-70.

Boisson-Dernier A, Lituiev DS, Nestorova A, Franck, CM, Thirugnanarajah S, Grossniklaus U. ANXUR receptor-like kinases coordinate cell wall integrity with growth at the pollen tube tip via NADPH oxidases. *PLoS biology*. **2013. 11 :** e1001719.

Bosch M, Hepler PK. Pectin Methylesterases and Pectin Dynamics in Pollen Tubes. *Plant Cell.* **2005. 17 :** 3219-3226.

Bouton S, Leboeuf E, Mouille G, Leydecker MT, Talbotec J, Granier F, Lahaye M, Höfte H, Truong HN. *QUASIMODO1* encodes a putative membrane-bound glycosyltransferase required for normal pectin synthesis and cell adhesion in *Arabidopsis*. *Plant Cell.* **2002. 14 :** 2577-2590.

Bove J, Vaillancourt B, Kroeger J, Hepler PK, Wiseman PW, Geitmann A. Magnitude and direction of vesicle dynamics in growing pollen tubes using spatiotemporal image correlation spectroscopy and fluorescence recovery after photobleaching. *Plant Physiol.* **2008. 147 :** 1646-1658.

Bright J, Hiscock SJ, James PE, Hancock JT. Pollen generates nitric oxide and nitrite: a possible link to pollen-induced allergic responses. *Plant Physiol Biochem.* **2009. 47 :** 49-55.

Brownlee C. Role of the extracellular matrix in cell-cell signalling : paracrine paradigms. *Curr Opin Plant Biol*. **2002. 5 :** 396-401.

Cai G, Parrotta L, Cresti M. Organelle trafficking, the cytoskeleton, and pollen tube growth. *J Integr Plant Biol.* **2015. 57 :** 63-78.

Carpin S, Crèvecoeur M, de Meyer M, Simon P, Greppin H, Penel C. Identification of a Ca^{2+}-pectate binding site on an apoplastic peroxidase. *Plant Cell*. **2001. 13 :** 11-20.

Carol RJ, Dolan L. The role of reactive oxygen species in cell growth: lessons from root hairs. *J Exp Bot*. **2006. 57 :** 1829-1834.

Cassab GI. Plant cell wall proteins. *Annu Rev Plant Bio*. **1998. 49 :** 281-309.

Chang F, Gu Y, Ma H, Yang Z. AtPRK2 promotes ROP1 activation via RopGEFs in the control of polarized pollen tube growth. *Mol Plant*. **2013. 6 :** 1187-1201.

Chebli Y, Kaneda M, Zerzour R, Geitmann A. The cell wall of the *Arabidopsis thaliana* pollen tube spatial distribution, recycling and network formation of polysaccharides. *Plant Physiol.* **2012. 160 :** 1940-1955.

Chen KM, Wu GL, Wang YH, Tian CT, Samaj J, Baluska F, Lin JX. The block of intracellular calcium release affects the pollen tube development of *Picea wilsonii* by changing the deposition of cell wall components. *Protoplasma.* **2008. 233 :** 39-49.

Chen X, Kim J. Callose synthesis in higher plants. *Plant Signal Behav.* **2009. 4 :** 489-492.

Cheung AY, Wang H, Wu HM. A floral transmitting tissue-specific glycoprotein attracts pollen tubes and stimulates their growth. *Cell.* **1995. 82 :** 383-393.

Cheung AY, Wu HM. Arabinogalactan proteins in plant sexual reproduction. *Protoplasma*. **1999. 208 :** 87-98.

Cheung AY, Wu HM. Structural and signaling networks for the polar cell growth machinery in pollen tubes. *Annu Rev Plant Physiol Plant Mol Biol.* **2008. 59 :** 547-572.

Coimbra S, Almeida J, Junqueira V, Costa ML, Pereira LG. Arabinogalactan proteins as molecular markers in *Arabidopsis thaliana* sexual reproduction. *J Exp Bot.* **2007. 58 :** 4027-4035.

Coimbra S, Costa M, Jones B, Mendes MA, Pereira LG. Pollen grain development is compromised in *Arabidopsis agp6 agp11* null mutants. *J Exp Bot*. **2009. 60 :** 3133-3142.

Coimbra S, Costa M, Mendes MA, Pereira AM, Pinto J, Pereira LG. Early germination of *Arabidopsis* pollen in a double null mutant for the arabinogalactan protein genes *AGP6* and *AGP11*. *Sex Plant Reprod.* **2010. 23 :** 199-205.

Coimbra S, Duarte C. Arabinogalactan proteins may facilitate the movement of pollen tubes from the stigma to the ovules in *Actinidia* deliciosa and *Amaranthus* hypochondriacus. *Euphytica*. **2003. 133 :** 171-178.

Coimbra S, Jones B, Pereira LG. Arabinogalactan proteins (AGPs) related to pollen tube guidance into the embryo sac in *Arabidopsis*. *Plant Signal Behav*. **2008. 3 :** 455-456.

Coimbra S, Pereira LG. Arabinogalactan proteins in *Arabidopsis thaliana* pollen development, transgenic plants - Advances and Limitations, PhD. Yelda Ozden Çiftçi (Ed.), ISBN: 978-953-51-0181-9, *InTech*. **2012.** 329-352.

Coimbra S, Salema R. Immunolocalization of arabinogalactan proteins in *Amaranthus* hypochondriacus L. ovules. *Protoplasma*. **1997. 199 :** 75-82.

Cornuault V, Buffetto F, Marcus SE, Crépeau MJ, Guillon F, Ralet MC, Knox JP. LM6-M: a high avidity rat monoclonal antibody to pectic α-1, 5-L-arabinan. *bioRxiv*. **2017.** 161604. doi: https://doi.org/10.1101/161604.

Costa M, Pereira AM, Rudall PJ, Coimbra S. Immunolocalization of arabinogalactan proteins (AGPs) in reproductive structures of an early-divergent angiosperm, *Trithuria* (Hydatellaceae). *Ann Bot.* **2013. 111 :** 183-190.

Dai S, Chen T, Chong K, Xue Y, Liu S, Wang T. Proteomics identification of differentially expressed proteins associated with pollen germination and tube growth reveals characteristics of germinated *Oryza sativa* pollen. *Mol Cell Proteomics.* **2007. 6 :** 207-230.

Dai S, Li L, Chen T, Chong K, Xue Y, Wang T. Proteomic analyses of *Oryza sativa* mature pollen reveal novel proteins associated with pollen germination and tube growth. *Proteomics.* **2006. 6 :** 2504-2529.

Dangl JL, Jones JD. Plant pathogens and integrated defence responses to infection. *Nature*. **2001. 411 :** 826.

Dardelle F, Le Mauff F, Lehner A, Loutelier-Bourhis C, Bardor M, Rihouey C, Causse M, Lerouge P, Driouich A, Mollet JC. Pollen tube cell walls of wild and domesticated tomatoes contain arabinosylated and fucosylated xyloglucan. *Ann Bot.* **2015. 115 :** 55-66.

Dardelle F, Lehner A, Ramdani Y, Bardor M, Lerouge P, Driouich A, Mollet JC. Biochemical and immunocytological characterization of *Arabidopsis* pollen tube cell wall. *Plant Physiol.* **2010. 153 :** 1563-1576.

Dearnaley JDW, Daggard GA. Expression of a polygalacturonase enzyme in germinating pollen of *Brassica napus*. *Sex Plant Reprod.* **2001. 13 :** 265-271.

Delmas F, Séveno M, Northey JG, Hernould M, Lerouge P, McCourt P, Chevalier C. The synthesis of the rhamnogalacturonan II component 3-deoxy-D-manno-2-octulosonic acid (Kdo) is required for pollen tube growth and elongation. *J Exp Bot.* **2008. 59 :** 2639-2647.

Deng Y, Wang W, Li WQ, Xia C, Liao HZ, Zhang XQ, Ye D. *MALE GAMETOPHYTE DEFECTIVE 2*, encoding a sialyltransferase-like protein, is required for normal pollen germination and pollen tube growth in *Arabidopsis*. *J Integr Plant Biol.* **2010. 52 :** 829-843.

Derksen J, Knuiman B, Hoedemaekers K, Guyon A, Bonhomme S, Pierson ES. Growth and cellular organization of *Arabidopsis* pollen tubes *in-vitro*. *Sex Plant Reprod*. **2002. 15 :** 133-139.

Derksen J, Li YQ, Knuiman B, Guerts H. The wall of *Pinus sylvestris* pollen tubes. *Protoplasma.* **1999. 208** : 26-36.

Desnos T, Orbović V, Bellini C, Kronenberger J, Caboche M, Traas J, Höfte H. *Procuste1* mutants identify two distinct genetic pathways controlling hypocotyl cell elongation, respectively in dark- and light-grown *Arabidopsis* seedlings. *Development*. **1996. 122 :** 683-693.

Dey PM, Del Campillo E. Biochemistry of the multiple forms of glycosidases in plants. *Adv Enzymol Relat Areas Mol Biol.* **1984. 56 :** 141-249.

Dong X, Hong Z, Sivaramakrishnan M, Mahfouz M, Verma DP. Callose synthase (*CalS5*) is required for exine formation during microgametogenesis and for pollen viability in *Arabidopsis*. *Plant J*. **2005. 42 :** 315-328.

Drakakaki G, Zabotina O, Delgado I, Robert S, Keegstra K, Raikhel N. *Arabidopsis* reversibly glycosylated polypeptides 1 and 2 are essential for pollen development. *Plant Physiol.* **2006. 142 :** 1480-1492.

Duan Q, Kita D, Johnson EA, Aggarwal M, Gates L, Wu HM, Cheung AY. Reactive oxygen species mediate pollen tube rupture to release sperm for fertilization in *Arabidopsis***.** *Nature Comm*. **2014. 5 :** 3129.

Dumont M. Rôle du rhamnogalacturonane de type 2 dans l'élongation cellulaire. Thèse de doctorat de l'Université de Rouen Normandie, 10 juillet 2015. 269 p.

Dumont M, Lehner A, Bouton S, Kiefer-Meyer MC, Voxeur A, Pelloux J, Lerouge P, Mollet JC. The cell wall pectic polymer rhamnogalacturonan-II is required for proper pollen tube

elongation: implications of a putative sialyltransferase-like protein. *Ann Bot.* **2014. 114 :** 1177-1188**.**

Dumont M, Lehner A, Bardor M, Burel C, Vauzeilles B, Lerouxel O, Anderson CT, Mollet JC, Lerouge P. Inhibition of fucosylation of cell wall components by 2-fluoro 2-deoxy-L-fucose induces defects in root cell elongation. *Plant J.* **2015. 84 :** 1137-1151.

Durand C, Vicre-Gibouin M, Follet-Gueye ML, Duponchel L, Moreau M, Lerouge P, Driouich A. The organization pattern of root border-likes cells of *Arabidopsis thaliana* is dependent on cell wall homogalacturonan. *Plant Physiol.* **2009. 150 :** 1411-1421.

Ellis M, Egelund J, Schultz CJ, Bacic A. Arabinogalactan-proteins: key regulators at the cell surface? *Plant Physiol.* **2010. 153 :** 403-419.

Fagard M, Desnos T, Desprez T, Goubet F, Refregier G, Mouille G, McCann M, Rayon C, Vernhettes S, Höfte H. *PROCUSTE1* encodes a cellulose synthase required for normal cell elongation specifically in roots and dark-grown hypocotyls of *Arabidopsis*. *Plant Cell*. **2000. 12 :** 2409-2424.

Faik A, Bar-Peled M, DeRocher AE, Zeng W, Perrin RM, Wilkerson C, ... Keegstra K. Biochemical characterization and molecular cloning of an α-1, 2-fucosyltransferase that catalyzes the last step of cell wall xyloglucan biosynthesis in pea. *J Biol Chem.* **2000. 275:** 15082-15089.

Feijó JA, Sainhas J, Hackett GR, Kunkel JG, Hepler PK. Growing pollen tubes possess a constitutive alkaline band in the clear zone and a growth-dependent acidic tip. *J Cell Biol*. **1999. 3 :** 483-496.

Ferguson C, Teeri TT, Siika-aho M, Read SM, Basic A. Location of cellulose and callose in pollen tubes and grains of *Nicotiana tabacum*. *Panta*. **1998. 206 :** 452-460.

Fry SC. Cell wall polysaccharide composition and covalent crosslinking. *Ann Plant Rev.* **2011. 41 :** 1-42.

Fry SC, York WS, Albersheim P, Darvill A, Hayashi T, Joseleau JP, Kato Y, Lorences EP, Maclachlan GA, McNeil M, Mort AJ, Reid JSG, Seitz HU, Selvendran RR, Voragen AGJ, White AR. An unambiguous nomenclature for xyloglucan-derived oligosaccharides. *Physiol Plant*. **1993. 89 :** 1-3.

Fu Y, Li H, Yang Z. The ROP2 GTPase controls the formation of cortical fine F-actin and the early phase of directional cell expansion during Arabidopsis organogenesis. *Plant Cell.* **2002. 14 :** 777-794.

Fu Y, Wu G, Yang Z. Rop GTPase–dependent dynamics of tip-localized F-actin controls tip growth in pollen tubes. *J Cell Biol.* **2001. 152 :** 1019-1032.

Fujita M, Fujita Y, Noutoshi Y, Takahashi F, Narusaka Y, Yamaguchi-Shinozaki K, Shinozaki K. Crosstalk between abiotic and biotic stress responses: a current view from the points of convergence in the stress signaling networks. *Curr Opin Plant Biol.* **2006. 9 :** 436-442.

Gaspar YM, Johnson KL, McKenna JA, Bacic A, Schultz CJ. The complex structures of arabinogalactan-proteins and the journey towards a function. *Plant Mol Biol.* **2001. 47 :** 116-176.

Ge W, Song Y, Zhang Y, Burlingame AL, Guo Y. Proteomic analysis of apoplastic proteins from germinating *Arabidopsis thaliana* pollen. *Biochim Biophys Acta.* **2011. 1814 :** 1964-1973.

Geitmann A. How to shape a cylinder : Pollen tube as a model system for the generation of complex cellular geometry. *Sex Plant Reprod.* **2010. 23 :** 63-71.

Gibeaut DM, Carpita NC. Biosynthesis of plant cell wall polysaccharides. *FASEB J.* **1994. 8 :** 904-915.

Gillmor CS, Lukowitz W, Brininstool G, Sedbrook JC, Hamann T, Poindexter P, Somerville C. Glycosylphosphatidylinositol-Anchored Proteins Are Required for Cell Wall Synthesis and Morphogenesis in *Arabidopsis*. *Plant Cell*. **2005. 17 :** 1128-1140.

Golovkin M, Reddy AS. A calmodulin-binding protein from Arabidopsis has an essential role in pollen germination. *Proc Natl Acad Sci USA*. **2003. 100 :** 10558-10563.

Gu F, Nielsen E. Targeting and regulation of cell wall synthesis during tip growth in plants. *J Integr Plant Biol.* **2013. 55 :** 835-846.

Gu Y, Fu Y, Dowd P, Li S, Vernoud V, Gilroy S, Yang Z. A Rho family GTPase controls actin dynamics and tip growth via two counteracting downstream pathways in pollen tubes. *J Cell Biol*. **2005. 169 :** 127-138.

Harholt J, Suttangkakul A, Scheller HV. Biosynthesis of pectin. *Plant Physiol.* **2010. 153 :** 384-395.

Hart DA, Kindel PK. Isolation and partial characterization of apiogalacturonans from the cell wall of Lemna minor. *Biochem J*. **1970. 116 :** 569-579.

Hepler PK, Winship LJ. The pollen tube clear zone: Clues to the mechanism of polarized growth. *J Integr Plant Biol.* **2015. 57 :** 79-92.

Hocq L, Sénéchal F, Lefebvre V, Lehner A, Domon J-M, Mollet J-C, Dehors J, Pageau K, Marcelo P, Guérineau F, Kolšek K, Mercadante D, Pelloux J. Combined Experimental and computational approaches reveal distinct pH-dependence of pectin methyl esterase inhibitors. *Plant Physiol.* **2017. 173 :** 1075-1093.

Hong Z, Delauney AJ, Verma DP. A cell plate-specific callose synthase and its interaction with phragmoplastin. *Plant Cell.* **2001. 13 :** 755-768.

Honkanen S, Dolan L. Growth regulation in tip-growing cells that develop on the epidermis. *Curr Opin Plant Biol.* **2016. 34 :** 77-83.

Hruba P, Honys D, Twell D, Capkova V, Tupy J. Expression of beta-galactosidase and beta-xylosidase genes during microspore and pollen development. *Planta.* **2005. 220 :** 931-940.

Huang L, Cao J, Ye Y, Zhang Y, Zhang A, Liu T. The polygalacturonase gene *BcMF2* from *Brassica campestris* is associated with intine development. *J Exp Bot.* **2009a. 60 :** 301-313.

Huang L, Ye Y, Zhang Y, Zhang A, Liu T, Cao J. BcMF9, a novel polygalacturonase gene, is required for both *Brassica campestris* intine and exine formation. *Ann Bot.* **2009b. 104 :** 1339-1351.

Hwang JU, Gu Y, Lee YJ, Yang Z. Oscillatory ROP GTPase activation leads the oscillatory polarized growth of pollen tubes. *Mol Biol Cell*. **2005. 16 :** 5385-5399.

Hwang JU, Vernoud V, Szumlanski A, Nielsen E, Yang Z. A tip-localized RhoGAP controls cell polarity by globally inhibiting Rho GTPase at the cell apex. *Curr Biol.* **2008. 18 :** 1907-1916.

Iwai H, Masaoka N, Ishii T, Satoh S. A pectin glucuronyltransferase gene is essential for intercellular attachment in the plant meristem. *Proc Natl Acad Sci USA*. **2002. 99 :** 16319-16324.

Jarvis MC, Briggs SPH, Knox JP. Intercellular adhesion and cell separation in plants. *Plant Cell Environ.* **2003. 26 :** 977-989.

Jauh GY, Lord EM. Localization of pectins and arabinogalatan-proteins in *lily* (*Lilium longiflorum L.*) pollen tube and style, and their possible roles in pollination. *Planta.* **1996. 199 :** 251-261.

Jensen JK, Sørensen SO, Harholt J, Geshi N, Sakuragi Y, Møller I, Zandleven J, Bernal AJ, Jensen NB, Sørensen C. Identification of a xylogalacturonan xylosyltransferase involved in pectin biosynthesis in *Arabidopsis*. *Plant Cell.* **2008. 20 :** 1289-1302.

Jiang L, Yang SL, Xie LF, Puah CS, Zhang XQ, Yang WC, Sundaresan V, Ye D. *VANGUARD1* encodes a pectin methylesterase that enhances pollen tube growth in the *Arabidopsis* style and transmitting tract. *Plant Cell.* **2005. 17 :** 584-596.

Jiang J, Yao L, Yu Y, Lv M, Miao Y, Cao J. *PECTATE LYASE-LIKE10* is associated with pollen wall development in *Brassica campestris*. *J Integr Plant Biol*. **2014. 56 :** 1095-1105.

Jones, M. A., Shen, J. J., Fu, Y., Li, H., Yang, Z., & Grierson, C. S. The Arabidopsis Rop2 GTPase is a positive regulator of both root hair initiation and tip growth. *Plant Cell*, **2002. 14 :** 763-776.

Kaya H, Nakajima R, Iwano M, Kanaoka MM, Kimura S, Takeda S, Kawarazaki T, Senzaki E, Hamamura Y, Higashiyama T, Takayama S, Abe M, Kuchitsu K. (2014). Ca2+-activated reactive oxygen species production by Arabidopsis RbohH and RbohJ is essential for proper pollen tube tip growth. *Plant Cell.* **2014. 26 :** 1069-1080.

Ketelaar T. The actin cytoskeleton in root hairs: all is fine at the tip. *Curr Opin Plant Biol*. **2013. 16 :** 749-756.

Kieliszewski MJ, Lamport DT. Extensin: repetitive motifs, functional sites, post-translational codes, and phylogeny. *Plant J.* **1994. 5 :** 157-172.

Kobayashi M, Kouzu N, Inami A, Toyooka K, Konishi Y, Matsuoka K, Matoh T. Characterization of *Arabidopsis* CTP : 3-deoxy-D-manno-2-octulosonate cytidylyltransferase (CMP-KDO synthetase), the enzyme that activates KDO during rhamnogalacturonan II biosynthesis. *Plant Cell Physiol.* **2011. 52 :** 1832-1843.

Kobayashi M, Matoh T, Azuma J. Two chains of rhamnogalacturonan II are cross-linked by borate-diol ester bonds in higher plant cell walls. *Plant Physiol.* **1996. 110 :** 1017-1020.

Kohorn BD, Kohorn SL. The cell wall-associated kinases, WAKs, as pectin receptors. *Front Plant Sci.* **2012. 3 :** 88.

Konishi T, Takeda T, Miyazaki Y, Ohnishi-Kameyama M, Hayashi T, O'Neill MA, Ishii T. A plant mutase that interconverts UDP-arabinofuranose and UDP-arabinopyranose. *Glycobiology.* **2007. 17 :** 345-354.

Kost B, Lemichez E, Spielhofer P, Hong Y, Tolias K, Carpenter C, Chua NH. Rac homologues and compartmentalized phosphatidylinositol 4, 5-bisphosphate act in a common pathway to regulate polar pollen tube growth. *J Cell Biol.* **1999. 145 :** 317-330.

Kotake T, Li YQ, Takahashi M, Sakurai N. Characterization and function of wall-bound exo-beta-glucanases of *Lilium longiflorum* pollen tubes. *Sex Plant Reprod.* **2000. 13 :** 1-9.

Kulikauskas R, McCormick S. Identification of the *tobacco* and *Arabidopsis* homologues of the pollen-expressed *LAT59* gene of tomato. *Plant Mol Biol.* **1997. 34 :** 809-814.

Lalanne E, Honys D, Johnson A, Borner GH, Lilley KS, Dupree P, Grossniklaus U, Twell D. *SETH1* and *SETH2*, two components of the glycosylphosphatidylinositol anchor biosynthetic pathway, are required for pollen germination and tube growth in *Arabidopsis*. *Plant Cell*. **2004. 16 :** 229-240.

Lamport DT, Kieliszewski MJ, Chen Y, Cannon MC. Role of the extensin superfamily in primary cell wall architecture. *Plant Physiol.* **2011. 156 :** 11-19.

Lampugnani ER, Moller IE, Cassin A, Jones DF, Koh PL, Ratnayake S, Beahan CT, Wilson SM, Bacic A. *In-vitro* grown pollen tubes of *Nicotiana alata* actively synthesise a fucosylated xyloglucan. *PLoS ONE*. **2013. 8 :** 77140.

Lang V, Usadel B, Obermeyer G. *De novo* sequencing and analysis of the lily pollen transcriptome : an open access data source for an orphan plant species. *Plant Mol Biol.* **2015. 87 :** 69-80.

Lehner A, Dardelle F, Soret-Morvan O, Lerouge P, Driouich A, Mollet JC. Pectins in the cell wall of *Arabidopsis thaliana* pollen tube and pistil. *Plant Signal Behav.* **2010. 5 :** 1282-1285.

Lehner A, Menu-Bouaouiche L, Dardelle F, Le Mauff F, Driouich A, Lerouge P, Mollet JC. *In silico* prediction of proteins related to xyloglucan fucosyltransferases in Solanaceae genomes. *Plant Signal Behav.* **2015. 10 :** e1026023.

Lennon KA, Lord EM. *In-vivo* pollen tube cell of *Arabidopsis thaliana* I. Tube cell cytoplasm and wall. *Protoplasma*. **2000. 214 :** 45-56.

Leroux C, Bouton S, Kiefer-Meyer MC, Ndinyanka Fabrice T, Mareck A, Guénin S, Fournet F, Ringli C, Pelloux J, Driouich A, Lerouge P, Lehner A, Mollet JC. *PECTIN METHYLESTERASE48* is involved in *Arabidopsis* pollen grain germination. *Plant Physiol*. **2015. 167 :** 347-380.

Lerouxel O, Choo TS, Séveno M, Usadel B, Faye L, Lerouge P, Pauly M. Rapid structural phenotyping of plant cell wall mutants by enzymatic oligosaccharide fingerprinting. *Plant Physiol.* **2002. 130 :** 1754-1763.

Li YQ, Faleri C, Geitmann A, Zhang HQ, Cresti M. Immunogold localization of arabinogalactan proteins, unesterified and esterified pectins in pollen grains and pollen tubes of *Nicotiana tabacum* L**.** *Protoplasma*. **1995. 189 :** 26-36.

Li YQ, Mareck A, Faleri C, Moscatelli A, Liu Q, Cresti M. Detection and localization of pectin methylesterase isoforms in pollen tubes of *Nicotiana tabacum L*. *Planta*. **2002. 214 :** 734-740.

Li H, Lin Y, Heath RM, Zhu MX, Yang Z. Control of pollen tube tip growth by a Rop GTPase–dependent pathway that leads to tip-localized calcium influx. *Plant Cell*. **1999. 11 :** 1731-1742.

Liepman AH, Wightman R, Geshi N, Turner SR, Scheller HV. *Arabidopsis* - a powerful model system for plant cell wall research. *Plant J.* **2010. 61 :** 1107-1121.

Lin Y, Wang Y, Zhu JK, Yang Z. Localization of a Rho GTPase implies a role in tip growth and movement of the generative cell in pollen tubes. *Plant Cell.* **1996. 8 :** 293-303.

Lin Y, Yang Z. Inhibition of pollen tube elongation by microinjected anti-Rop1Ps antibodies suggests a crucial role for Rho-type GTPases in the control of tip growth. *Plant Cell.* **1997. 9 :** 1647-1659.

Lindsay SE, Fry SC. Control of diferulate formation in dicotyledonous and gramineous cell-suspension cultures. *Planta*. **2008. 227 :** 439-452.

Liszkay A, van der Zalm E, Schopfer P. Production of reactive oxygen intermediates (O2−, H_2O_2, and OH) by maize roots and their role in wall loosening and elongation growth. *Plant Physiol*. **2004. 136 :** 3114-3123.

Liu XL, Liu L, Niu QK, Xia C, Yang KZ, Li R, Chen LQ, Zhang XQ, Zhou Y, Ye D. *MALE GAMETOPHYTE DEFECTIVE 4* encodes a rhamnogalacturonan II xylosyltransferase and is important for growth of pollen tubes and roots in *Arabidopsis*. *Plant J.* **2011. 65 :** 647-660.

Macquet A, Ralet MC, Kronenberger J, Marion-Poll A, North HM. In Situ, chemical and macromolecular study of the composition of *Arabidopsis thaliana* seed coat mucilage. *Plant Cell Physiol.* **2007. 48 :** 984-999.

Mangano S, Juárez SPD, Estevez JM. ROS regulation of polar growth in plant cells. *Plant Physiol.* **2016. 171 :** 1593-1605.

Marin-Rodriguez MV, Orchard J, Seymour GB. Pectate lyases, cell wall degradation and fruit softening. *J Exp Bot.* **2002. 53 :** 2115-2119.

Matoh T, Takasaki M, Takabe K, Kobayashi M. Immunocytochemistry of rhamnogalacturonan II in cell walls of higher plants. *Plant Cell Physiol.* **1998**. **39 :** 483-491.

Matsunaga T, Ishii T, Matsumoto S, Higuchi M, Darvill A, Albersheim P, O'Neill MA. Occurrence of the primary cell wall polysaccharide rhamnogalacturonan II in pteridophytes, lycophytes, and bryophytes. Implications for the evolution of vascular plants. *Plant Physiol.* **2004. 134 :** 339-351.

McCann MC, Carpita NC. Designing the deconstruction of plant cell walls. *Curr Opin Plant Biol.* **2008. 11 :** 314-320.

McCann MC, Wells B, Roberts K. Direct visualization of cross-links in the primary plant cell wall. *J Cell Sci*. **1990. 96 :** 323-334.

McCartney L, Ormerod AP, Gidley MJ, Knox JP. Temporal and spatial regulation of pectic (1-->4)-beta-D-galactan in cell walls of developing pea cotyledons : implications for mechanical properties. *Plant J*. **2000. 22 :** 105-113.

Mendrinna A, Persson S. Root hair growth: it's a one way street. *F1000 Prime Rep.***2015. 7.**

Micheli F. Pectin methylesterases : cell wall enzymes with important roles in Plant Physiol. *Trends Plant Sci.* **2001. 6 :** 414-419.

Micheli F, Holliger C, Goldberg R and Richard L. Characterization of the *pectin methylesterase-like* gene *AtPME3* : a new member of a gene family comprising at least 12 genes in *Arabidopsis thaliana. Gene.* **1998. 220 :** 13-20.

Molendijk AJ, Bischoff F, Rajendrakumar CS, Friml J, Braun M, Gilroy S, Palme, K. Arabidopsis thaliana Rop GTPases are localized to tips of root hairs and control polar growth. *EMBO J.* **2001. 20 :** 2779-2788.

Mollet JC, Faugeron C, Morvan H. Cell adhesion, separation and guidance in compatible plant reproduction. *Annu Plant Rev.* **2007. 25 :** 69-90.

Mollet JC, Kim S, Jauh GY, Lord EM. AGPs, pollen tube growth and the reversible effects of Yariv phenylglycoside. *Protoplasma.* **2002. 219 :** 89-98.

Mollet JC, Leroux C, Dardelle F, Lehner A. Cell wall composition, biosynthesis and remodeling during pollen tube growth. *Plants.* **2013. 2 :** 107-147.

Mollet JC, Park SY, Nothnagel EA, Lord EM. A lily stylar pectin is necessary for pollen tube adhesion to an *in-vitro* stylar matrix. *Plant Cell.* **2000. 12 :** 1737-1749.

Moscatelli A, Idilli AI. Pollen tube growth : A delicate equilibrium between secretory and endocytic pathways. *J Integr Plant Biol.* **2009. 51 :** 727-739.

Mouille G, Ralet MC, Cavelier C, Eland C, Effroy D, Hématy K, McCartney L, Truong HN, Gaudon V, Thibault JF, Marchant A, Höfte H. Homogalacturonan synthesis in *Arabidopsis thaliana* requires a Golgi-localized protein with a putative methyltransferase domain. *Plant J.* **2007. 50 :** 605-614.

Nezames CD, Sjogren CA, Barajas JF, Larsen PB. The *Arabidopsis* cell cycle checkpoint regulators TANMEI/ALT2 and ATR mediate the active process of aluminum-dependent root growth inhibition. *Plant Cell.* **2012. 24 :** 608-621.

Nguema-Ona E, Andème-Onzighi C, Aboughe-Angone S, Bardor M, Ishii T, Lerouge P, Driouich A. The *reb1-1* mutation of *Arabidopsis*. Effect on the structure and localization of galactose-containing cell wall polysaccharides. *Plant Physiol*. **2006. 140 :** 1406-1417.

Nguema-Ona E, Coimbra S, Vicré-Gibouin M, Mollet JC, Driouich A. Arabinogalactan-proteins in root and pollen tube cells : Distribution and functional aspects. *Ann Bot.* **2012. 110 :** 383-404.

Nishikawa S, Zinkl GM, Swanson RJ, Maruyama D, Preuss D. Callose (beta-1,3 glucan) is essential for *Arabidopsis* pollen wall patterning, but not tube growth. *BMC Plant Biol.* **2005. 5 :** 22-32.

Obel N, Erben V, Schwarz T, Kühnel S, Fodor A, Pauly M. Microanalysis of plant cell wall polysaccharides. *Mol Plant*. **2009. 2 :** 922-932.

O'Neill MA, Eberhard S, Albersheim P, Darvill AG. Requirement of borate cross-linking of cell wall rhamnogalacturonan II for *Arabidopsis* growth. *Science*. **2001. 294 :** 846-849.

O'Neill MA, Warrenfeltz D, Kates K, Pellerin P, Doco T, Darvill AG, Albersheim P. Rhamnogalacturonan-II, a pectic polysaccharide in the walls of growing plant cell, forms a dimer that is covalently cross-linked by a borate ester. *In-vitro* conditions for the formation and hydrolysis of the dimer. *J Biol Chem.* **1996. 271 :** 22923-22930.

Oxley D, Bacic A. Structure of the glycosylphosphatidylinositol anchor of an arabinogalactan protein from Pyrus communis suspension-cultured cells. *Proc Natl Acad Sci USA*. **1999. 96 :** 14246-14251.

Palusa SG, Golovkin M, Shin SB, Richardson DN, Reddy AS. Organ-specific, developmental, hormonal and stress regulation of expression of putative pectate lyase genes in *Arabidopsis*. *New Phytol.* **2007. 174 :** 537-550.

Parre E, Geitmann A. More than a leak sealant. The mechanical properties of callose in pollen tubes. *Plant Physiol.* **2005a. 137 :** 274-286.

Parre E, Geitmann A. Pectin and the role of the physical properties of the cell wall in pollen tube growth of *Solanum chacoense*. *Planta.* **2005b. 220 :** 582-592.

Paynel F, Leroux C, Surcouf O, Schaumann A, Pelloux J, Driouich A, Mollet JC, Lerouge P, Lehner A, Mareck A. Kiwi fruit PMEI inhibits PME activity, modulates root elongation and induces pollen tube burst in *Arabidopsis thaliana*. *Plant Growth Reg.* **2014. 74 :** 285-297.

Peaucelle A, Braybrook SA, Le Guillou L, Bron E, Kuhlemeier C, Hofte H. Pectin-induced changes in cell wall mechanics underlie organ initiation in Arabidopsis. *Curr Biol.* **2011. 21 :** 1720–1726.

Pereira LG, Coimbra S, Oliveira H, Monteiro L, Sottomayor M. Expression of arabinogalactan protein genes in pollen tubes of *Arabidopsis thaliana*. *Planta.* **2006. 223 :** 374-380.

Pereira AM, Masiero S, Nobre MS, Costa ML, Solís MT, Testillano PS, Sprunck S, Coimbra S. Differential expression patterns of *Arabinogalactan Proteins* in *Arabidopsis thaliana* reproductive tissues. *J Exp Bot*. **2014. 65 :** 5459-5471.

Pelloux J, Rustérucci C, Mellerowicz EJ. New insights into pectin methylesterase structure and function. *Trends Plant Sci.* **2007. 12 :** 267-277.

Pérez S, Rodríguez-Carvajal MA, Doco T. A complex plant cell wall polysaccharide: rhamnogalacturonan II. A structure in quest of a function. *Biochimie.* **2003. 85** : 109-121.

Perrin RM, DeRocher AE, Bar-Peled M, Zeng W, Norambuena L, Orellana A, ... , Keegstra K. Xyloglucan fucosyltransferase, an enzyme involved in plant cell wall biosynthesis. S*cience*. **1999. 284:** 1976-1979.

Pina C, Pinto F, Feijó JA, Becker JD. Gene family analysis of the *Arabidopsis* pollen transcriptome reveals biological implications for cell growth, division control, and gene expression regulation. *Plant Physiol.* **2005. 138 :** 744-756.

Potocký M, Jones MA, Bezvoda R, Smirnoff N, Žárský V. Reactive oxygen species produced by NADPH oxidase are involved in pollen tube growth. *New Phytol.* **2007. 174 :** 742-751.

Prado AM, Porterfield DM, Feijo JA. Nitric oxide is involved in growth regulation and re-orientation of pollen tubes. *Development*. **2004. 131 :** 2707-2714.

Prado AM, Colaco R, Moreno N, Silva AC, Feijo JA. Targeting of pollen tubes to ovules is dependent on nitric oxide (NO) signaling. *Mol Plant*. **2008. 1 :** 703-714.

Qin Y, Chen D, Zhao J. Localization of arabinogalactan proteins in anther, pollen, and pollen tube of *Nicotiana tabacum* L. *Protoplasma*. **2007. 231 :** 43-53.

Qin Y, Leydon AR, Manziello A, Pandey R, Mount D, Denic S, Vasic B, Johnson MA, Palanivenu R. Penetration of the stigma and style elicits a novel transcriptome in pollen tubes, Pointing to genes critical for growth in a pistil. *PLoS Genet.* **2009. 5 :** e1000621.

Raiola A, Camardella L, Giovane A, Mattei B, De Lorenzo G, Cervone F, Bellicampi D. Two *Arabidopsis thaliana* genes encode functional pectin methylesterase inhibitors. *FEBS Lett*. **2004. 557 :** 199-203.

Ralet MC, Crepeau MJ, Lefebvre J, Mouille G, Hofte H, Thibault JF. Reduced number of homogalacturonan domains in pectins of an *Arabidopsis* mutant enhances the flexibility of the polymer. *Biomacromol*. **2008. 9 :** 1454-1460.

Ralet MC, Tranquet O, Poulain D, Moïse A, Guillon F. Monoclonal antibodies to rhamnogalacturonan I backbone. *Planta*. **2010. 231 :** 1373-1383.

Rautengarten C, Ebert B, Herter T, Petzold CJ, Ishii T, Mukhopadhyay A, Usadel B, Scheller HV. The interconversion of UDP-arabinopyranose and UDP-arabinofuranose is indispensable for plant development in *Arabidopsis*. *Plant Cell.* **2011. 23 :** 1373-1390.

Ray PM, Green PB, Cleland R. Role of turgor in plant cell growth. *Nature.* **1972. 239 :** 163-164.

Roberts K. How the cell wall acquired a cellular context. *Plant Physiol.* **2001. 125 :** 127-130.

Roggen HPJ, Stanley RG. Cell-wall-hydrolysing enzymes in wall formation as measured by pollen-tube extension. *Planta.* **1969. 84 :** 295-303.

Rong D, Luo N, Mollet JC, Liu X, Yang Z. Salicylic acid regulates pollen tip growth through an NPR3/NPR4-independent pathway. *Mol Plant.* **2016. 9 :** 1478-1491.

Roy S, Eckard KJ, Lancelle S, Hepler PK, Lord EM. High-pressure freezing improves the ultrastructural preservation of in-vivo grown lily pollen tubes. *Protoplasma*. **1997. 200 :** 87-98.

Roy S, Jauh GY, Hepler PK, Lord EM. Effects of Yariv phenylglycoside on cell wall assembly in the lily pollen tube. *Planta*. **1998. 204 :**450-458.

Rubinstein AL, Márque J, Cervera MS, Bedinger PA. Extensin-like glycoproteins in the maize pollen tube wall. *Plant Cell.* **1995. 7 :** 2211-2225.

Scheller HV, Ulvskov P. Hemicelluloses. *Annu Rev Plant Physiol Plant Mol Biol*. **2010. 61 :** 263-289.

Schlüpmann H, Bacic A, Read SM. Uridine diphosphate glucose metabolism and callose synthesis in cultured pollen tubes of *Nicotiana alata* Link et Otto. *Plant Physiol*. **1994. 105 :** 659-670.

Schols HA, Vierhuis E, Bakx EJ, Voragen AG. Different populations of pectic hairy regions occur in apple cell walls. *Carbohydr Res.* **1995. 275 :** 343-360.

Schopfer P, Plachy C, Frahry G. Release of reactive oxygen intermediates (superoxide radicals, hydrogen peroxide, and hydroxyl radicals) and peroxidase in germinating radish seeds controlled by light, gibberellin, and abscisic acid. *Plant Physiol*. **2001. 125 :** 1591-1602.

Schultz CJ, Rumsewicz MP, Johnson KL, Jones BJ, Gaspar YG, Bacic A. Using genomic resources to guide research directions. The arabinogalactan protein gene family as a test case. *Plant Physiol*. **2002. 129 :** 1448-1463.

Shin SB, Golovkin M, Reddy AS. A pollen-specific calmodulin-binding protein, NPG1, interacts with putative pectate lyases. *Sci Rep*. **2014. 4.**

Seifert GJ, Roberts K. The biology of arabinogalactan proteins. *Annu Rev Plant Biol.* **2007. 58 :** 137-161.

Sénéchal F, Graff L, Surcouf O, Marcelo P, Rayon C, Bouton S, Mareck A, Mouille G, Stintzi A, Höfte H, Lerouge P, Schaller A, Pelloux J. *Arabidopsis PECTIN METHYLESTERASE 17* is co-expressed with and processed by *SBT3.5*, a subtilisin-like serine protease. *Ann Bot*. **2014. 114 :** 1161-1175.

Shibuya N, Minami E. Oligosaccharide signalling for defence responses in plant. *Physiol Mol Plant Pathol.* **2001. 59 :** 223-233.

Showalter AM. Structure and function of plant cell wall proteins. *Plant Cell*. **1993. 5 :** 9-23.

Silipo A, Erbs G, Shinya T, Dow JM, Parrilli M, Lanzetta R, Shibuya N, Newman M, Molinaro A. Glyco-conjugates as elicitors or suppressors of plant innate immunity. *Glycobiology*. **2010. 20 :** 406-419.

Smallwood M, Beven A, Donovan N, Neill SJ, Peart J, Roberts K, Knox JP. Localization of cell wall proteins in relation to the developmental anatomy of the carrot root apex. *Plant J.* **1994. 5 :** 237-246.

Sommer-Knudsen J, Clarke AE, Bacic A. Proline- and hydroxyproline-rich gene products in the sexual tissues of flowers. *Sex Plant Reprod.* **1997. 10 :** 253-260.

Sørensen I, Pettolino FA, Wilson SM, Doblin MS, Johansen B, Bacic A, Willats WGT. Mixed-linkage (1-->3),(1-->4)-beta-D-glucan is not unique to the Poales and is an abundant component of Equisetum arvense cell walls. *Plant J.* **2008. 54 :** 510-521.

Speranza A, Crinelli R, Scoccianti V, Geitmann A. Reactive oxygen species are involved in pollen tube initiation in kiwifruit. *Plant Biol.* **2012. 14 :** 64-76.

Sun L, Van Nocker S. Analysis of promoter activity of members of the *PECTATE LYASE-LIKE* (*PLL*) gene family in cell separation in *Arabidopsis*. *BMC Plant Biol.* **2010. 10 :** 152.

Svetek J, Yadav MP, Nothnagel EA. Presence of a glycosylphosphatidylinositol lipid anchor on rose arabinogalactan proteins. *J Biol Chem*. **1999. 274 :** 14724-14733.

Takeda H, Yoshikawa T, Liu XZ, Nakagawa N, Li YQ, Sakurai N. Molecular cloning of two exo-beta-glucanases and their *in-vivo* substrates in the cell walls of *lily* pollen tubes. *Plant Cell Physiol.* **2004. 45 :** 436-444.

Takos AM, Dry LB, Soole KL. Glycosyl-phosphatidylinositol-anchor addition signals are processed in *Nicotiana tabacum. Plant J.* **2000. 21 :** 43-52.

Tamari F, Shore JS. Allelic variation for a short-specific polygalacturonase in *Turnera subulata*: Is it associated with the degree of self-compatibility? *Int J Plant Sci.* **2006. 167 :** 125-133.

Tenhaken R. Cell wall remodeling under abiotic stress. *Front Plant Sci.* **2014. 5.**

Testerink C, Munnik T. Molecular, cellular, and physiological responses to phosphatidic acid formation in plants. *J Exp Bot*. **2011. 62 :** 2349-2361.

Thompson JE, Fry SC. Evidence for covalent linkage between xyloglucan and acidic pectins in suspension-cultured rose cells. *Planta.* **2000. 211 :** 275-286.

Tian GW, Chen MH, Zaltsman A, citovsky V. Pollen-specific pectin methylesterase involved in pollen tube growth. *Dev Biol.* **2006. 294 :** 83-91.

Tryfona T, Liang HC, Kotake T, Kaneko S, Marsh J, Ichinose H, Lovegrove A, Tsumuraya Y, Shewry PR, Stephens E, Dupree P. Carbohydrate structural analysis of wheat flour arabinogalactan protein. *Carbohyd Res*. **2010. 345 :** 2648-2656.

Verma DP, Hong Z. Plant callose synthase complexes. *Plant Mol Biol.* **2001. 47 :** 693-701.

Vidal S, Williams P, O'Neill MA, Pellerin P. Polysaccharides from grape berry cell walls. Part I : tissue distribution and structural characterization of the pectic polysaccharides. *Carbohydr Polymers.* **2001. 45 :** 315-323.

Vidali L, Rounds CM, Hepler PK, Bezanilla M. Lifeact-mEGFP reveals a dynamic apical F-actin network in tip growing plant cells. *PloS one*. **2009. 4 :** e5744.

Vogler F, Konrad SS, Sprunck S. Knockin'on pollen's door: live cell imaging of early polarization events in germinating Arabidopsis pollen. *Front. Plant Sci.* **2015. 6.**

Vogler F, Sprunck S. F-actin forms mobile and unwinding ring-shaped structures in germinating Arabidopsis pollen expressing Lifeact. *Plant Signal Behav.* **2015. 10 :** e1075684.

Voxeur A, Gilbert L, Rihouey C, Driouich A, Rothan C, Baldet P, Lerouge P. Silencing of the GDP-D-mannose 3,5-epimerase affects the structure and cross-linking of the pectic

polysaccharide rhamnogalacturonan II and plant growth in tomato. *J Biol Chem.* **2011. 286 :** 8014-8020.

Whitcombe AJ, O'Neill MA, Steffan W, Albersheim P, Darvill AG. Structural characterization of the pectic polysaccharide, rhamnogalacturonan-II. *Carbohydr Res.* **1995. 271 :** 15-29.

Willats WG, McCartney L, Steele-King CG, Marcus SE, Mort A, Huisman M, Van Alebeek GJ, Schols HA, Voragen AGJ, Le Goff A, Bonnin E, Thibault JF, Knox JP. A xylogalacturonan epitope is specifically associated with plant cell detachment. *Planta*. **2004. 218 :** 673-681.

Willats WG, Marcus SE, Knox JP. Generation of a monoclonal antibody specific to (1→5)-α-L-arabinan. *Carbohydr Res*. **1998. 308 :** 149-152.

Wing RA, Yamaguchi J, Larabell SK, Ursin VM, McCormick S. Molecular and genetic characterization of two pollen-expressed genes that have sequence similarity to pectate lyases of the plant pathogen *Erwinia*. *Plant Mol Biol.* **1989. 14 :** 17-28.

Wolf S, Höfte H. Growth control: a saga of cell walls, ROS, and peptide receptors. *Plant Cell*. **2014. 26 :** 1848-1856.

Wolf S, Grsic-Rausch S, Rausch T, Greiner S. Identification of pollen-expressed pectin methylesterase inhibitors in *Arabidopsis*. *FEBS Lett.* **2003. 555 :** 551-555.

Wolf S, Mouille G, Pelloux J. Homogalacturonan methyl-esterification and plant development. *Mol Plant.* **2009. 2 :** 851-560.

Woriedh M, Wolf S, Márton ML. External application of gametophyte-specific *Zm*PMEI1 induces pollen tube burst in maize. *Plant Reprod.* **2013. 26 :** 255-266.

Wu HM, Wang H, Cheung AY. A pollen tube growth stimulatory glycoprotein is deglycosylated by pollen tubes and displays a glycosylation gradient in the flower. *Cell.* **1995. 82 :** 395-403.

Xie B, Wang X, Zhu M, Zhang Z, Hong Z. *CalS7* encodes a callose synthase responsible for callose deposition in the phloem. *Plant J.* **2011. 65 :** 1-14.

Yariv J, Lis E, Katchalski E. Precipitation of arabic acid and some seed polysaccharides by glycosylphenylazo dyes. *Biochem J.* **1967. 105 :** 1-2.

Yariv J, Rapport MM, Graf L. The interaction of glycosides and saccharides with antibody to the corresponding phenylazo glycosides. *Biochem J*. **1962. 85 :** 383-388.

Zablackis E, Huang J, Müller B, Darvill AG, Albersheim P. Characterization of the cell-wall polysaccharides of *Arabidopsis thaliana* leaves. *Plant Physiol.* **1995. 107 :** 1129-1138.

Zaidi MA, O'Leary S, Wu S, Gleddie SC, Eudes F, Laroche A, Robert LS. A molecular and proteomic investigation of proteins rapidly released from triticale pollen upon hydration. *Plant Mol Biol.* **2012. 79 :** 101-121.

Zandleven J, Sørensen SO, Harholt J, Beldman G, Schols HA, Scheller HV, Voragen AJ. Xylogalacturonan exists in cell walls from various tissues of Arabidopsis thaliana. *Phytochem*. **2007. 68 :** 1219-1226.

Zhang X, Ma H, Qi H, Zhao J. Roles of hydroxyproline-rich glycoproteins in the pollen tube and style cell growth of tobacco (*Nicotiana tabacum L.*). *J Plant Physiol.* **2014. 171 :** 1036-1045.

Zhang GF, Staehelin LA. Functional compartmentation of the Golgi apparatus of plant cells: Immunocytochemical analysis of high-pressure frozen- and freeze-substituted sycamore maple suspension culture cells. *Plant Physiol.* **1992. 99 :** 1070-1083.

Zhu Y, Zhao P, Wu X, Wang W, Scali M, Cresi M. Proteomic identification of differentially expressed proteins in mature and germinated maize pollen. *Acta Physiol Planta.* **2011. 33 :** 1467-1474.

10. Principales publications

ACL-12 Dardelle F, **Lehner A**, Ramdani Y, Bardor M, Lerouge P, Driouich A, Mollet JC. 2010. Biochemical and immunocytological characterizations of Arabidopsis thaliana pollen tube cell wall. ***Plant Physiology***, 153, 1563-1576. (IF_{2010} 6.45).

ACL-15 Mollet JC, Leroux C, Dardelle F, **Lehner A**. 2013. Cell wall composition, biosynthesis and remodeling during pollen tube growth. ***Plants,*** 2, 107-147. Revue sur invitation

ACL-17 Dumont M, **Lehner A**, Bouton S, Kiefer-Meyer MC, Voxeur A, Pelloux J, Lerouge P, Mollet JC. 2014. The cell wall pectic polymer rhamnogalacturonan-II is required for proper pollen tube elongation: implication of a putative sialyltransferase-like protein. ***Annals of Botany***, 114, 1177-1188. (IF_{2014} 3.65).

ACL-19 Leroux C, Bouton S, Kiefer-Meyer MC, Ndinyanka Fabrice T, Mareck A, Guénin S, Fournet F, Ringli C, Pelloux J, Driouich A, Lerouge P, **Lehner A***, Mollet JC*. 2015. PECTIN METHYLESTERASE48 is involved in Arabidopsis pollen grain germination. ***Plant Physiology***, 167, 367-380. (IF_{2015} 6.28). * Equal contribution of the senior authors.

ACL-23 Dumont M, **Lehner A**, Bardor M, Burel C, Vauzeilles B, Lerouxel O, Anderson CT, Mollet JC, Lerouge P. 2015. Inhibition of fucosylation of cell wall components by 2-fluoro 2-deoxy-L-fucose induces defects in root cell elongation. ***Plant Journal***, 84, 1137-1151. (IF_{2015} 5.47).

Biochemical and Immunocytological Characterizations of Arabidopsis Pollen Tube Cell Wall[1][C][W][OA]

Flavien Dardelle, Arnaud Lehner, Yasmina Ramdani, Muriel Bardor, Patrice Lerouge, Azeddine Driouich, and Jean-Claude Mollet*

Laboratoire de Glycobiologie et Matrice Extracellulaire Végétale, UPRES EA 4358, Institut Fédératif de Recherche Multidisciplinaire sur les Peptides 23 (F.D., A.L., M.B., P.L., J.-C.M.), and Plate-forme de Recherche en Imagerie Cellulaire de Haute Normandie (Y.R., A.D.), Université de Rouen, 76821 Mont Saint-Aignan cedex, France

During plant sexual reproduction, pollen germination and tube growth require development under tight spatial and temporal control for the proper delivery of the sperm cells to the ovules. Pollen tubes are fast growing tip-polarized cells able to perceive multiple guiding signals emitted by the female organ. Adhesion of pollen tubes via cell wall molecules may be part of the battery of signals. In order to study these processes, we investigated the cell wall characteristics of in vitro-grown Arabidopsis (*Arabidopsis thaliana*) pollen tubes using a combination of immunocytochemical and biochemical techniques. Results showed a well-defined localization of cell wall epitopes. Low esterified homogalacturonan epitopes were found mostly in the pollen tube wall back from the tip. Xyloglucan and arabinan from rhamnogalacturonan I epitopes were detected along the entire tube within the two wall layers and the outer wall layer, respectively. In contrast, highly esterified homogalacturonan and arabinogalactan protein epitopes were found associated predominantly with the tip region. Chemical analysis of the pollen tube cell wall revealed an important content of arabinosyl residues (43%) originating mostly from (1→5)-α-L-arabinan, the side chains of rhamnogalacturonan I. Finally, matrix-assisted laser desorption ionization time-of-flight mass spectrometry analysis of endo-glucanase-sensitive xyloglucan showed mass spectra with two dominant oligosaccharides (XLXG/XXLG and XXFG), both being mono *O*-acetylated, and accounting for over 68% of the total ion signals. These findings demonstrate that the Arabidopsis pollen tube wall has its own characteristics compared with other cell types in the Arabidopsis sporophyte. These structural features are discussed in terms of pollen tube cell wall biosynthesis and growth dynamics.

Fertilization of flowering plants requires the delivery of the two sperm cells, carried by a fast growing tip-polarized pollen tube, to the egg cell. In plants with dry stigma and solid style such as Arabidopsis (*Arabidopsis thaliana*), this process begins with the deposition and specific adhesion of the pollen grains on the stigmatic tissue, subsequent hydration of the pollen grains, and germination of pollen tubes (Palanivelu and Preuss, 2000). Pollen tubes invade the papillae cell wall of the stigma, enter the short style, and grow through the apoplast of the specialized transmitting tract (TT) that is filled with a nutrient-rich extracellular matrix (Kandasamy et al., 1994; Lennon et al., 1998). During this invasive growth, pollen tubes are guided to the ovules via signals that need to pass through the cell wall to reach their membrane-associated or intracellular targets (Lord and Russell, 2002; Kim et al., 2003; Boavida et al., 2005; McCormick and Yang, 2005; Johnson and Lord, 2006). In plant species with wet stigma and hollow style such as lily (*Lilium longiflorum*), adhesion between the pollen tube wall and the TT epidermis extracellular matrix is important for the growth of the pollen tubes toward the ovules (Mollet et al., 2000, 2007; Park et al., 2000; Chae et al., 2007). In addition to being the interface between the tube cells and the surroundings (female sporophyte or culture medium), the pollen tube wall also controls the cell shape, protects the generative cells, and allows resistance against turgor pressure (Geitmann and Steer, 2006; Geitmann, 2010).

Most of our knowledge on cell wall polymers of higher plants comes from investigations on vegetative organs in which cells have diffuse growth. The cell wall is mainly composed of polysaccharides (cellulose, hemicellulose, pectin, and occasionally callose, depending on the tissue) and proteoglycans (e.g. extensin and arabinogalactan proteins [AGPs]) forming a complex network with processing enzymes.

Pectins are complex wall macromolecules with uncertain supramolecular organization (Vincken et al., 2003) consisting of homogalacturonan (HG) that can be methylesterified and acetylesterified, rhamnogalac-

[1] This work was supported by the University of Rouen, le Grand Réseau de Recherche Végétal, Agronomie et Transformation des Agroressources de Haute Normandie, and the CNRS.

* Corresponding author; e-mail jean-claude.mollet@univ-rouen.fr.

The author responsible for distribution of materials integral to the findings presented in this article in accordance with the policy described in the Instructions for Authors (www.plantphysiol.org) is: Jean-Claude Mollet (jean-claude.mollet@univ-rouen.fr).

[C] Some figures in this article are displayed in color online but in black and white in the print edition.

[W] The online version of this article contains Web-only data.

[OA] Open Access articles can be viewed online without a subscription.

www.plantphysiol.org/cgi/doi/10.1104/pp.110.158881

turonan I (RG-I), rhamnogalacturonan II (RG-II), and xylogalacturonan (Carpita and McCann, 2000). HG is a polymer of repeated units of (1→4)-α-D-GalUA that can be cross-linked with calcium upon block-wise action of pectin methylesterases (PMEs) on methylesterified HG (Micheli, 2001). RG-II has the same homopolymer backbone as HG but is substituted with four different oligosaccharides composed of unusual sugars, such as apiose, aceric acid, and 3-deoxy-D-manno-2-octulosonic acid, of unknown function (for review, see Caffall and Mohnen, 2009). RG-I consists of the repeating disaccharide (1→4)-α-D-GalUA-(1→2)-α-L-Rha, with a wide variety of side chains attached to the rhamnosyl residues, ranging from monomers to large oligosaccharides such as (1→4)-β-D-galactan, (1→5)-α-L-arabinan, and/or type I arabinogalactan (Caffall and Mohnen, 2009).

Xyloglucan (XyG) is the major hemicellulosic polysaccharide of the primary wall of flowering plants. Classic XyG consists of a (1→4)-β-D-glucan backbone substituted with Xyl, Gal-Xyl, or Fuc-Gal-Xyl motifs, which correspond, according to the one-letter code proposed by Fry et al. (1993), to X, L, and F, respectively, G being the unsubstituted glucosyl residue of the glucan backbone. The main XyG fragments released after endo-glucanase treatment of the cell wall from wild-type Arabidopsis vegetative organs are generally XXXG, XXLG/XLXG, XXFG, and XLFG (Zablackis et al., 1995; Lerouxel et al., 2002; Nguema-Ona et al., 2006; Obel et al., 2009). In addition, *O*-acetylation of XyG can occur, most generally on the galactosyl residues, but its biological function is unknown (Cavalier et al., 2008). In the primary wall, XyG interacts with cellulose microfibrils via hydrogen bonds and participates in the control of cell expansion (Cosgrove, 1999).

AGPs and extensin belong to the Hyp-rich glycoproteins superfamily with very high levels of type II arabinogalactan glycosylation (Nothnagel, 1997; Showalter, 2001). These proteoglycans have been implicated in many aspects of plant development, including cell expansion, cell signaling and communication, embryogenesis, wound response, and pollen tube guidance (Wu et al., 1995; Nothnagel, 1997; Seifert and Roberts, 2007; Driouich and Baskin, 2008).

Despite the importance of pollen tubes for the delivery of the sperm cells to the egg, little is known about the underlying molecular mechanisms that regulate the mechanical interaction of pollen tubes with female floral tissues. There are very scarce data concerning the different components of the pollen tube cell wall. Past approaches to characterize the pollen tube cell wall are limited to a few plant genera, including *Camellia* (Nakamura and Suzuki, 1981), *Lilium* (Jauh and Lord, 1996; Mollet et al., 2002), *Nicotiana* (Rae et al.,1985; Li et al., 1995; Ferguson et al., 1998; Qin et al., 2007), *Pinus* (Derksen et al., 1999), and *Zea* (Rubinstein et al., 1995), and are mostly based on immunocytochemistry. These studies revealed that, depending on the species, the pollen tube cell wall contains epitopes that are found in the polymers described above, including HGs with varying levels of methylesterification, AGPs, extensin-like proteins, and low amounts of cellulose. Unlike most other plant cells, callose, a (1→3)-β-glucan, is predominant and is deposited in the wall back from the tip. Moreover, it is deposited at regular intervals to form callose plugs that maintain the tube cell in the apical expanding region of the tube and separate the viable from the degenerating region of the tube (for review, see Geitmann and Steer, 2006). Only a few reports have investigated the pollen tube of the model plant Arabidopsis. They have focused either on in vivo-grown or on in vitro-grown pollen tubes using monoclonal antibodies (MAbs) directed against a subset of cell wall epitopes present in HG, XyG, and AGPs (Lennon and Lord, 2000; Freshour et al., 2003; Pereira et al., 2006), but quantitative chemical analyses are lacking. This lack of information is most likely due to the fact that substantial amounts of pollen tube material are needed for chemical analysis, and a reproducible and efficient method for liquid culture of Arabidopsis pollen tubes had not been established until recently (Boavida and McCormick, 2007; Bou Daher et al., 2009).

Here, we report the composition and localization of different cell wall polymers of in vitro-grown wild-type Arabidopsis pollen tubes based on biochemical analyses coupled to immunocytochemical investigations both at light and transmission electron microscopy (TEM) levels using recently developed MAbs. Our results show distinct patterns of labeling (tip, whole tube, and shank of the tube) depending on the recognized epitope. The most striking observations are (1) the abundance of (1→5)-α-L-arabinan in the tube wall (greater than 40 mol % of Ara), mostly localized, with LM6 and LM13, in the outer wall layer of the tube and (2) an atypical XyG matrix-assisted laser desorption ionization time-of-flight mass spectrometry (MALDI-TOF MS) profile with over 68% of the oligosaccharide fragments being *O*-acetylated.

RESULTS

In Vitro Pollen Tube Growth and β-Glucan Localization

In order to study the cell wall of Arabidopsis pollen tubes, sufficient material was necessary to perform the biochemical analysis. To achieve this, a large number of flowers, a good in vitro pollen germination rate, and sufficient pollen tube length were required. As shown in Figure 1A, high rates of pollen germination were obtained (67% ± 12%), with an average pollen tube length of 1,248 ± 374 μm and a growth rate of 0.46 ± 0.05 μm min^{-1} after 16 h of culture in liquid medium. Moreover, 16-h-old pollen tubes displayed typical tip organization (Fig. 1A, inset) without any plasmolysis event. These results showed that using these in vitro conditions, pollen tube length is approaching what we should expect in in vivo conditions given the distance between stigma and ovules. By comparison, 6-h-old

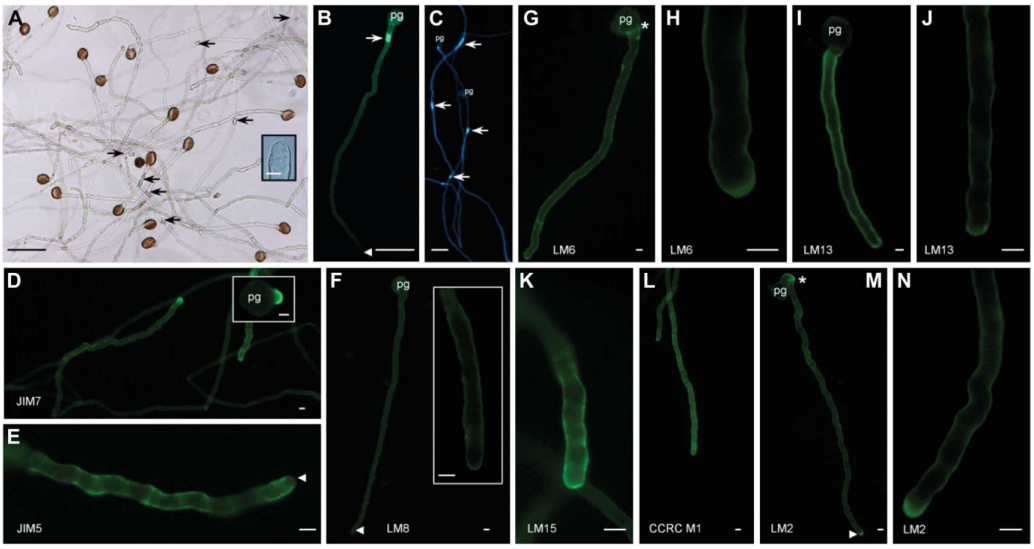

Figure 1. In vitro pollen tube growth, β-glucan staining, and immunolocalization of Arabidopsis pollen tube wall epitopes. A, Sixteen-hour-old in vitro pollen tubes grown in liquid medium (arrows show callose plugs). The inset is a closeup of a 16-h-old in vitro pollen tube tip. B, Cytochemical staining of β-glucan (callose) with aniline blue showing a callose plug (arrow) and a lack of staining in the pollen tube tip region (arrowhead). C, Cytochemical staining with calcofluor white showing callose plugs (arrows) and the localization of β-glucans in the wall. D to N, Immunofluorescence labeling of cell wall polymer epitopes at the surface of pollen tubes. D to F, Arabidopsis pollen tube wall epitopes probed with anti-pectin MAbs JIM7 (D), JIM5 (E), and LM8 (F), specific for highly and low methylesterified HG and xylogalacturonan, respectively. D, The JIM7 tag showed a strong signal at the tip in a well-developed pollen tube and emerging tube tip from the pollen grain (inset). E, Pollen tube stained with JIM5 showing a very weak intensity of labeling at the tip (arrowhead) compared with the wall back from the tip. F, LM8 labeled evenly the entire pollen tube wall. The insert is a closeup of an in vitro pollen tube tip. G to J, Detection of (1→5)-α-L-arabinan epitopes with LM6 (G and H) and LM13 (I and J). Labeling was evenly distributed along the entire tube wall, with a strong signal at the pollen tube tip. Note a collar-like structure (asterisk) labeled at the emergence of the pollen tube from the pollen grain in G. K and L, Immunofluorescence staining of the nongalactosylated (XXXG motif) and fucosylated XyG with LM15 (K) and CCRC-M1 (L), respectively. Labeling with both MAbs was not evenly detected in the wall and displayed periodic deposition of the epitopes containing polysaccharides during pollen tube growth. M and N, LM2, which recognizes β-D-Glc*p*UA-(1→3)-α-D-Gal*p*UA-(1→2)-L-Rha moieties of AGPs, labeled weakly the whole tube, with the strongest signal at the tip. In M, a more intense labeling (asterisk) was observed at the emergence of the tube from the pollen grain. Pollen tubes were grown for 6 h except in A and C (16 h). pg, Pollen grain. Bars = 50 μm (A–C) and 5 μm (A inset and D–N).

pollen tubes were 4-fold shorter, with an average length of 307 ± 102 μm and an estimated growth rate of 1.6 ± 0.17 μm min^{-1}.

Cytochemical staining of β-glucans with aniline blue (for callose) and calcofluor white (mainly callose and cellulose) was performed in order to visualize the distribution of these β-glucans along the tube wall and within the tube. Aniline blue staining was not detectable in the tip region and was mainly localized in the wall, back from the tip, and within the tube as callose plugs that are periodically synthesized (Fig. 1B; Table I). In contrast, staining with calcofluor white was uniform along the whole tube and the tip. The bright regions within the tubes revealed several plugs (Fig. 1C). At the ultrastructural level, the Arabidopsis pollen tube wall back from the tip appeared as a bilayered structure consisting of a fibrillar outer and a weakly electron-dense inner wall layer (Fig. 2A). Immunogold localization of callose resulted in dense labeling in the inner wall layer back from the tip (Supplemental Fig. S1A).

Immunolocalization of Arabidopsis Pollen Tube Cell Wall Epitopes

Immunolabeling Pattern of Pectin Domains

Probing with JIM7 and JIM5, which recognize highly and partially methylesterified HGs, revealed that JIM7 epitopes were dominantly localized in the tip region of the pollen tubes (Table I; Fig. 1D). Similar observations were made at tube tips emerging from

Table I. *Summary of cytochemical staining and immunolocalization of cell wall polymers in in vitro-grown Arabidopsis pollen tubes*

Data are based on observations at the fluorescence microscopy (FM) and electron microscopy (EM) levels. −, No labeling detected (at over 500-ms exposure time); ±, weak labeling detected; +, strong labeling detected. iw, Inner wall layer; na, not applicable; nd, not determined; ow, outer wall layer.

Target	Probe	Back from the Tip		Tip
		FM Level	EM Level	FM Level
β-Glucan	Calcofluor white	+	na	+
Callose	Aniline blue	+	na	−
	Anti-callose	nd	iw	nd
Extensin	LM1	−	nd	−
AGP	LM2	±	nd	+
	MAC207	±	nd	+
	JIM13	−	nd	−
HG	JIM5	+	nd	±
	JIM7	±	nd	+
Galactan	LM5	±	nd	±
Arabinan	LM6	+	ow	+
	LM13	+	nd	+
Xylogalacturonan	LM8	+	nd	+
XyG	CCRC-M1	+	iw/ow	+
	LM15	+	iw/ow	+
Controls		−	−	−

pollen grains (Fig. 1D, inset). In contrast, JIM5 staining was observed mostly back from the tip with brighter ring-like deposits, presumably originating from successive temporary slowdowns in the growth of the tubes (Fig. 1E). LM8, specific for xylogalacturonan epitopes, uniformly labeled the whole pollen tube wall (Fig. 1F, inset). (1→5)-α-L-Arabinan epitopes, localized with LM6 and LM13, were clearly detected in the entire pollen tube wall (Fig. 1, G and I), with stronger fluorescent signal at the pollen tube tip (Fig. 1, H and J). A ring-like structure was also noticeable as a collar at the emergence of the pollen tube from the pollen grain (Fig. 1G). Immunogold labeling of epitopes recognized by LM6 was mostly found in the fibrillar outer wall layer (Fig. 2, B and C). A strong concentration of gold particles was also observed over densely stained vesicles, possibly associated with the trans-Golgi network (Fig. 2B). Epitopes recognized by LM6 were also detected in the intine wall of the pollen grain (Supplemental Fig. S1B).

Immunolabeling of XyG Motifs

To investigate the distribution of XyG, pollen tubes were probed with the MAbs LM15 and CCRC-M1, which recognize nongalactosylated (XXXG motif) and fucosylated XyG domains, respectively. As shown in Figure 1, K and L, both MAbs bound to the entire pollen tube wall.

TEM observations showed that fucosylated XyG epitopes probed with the MAb CCRC-M1 were mainly found in the inner pollen tube wall (Fig. 2D), whereas the nongalactosylated XyG epitopes tagged with LM15 were detected in both the inner and outer layers of the wall (Fig. 2, E and F; Table I). Immunolabeling of pollen grains with the LM15 and CCRC-M1 MAbs resulted in a strong detection of XyG epitopes, mostly in the intine wall and at the vicinity of the plasma membrane (Supplemental Fig. S1, C and D).

Immunolabeling of AGPs

Epitopes of AGPs recognized by the MAb LM2 were found slightly labeled throughout the pollen tube wall, with a stronger signal in the tip region (Fig. 1, M and N; Table I). Similar results were observed with MAC207, whereas JIM13 did not label the tube cell wall (Table I).

Immunolabeling at the fluorescence microscopy level was carried out on 6- and 16-h-old pollen tubes and did not show any difference in labeling pattern between the two time points (data not shown). Controls for immunofluorescent labeling did not show any fluorescence of the pollen tubes and showed a weak autofluorescence of the pollen grain exine (data not shown). Controls for immunogold detection did not exhibit any significant nonspecific gold particles on the resin, pollen tubes, and pollen grains (Supplemental Fig. S1, E–H). A summary of immunolocalization data on the Arabidopsis pollen tube wall is shown in Table I.

Contribution of Pollen Grain Wall versus Pollen Tube Wall for Biochemical Analysis

We estimated the relative abundance of the pollen tube cell wall versus the pollen grain cell wall by measuring the cell wall thickness based on TEM observations, pollen germination rates, and pollen tube length (Supplemental Table S1). The estimated

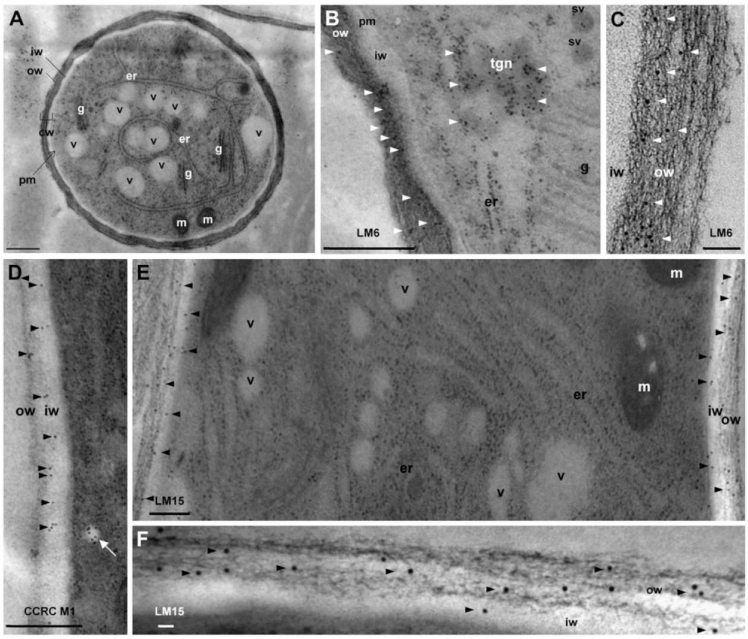

Figure 2. Electron micrographs showing the ultrastructure (A) and immunogold labeling of cell wall epitopes (B–F) of high-pressure frozen/freeze-substituted Arabidopsis pollen tube grown in vitro for 6 h. A, Cross section of a pollen tube showing the cell wall (cw) composed of two distinct layers: a fibrillar outer wall (ow) and a weakly electron-dense inner wall (iw). Well-preserved organelles are also clearly distinguishable, including endoplasmic reticulum (er), Golgi stacks (g), mitochondria (m), and vacuoles (v). pm, Plasma membrane. B and C, Immunogold labeling of (1→5)-α-L-arabinan epitopes with LM6. Gold particles (arrowheads) are mostly localized in the outer wall layer. In B, possible trans-Golgi network (tgn) and secretory vesicles (sv) labeled with LM6 are seen. D, Immunogold labeling of fucosylated XyG motif recognized by CCRC-M1 in the inner and outer wall layers. Note the presence of gold particles in vesicles in the vicinity of the plasma membrane (white arrow). E and F, Immunogold labeling of nonfucosylated XyG motif (XXXG) with LM15. Gold particles (arrowheads) are visible in the inner and mainly in the outer walls. Bars = 1 μm (A), 0.5 μm (B, D, and E), and 100 nm (C and F).

ratio of the pollen grain cell wall on the pollen tube cell wall was about 1:7.4. Similarly, we also quantified, by gas chromatography (GC), the amount of carbohydrates present in nongerminated pollen grains and 16-h-old germinated pollen tubes isolated from 520 flowers (Supplemental Fig. S2). Monosaccharide composition of the pollen grain and the pollen tube cell walls was similar, and the amount of carbohydrates contained in the pollen grain cell wall was 8-fold lower than the amount of carbohydrates contained in the pollen tube cell wall. These data indicate that the quantity of pollen grain cell wall material would interfere only weakly in the cell wall analysis and were used as a baseline for the monosaccharide composition of Arabidopsis pollen tubes.

Monosaccharide Composition of the Arabidopsis Pollen Tube Wall

Monosaccharide analysis of Arabidopsis pollen tube cell wall (Table II) displayed a high level of Glc (19.8 mol %), originating probably mostly from callose and to a lesser extent from XyG polymers. The most abundant monosaccharide, Ara (43.6 mol %), and Gal (8.4 mol %) may come from AGP glycans and/or the pectic RG-I domain. Indeed, both sugars composing the backbone of RG-I (i.e. Rha and GalUA) were present in the extract in equimolar amounts (approximately 5 mol %). The remaining GalUA (approximately 5 mol %) composes undoubtedly the pectic HG backbone. XyG polymers generally consist of Xyl and Fuc residues that are also found in this analysis, although in low amounts (1.2 mol % Fuc and 6.2 mol % Xyl), suggesting that XyG is not a major cell wall component of the pollen tube cell wall.

The sequential extraction of the Arabidopsis pollen tube cell wall with ammonium oxalate and KOH aimed at yielding pectin- and hemicellulose-enriched fractions. Both extracts were analyzed for monosaccharide composition by GC and linkage/substitution sites by GC-mass spectrometry (MS; Table II). The

Table II. *Monosaccharide composition and linkage analysis of total pollen tube cell wall and pectin-enriched (ammonium oxalate) and hemicellulose-enriched (KOH) extracts*

Carbohydrate Analysis	Pollen Tube Wall	Oxalate Extract	KOH Extract
Neutral sugar[a] (%)	–	78.5	97.6
Uronic acid[b] (%)	–	21.5	2.4
Monosaccharide composition[b]			
Ara	43.6 ± 4.5	24.7 ± 1.9	23 ± 7.4
Fuc	1.2 ± 0.2	1.0 ± 0.5	0.9 ± 0.7
Gal	8.4 ± 1.0	18.3 ± 0.6	14 ± 3.2
Glc	19.8 ± 5.1	19.3 ± 2.8	40.1 ± 6.6
GalUA	10.9 ± 0.7	21.5 ± 1.4	6.8 ± 0.2
GlcUA	2.2 ± 3.0	3.4 ± 0.8	1.5 ± 0.4
Rha	5.3 ± 0.8	4.2 ± 0.2	2.4 ± 0.7
Man	2.2 ± 1.5	1.7 ± 3.0	4.9 ± 0.1
Xyl	6.2 ± 1.2	5.8 ± 0.6	6.5 ± 0.4
Linkage analysis[c]			
t-Ara*f*	–	27.4	8.5
5-Ara*f*	–	28.2	14.6
2,5-Ara*f*	–	3.7	2.2
3,5-Ara*f*	–	3.9	2.7
t-Xyl	–	1.4	1.1
2-Xyl	–	1	2.4
t-Gal	–	1.7	6
3-Gal	–	2	1.2
4-Gal	–	1.5	nd
6-Gal	–	4	1.8
3,6-Gal	–	5.6	7.3
4,6-Gal	–	1.2	2.2
3-Glc	–	10	27.6
4-Glc	–	8.4	15.4
2,3-Glc	–	nd	7

[a]Determined by the phenol sulfuric and *m*-hydroxydiphenyl colorimetric assays. [b]Determined by GC and expressed as mol %. Values are means ± SD from two independent experiments. [c]Determined by GC-MS of partially methylated alditol acetates and expressed as percentage of total area of the identified peaks. *t*-Ara*f* denotes 1,4-di-*O*-acetyl-1-deuterio-2,3,5-tri-*O*-methyl-D-arabinitol, etc. –, Not determined; nd, not detected.

oxalate extract showed similar levels of uronic acid content by colorimetric assay (21.5 mol %) and GC (24.9 mol %) analyses. This extract was enriched in GalUA (21.5 mol %), indicating the presence of the pectin domains HG and highly branched RG-I, as shown by the detection of 4.2 mol % Rha, 24.7 mol % Ara, and 18.3 mol % Gal. These data are supported by the immunodot assay (Fig. 3), showing a strong interaction of the oxalate extract with JIM5 for partially methylesterified HG and LM6 for (1→5)-α-L-arabinan. This labeling was consistent with the presence of 28.2% 5-Ara*f* (Table II). Labeling with LM5 was weak, which suggests a low amount of (1→4)-β-D-galactan. This observation was confirmed by the detection of only 1.5% 4-linked galactosyl residues (Table II). Instead, galactosyl residues detected in the monosaccharide analysis originate probably from type II arabinogalactans, as shown by the detection of 3-Gal, 6-Gal, and 3,6-Gal (Table II).

In the KOH extract, levels of HG (GalUA) and RG-I backbone (Rha and GalUA) decreased significantly compared with the oxalate extract, but the remaining RG-I domains were probably highly substituted by arabinans and/or arabinogalactans, as both arabinosyl and galactosyl residues counted for 37 mol % of the total sugars (Table II). The dot-blot immunoassay (Fig. 3) revealed a significant reduction of the signal in the KOH extract with JIM5 compared with the oxalate extract, indicating that KOH treatment had substantially removed methylester groups from the partially methylesterifed HG, leaving a low amount of nonesterified HG. In contrast, labeling for (1→5)-α-L-arabinan with LM6 was still strong (Fig. 3) and was confirmed with the detection of 14.6% 5-Ara*f* (Table II). The different components of XyG (i.e. Glc, Xyl, Gal, and Fuc) were also present in the KOH extract (Table II), with a large increase in the Glc level (40.1 mol %) compared with the oxalate extract. As revealed by methylation analysis, the latter originated from XyG (2.2% 4,6-Glc), starch, and/or amorphous cellulose (15.4% 4-Glc) but dominantly from callose with the presence of 3-Glc (27.6%) and possibly 2,3-Glc (7%), which may suggest that callose can be substituted on

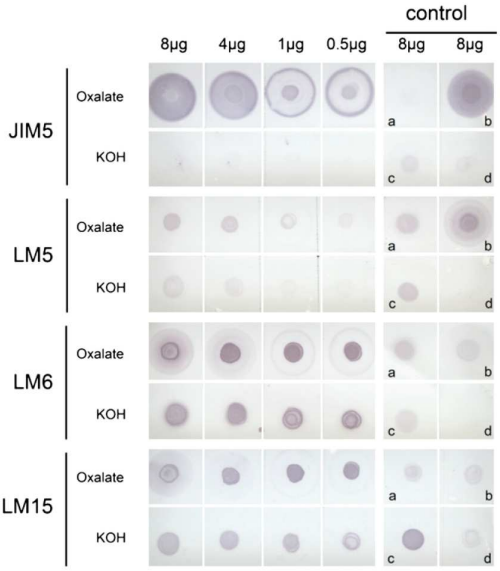

Figure 3. Immunodot blot assay of pectin-enriched (oxalate extract) and hemicellulose-enriched (KOH extract) fractions isolated from Arabidopsis pollen tube cell wall. Oxalate and KOH extracts (8, 4, 1, and 0.5 μg) were probed with JIM5 for partially methylesterified HG, LM5 for (1→4)-β-D-galactan, LM6 for (1→5)-α-L-arabinan, and LM15 for nongalactosylated XyG (XXXG). Controls (8 μg) are as follows: a, arabinan from sugar beet; b, pectin with 8.6% methylesterification from citrus; c, XyG from tamarind seed; d, gum arabic from acacia. [See online article for color version of this figure.]

the C2 of the glucosyl residues (Table II). The MAb LM15 reacted strongly with both oxalate and KOH extracts (Fig. 3), suggesting that XyG was present in both extracts.

MALDI-TOF MS Analysis of Pollen Tube Cell Wall XyG Fragments

Analysis by MALDI-TOF MS of XyG fragments released after XyG endo-glucanase treatment of Arabidopsis pollen tube cell wall (Fig. 4A) showed the typical ions, XXXG, XLXG/XXLG, and XXFG (14.7%, 5.7%, and 8.4%, respectively), found in XyG (Table III). However, these oligosaccharides were not the main motifs. Instead, the two principal ions identified (XLXG/XXLG and XXFG) present a shift of mass-to-charge ratio = 42, characteristic of an *O*-acetyl group, branching presumably the galactosyl residue. These two *O*-acetylated fragments count for over 68% of the total oligosaccharide released. Overall, galactosylated and fucosylated XyG oligosaccharides showed a relative abundance of 85% and 52%, respectively. By comparison, the main XyG fragment released after endo-glucanase treatment of Arabidopsis leaf cell wall was XXXG (Supplemental Fig. S3) and the total level of *O*-acetylated fragments was 33%. Moreover, based on the signal intensity, the ratio of Fuc to Xyl can be estimated as 1:5.7, similar to what was found in the compositional analysis of the pollen tube wall extract (1:5.2), which suggests that other Xyl-containing polymers such as xylan may not be present or in very low amount in the pollen tube cell wall. Finally, monosaccharide analysis of the endo-glucanase-resistant pollen tube cell wall residue (Fig. 4B) revealed, despite a clear decrease in the carbohydrate content of Xyl, Gal, and Fuc compared with the untreated cell wall material, that all the XyGs have not been completely degraded by the enzyme, perhaps due to their tight association with other cell wall components.

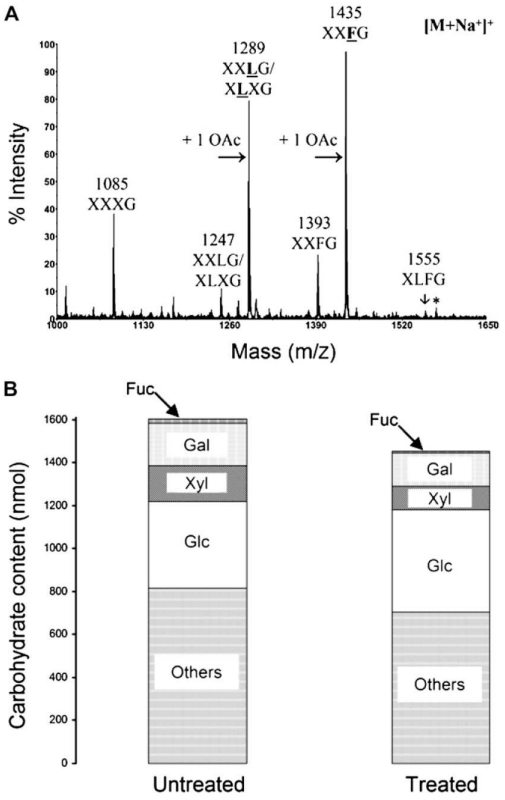

Figure 4. Analysis of Arabidopsis pollen tube XyG. A, MALDI-TOF mass spectrum of endo-glucanase-generated XyG fragments from the cell wall of 16-h-grown Arabidopsis pollen tubes. The structures of the XyG fragments are shown according to the nomenclature proposed by Fry et al. (1993). Underlined and boldface structures represent *O*-acetylated side chains (+ 1 OAc). The asterisk indicates the signal of the XLFG fragment with K^+ adduct ion instead of Na^+. B, Monosaccharide composition of 16-h-grown Arabidopsis pollen tube cell wall before (untreated) and after (treated) endo-glucanase treatment. Only the monosaccharides composing XyG are shown. "Others" include Ara, GalUA, GlcUA, Man, and Rha.

DISCUSSION

Since the Arabidopsis Genome Initiative (2000), increasing genomic, transcriptomic, and proteomic data on Arabidopsis have become available (Becker et al., 2003; Honys and Twell, 2004; Tung et al., 2005; Qin et al., 2009; Zou et al., 2009). The use of male and female gametophyte or sporophyte mutants has allowed major insight into pollen formation, pollen tube growth, guidance, and signaling (Rhee et al., 2003; Dong et al., 2005; Escobar-Restrepo et al., 2007), but the biosynthesis, the remodeling, and the overall role of the cell wall of the tip-growing pollen tube cell are far from being fully understood. Using the in vitro pollen tube method developed by Boavida and McCormick (2007), we obtained high levels of pollen germination, ranging from 55% to 79%, with pollen tubes that can expand over 1.5 mm after 16 h of culture. Based on this, we decided to investigate one of the main components, the cell wall, of this tip-growing cell by means of immunolocalization at light and electron microscopy levels and analytical polysaccharide biochemistry. Our results showed that (1) the pectin wall is enriched in HG and (1→5)-α-L-arabinan and (2) *O*-acetylation of XyG fragments released by endo-glucanase is high compared with other sporophytic tissues.

Most of the precursor studies on the pollen tube wall of the so-called "pollen tube model plants" (i.e. *Nicotiana* or *Lilium*) employed MAbs recognizing the HG pectin domains (JIM5 and JIM7) and a subset of carbohydrate epitopes of the cell surface AGPs (mainly

Table III. *Relative quantification of XyG oligosaccharides obtained after endo-glucanase digestion of Arabidopsis pollen tube wall*

Mass[a]	Composition[b]	Structure[c]	Relative Abundance[d]
1,085	Hex_4Pent_3	XXXG	14.7 ± 3.3
1,247	Hex_5Pent_3	XLXG/XXLG	5.7 ± 0.6
1,289	$Hex_5Pent_3OAc_1$	XLXG/XXLG + 1 OAc	27.6 ± 3.9
1,393	$Hex_5Pent_3Dox_1$	XXFG	8.4 ± 0.5
1,435	$Hex_5Pent_3Dox_1OAc_1$	XXFG + 1 OAc	41.2 ± 6.6
1,555	$Hex_6Pent_3Dox_1$	XLFG	2.5 ± 0.1[e]

[a]Mass of the fragments $[M+Na^+]^+$. [b]Hex, Hexose; Pent, pentose; OAc, *O*-acetyl substituent; Dox, deoxyhexose. [c]Based on XyG oligosaccharide structures found in Pauly et al. (2001). [d]Values are expressed as percentage and are means ± SD from MALDI spectra obtained after endo-glucanase digestion from three different Arabidopsis pollen tube cell wall extracts. [e]Relative abundance of this oligosaccharide corresponds to the total of the K^+ and Na^+ adduct fragments.

JIM13, MAC207, LM2, and JIM8). To date, only scarce reports on the pollen tube wall have been published using other well-defined MAbs such as anti-XyG (CCRC-M1; Freshour et al., 2003) and, to our knowledge, none with the more recently produced MAbs on pollen tube wall.

Arabidopsis Pollen Tube Wall Is Composed of an Inner Layer Enriched in Callose and an Outer Fibrillar Layer

TEM observations of in vitro rapidly frozen Arabidopsis pollen tubes showed the typical two wall layers at the shank of the tip (a fibrillar outer and a weakly electron-dense inner wall layer), as observed in in vitro-grown tobacco (*Nicotiana tabacum*) pollen tube (Li et al., 1995; Ferguson et al., 1998) and in in vivo-grown pollen tube from lily (Roy et al., 1997) and Arabidopsis (Lennon and Lord, 2000; Derksen et al., 2002). Our data and those of others have shown that callose is the main component of the inner wall layer but is not detectable at the tip, whereas cellulose is weakly detected (Ferguson et al., 1998).

Arabidopsis Pollen Tube Wall Contains a Subset of AGPs Recognized by LM2

We found that AGPs were labeled in the whole tube, with a stronger signal at the tip with LM2, whereas JIM13 labeling was almost absent. In contrast, JIM13 labeled lily pollen tube at the tip (Mollet et al., 2002) and uniformly or in a ring-like deposition along the tube of tobacco (Li et al., 1992; Qin et al., 2007). Pereira et al. (2006) also noted a lack of labeling of Arabidopsis pollen tube with JIM13, unlike MAC207, which labels uniformly the whole tube (Coimbra et al., 2008). These divergent data depend on the MAb used [despite the apparent identical epitope, β-D-Glc*p*UA-(1→3)-α-D-Gal*p*UA-(1→2)-L-Rha, recognized by MAC207 and JIM13] and the species investigated. These differences may suggest that the carbohydrate moieties of AGPs are species and/or cell type specific (vegetative and sperm cells) or that the cell wall organization is different in these species, which may alter the accessibility of the epitopes.

HG Pectin Domains Are Present in Different Locations in Arabidopsis Pollen Tube Wall

Immunofluorescent labeling with JIM5 and JIM7 shows a pattern similar to that observed in pollen tubes from families possessing a solid style, such as the Solanaceae (potato [*Solanum tuberosum*], tobacco, petunia [*Petunia hybrida*]), Oleaceae (jasmine [*Jasminum* species]), and Poaceae (corn [*Zea mays*]; Li et al., 1994; Qin et al., 2007). A dominant localization of highly methylesterified HG, recognized by JIM7, was present at the tip, and a periodic patterning of low methylesterified HG epitopes, labeled with JIM5, was visible behind the tip region. Pollen tube wall contains 10 mol % GalUA, half of it being presumably dedicated to HG building, which explains the weak labeling by JIM5 along the wall compared with other species (Jauh and Lord, 1996; Qin et al., 2007), even though reduced accessibility of the MAb to the epitopes may occur due to other polymers. In fact, the pectin-enriched extract isolated from the pollen tube wall showed a strong interaction with JIM5 (Fig. 3). Highly methylesterified HG and other pectic motifs are deposited at the growing tip by Golgi-derived vesicles and deesterified via PMEs in the wall back from the tip, to allow calcium cross-linking of the carboxyl groups (Geitmann and Steer, 2006). In the tobacco pollen tube, two PME isoforms have been localized in the Golgi, secretory vesicles, and at the outer surface of the plasma membrane, where they may deesterify HG (Li et al., 2002). Two Arabidopsis mutants, *vanguard1* (Jiang et al., 2005) and *Atppme1* (Tian et al., 2006), defective in two different pollen-specific PMEs, showed slight reduction (about 20%) of overall PME activity, reduced growth compared with wild-type pollen tubes, but different pollen tube phenotypes. *vanguard1* pollen tubes were unstable in vitro, resulting in tip bursting, and in vivo, *vanguard1* plants showed reduced male fertility. In contrast, *Atppme1* pollen tubes showed an

in vitro branching pattern with numerous tips but did not show male sterility in vivo. These reports suggest that these mutant pollen tubes have modified cell wall mechanical properties, despite a lack of either immunolocalization or biochemical data showing a modification in the methylesterification level of the HG motif. It is noteworthy to point out, as suggested by Jiang et al. (2005), that these PMEs may also have a role in modifying the female TT wall to facilitate pollen tube progression through the female tissue. *AtPPME1* and *VANGUARD1* are among a group of 15 other pollen-specific genes that are separated in two groups (I and II) and encode putative PMEs containing either a catalytic domain only (five genes) or a catalytic domain and a putative PME inhibitor (PMEI) domain (10 genes; Chen and Ye, 2007; Pelloux et al., 2007). More studies on these important protein members are required to understand the fine-tuning of demethylesterification of HG and to determine the interaction between PME and PMEI and their roles in modifying the pollen tube mechanics and sensing (Bosch et al., 2005). Low esterified HGs have been implicated in important physiological processes, such as cell attachment in vegetative cells or organs (Bouton et al., 2002; Leboeuf et al., 2005; Durand et al., 2009) and, associated with a stigma/style Cys-rich adhesin, a secreted plant lipid transfer protein (LTP), in lily pollen tube adhesion (Mollet et al., 2000; Park et al., 2000). Several LTPs are present in the TT of the Arabidopsis pistil along the pollen tube path (Tung et al., 2005). Recently, the LTP5, produced in Arabidopsis pollen tube and in the pistil TT, has been proposed to play important roles in maintaining cell polarity at the tube tip and adhesion-mediated guidance perhaps by interaction with pectins (Chae et al., 2009).

Arabidopsis Pollen Tube Wall Is Enriched in Pectin Arabinan

In addition to HG motifs, Arabidopsis pollen tube wall contains highly branched RG-I with arabinan. Our results based on immunolocalization using LM6 and LM13, both recognizing (1→5)-α-L-arabinan epitopes, and biochemical analysis indicate, first, a strong and evenly distributed labeling in the shank of the tube with a slight increase of the signal in the tip region. Second, the most striking point is the high level of arabinosyl residues present in the pollen tube wall, oxalate, and KOH extracts, which counts for over 40 mol % of the total analyzed sugar. Chemical analysis of the pollen tube cell wall from tobacco (Rae et al., 1985) revealed also a high level of Ara (between 15.4 and 26.4 mol % depending on the hydrolysis method), mostly 5-linked and to a lesser extent 5,2-linked. Moreover, tobacco pollen tube wall displayed a low level of galactosyl residues and uronic acids (Rae et al., 1985). Similarly, *Lilium*, *Camellia*, and *Tulipa* pollen tube wall also showed high levels of arabinosyl residues (Nakamura and Suzuki, 1981). Golgi vesicles from *Camellia* pollen tubes were also enriched in Ara, Gal, and uronic acid (Hasegawa et al., 1998). Altogether, our data suggest that Arabidopsis pollen tube wall contains a short RG-I backbone harboring long chains of (1→5)-α-L-arabinans in the outer wall layer. The significance of this common feature (high level of arabinan) between the pollen tubes originating from nonrelated species is not known but may suggest an important role of this polymer in pollen tube biology. The role of arabinan side chains of RG-I is not clear. Indeed, mutation in the *ARABINAN DEFICIENT1* gene, a putative arabinosyltransferase involved in the biosynthesis of pectic arabinan in Arabidopsis, showed high reduction of arabinan side chains of RG-I without any compensation by other polymers. However, no obvious phenotype was detected, suggesting that a loss of arabinan in RG-I does not affect vegetative growth (Harholt et al., 2006). On the other hand, plants exhibiting mutations in two *Reversibly Glycosylated Peptides* (*RGP1* and *RGP2*) that may be involved in cell wall biosynthesis showed a strong defect in the inner pollen wall and pollen lethality (Drakakaki et al., 2006). Interestingly, rice RGPs show strong amino acid sequence identity (approximately 80%), with UDP-arabinopyranose mutase implicated in UDP-Ara*p* and UDP-Ara*f* interconversion (Konishi et al., 2007). We might speculate that RGP may be part of the arabinan biosynthesis network, but further biochemical studies are required to validate this, as many other molecules contain arabinosyl residues such as arabinoxylans and arabinogalactans. In *Commelina communis*, arabinan side chains of RG-I have been implicated in guard cell opening and closing. The authors suggested that they may prevent HG polymers from forming tight associations (Jones et al., 2003). A similar effect may occur between the pollen tube wall and the TT cell wall. Finally, pectic arabinans have also been implicated in cell attachment (Iwai et al., 2001; Orfila et al., 2001; Leboeuf et al., 2004, 2005; Peňa and Carpita, 2004). Adhesion of pollen tubes to the TT cells may be an important cue for guiding the tube cell within the female tissue, as was shown in the hollow style plant, lily (Mollet et al., 2007). Investigation of mutant pollen defective in arabinosyltransferase will undoubtedly give insight into the function of arabinan side chains of RG-I in pollen/pollen tube biology.

Arabidopsis Pollen Tube Wall Endo-Glucanase-Sensitive XyG Is Highly Acetylated

MAbs directed against two different XyG epitopes labeled the whole tube mostly in the outer wall layer and the tip. Oligosaccharide fragments containing these two epitopes (XXXG and XXFG) were also detected with MALDI-TOF MS after pollen tube cell wall digestion. Interestingly, XyG analysis from vegetative organs (leaf, stem, or root) revealed consistently that the main fragments are XXXG and XXFG (Zablackis et al., 1995; Pauly et al., 2001; Lerouxel et al., 2002). Arabidopsis pollen tube XyG shows distinct mass spectra with two major fragments detected (XLXG/XXLG and XXFG),

both being substituted by one acetyl group, presumably linked to the galactosyl residue. The signal intensity of these two fragments consistently accounted for over 68%. Recent investigations of XyG from leaf tissues isolated after laser microdissection has allowed a more detailed analysis showing subtle modification of XyG (Obel et al., 2009). As an example, the level of acetylation of XLFG fragments in the mesophyll tissue was significantly higher than in the vascular tissue, but the overall acetylation level in these tissues did not exceed 35% to 40% (Obel et al., 2009). Together, these findings indicate that subtle changes in the acetylation level of XyG can occur, but the function of these hydrophobic groups in cell wall biology is still unknown.

XyGs are known to interact with cellulose microfibrils. Despite the low amount of cellulose in the pollen tube wall (Doblin et al., 2001), cellulose is present at the tip and plays an important role in stabilizing the pollen tube tip wall. Cellulase treatment on growing pollen tubes resulted in tip swelling and eventually bursting (Aouar et al., 2010). Cellulose at the tip region may also serve as an interacting partner for XyG cross-linking. Acetylation of XyG does not seem to play a major role in the interaction with cellulose. In vitro experiments have shown that native (acetylated) and deacetylated XyG were able to cross-link cellulose microfibrils in a similar manner (Whitney et al., 2006). In contrast, the high molecular mass of the XyG (880 kD) and the presence of galactosyl residues appeared to be necessary to promote the interaction with cellulose. A lack of Gal in the XyG resulted in the self-association of XyG polymers instead of the interaction between XyG and cellulose (Whitney et al., 2006). Similarly, Arabidopsis mutants with XyG lacking xylosyl, galactosyl, or fucosyl residues showed reduction of tensile strength (Peña et al., 2004) or abnormal bulging in the tip-growing root hairs, possibly due to impaired cellulose-XyG assembly (Nguema-Ona et al., 2006; Zabotina et al., 2008). A similar phenotype was also noticed in plants exhibiting double mutations in the two XyG xylosyltransferase 1 and 2 genes (*XXT1* and *XXT2*) that are apparently lacking XyG (Cavalier et al., 2008). In the moss *Physcomitrella*, AGPs were found to be enriched in 3-*O*-methyl-rhamnosyl residues compared with AGPs from more evolved plant species. This suggests a possible hydrophobic interaction of AGPs, which for a long time had been considered to have large capacity for interacting with water (Fu et al., 2007). Altogether, acetyl groups of XyG may promote hydrophobic interactions with other molecules within the pollen tube cell wall but also with other female components of the TT extracellular matrix during the intrusive growth of pollen tubes. Moreover, acetylation may modulate water uptake due to the nonpolar property of these groups, but this requires further investigation.

In summary, this study provides a solid foundation for the use of Arabidopsis pollen tubes in cell wall biology and for the investigation of the male gametophyte cell elongation with mutants impaired in proteins implicated in the biosynthesis of specific cell wall polymers (XyG, HG, RG-I, RG-II, and AGPs), cell wall deposition, and cell wall remodeling. It may also help to dissect the mechanisms controlling the interaction between the pollen tube wall with the female counterpart. The challenge in this field is to overcome the generally observed phenotypes, such as arrest of pollen formation, lack of pollen viability, absence of pollen tube germination or growth resulting in reduced male fertility, when mutations are located in important male gametophyte genes (Lalanne et al., 2004; Drakakaki et al., 2006; Iwai et al., 2006; Delmas et al., 2008; Boavida et al., 2009). Chemical genetic screens on in vitro-grown pollen tubes may be an alternative. Nevertheless, studies on the two distinct features of Arabidopsis pollen tube wall (high levels of pectic arabinan side chains and XyG acetylation) require closer attention and investigation to better understand their possible roles in pollen tube growth, signaling, guidance, and adhesion.

MATERIALS AND METHODS

Plant Materials

Arabidopsis (*Arabidopsis thaliana* ecotype Columbia) seeds stored at 4°C were spread on the surface of sterile soil and cultured in a growth chamber with a photoperiod of 16 h of light/8 h of dark at 20°C during the light phase and at 16°C in the dark phase with 60% humidity and daily watering. Only recently opened flowers were collected.

In Vitro Pollen Tube Growth

Pollen was grown in vitro in a liquid medium according to the method described by Boavida and McCormick (2007). Briefly, flowers (40 per 1.5-mL tube) were submerged in 1 mL of germination medium (GM) containing 5 mM $CaCl_2$ $2H_2O$, 0.01% (w/v) H_3BO_3, 5 mM KCl, 1 mM $MgSO_4$ $7H_2O$, and 10% (w/v) Suc, pH 7.5. Tubes were shaken with a vortex to release the pollen grains from the anthers. Flowers were removed with a pair of tweezers, and the pollen suspension was then pelleted down at 3,200*g* for 6 min. New GM (250 μL) was added to the pellet, and pollen grains were transferred into glass vials (14 × 45 mm) and grown in a growth chamber in the dark at 22°C. For large-scale culture, pollen from 200 flowers was grown in glass vials (25 × 50 mm) in 1.25 mL of GM. Using this harvesting method, the number of pollen grains collected per flower was estimated at 291 ± 63.3 (n = 10 independent experiments). Pollen tubes were grown for 6 h for TEM sample preparation, 6 and 16 h for immunolabeling at the fluorescence microscopy level, and 16 h for biochemical analysis. Before any further manipulation, pollen germination and pollen tube growth were assessed with an inverted microscope.

Cytochemical Staining

Calcofluor white (0.01%, w/v) and decolorized aniline blue (0.1%, w/v) in 100 mM K_3PO_4, pH 11 (Johnson-Brousseau and McCormick, 2004), were used to localize β-glucans (cellulose and callose) and callose, respectively.

MAbs

JIM13, MAC207, and LM2 MAbs recognize a carbohydrate moiety of AGPs (Yates et al., 1996). Extensins were probed with LM1 (Smallwood et al., 1995). The MAbs JIM5 and JIM7 recognize different levels of esterification of HG regions of pectins (Clausen et al., 2003). (1→4)-β-D-Galactans were probed with LM5 (Jones et al., 1997) and (1→5)-α-L-arabinans with LM6 (Willats et al., 1998) and LM13 (Verhertbruggen et al., 2009). The MAbs directed against XyG were CCRC-M1, which recognizes an α-Fuc-(1→2)-β-Gal epitope (Puhlmann et al., 1994), and LM15, which binds to the XXXG motif (Marcus et al., 2008).

MAbs were kindly provided by P. Knox (University of Leeds) and M. Hahn (Complex Carbohydrate Research Center, University of Georgia) or purchased at Plant Probes. Finally, callose was localized with a mouse anti-(1→3)-β-glucan (Biosupplies Australia).

Immunolocalization of Arabidopsis Pollen Tube Wall Epitopes

Pollen tubes in GM were mixed (v/v) with a fixation medium containing 100 mM PIPES buffer, pH 6.9, 4 mM $MgSO_4$ $7H_2O$, 4 mM EGTA, 10% (w/v) Suc, and 5% (w/v) formaldehyde and incubated for 90 min at room temperature. Pollen tubes were rinsed three times by centrifugation with 50 mM PIPES buffer, pH 6.9, 2 mM $MgSO_4$ $7H_2O$, and 2 mM EGTA and three times with phosphate-buffered saline (100 mM potassium phosphate, 138 mM NaCl, and 2.7 mM KCl, pH 7.4) supplemented or not with 3% fat-free milk. Primary antibodies were diluted at 1:5 or 1:10 as described previously (Mollet et al., 2002) with phosphate-buffered saline (with or without 3% milk). Pollen tubes were rinsed with the buffer and incubated overnight at 4°C in the dark with the secondary antibody combined with fluorescein isothiocyanate (FITC; Sigma) diluted at 1:50 with the appropriate buffer for 3 h at 30°C. For JIM, LM, and MAC antibody detection, goat anti-rat IgG (whole molecule)-FITC was used; for CCRC antibody detection, sheep anti-mouse IgG (whole molecule)-FITC was used. Controls were carried out by incubation of the pollen tubes with the secondary antibody only.

Microscope Observation and Acquisition of Pollen Tube Images

Pollen tubes were observed under Nomarski differential interference contrast optics or fluorescence illumination on a Leica DLMB microscope equipped with FITC (absorption, 485–520 nm; emission, 520–560 nm wavelength) or calcofluor white filter sets. Images were acquired with a Leica DFC300FX camera.

Pollen count and germination rate were estimated with a Nageotte chamber. A pollen grain was considered germinated if the pollen tube length was greater than the pollen grain diameter. Pollen tube length was measured from the image using the program ImageJ (Abramoff et al., 2004). At least 350 pollen tubes were measured in three independent experiments.

Electron Microscopy Preparation of in Vitro-Grown Pollen Tubes

High-Pressure Freezing/Freeze Substitution Sample Preparation

Centrifuged 6-h-old pollen tubes were transferred into the cavity of gold cupules (200 μm in depth and 1.2 mm in diameter) coated with soybean (*Glycine max*) lecithin (100 mg mL^{-1} in chloroform). Excess medium was removed using a filter paper. Then, samples were frozen using a high-pressure freezing EM-PACT (Leica) according to a maximum cooling rate of 10,000°C s^{-1}, incoming pressure of 7.5 bars, and working pressure of 4.8 bars. Cupules containing frozen samples were stored in liquid nitrogen until the freeze substitution procedure was initiated.

After high-pressure freezing, samples were transferred to a freeze substitution automate (EM-AFS; Leica) precooled to −140°C. Freeze substitution conditions followed a modified procedure from D. Studer (personal communication). Substitution media were composed of 2% osmium in anhydrous acetone. Samples were substituted at −90°C for 72 h. The temperature was gradually raised (2°C h^{-1}) to −60°C and stabilized during 12 h, then gradually raised (2°C h^{-1}) to −30°C (12 h) and gradually raised again (2°C h^{-1}) to 0°C for 2 h. Samples were washed at room temperature with fresh anhydrous acetone. Infiltration was done at +4°C in acetone-Spurr resin (2:1, 1:1, 1:2, 8 h each step) and with pure resin for at least 2 d. Polymerization was performed at 60°C for 16 h. Using an ultracut EM-UC6 (Leica), thin sections (90 nm) were mounted on formvar-coated nickel grids.

Immunogold Labeling and TEM Observation

Grids were rehydrated in a Tris-buffered saline (TBS) + bovine serum albumin (BSA) 0.2% buffer and blocked in a TBS/BSA 0.2%/milk 3% solution for 30 min. After three brief rinses in TBS/BSA 0.2% solution, grids were incubated 3 h at 25°C in primary antibodies: nondiluted for LM15 and CCRC-M1 or diluted (LM6, 1:2; anti-callose, 1:100) in TBS/BSA 0.2% buffer. Then, grids were washed (six times for 5 min each) in TBS/BSA 0.2% and incubated for 1 h at 25°C in a 1:20 secondary antibody (goat anti-rat for LM6 and LM15, goat anti-mouse for CCRC-M1 and anti-callose) conjugated to 10-nm gold particles (British Biocell International). Finally, grids were washed (six times for 5 min each) in a TBS + BSA 0.2% buffer, 1 min in TBS, 10 min in TBS + glutaraldehyde 2%, 5 min in TBS, and then two times for 5 min each in double deionized water.

The sections were stained with 0.5% (w/v) uranyl acetate in methanol for 10 min in the dark, rapidly rinsed 10 times with water and stained with lead citrate for 10 min, and briefly rinsed 10 times with water.

Grids were observed at 80 kV with a TEM apparatus (Tecnai 12 Bio-Twin; Philips), and images were acquired with an Erlangshen ES500W camera.

Cell Wall Extraction of Arabidopsis Pollen Tubes

Sixteen-hour-old pollen tubes from pollen grains from 8,500 flowers collected manually were pooled after addition of 3 volumes of 95% ethanol to the GM. This experiment was performed three times to allow three independent replicates. Pollen tubes were centrifuged at 5,000*g* and rinsed three times with 70% ethanol to remove salts and Suc from the GM. The insoluble material (3 × 12 mg) was ground and then treated three times with 70% ethanol at 70°C for 15 min followed by incubation with a mixture of chloroform:methanol (1:1, v/v). The remaining insoluble material was then dried to yield the cell wall fraction (3 × 10 mg). As a baseline control, cell wall from nongerminated pollen grains was extracted. A similar extraction method was applied to Arabidopsis mature rosette leaves to yield a leaf wall extract, except that an acetone incubation was added after the chloroform:methanol treatment for pigment removal. This extract was used to compare the XyG fragments analyzed by MALDI-TOF MS with the pollen tube cell wall extract.

As described by Ray et al., (2004), a pectin-enriched fraction was obtained by extraction with boiling ammonium oxalate 0.5% (w/v) for 1 h. After centrifugation, the supernatant was dialyzed against double deionized water and freeze dried. The ammonium oxalate-insoluble residue was then treated with 4 M KOH supplemented with 20 mM $NaBH_4$ at room temperature for 12 h. The alkaline-soluble fraction was acidified to pH 5.5 with acetic acid, dialyzed against water, and freeze dried to yield a hemicellulose-enriched fraction.

Analysis of Cell Wall Polysaccharides

Photometric Assays

Total uronic acid and neutral sugars were estimated with the *m*-hydroxydiphenyl assay (Blumenkrantz and Asboe-Hansen, 1973) and the phenol sulfuric method (Dubois et al., 1956) with Gal and GalUA as standards. Estimation of uronic acid and neutral sugar contents was calculated after correction of the interference of GalUA with the phenol sulfuric assay and that of Gal with the *m*-hydroxydiphenyl assay.

Immunodot Blot Assays

Ammonium oxalate and KOH extracts (8, 4, 1, and 0.5 μg) were blotted onto nitrocellulose membranes. Immunodot blots were processed according to Jauh and Lord (1996). Arabinan from sugar beet (*Beta vulgaris*; Megazyme), gum arabic from acacia (Fisher), pectin with 8.6% *O*-methylation from citrus fruits (Sigma), and XyG from tamarind seeds (*Tamarindus indica*; Megazyme) were used as controls. MAb binding was revealed with a goat anti-rat IgG (whole molecule) antibody conjugated with alkaline phosphatase (Sigma) diluted 1:1,000 and developed with the nitroblue tetrazolium/5-bromo-4-chloro-3-indolyl phosphate kit (Promega).

GC-MS

Monosaccharide compositions of the total cell wall and pectin- and hemicellulose-enriched fractions were determined by gas liquid chromatography according to York et al. (1985) using inositol as an internal standard. Briefly, each fraction (500 μg) was treated with 1 M methanolic-HCl at 80°C for 16 h, and the free monosaccharides were converted to their methyl glycosides.

After silylation at 110°C for 20 min, samples were dried, dissolved in cyclohexane, and analyzed using a GC 3800 Varian GC system equipped with a DB1 capillary column and a flame ionization detector. A temperature program optimized for separation of the most common cell wall monosaccharides (Ara, Fuc, Gal, GalUA, Glc, GlcUA, Man, Rha, Xyl) was used. Data were analyzed and integrated using Varian GC Star Workstation software, with the quantity of each monosaccharide was corrected according to its response factor.

Preparation and linkage analysis of the partially methylated alditol acetates of pectin- and hemicellulose-enriched fractions were performed according to Smith et al. (1994), except that the ultrasonic bath was performed for 1 h instead of 15 min, dichloromethane was used instead of chloroform, and a stream of air was used to dry samples instead of nitrogen. The resulting partially methylated alditol acetates were separated by GC (Hewlett-Packard 6890) on an Optima 5-MS capillary column (30 m i.d., 0.25 mm; Macherey Nagel) and analyzed by electron-impact MS using an Autospec mass spectrometer (Micromass) equipped with an Opus 3.1 data system.

Preparation of XyG Oligosaccharides

A total of 0.5 mg of pollen tube cell wall or leaf cell wall extract was incubated under agitation for 16 h at 37°C with 500 μL of endo-(1→4)-β-D-glucanase (5 units; EC 3.2.1.4; Megazyme) prepared in 10 mM ammonium acetate buffer, pH 5.0. Glucanase-resistant material was removed by centrifugation after the addition of ethanol to reach a final concentration of 80%. The ethanol-soluble XyG oligosaccharides were concentrated by evaporation under a stream of air.

MALDI-TOF MS Analysis of XyG-Derived Oligosaccharides

MALDI-TOF mass spectra were acquired on a Voyager DE-Pro MALDI-TOF instrument (Applied Biosystems) equipped with a 337-nm nitrogen laser. MS was performed in the reflector delayed extraction mode using 2,5-dihydroxybenzoic acid (Sigma) as matrix. The matrix, freshly dissolved at 5 mg mL^{-1} in 70:30 acetonitrile:0.1% trifluoroacetic acid, was mixed with the water-solubilized oligosaccharides at a ratio of 1:1 (v/v). These spectra were recorded in positive mode using an acceleration voltage of 20,000 V with a delay time of 100 ns and above 50% of the laser energy. They were externally calibrated using commercially available mixtures of peptides and proteins (Applied Biosystems). In this study, the spectra were calibrated using des-Arg-1-bradykinin (904.4681 D), angiotensin I (1,296.6853 D), Glu-1-fibrinopeptide B (1,570.6774 D), and ACTH18-39 (2,465.1989 D). Laser shots were accumulated for each spectrum in order to obtain an acceptable signal-to-noise ratio (sum of 10 spectra of 1,000 shots per spectrum).

Supplemental Data

The following materials are available in the online version of this article.

Supplemental Figure S1. Immunogold labeling of cell wall epitopes in Arabidopsis pollen tube, hydrated pollen grain, and controls.

Supplemental Figure S2. Monosaccharide composition and carbohydrate content of the cell wall of nongerminated pollen grains and 16-h in vitro-grown pollen tubes isolated from 520 flowers.

Supplemental Figure S3. MALDI-TOF MS of XyG fragments of Arabidopsis cell wall leaf released by endo-glucanase treatment.

Supplemental Table S1. Estimation of the amount of pollen grain wall versus pollen tube cell wall.

ACKNOWLEDGMENTS

A. Geitmann (University of Montreal) is greatly acknowledged for her comments on and proofreading of the manuscript. We are also grateful to F. Richard, L. Chevalier, and M.L. Follet-Gueye for their expertise in high-pressure freezing/freeze substitution sample preparation and technical assistance with the TEM at PRIMACEN (Institut Fédératif de Recherche Multidisciplinaire sur les Peptides 23) and to C. Loutelier-Bourhis (Institut de Recherche en Chimie Organique Fine) for the GC-MS analysis, both part of the University of Rouen. Finally, R. Ngouala Finassi is greatly acknowledged for his help in flower harvest and pollen tube wall immunolocalization.

Received May 5, 2010; accepted June 11, 2010; published June 14, 2010.

LITERATURE CITED

Abramoff MD, Magelhaes PJ, Ram SJ (2004) Image processing with ImageJ. Biophotonics Int **11:** 36–42

Aouar L, Chebli Y, Geitmann A (2010) Morphogenesis of complex plant cell shapes: the mechanical role of crystalline cellulose in growing pollen tubes. Sex Plant Reprod **23:** 15–27

Arabidopsis Genome Initiative (2000) Analysis of the genome sequence of the flowering plant *Arabidopsis thaliana*. Nature **408:** 796–815

Becker JD, Boavida LC, Carneiro J, Haury M, Feijo JA (2003) Transcriptional profiling of Arabidopsis tissues reveals the unique characteristics of the pollen transcriptome. Plant Physiol **133:** 713–725

Blumenkrantz N, Asboe-Hansen G (1973) New method for quantitative determination of uronic acids. Anal Biochem **54:** 484–489

Boavida LC, McCormick S (2007) Temperature as a determinant factor for increased and reproducible in vitro pollen germination in *Arabidopsis thaliana*. Plant J **52:** 570–582

Boavida LC, Shuai B, Yu HJ, Pagnussat GC, Sundaresan V, McCormick S (2009) A collection of Ds insertional mutants associated with defects in male gametophyte development and function in *Arabidopsis thaliana*. Genetics **181:** 1369–1385

Boavida LC, Vieira AM, Becker JD, Feijò JA (2005) Gametophyte interaction and sexual reproduction: how plants make a zygote. Int J Dev Biol **49:** 615–632

Bosch M, Cheung AY, Hepler PK (2005) Pectin methylesterase, a regulator of pollen tube growth. Plant Physiol **138:** 1334–1346

Bou Daher F, Chebli Y, Geitmann A (2009) Optimization of conditions for germination of cold-stored *Arabidopsis thaliana* pollen. Plant Cell Rep **28:** 347–357

Bouton S, Leboeuf E, Mouille G, Leydecker MT, Talbotec J, Granier F, Lahaye M, Höfte H, Truong HN (2002) QUASIMODO1 encodes a putative membrane-bound glycosyltranferase required for normal pectin synthesis and cell adhesion in *Arabidopsis*. Plant Cell **14:** 2577–2590

Caffall KH, Mohnen D (2009) The structure, function, and biosynthesis of plant cell wall pectic polysaccharides. Carbohydr Res **344:** 1879–1900

Carpita NC, McCann MC (2000) The cell wall. *In* BB Buchanan, W Gruissem, R Jones, eds, Biochemistry and Molecular Biology of Plants. American Society of Plant Physiologists, Rockville, MD, pp 52–109

Cavalier DM, Lerouxel O, Neumetzler L, Yamauchi K, Reinecke A, Freshour G, Zabotina OA, Hahn MG, Burgert I, Pauly M, et al (2008) Disrupting two *Arabidopsis thaliana* xylosyltransferase genes results in plants deficient in xyloglucan, a major primary cell wall component. Plant Cell **20:** 1519–1537

Chae K, Kieslich CA, Morikis D, Kim SC, Lord EM (2009) A gain-of-function mutation of *Arabidopsis* Lipid Transfer Protein 5 disturbs pollen tube tip growth and fertilization. Plant Cell **21:** 3902–3914

Chae K, Zhang K, Zhang L, Morikis D, Kim S, Mollet JC, de la Rosa N, Tan K, Lord EM (2007) A relationship between structural features and lily pollen tube adhesion activity of SCA (stigma/style cysteine-rich adhesin) isoforms. J Biol Chem **282:** 33845–33858

Chen LQ, Ye D (2007) Roles of pectin methylesterases in pollen tube growth. J Integr Plant Biol **49:** 94–98

Clausen MH, Willats WGT, Knox JP (2003) Synthetic methyl hexagalacturonate hapten inhibitors of anti-homogalacturonan monoclonal antibodies LM7, JIM5 and JIM7. Carbohydr Res **338:** 1797–1800

Coimbra S, Jones B, Pereira LG (2008) Arabinogalactan proteins (AGPs) related to pollen tube guidance into the embryo sac in *Arabidopsis*. Plant Signal Behav **3:** 455–456

Cosgrove DJ (1999) Enzymes and other agents that enhance cell wall extensibility. Annu Rev Plant Physiol Plant Mol Biol **50:** 391–417

Delmas F, Séveno M, Northey JGB, Hernould M, Lerouge P, McCourt P, Chevalier C (2008) The synthesis of the rhamnogalacturonan II component 3-deoxy-D-manno-2-octulosonic acid (Kdo) is required for pollen tube growth and elongation. J Exp Bot **59:** 2639–2647

Derksen J, Knuiman B, Hoedemaekers K, Guyon A, Bonhomme S,

Pierson ES (2002) Growth and cellular organization of *Arabidopsis* pollen tubes *in vitro*. Sex Plant Reprod **15:** 133–139
Derksen J, Li YQ, Knuiman B, Geurts H (1999) The wall of *Pinus sylvestris* L. pollen tubes. Protoplasma **208:** 26–36
Doblin MS, De Melis L, Newbigin E, Bacic A, Read SM (2001) Pollen tubes of *Nicotiana alata* express two genes from different β-glucan synthase families. Plant Physiol **125:** 2040–2052
Dong J, Kim ST, Lord EM (2005) Plantacyanin plays a role in reproduction in Arabidopsis. Plant Physiol **138:** 778–789
Drakakaki G, Zabotina O, Delgado I, Robert S, Keegstra K, Raikhel N (2006) Arabidopsis reversibly glycosylated polypeptides 1 and 2 are essential for pollen development. Plant Physiol **142:** 1480–1492
Driouich A, Baskin TI (2008) Intercourse between cell wall and cytoplasm exemplified by arabinogalactan proteins and cortical microtubules. Am J Bot **95:** 1491–1497
Dubois M, Gilles KA, Hamilton JK, Rebers PA, Smith F (1956) Colorimetric method for determination of sugars and related substances. Anal Chem **28:** 350–356
Durand C, Vicré-Gibouin M, Follet-Gueye ML, Duponchel L, Moreau M, Lerouge P, Driouich A (2009) The organization pattern of root border-like cells of *Arabidopsis thaliana* is dependent on cell wall homogalacturonan. Plant Physiol **150:** 1411–1421
Escobar-Restrepo JM, Huck N, Kessler S, Gagliardini V, Gheyselinck J, Yang WC, Grossniklaus U (2007) The FERONIA receptor-like kinase mediates male-female interactions during pollen tube reception. Science **317:** 656–660
Ferguson C, Teeri TT, Siika-aho M, Read SM, Bacic A (1998) Location of cellulose and callose in pollen tubes and grains of *Nicotiana tabacum*. Planta **206:** 452–460
Freshour G, Bonin CP, Reiter WD, Albersheim P, Darvill AG, Hahn MG (2003) Distribution of fucose-containing xyloglucans in cell walls of the *mur1* mutant of Arabidopsis. Plant Physiol **131:** 1602–1612
Fry SC, York WS, Albersheim P, Darvill A, Hayashi T, Joseleau JP, Seitz HU, Kato Y, Pérez Lorences E, Maclachlan GA, et al (1993) An unambiguous nomenclature for xyloglucan-derived oligosaccharides. Physiol Plant **89:** 1–3
Fu H, Yadav MP, Nothnagel EA (2007) *Physcomitrella patens* arabinogalactan proteins contain abundant terminal 3-O-methyl-L-rhamnosyl residues not found in angiosperms. Planta **226:** 1511–1524
Geitmann A (2010) How to shape a cylinder: pollen tube as a model system for the generation of complex cellular geometry. Sex Plant Reprod **23:** 63–71
Geitmann A, Steer M (2006) The architecture and properties of the pollen tube cell wall. *In* R Malhó, ed, The Pollen Tube. Plant Cell Monographs, Vol 3. Springer-Verlag, Berlin, pp 177–200
Harholt J, Jensen JK, Sørensen SO, Orfila C, Pauly M, Scheller HV (2006) ARABINAN DEFICIENT 1 is a putative arabinosyltransferase involved in biosynthesis of pectic arabinan in Arabidopsis. Plant Physiol **140:** 49–58
Hasegawa Y, Nakamura S, Kakizoe S, Sato M, Nakamura N (1998) Immunocytochemical and chemical analyses of Golgi vesicles isolated from the germinated pollen of *Camellia japonica*. J Plant Res **111:** 421–429
Honys D, Twell D (2004) Transcriptome analysis of haploid male gametophyte development in *Arabidopsis*. Genome Biol **5:** R85
Iwai H, Hokura A, Oishi M, Chida H, Ishii T, Sakai S, Satoh S (2006) The gene responsible for borate cross-linking of pectin rhamnogalacturonan-II is required for plant reproductive tissue development and fertilization. Proc Natl Acad Sci USA **103:** 16592–16597
Iwai H, Ishii T, Satoh S (2001) Absence of arabinan in the side chains of the pectic polysaccharides strongly associated with cell walls of *Nicotiana plumbaginifolia* non-organogenic callus with loosely attached constituent cells. Planta **213:** 907–915
Jauh GY, Lord EM (1996) Localization of pectins and arabinogalactan-proteins in lily (*Lilium longiflorum* L.) pollen tube and style, and their possible roles in pollination. Planta **199:** 251–261
Jiang L, Yang SL, Xie LF, Puah CS, Zhang XQ, Yang WC, Sundaresan V, Ye D (2005) *VANGUARD1* encodes a pectin methylesterase that enhances pollen tube growth in the *Arabidopsis* style and transmitting tract. Plant Cell **17:** 584–596
Johnson MA, Lord EM (2006) Extracellular guidance cues and intracellular signaling pathways that direct pollen tube growth. *In* R Malhó, ed, The Pollen Tube. Plant Cell Monographs, Vol 3. Springer-Verlag, Berlin, pp 223–242
Johnson-Brousseau SA, McCormick S (2004) A compendium of methods useful for characterizing Arabidopsis pollen mutants and gametophytically expressed genes. Plant J **39:** 761–775
Jones L, Milne JL, Ashford D, McQueen-Mason SJ (2003) Cell wall arabinan is essential for guard cell function. Proc Natl Acad Sci USA **100:** 11783–11788
Jones L, Seymour GB, Knox JP (1997) Localization of pectic galactan in tomato cell walls using a monoclonal antibody specific to (1-4)-β-D-galactan. Plant Physiol **113:** 1405–1412
Kandasamy MK, Nasrallah JB, Nasrallah ME (1994) Pollen-pistil interactions and developmental regulation of pollen tube growth in *Arabidopsis*. Development **120:** 3405–3418
Kim S, Mollet JC, Dong J, Zhang K, Park SY, Lord EM (2003) Chemocyanin, a small basic protein from the lily stigma, induces pollen tube chemotropism. Proc Natl Acad Sci USA **100:** 16125–16130
Konishi T, Takeda T, Miyazaki Y, Ohnishi-Kameyama M, Hayashi T, O'Neill MA, Ishii T (2007) A plant mutase that interconverts UDP-arabinofuranose and UDP-arabinopyranose. Glycobiology **17:** 345–354
Lalanne E, Honys D, Johnson A, Borner GH, Lilley KS, Dupree P, Grossniklaus U, Twell D (2004) SETH1 and SETH2, two components of the glycosylphosphatidylinositol anchor biosynthetic pathway, are required for pollen germination and tube growth in *Arabidopsis*. Plant Cell **16:** 229–240
Leboeuf E, Guillon F, Thoiron S, Lahaye M (2005) Biochemical and immunohistochemical analysis of pectic polysaccharides in the cell walls of *Arabidopsis* mutant *quasimodo 1* suspension-cultured cells: implications for cell adhesion. J Exp Bot **56:** 3171–3182
Leboeuf E, Thoiron S, Lahaye M (2004) Physico-chemical characteristics of cell walls from *Arabidopsis thaliana* microcalli showing different adhesion strengths. J Exp Bot **55:** 2087–2097
Lennon KA, Lord EM (2000) The *in vivo* pollen tube cell of *Arabidopsis thaliana*. I. Tube cell cytoplasm and wall. Protoplasma **214:** 45–56
Lennon KA, Roy S, Hepler PK, Lord EM (1998) The structure of the transmitting tissue of *Arabidopsis thaliana* (L.) and the path of pollen tube growth. Sex Plant Reprod **11:** 49–59
Lerouxel O, Choo TS, Seveno M, Usadel B, Faye L, Lerouge P, Pauly M (2002) Rapid structural phenotyping of plant cell wall mutants by enzymatic oligosaccharide fingerprinting. Plant Physiol **130:** 1754–1763
Li YQ, Bruun L, Pierson ES, Cresti M (1992) Periodic deposition of arabinogalactan epitopes in the cell wall of pollen tubes of *Nicotiana tabacum* L. Planta **188:** 532–538
Li YQ, Chen F, Linskens HF, Cresti M (1994) Distribution of unesterified and esterified pectins in cell walls of pollen tubes of flowering plants. Sex Plant Reprod **7:** 145–152
Li YQ, Faleri C, Geitmann A, Zhang HQ, Cresti M (1995) Immunogold localization of arabinogalactan proteins, unesterified and esterified pectins in pollen grains and pollen tubes of *Nicotiana tabacum* L. Protoplasma **189:** 26–36
Li YQ, Mareck A, Faleri C, Moscatelli A, Liu Q, Cresti M (2002) Detection and localization of pectin methylesterase isoforms in pollen tubes of *Nicotiana tabacum* L. Planta **214:** 734–740
Lord EM, Russell SD (2002) The mechanisms of pollination and fertilization in plants. Annu Rev Cell Dev Biol **18:** 81–105
Marcus SE, Verhertbruggen Y, Hervé C, Ordaz-Ortiz JJ, Farkas V, Pedersen HL, Willats WGT, Knox JP (2008) Pectic homogalacturonan masks abundant sets of xyloglucan epitopes in plant cell walls. BMC Plant Biol **8:** 60
McCormick S, Yang H (2005) Is there more than one way to attract a pollen tube? Trends Plant Sci **10:** 260–263
Micheli F (2001) Pectin methylesterases: cell wall enzymes with important roles in plant physiology. Trends Plant Sci **6:** 414–419
Mollet JC, Faugeron C, Morvan H (2007) Cell adhesion, separation and guidance in compatible plant reproduction. Annu Plant Rev **25:** 69–90
Mollet JC, Kim S, Jauh GY, Lord EM (2002) Arabinogalactan proteins, pollen tube growth, and the reversible effects of Yariv phenylglycoside. Protoplasma **219:** 89–98
Mollet JC, Park SY, Nothnagel EA, Lord EM (2000) A lily stylar pectin is necessary for pollen tube adhesion to an *in vitro* stylar matrix. Plant Cell **12:** 1737–1749
Nakamura N, Suzuki H (1981) Sugar composition of pollen grain and pollen tube cell walls. Phytochemistry **20:** 981–984
Nguema-Ona E, Andème-Onzighi C, Aboughe-Angone S, Bardor M, Ishii T, Lerouge P, Driouich A (2006) The reb1-1 mutation of Arabi-

dopsis: effect on the structure and localization of galactose-containing cell wall polysaccharides. Plant Physiol **140:** 1406–1417

Nothnagel EA (1997) Proteoglycans and related components in plant cells. Int Rev Cytol **174:** 195–291

Obel N, Erben V, Schwarz T, Kuhnel S, Fodor A, Pauly M (2009) Microanalysis of plant cell wall polysaccharides. Mol Plant **2:** 922–932

Orfila C, Seymour GB, Willats WG, Huxham IM, Jarvis MC, Dover CJ, Thompson AJ, Knox JP (2001) Altered middle lamella homogalacturonan and disrupted deposition of (1→5)-α-L-arabinan in the pericarp of *Cnr*, a ripening mutant of tomato. Plant Physiol **126:** 210–221

Palanivelu R, Preuss D (2000) Pollen tube targeting and axon guidance: parallels in tip growth mechanisms. Trends Cell Biol **10:** 517–524

Park SY, Jauh GY, Mollet JC, Eckard KJ, Nothnagel EA, Walling LL, Lord EM (2000) A lipid transfer-like protein is necessary for lily pollen tube adhesion to an *in vitro* stylar matrix. Plant Cell **12:** 151–163

Pauly M, Qin Q, Greene H, Albersheim P, Darvill G, York WS (2001) Changes in the structure of xyloglucan during cell elongation. Planta **212:** 842–850

Pelloux J, Rustérucci C, Mellerowicz EJ (2007) New insights into pectin methylesterase structure and function. Trends Plant Sci **12:** 267–277

Peña MJ, Carpita NC (2004) Loss of highly branched arabinans and debranching of rhamnogalacturonan I accompany loss of firm texture and cell separation during prolonged storage of apple. Plant Physiol **135:** 1305–1313

Peña MJ, Ryden P, Madson M, Smith AC, Carpita NC (2004) The galactose residues of xyloglucan are essential to maintain mechanical strength of the primary cell walls in Arabidopsis during growth. Plant Physiol **134:** 443–451

Pereira LG, Coimbra S, Oliveira H, Monteiro L, Sottomayor M (2006) Expression of arabinogalactan protein genes in pollen tubes of *Arabidopsis thaliana*. Planta **223:** 374–380

Puhlmann J, Bucheli E, Swain MJ, Dunning N, Albersheim P, Darvill AG, Hahn MG (1994) Generation of monoclonal antibodies against plant cell wall polysaccharides. I. Characterization of a monoclonal antibody to a terminal α-(1,2)-linked fucosyl-containing epitope. Plant Physiol **104:** 699–710

Qin Y, Chen D, Zhao J (2007) Localization of arabinogalactan proteins in anther, pollen, and pollen tube of *Nicotiana tabacum* L. Protoplasma **231:** 43–53

Qin Y, Leydon AR, Manziello A, Pandey R, Mount D, Denic S, Vasic B, Johnson MA, Palanivelu R (2009) Penetration of the stigma and style elicits a novel transcriptome in pollen tubes, pointing to genes critical for growth in a pistil. PLoS Genet **5:** e1000621

Rae AL, Harris PJ, Bacic A, Clarke AE (1985) Composition of the cell walls of *Nicotiana alata* Link et Otto pollen tubes. Planta **166:** 128–133

Ray B, Loutelier-Bourhis C, Lange C, Condamine E, Driouich A, Lerouge P (2004) Structural investigation of hemicellulosic polysaccharides from *Argania spinosa*: characterisation of a novel xyloglucan motif. Carbohydr Res **339:** 201–208

Rhee SY, Osborne E, Poindexter PD, Somerville CR (2003) Microspore separation in the *quartet3* mutants of Arabidopsis is impaired by a defect in a developmentally regulated polygalacturonase required for pollen mother cell wall degradation. Plant Physiol **133:** 1170–1180

Roy S, Eckard KJ, Lancelle S, Hepler PK, Lord EM (1997) High-pressure freezing improves the ultrastructural preservation of *in vivo* grown lily pollen tubes. Protoplasma **20:** 87–98

Rubinstein AL, Márque J, Cervera MS, Bedinger PA (1995) Extensin-like glycoproteins in the maize pollen tube wall. Plant Cell **7:** 2211–2225

Seifert GJ, Roberts K (2007) The biology of arabinogalactan proteins. Annu Rev Plant Biol **58:** 137–161

Showalter AM (2001) Arabinogalactan-proteins: structure, expression and function. Cell Mol Life Sci **58:** 1399–1417

Smallwood M, Martin H, Knox JP (1995) An epitope of rice threonine- and hydroxyproline-rich glycoprotein is common to cell wall and hydrophobic plasma-membrane glycoproteins. Planta **196:** 510–522

Smith K, Davies M, Hounsells E (1994) Structural profiling of oligosaccharides of glycoproteins. Methods Mol Biol **32:** 143–155

Tian GW, Chen MH, Zaltsman A, Citovsky V (2006) Pollen-specific pectin methylesterase involved in pollen tube growth. Dev Biol **294:** 83–91

Tung CW, Dwyer KG, Nasrallah ME, Nasrallah JB (2005) Genome-wide identification of genes expressed in Arabidopsis pistils specifically along the path of pollen tube growth. Plant Physiol **138:** 977–989

Verhertbruggen Y, Marcus SE, Haeger A, Verhoef R, Schols HA, McCleary BV, McKee L, Gilbert HJ, Knox JP (2009) Developmental complexity of arabinan polysaccharides and their processing in plant cell walls. Plant J **59:** 413–425

Vincken JP, Schols HA, Oomen R, McCann MC, Ulvskov P, Voragen AGJ, Visser RGF (2003) If homogalacturonan were a side chain of rhamnogalacturonan I: implications for cell wall architecture. Plant Physiol **132:** 1781–1789

Whitney SEC, Wilson E, Webster J, Bacic A, Reid JSG, Gidley MJ (2006) Effects of structural variation in xyloglucan polymers on interactions with bacterial cellulose. Am J Bot **93:** 1402–1414

Willats WGT, Marcus SE, Knox JP (1998) Generation of a monoclonal antibody specific to (1-5)-alpha-L-arabinan. Carbohydr Res **308:** 149–152

Wu H, Wang H, Cheung AY (1995) A floral transmitting tissue specific glycoprotein attracts pollen tubes and stimulates their growth. Cell **82:** 383–393

Yates EA, Valdor JF, Haslam SM, Morris HR, Dell A, Mackie W, Knox JP (1996) Characterization of carbohydrate structural features recognized by anti-arabinogalactan-protein monoclonal antibodies. Glycobiology **6:** 131–139

York W, Darvill A, McNeil M, Stevenson TT, Albersheim P (1985) Isolation and characterization of plant cell walls and cell wall components. Methods Enzymol **118:** 3–40

Zablackis E, Huang J, Müller B, Darvill AG, Albersheim P (1995) Characterization of the cell-wall polysaccharides of *Arabidopsis thaliana* leaves. Plant Physiol **107:** 1129–1138

Zabotina OA, van de Ven WTG, Freshour G, Drakakaki G, Cavalier D, Mouille G, Hahn MG, Keegstra K, Raikhel NV (2008) Arabidopsis *XXT5* gene encodes a putative α-1,6-xylosyltransferase that is involved in xyloglucan biosynthesis. Plant J **56:** 101–115

Zou J, Song L, Zhang W, Wang Y, Ruan S, Wu WH (2009) Comparative proteomic analysis of Arabidopsis mature pollen and germinated pollen. J Integr Plant Biol **51:** 438–455

Supplemental data

Estimation of the amount of pollen grain wall *versus* pollen tube wall

From TEM pictures, we measured the diameter of pollen grains and pollen tubes, the thickness of the intine wall and pollen tube cell wall (inner and outer wall) as shown in the drawing of Table SI.A. We considered (1) that the dehydration step used for sample preparation will have the same affect on both pollen grains and pollen tubes and (2) the thickness of the pollen tube wall is constant throughout the length of the tube. We calculated the volume of the intine wall (using the formula $4/3\pi r^3$) and the volume of pollen tube wall (using the formula $L\pi r^2$, with an average of L (averaged pollen tube length) = 1248 µm (1248 µm ± 374) (Table SI.B). We considered the pollen tube as a cylinder and did not take into account the tip which is negligible. We calculated the contribution of pollen tube wall and pollen grain intine wall based on the average 67% germination rate (67% ± 12) (Table SI. B).

Table SI. (A) Measurement of pollen grain and pollen tube diameters and (B) calculations of cell wall volumes and estimation of the contribution of pollen tube wall *versus* pollen grain wall

A

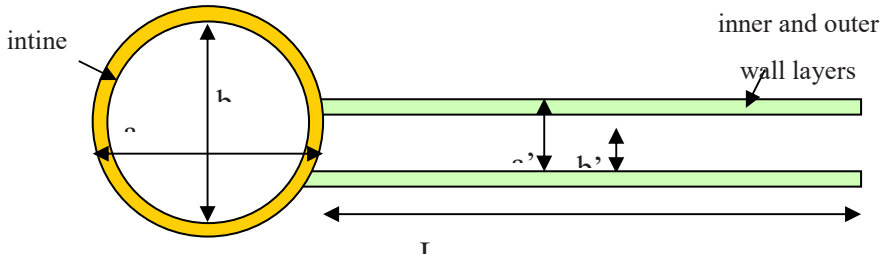

B

	Pollen grain	Pollen tube
External diameter (µm), (a and a')	a = 18.1 µm ± 4.53	a' = 3.74 µm ± 0.17
Internal diameter (µm), (b and b')	b = 17.82 µm ± 4.55	b' = 3.52 µm ± 0.18
Thickness of wall (µm)	a-b = 0.28 µm ± 0.06	a'-b' = 0.22 µm ± 0.03
Volume formula	$V = 4/3\pi r^3$	$V = L\pi r^2$ with L = 1248 µm
Volume with wall (μm^3)	3104 μm^3	13710.32 μm^3
Volume without wall (μm^3)	2963 μm^3	12144.78 μm^3
Volume of wall (μm^3)	141 μm^3	1565.54 μm^3
Volume of wall for 67% germination rate		1048.91 μm^3
Ratio volume of wall from pollen tube / volume of wall from pollen grain		7.44 (for 67 % germination)

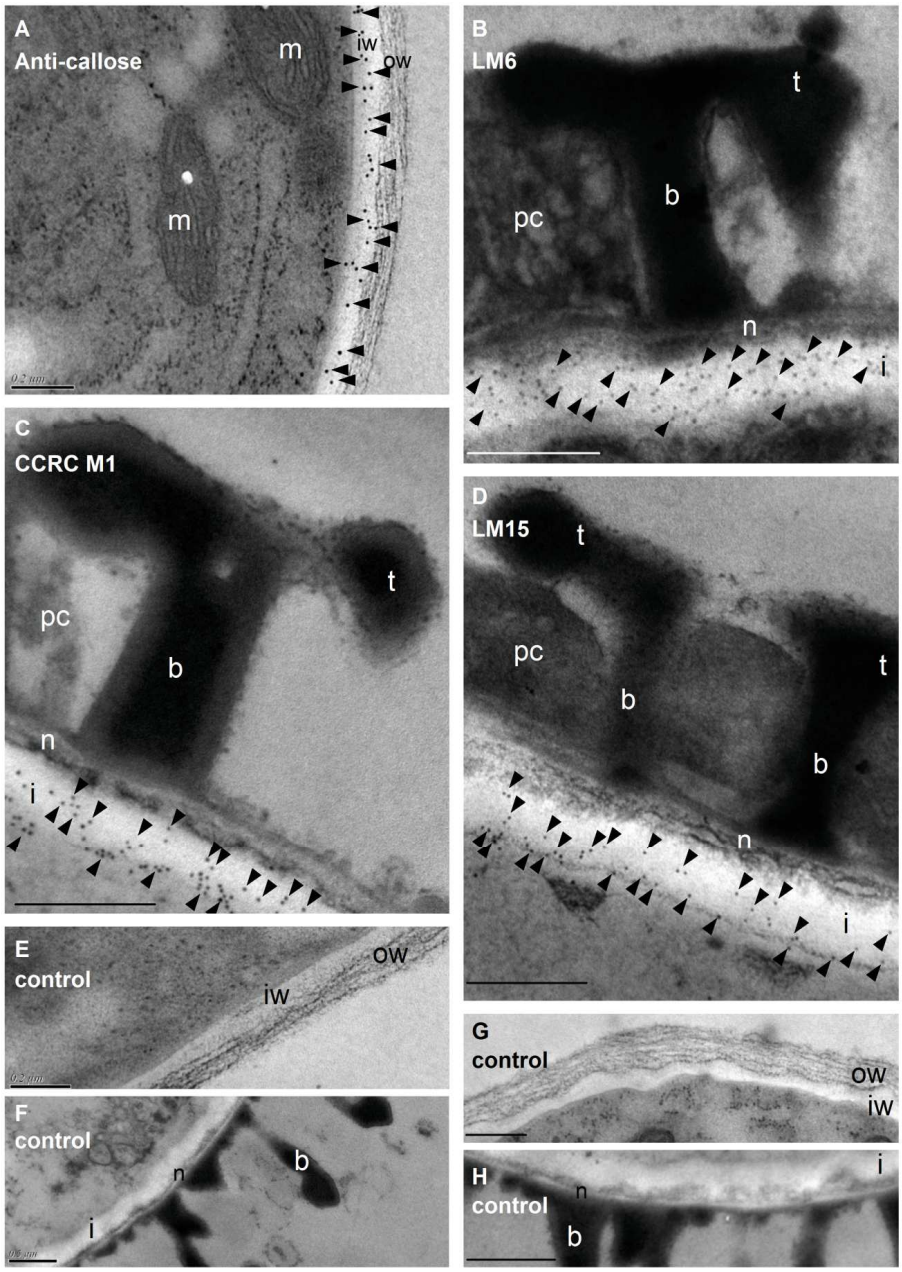

Figure S1. Immunogold localization of cell wall polymers in Arabidopsis pollen tube (A), pollen grain (B-D) and controls (E-H). **A**, Localization of callose in pollen tube. Gold particles (arrowhead) are localized in the translucent inner wall layer. **B**, Localization of (1→5)-α-L-arabinan epitopes with LM6 in pollen grain. Gold particles (arrowhead) are uniformly dispatched over the entire intine wall. The outer wall (bacula, nexine and tectum) forming the exine of the pollen grain and pollen coat (pc) are visible. **C**, Localization of fucosylated XyG with CCRC-M1 in the pollen grain. Gold particles (arrowhead) appeared located in the inner part of the intine. **D**, Localization of non galactosylated XyG with LM15 in the pollen grain. The MAb also labeled the inner part of the intine wall, close to the plasma membrane. **E-F**, Controls with anti-rat-gold conjugate in pollen tube and pollen grain, respectively. No significant non specific labeling was observed. **G-H**, Controls with anti-mouse-gold conjugate in pollen tube and pollen grain, respectively. No significant labeling was observed.

b, bacula; i, intine; iw, inner wall; m, mitochondria; n, nexine; ow, outer wall; pc, pollen coat; t, tectum. Scale bars = 0.5 µm (B-E, G, I) and 0.2 µm (A, F, H).

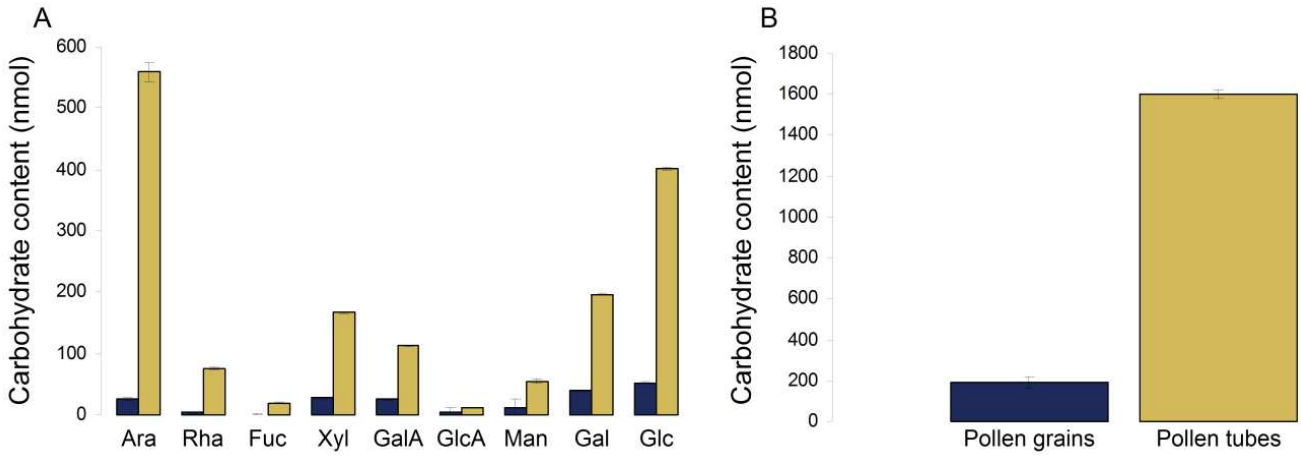

Figure S2. Monosaccharide composition (**A**) and carbohydrate content (**B**) of the cell wall of non-germinated pollen grains (blue) and 16h-*in vitro* grown pollen tubes (yellow) isolated from 520 flowers.

Ara, arabinose; Fuc, fucose; Gal, galactose; Glc, glucose; GalA, galacturonic acid; GlcA, glucuronic acid; Man, mannose; Rha, rhamnose; Xyl, xylose.

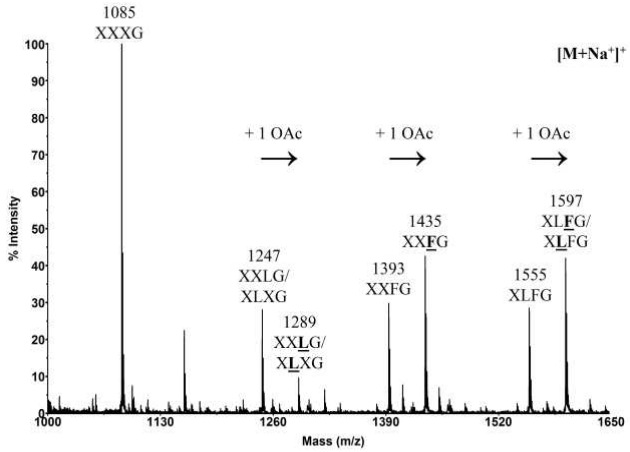

Figure S3. MALDI-TOF mass spectrum of endoglucanase-generated XyG fragments from mature leaf cell wall. The structures of the XyG fragments are shown according to the nomenclature proposed by Fry et al., (1993). Underlined and bold structures represent O-acetylated side chains (+ 1 OAc).

Plants **2013**, *2*, 107-147; doi:10.3390/plants2010107

OPEN ACCESS

plants

ISSN 2223-7747

www.mdpi.com/journal/plants

Review

Cell Wall Composition, Biosynthesis and Remodeling during Pollen Tube Growth

Jean-Claude Mollet *, Christelle Leroux, Flavien Dardelle and Arnaud Lehner

Laboratoire de Glycobiologie et Matrice Extracellulaire Végétale, EA4358, IRIB, Normandy University, University of Rouen, 76821 Mont Saint-Aignan, France; E-Mails: christelle.leroux@etu.univ-rouen.fr (C.L.); flavien.dardelle@gmail.com (F.D.); arnaud.lehner@univ-rouen.fr (A.L.)

* Author to whom correspondence should be addressed; E-Mail: jean-claude.mollet@univ-rouen.fr; Tel.: +332-351-466-89; Fax: +332-351-466-15.

Received: 13 December 2012; in revised form: 19 February 2013 / Accepted: 19 February 2013 / Published: 7 March 2013

Abstract: The pollen tube is a fast tip-growing cell carrying the two sperm cells to the ovule allowing the double fertilization process and seed setting. To succeed in this process, the spatial and temporal controls of pollen tube growth within the female organ are critical. It requires a massive cell wall deposition to promote fast pollen tube elongation and a tight control of the cell wall remodeling to modify the mechanical properties. In addition, during its journey, the pollen tube interacts with the pistil, which plays key roles in pollen tube nutrition, guidance and in the rejection of the self-incompatible pollen. This review focuses on our current knowledge in the biochemistry and localization of the main cell wall polymers including pectin, hemicellulose, cellulose and callose from several pollen tube species. Moreover, based on transcriptomic data and functional genomic studies, the possible enzymes involved in the cell wall remodeling during pollen tube growth and their impact on the cell wall mechanics are also described. Finally, mutant analyses have permitted to gain insight in the function of several genes involved in the pollen tube cell wall biosynthesis and their roles in pollen tube growth are further discussed.

Keywords: biosynthesis; callose; cellulose; cell wall; pectin; glycoside hydrolases; pollen tube growth; remodeling; xyloglucan

1. Introduction

Fertilization of flowering plants requires the delivery of two sperm cells carried by the pollen tube, a fast tip-polarized growing cell, to the egg cell. In plants such as *Arabidopsis thaliana*, this process begins with the adhesion of the pollen grains on the stigmatic papillae after the pollen coat has contacted the papillae (Figure 1a–d). Following hydration of the pollen grain, the pollen tube emerges either from one of the three pollen grain apertures (Figure 1c) or through the exine wall (Figure 1e) [1]. Then, pollen tubes invade the cell wall of the papillae (Figure 1b–d), enter the short style, and grow in the apoplast of the specialized transmitting tract cells (Figure 1b) enriched in extracellular nutrient [2,3].

Figure 1. Scanning electron (**a**–**d**) and fluorescent (**e**) micrographs of *Arabidopsis thaliana* (**a**) dry pollen grain showing the three apertures (arrows), (**b**) emerging pollen tube from a pollen grain, (**c**) pollen germination on the papillae, (**d**) self-pollinated pistil with adhering pollen grains on the papillae and (**e**) aniline blue staining of self-pollinated stigma showing pollen tubes within the transmitting tract and reaching the ovules (dashed line and *). ex. exine, p. papillae, o. ovule, ov. ovary, pg. pollen grain, pt. pollen tube, s. stigma, st. style, tt. transmitting tract.

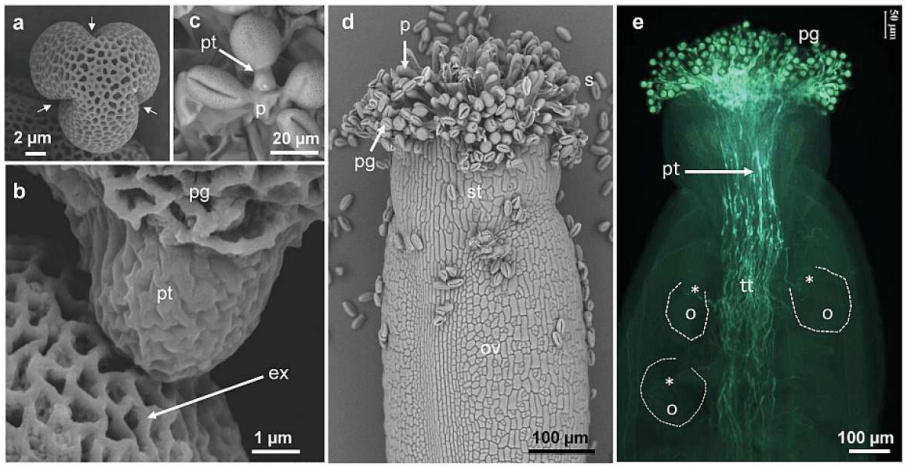

During this invasive growth, pollen tubes are guided to the ovules via signals that need to pass through the cell wall to reach their membrane-associated or intracellular targets [4–11]. In addition to being the interface between the tube cell and the surrounding (culture medium or female tissues), the cell wall of pollen tubes plays a crucial role in the control of the cell shape, in the protection of the generative cells and in the resistance against turgor pressure induced tensile stress [12,13]. Thus, a tight control of cell wall deposition and remodeling during pollen tube growth is required to fulfill all these functions.

In this review, we describe our current knowledge on the biosynthesis, distribution and biochemistry of cell wall polymers including pectin, hemicellulose, cellulose and callose from several pollen tube species (including plants with dry stigma and solid style like *Arabidopsis thaliana* and

tobacco and wet stigma and hollow style like in lily). The structure and functions of arabinogalactan-proteins in pollen tube growth will not be addressed as it was recently detailed by [14]. Finally, the enzymes from the male gametophyte and the female sporophytic counterpart possibly involved in the cell wall remodeling during pollen tube growth are further discussed in relation with the mechanical properties of the cell wall.

2. Cell Wall Polymers in Pollen Tubes

Despite the importance of pollen tubes for the delivery of the sperm cells to the egg, little is known about the underlying molecular mechanisms that regulate the mechanical interaction of pollen tubes with the female floral tissues and only very scarce data are available concerning the biosynthesis and remodeling of the pollen tube cell wall.

Pollen tubes in most species display in the tip region a clear zone like in *A. thaliana* (Figure 2a), composed of numerous Golgi-derived vesicles that migrate toward the apex in the cell cortex and accumulate in an annulus-shaped region adjacent to the extreme tip (apical flank) where they fuse with the plasma membrane to sustain pollen tube growth [15]. At the extreme apex and in the distal region of the pollen tube, endocytosis takes place possibly by clathrin-dependent and -independent pathways [10,16–19].

Figure 2. *A. thaliana* pollen tube grown *in vitro*. (**a**) High magnification of eight-hour-old pollen tube grown in liquid medium showing the clear zone at the tip (arrow). (**b**) Transmission electron micrograph of high pressure-freeze substituted pollen tube showing the two cell wall layers. (**c**) Pollen tube stained with decolorized aniline blue showing the callose wall and two callose plugs. Note the absence of staining at the tip (arrow). (**d**) Immunolocalization of highly methylesterified HG with LM20 in a pollen tube showing a strong labeling at the tip (arrow). cp: callose plug, er: endoplasmic reticulum, g: Golgi apparatus, iw: inner wall, m: mitochondria, ow: outer wall. Dotted circle indicates the location of the pollen grain.

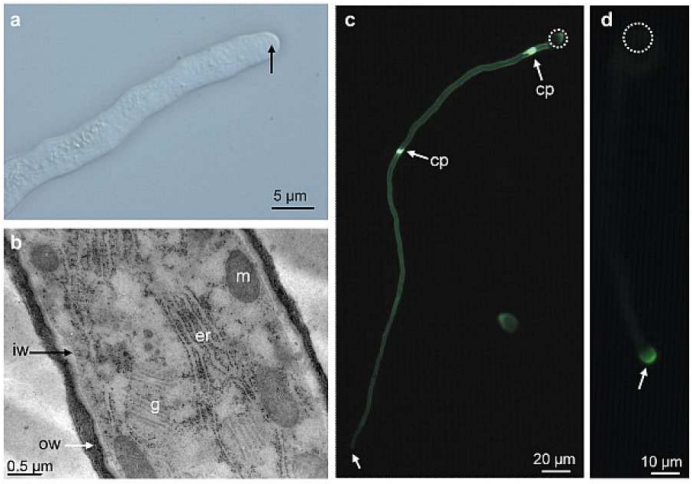

Transmission electron microscope observations of *in vitro* and *in vivo* grown pollen tubes from many species including lily [20], tobacco [21,22], *A. thaliana* [23–26] and in several but not all the gymnosperm investigated species like *Pinus sylvestris* [27], *Podocarpus nagi* or *Pinus banksiana* [28] showed a cell wall composed of two layers at the shank of the pollen tube: a fibrillar outer layer and a weakly electron-dense inner wall (Figure 2b). In contrast, the inner cell wall layer is generally lacking at the pollen tube tip in normal condition [20,23,24,27].

2.1. Distribution of Carbohydrate Epitopes in the Pollen Tube Cell Wall

Distribution of pollen tube cell wall polymers was investigated by using mostly cytochemical reagents, enzymes and/or antibodies (Table 1). In most of the immunolocalization studies, monoclonal antibodies (mAbs) are applied on the whole pollen tube [24–32], allowing a cell surface labeling that may mislead in the interpretation as epitopes may have been masked by other polymers. To avoid this problem, enzyme treatments were sometimes applied on fixed tubes or pollen tubes were embedded in resin and sectioned [33]. Another possible artifact is caused by the slow penetration of the chemical fixative that arrests pollen tube growth while exocytosis is still ongoing, or the other way round, that arrests of enzymatic reactions in the wall while the tube is still growing.

Table 1. List of probes (antibody, cytochemical reagent and enzyme) used to detect pollen tube cell wall polysaccharides.

Probe [a]	Polysaccharide [b]	Epitope recognized [c]	Refs.
Antibody			
CCRC-M1	XyG	α-Fuc-(1→2)-β-Gal	[34]
LM15	XyG	XXXG, XXLG, XLXG, XXGG	[35]
JIM5	weakly methylesterified HG	α-MeGalA-(1→4)-α-GalA$_{(4)}$-(1→4)-α-MeGalA	[36]
LM19	weakly methylesterified HG	α-GalA-(1→4)$_{(4)}$	[37]
JIM7	partially methylesterified HG	α-GalA-(1→4)-α-MeGalA$_{(4)}$-(1→4)-α-GalA	[36]
LM20	partially methylesterified HG	α-MeGalA-(1→4)$_{(4)}$	[37]
LM8	xylogalacturonan	unknown	[38]
LM5	(1→4)-β-D-galactan (RG-I)	β-Gal-(1→4)$_{(3)}$	[39]
LM6	(1→5)-α-L-arabinan (RG-I)	Branched α-Ara-(1→5)$_{(5)}$	[40]
LM13	(1→5)-α-L-arabinan (RG-I)	Linear α-Ara-(1→5)$_{(5)}$	[41]
LAMP	callose	β-Glc-(1→3)$_{(5)}$	[42]
Anti-RG-II	Monomeric and dimeric RG-II	unknown	[43]
Cytochemical reagent			
Calcofluor white	β-Glucan	na	
Aniline blue	callose	na	[44]
PI	HG	na	[45]
Protein			
CBH-I	cellulose	na	[22]
CBM3a	Crystalline cellulose	na	[46]

[a] CCRC-M. Complex Carbohydrate Research Center-Monoclonal, LM, Leeds Monoclonal, JIM, John Innes Monoclonal, LAMP, LAMinarin Pentaose, RG-II. Rhamnogalacturonan-II, PI. Propidium iodide, CBH-I. Cellobiohydrolase-I, CBM3a. Cellulose binding module3a. [b] XyG. Xyloglucan, HG. Homogalacturonan, RG-I. Rhamnogalacturonan-I. [c] Ara. arabinose, Fuc. fucose, Gal. galactose, GalA. galacturonic acid, Glc, glucose, MeGalA, 6-*O*-methyl-galacturonate, na. not applicable. For more information see [47].

Distribution of cell wall polymers in pollen tubes was investigated in plant species of the angiosperm eudicots such as *A. thaliana* [23–26], *Nicotiana tabacum* [21,22,29], *Solanum chacoense* [30], *Camellia japonica* [31], *Torenia fournieri* [32] and *Actinidia deliciosa* [33] as well as angiosperm monocots like *Lilium longiflorum* [48,49] and *Zea mays* [50]. More recent studies have focused on the gymnosperms like *Pinus sylvestris* [27], *Picea meyeri* [51] and several others [28,52].

One of the main differences between the primary cell wall of somatic and pollen tube cells is despite its presence, the low abundance of cellulose, a β-(1→4)-glucan. Instead, callose, a β-(1→3)-glucan, is the main cell wall polysaccharide. Callose is mostly localized in the inner cell wall and is absent from the tube tip of most angiosperm pollen tubes [53,54] including *A. thaliana* (Figure 2c) [25]. In contrast, in *Cycas* and several *Pinus* species, callose was not detected in the pollen tube wall by aniline blue staining [28]. However, in *P. sylvestris*, a strong fluorescence was detected with aniline blue at the tube tip [27]. In addition, callose is deposited at periodic intervals to form callose plugs that maintain the tube cell in the apical expanding region of angiosperm pollen tubes (Figure 2c) and separates the viable from the degenerating region of the tube [12]. In tobacco using CBH-I-gold and LAMP MAb [22] and in *A. thaliana* using CBM3a [26] and LAMP MAb [25], callose and cellulose are localized in the plugs and in the inner cell wall of the pollen tube. In contrast, in long-living and slow-growing gymnosperm pollen tubes, the callose plug deposition is apparently not a consistent feature as well as the permanent callose wall in pollen tubes [52]. This observation suggests that in the evolution of flowering plants a permanent callose wall and callose plug deposition appeared through the short-lived and fast-growing pollen tubes of angiosperms [55]. Cellulose is present in the entire cell wall of pollen tubes with a weaker staining with calcofluor white or CBH-I-gold labeling at the tip in most angiosperms [22,25,27,30]. Recently, Chebli *et al*. [26] using CBM3a that binds to crystalline cellulose found two populations of *A. thaliana* pollen tubes displaying intense or weak labeling at their tips suggesting that the labeling was related to temporal growth rate. Similarly, in *T. fournieri*, the distribution of cellulose changed temporally and spatially, being abundant in freshly germinated pollen tubes, and absent from the tube tip of older pollen tubes [32]. Using atomic force microscopy, Wu *et al.* [32] also revealed that cellulose microfibrils were more abundant in the apical region of slow-growing tubes whereas only few microfibrils were observed in the auxin-stimulated pollen tubes suggesting a correlation between cellulose abundance and pollen tube growth. In Conifers, pollen tubes have cellulose in the entire cell wall and may contain more cellulose deposited at the tube tip, which may explain the slower growth [52,56].

Pectins are complex polymers consisting of homogalacturonan (HG), which can be methyl- and acetyl-esterified, rhamnogalacturonan-I (RG-I), rhamnogalacturonan-II (RG-II), and xylogalacturonan [57]. HG is a polymer of repeated units of (1→4)-α-D-galacturonic acid. Upon block wise action of pectin methylesterases on methylesterified HG, several parallel HG chains can be cross-linked via the interaction of the negative charges of the carboxyl groups of galacturonic acid and calcium [58]. RG-II has a galacturonan backbone with four well defined oligosaccharides composed of unusual sugars such as apiose, aceric acid and 3-deoxy-D-manno-2-octulosonic acid (Kdo) of unknown function [57]. RG-II is present in the primary cell wall of all higher plants and its structure is evolutionarily conserved in the plant kingdom. In the cell wall, it exists predominantly in the form of a dimer that is cross-linked by a borate di-ester between two apiosyl residues [57]. On the other hand, RG-I consists of the repeating disaccharide unit, (1→4)-α-D-galacturonic acid-(1→2)-α-L-rhamnose. On the rhamnosyl

residues, a wide variety of side chains can be detected ranging from monomers to large oligosaccharides such as (1→4)-β-D-galactan, (1→5)-α-L-arabinan, and/or type I arabinogalactan [57].

Most of the studies on the pectic wall of the pollen tube focused on the detection of HG domains using the JIM5 and JIM7 mAbs (Table 1). To date, localization data of other pectic domains such as xylogalacturonan and RG-I side chains in the pollen tube wall are scarce. Immunofluorescence labeling of weakly and highly methylesterified HG with JIM5 and JIM7 or the newly introduced LM19 and LM20 depends clearly on the species, the *in vitro* growth condition and the growth rate of the pollen tube [59]. It is however generally observed that in most angiosperms, highly methylesterified HG is mostly detected at the tip (Figure 2d) and weakly methylesterified HG epitopes are preferentially detected either in the entire pollen tube or in the pollen tube except in the tip region as shown in the Brassicacae (*A. thaliana*) [25], Solanaceae (wild potato, tobacco, petunia), Oleaceae (jasmine), Poaceae (corn) [60], Scrophulariaceae (*T. fournieri*) [32] and Liliaceae (lily) [48,49]. Similar observations were obtained in *Picea meyeri* [51] and *Picea wilsonii* [61] pollen tubes. In other gymnosperm species like *P. macrophyllus* and *P. banksiana,* pollen tubes were not labeled with JIM5 and JIM7 using electron microscopy observation [28].

Based on Elisa assays and dot-blots, it was clearly shown that JIM5 and JIM7 as well as LM19 and LM20 have specific but also overlapping binding capabilities to different degrees of methylesterification (DM) of HG domains after random or blockwise action of pectin methylesterases (PME) [37,62]. LM20 binds to HG with DM ranging between 85 and 16%, whereas LM19 binds to HG with DM between 66% and the demethylesterified form [37]. Using these data and assuming that PME has a blockwise action to allow calcium cross-linking in the shank of the tube, we can estimate that the DM of HG at the tip is probably over 70% and back from the tip, the DM is less than 15%. In lily, this change of methylesterification level occurs between 15 and 20 μm from the pole of the pollen tube corresponding exactly to the transition zone between the apical dome and the cylindrical shank of the cell [63]. In *A. thaliana*, this modification takes place closer to the tip (between 3 and 10 μm) [26]. Recently, propidium iodide (PI) was used to probe low methylesterified HG on living *A. thaliana* and *L. longiflorum* pollen tubes, which allowed following the dynamics of the pectin during pollen tube growth. The fluorescence of PI was detected at the tip and the shank of the pollen tubes with PI fluorescence oscillations preceding growth rate oscillations [45]. Finally, in certain species such as lily [49], *Ornithogalum* [59], tobacco [54] and others [60], periodic ring-like labeling patterns of weakly methylesterified HG were clearly visible along the pollen tube and originated from cell wall deposition during the slow growth pulses [54].

Side chains of RG-I are also present in the cell wall of pollen tubes. Using LM6 and/or LM13, epitopes associated with arabinan are evenly distributed along the entire pollen tube in *A. thaliana* [25], *A. deliciosa* [33] and *P. wilsonii* [61]. At the electron microscopy level, arabinan is mostly detected in the outer cell wall layer in *A. thaliana* [25] consistent with the location of other pectic motifs such as HG. Galactan is also detected in *A. thaliana* pollen tubes but the labeling intensity is weak [25] and almost absent in *Picea* [61].

Finally, RG-II, the major boron-binding component of the cell wall, is detected in the entire lily pollen tube cell wall [43] but is not in *Picea* [61].

Xyloglucan (XyG) is the major hemicellulosic polysaccharide of the primary cell wall of angiosperm eudicots and non-commelinid monocots [64,65]. Classic XyG consists of a (1→4)-β-D-

glucan backbone substituted with xylose, galactose-xylose or fucose-galactose-xylose motifs [66]. In the primary cell wall, XyG interacts with cellulose via hydrogen bonds and participates in the control of cell expansion [67]. The presence of fucosylated and galactosylated XyG was assessed only recently in *A. thaliana* pollen tubes using CCRC-M1 [25,68] and LM15 [25]. Labeling with both mAbs is detected in the entire pollen tube wall and at the electron microscopy level; it was shown that XyG is present in the outer and inner layers of the pollen tube cell wall [25] suggesting a possible interaction with cellulose microfibrils.

All these data reveal a common organization of the pollen tube cell wall in the species from the angiosperm eudicots and the non-commelinid monocots. In contrast, with the slow-growing and short-traveling gymnosperm pollen tubes, it appears that the distribution of cell wall polymers, especially the callose, is altered [69]. However, more studies using the probes listed in Table 1 are required to draw a general conclusion. To date, the investigation on the distribution of RG-II in pollen tubes is very limited but with the development of new specific probes for each individual side chains, the gap might be soon overcome. Another attracting method that may develop in the near future in the study of cell wall dynamics during pollen tube growth is the use of sugar analogs compatible to click chemistry associated with *in vivo* cell imaging [70]. In this method, sugar analogs are metabolically incorporated into cell wall polymers and subsequently labeled with covalent linkages to fluorescent probes [71] as shown with alkynylated fucose analog incorporated in the pectin of *A. thaliana* root cell wall [72]. This method will allow for insight into the dynamics and recycling of cell wall polymers on living pollen tubes.

2.2. Chemical Composition of Pollen Tube Cell Wall

Only very scarce studies have focused on the biochemical characterization of the pollen tube cell wall. The most striking point observed in the few biochemical characterizations of the cell wall of tobacco, *C. japonica*, lily, tulipa and *A. thaliana* pollen tubes is consistently the high level of arabinosyl residues [25,73,74]. In *A. thaliana*, Ara represents 43%, Glc 20%, GalA 11%, Gal 8% and Rha 5% of the total sugars [25]. Linkage analyses show that most of the arabinosyl residues are T-Ara, 5-linked and to a lesser extent 2,5-linked. These data indicate that the pectin of *A. thaliana* pollen tube cell wall is composed of 6% HG, 5% RG-I backbone harboring abundant chains of (1→5)-α-L-arabinan. This common feature suggests that arabinan may have an important role during pollen tube growth. Finally, linkage analyses also indicate (1) that most of the Glc is 3-linked indicating the abundance of callose [25,73] and (2) confirm that XyG is also present based on the detection of 4-Glc, 2-Xyl and T-Xyl, T-Gal and Fuc residues [25]. According to the one letter code proposed by Fry *et al.* [75], the unsubtituted glucosyl residue of the backbone is represented by the letter G. X, L and F represent the substitution by xylose, galactose-xylose and fucose-galactose-xylose, respectively. XyG can also be *O*-acetylated generally on the galactose, indicated by an underline letter, but the biological significance of *O*-acetylation is not known yet [76]. Generally, every four or five glucoses of the glucan backbone are not substituted allowing the cleavage of the polymer by *endo*-glucanase. The small oligosaccharides can then be analyzed by MALDI-TOF mass spectrometry, known as OLIMP method (OLIgosaccharide Mass Profiling) [77]. Using this technique, the fine structure of *A. thaliana* pollen tube XyG was recently determined. It revealed significant differences with the XyG from

vegetative organs such as leaves (Figure 3). Whereas XXXG is the main fragment of leaf XyG [25,78], the fucosylated and *O*-acetylated fragments (XXFG and XLFG) are the major motifs in *A. thaliana* pollen tube XyG [25] suggesting an important role of these two features in pollen tube growth and/or in the interaction with the female tissues.

Figure 3. MALDI-TOF mass spectra of *endo*-glucanase-generated XyG fragments from *A. thaliana* (**a**) Spectrum from pollen tubes. (**b**) Spectrum from mature leaves. The structures of the XyG fragments are shown according to the nomenclature proposed by Fry *et al.* [19]. Underlined structures represent *O*-acetylated side chains (+1 *O*Ac). The asterisk indicates the signal of XLFG fragment with K^+ adduct ion instead of Na^+. From Dardelle *et al.* [25], Copyright American Society of Plant Biologists [79].

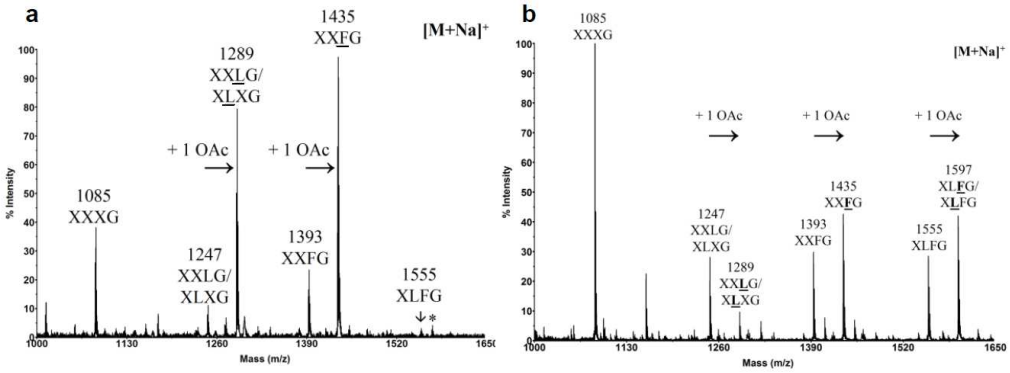

Used in the mid-90s to study the cell wall composition of algae [80] and later widely adopted to screen flax and *A. thaliana* cell wall mutants [81,82], Fourier transform infrared (FT-IR) microspectrometry associated with principal component analysis was recently used to study the effect of hormones, minerals or drugs on the cell wall composition of elongating pollen tubes [51,83]. It shows that treatments of *P. meyeri* pollen grains with brefeldin A, a drug able to inhibit the secretory pathway, reduce the pollen germination and tube growth by disrupting the secretory vesicles at the tip and significantly decrease the content of pectin in the apical region [84]. Treatments with nitric oxide donor or NO synthase inhibitor induce the accumulation of acidic HG and callose in the tip region [85]. Interestingly, blocking the release of intracellular calcium with drugs significantly alters the cell wall structure in *Picea* pollen tubes with the accumulation of callose and the disappearance of methylesterified HG at the tube tip [61]. Finally, treatment of *T. fournieri* pollen tubes with auxin promotes the growth by stimulating the synthesis of pectin, reducing the cellulose density and modifying the orientation of cellulose microfibrils as observed by atomic force microscopy [32]. However, whereas the vibrations associated with cellulose, phenolics, the methylester and the carboxyl groups of GalA are well assigned by FT-IR, the technique does not allow discriminating clearly other pectin motifs such as arabinan and/or galactan side chains of RG-I in the cell wall network. It is, however, a non destructive method that may be convenient to use in the future for determining the overall composition of pollen tube cell wall mutants compared to wild type. It may also be useful to follow the evolution of the cell wall composition in different portions of the pollen tube during growth.

Due to the technical challenges involved such as the labor intensive work to collect enough material, the number of studies focused on the biochemistry of pollen tube cell wall is limited. As a consequence, it does not permit to assess clearly the differences in the cell wall composition between angiosperm (monocot and eudicot) and gymnosperm. However, with the development of more sensitive equipments such as mass spectrometry, more information may be soon collected.

3. Cell Wall Polymer Biosynthesis in Pollen Tubes

3.1. Pectin Biosynthesis

Pectin represents one of the main carbohydrate polymers found in the cell wall of pollen tubes. Given the complexity of its structure, it is predicted that 67 different glycosyltransferases, methyltransferases and acetyltransferases are required for its biosynthesis [86]. The synthesis of the different pectin motifs is carried out in the Golgi apparatus and they are secreted via Golgi-derived vesicles [87].

3.1.1. Homogalacturonan

The synthesis of HG requires the activity of GALACTURONOSYLTRANSFERASEs (GAUTs) that was biochemically demonstrated in *Petunia axillaris* pollen tubes [88]. In *A. thaliana*, the multigenic family of *GALACTURONOSYLTRANSFERASE (GAUTs)* is composed of 15 genes [86,89] whose members are related to another family representing the *GALACTURONOSYLTRANSFERASE-LIKE* (*GATLs*), composed of 10 genes [90]. *GAUT1* (CAZy family GT8) is a galacturonosyltransferase gene that first was shown to be functionally implicated in the HG synthesis in *A. thaliana* vegetative organs [91]. The inactivation of *GAUT8* induces a reduction of the level of HG epitopes, a decrease of the amount of GalA in the cell wall of vegetative organs and a partial sterile phenotype [92]. Among all these genes, 13 *GAUTs* and 8 *GATLs* are expressed in the inflorescence of *A. thaliana* [89,90]. According to transcriptomic data, only two *GAUTs* (*GAUT13* and *GAUT14*) and two *GATLs* (*GATL4* and *GATL7*) are expressed in pollen tubes [90,93]. Interestingly, the *GALT4* expression seems to be pollen specific and is highly expressed in *A. thaliana* pollen tubes [90], which may suggest its implication in the synthesis of HG in pollen tubes but functional studies are necessary to assess the role of these genes in pollen tube growth.

3.1.2. Xylogalacturonan

In *A. thaliana*, the gene At5g33290 is involved in the xylogalacturonan biosynthesis, but the *xgd1* (*xylogalacturonan deficient1*) mutants do not display any visible pollen or pollen tube phenotype [94]. Other xylogalacturonan biosynthesis genes are undoubtedly implicated in this process but it remains to be established.

3.1.3. Rhamnogalacturonan-I

The backbone of RG-I is made of a repeating disaccharide α-(1→4)-D-GalA-α-(1→2)-L-Rha with Rha residues that can be substituted with galactan, arabinan and/or arabinogalactan [95]. In the

arabinan side chain, arabinosyl residues are almost entirely in the *furanose* configuration. Interestingly, rice REVERSIBLY GLYCOSYLATED PEPTIDEs (RGPs) show strong amino acid sequence identity (~80%) with an UDP-arabino*pyranose* mutase implicated in the interconversion of UDP-Ara*p* and UDP-Ara*f* [96]. Moreover, in *A. thaliana*, double knock-out mutations in two *RGPs* (*RGP1* and *RGP2*) showed a strong defect in the inner pollen wall and pollen lethality [97] suggesting that *RGP1* and *RGP2* act redundantly during pollen development. More recently, Rautengarten *et al.* [98] have shown that RGP1 and RGP2 are cytosolic and able to perform this interconversion indicating that RGPs may be part of the arabinan biosynthesis network. However, further studies are required to verify if RGP1 and RGP2 are also involved in the growth of pollen tubes. Moreover, biochemical evidence is needed to verify if the arabinan side chains of RG-I in the mutants are structurally different to the one found in wild type pollens and if other cell wall molecules containing Ara residues such as arabinogalactan proteins are not also affected.

3.1.4. Rhamnogalacturonan-II

Studies of the possible involvement of RG-II in pollen tube growth are very recent. In 2006, it was shown in tobacco that the mutation in *NpGUT1* (*Nicotiana plumbaginifolia GLUCURONOSYLTRANSFERASE1*) resulted in the inhibition of pollen tube elongation, presumably due to an abnormal deposition of RG-II and boron in the pollen tube tip cell wall [99]. However, it was shown recently that in *A. thaliana*, IRX10 (IRREGULAR XYLEM10) and IRX10-L (IRREGULAR XYLEM10-LIKE) proteins, which are closely related to *Np*GUT1, play a critical role in the synthesis of glucuronoxylan and not RG-II. [100,101]. To our knowledge, no report has shown any glucuronoxylan in the cell wall of *A. thaliana* or tobacco pollen tubes and these data contrast with the proposed function of *Np*GUT1 in the RG-II synthesis in pollen tubes.

Recently, three other genes involved in the biosynthesis of RG-II were shown to play an important role during *A. thaliana* pollen tube elongation. *KDO-8-P SYNTHASEs* (*AtKDSA1* and *AtKDSA2*) are involved in the synthesis of Kdo, one of the rare sugars composing the RG-II, with eight carbons. *Atkdsa1* and *Atkdsa2* double pollen mutants in *quartet* background are unable to form an elongated pollen tube properly and to perform fertilization [102]. In 2010, two *male gametophyte defective* (*mgp*) mutants, impaired in the biosynthesis of RG-II were isolated: *mgp4*, knock-out for a RG-II XYLOSYLTRANSFERASE [103] and *mgp2*, knock-out for a SIALYLTRANSFERASE-LIKE [104]. Both mutants display similar phenotypes with a strong inhibition of pollen germination and a delayed pollen tube growth *in vitro* and *in vivo* compared to wild type. Because the three *A. thaliana* sialyltransferase-like proteins, homologous to mammalian sialyltransferases, do not show any sialyltransferase activity *in vitro* and that the nucleotide sugar donor of the sialyltransferase CMP-Sia is similar to CMP-Kdo, Deng *et al.* [104] suggested that these genes may be involved in the RG-II biosynthesis pathway. Another contribution pointing out the critical role of RG-II in pollen tube growth was recently brought by Kobayashi *et al.* [105]. They studied the gene coding for the enzyme CTP:Kdo cytidylyltransferase (CMP:Kdo Synthetase, CKS) that activates Kdo as a nucleotide sugar during the biosynthesis of RG-II. They showed that the protein is located in the mitochondria and that this gene is essential for pollen tube development as the mutation in *CKS* induces the inhibition of pollen tube elongation [105]. All these studies indicate that RG-II is important for pollen tube growth

but none of the studies have shown biochemically that the RG-II structure in the pollen or the pollen tube was impaired. The development of specific probes targeting the different side chains of RG-II should facilitate studies on this non-abundant but important pectin motif in pollen tube growth but to date such tools are not available.

3.1.5. Pectin Methyltransferase and Pectin/XyG Acetyltransferase

The transferase activity of methyl and acetyl groups on HG was shown *in vitro* [106,107]. *QUASIMODO2* and *3* (*QUA2* and *QUA3*) are two genes coding for putative HG methyltransferases but their biochemical activities and their function during pollen tube growth have not been confirmed [108,109]. In 2011, a mutant designated as *reduced wall acetylation2* (*rwa2*) was studied. The loss-of-function in the *RWA2* gene was accompanied by a decrease of the level of acetylated cell wall polymers [110] but no phenotype was observed on the pollen tube indicating that other genes are likely to be involved in this process.

3.2. Xyloglucan Biosynthesis

Based on the structure of XyG, its biosynthesis requires a combination of (1→4)-β-glucan synthases, (1→6)-α-xylosyltransferases, (1→2)-β-galactosyltransferases, (1→2)-α-fucosyltransferases and *O*-acetyltransferases [111]. In *A. thaliana*, *CSL4* codes for a (1→4)-β-glucan synthase involved in the synthesis of the XyG backbone but transcriptomic data indicate that this gene is not expressed in pollen [112]. At least five *XYLOGLUCAN XYLOSYLTRANSFERASEs* (*XXTs*) have been identified in *A. thaliana* [76,113,114] but their implications during pollen tube growth have not been assessed yet. Two *XYLOGLUCAN GALACTOSYLTRANSFERASEs* were also characterized: *MUR3* in *A. thaliana* [115] and more recently *XLT2* in *Tropaeolum majus* [116]. However, none of these genes is expressed in pollen grains or pollen tubes [93]. *MUR1* codes for an enzyme that catalyzes the first step of the biosynthesis of GDP-fucose and the *mur1* mutants show a lack of labeling of fucosylated XyG epitopes with CCRC-M1 in hypocotyls, shoots or leaves [68]. However, the mutation does not affect the distribution of the fucosylated XyG epitopes in the pollen tube suggesting that this gene is not implicated in the XyG biosynthesis in pollen tubes. Mutation in the *FUCOSYLTRANSFERASE* gene (*FUT1*, *FT1* or *MUR2*) eliminates the fucosyl residues on the XyG side chains in all major plant organs indicating that FUT1 is involved in most of the XyG fucosyltransferase activity in *A. thaliana* [117,118]. *MUR1* and *FUT1* are not expressed in pollen grains or pollen tubes but are strongly expressed in the stigma and in ovarian tissues in *A. thaliana* [93] suggesting that XyG from the female tissues may be highly fucosylated but more direct experimental evidence is required.

3.3. Cellulose Biosynthesis

It is generally assumed that cellulose microfibrils are assembled by cellulose synthases (CESs) located at the plasma membrane in a form of rosette terminal complex. However, the possibility that the first step of cellulose biosynthesis begins in the Golgi apparatus in higher plants cannot be ruled out [119]. Different multigenic families are implicated in cellulose biosynthesis. Ten CESA (CELLULOSE SYNTHASE A) genes were found in the A. thaliana genome and it was shown by

mutant analyses that they play distinct roles in the cellulose synthesis process [120,121]. Another multigenic family, CSLD (CELLULOSE SYNTHASE LIKE-D), related to CESA, seems also to be involved in cellulose biosynthesis and contains six members in the A. thaliana genome [122,123]. In rice, the genome contains 7 CESA and 5 CSLD genes [124]. In tobacco, NaCSLD1 (Nicotiana alata *CELLULOSE SYNTHASE-LIKE D1*) was found to be only expressed in the anther and *in vitro*-grown pollen tubes and was predicted to code for a cellulose synthase in pollen [125]. In *N. tabacum* pollen tubes, CESA and CSLD were detected along the entire length of the pollen tubes with a higher concentration at the apex [126]. Similarly, in A. thaliana, CESA6, CSLD1 and CSLD4 were found at the plasma membrane of the pollen tube both at the tip and in the shank [26,127]. Moreover, crystalline cellulose was also found inside cytoplasmic vesicles and the trans Golgi network in A. thaliana pollen tubes leading to the hypothesis that the synthesis of short cellulose microfibrils may initiate in this compartment giving the pollen tubes the head start in assembling the cell wall necessary to promote rapid elongation [26]. Alternatively, the vesicles containing the cellulose may originate from endocytosis suggesting that cellulose in the shank of the tube may be degraded and recycled [26].

The CESA1 and CESA3 mutations are both gametophytic lethal. 50% of pollen grains from the heterozygous cesa1+/− or cesa3+/− plants are significantly deformed and do not produce pollen tube [128]. The cesa6 null mutants display subtle growth defect and the pollen is not deformed [128]. On the other hand, the triple cesa2/6/9 mutants are sterile and pollen grains are strongly deformed [128]. The data indicates that *CESA2* is functionally redundant with *CESA6*. As CESA9 is strongly expressed in pollen grains, these studies suggest that *CESA1*, *3*, *6* and *9* play a critical role during pollen grain formation. Recently, it was shown using pCESA6::GFP-CESA6 construction that CESA6 is expressed in pollen tubes indicating that in addition to CESA1, 3 and 9, CESA6 may also play a role during pollen tube growth [26].

Three genes from the CSLD family are also implicated in pollen tube growth. *Csld1* and *csld4* homozygous mutants are sterile. Mutant pollen grains show abnormal germination and reduce pollen tube growth *in vitro* and *in vivo*. In addition, high level of pollen tubes is bursting due to a reduced cellulose content, abnormal callose deposition and thickened and highly irregular cell wall [123,127]. Finally, mutation in CSLC6 results in a strong reduction of pollen tube growth [129]. All these data support the fact that despite the low abundance of cellulose in the cell wall of pollen tubes, it has an important function in maintaining the integrity of the tube cell.

3.4. Callose Biosynthesis

Callose is also synthesized at the plasma membrane by callose synthases (CALSs) located at the apex and the distal regions of tobacco pollen tubes. In longer pollen tubes, CALS accumulates also close to the callose plug [126]. Twelve putative *CALS* genes (*CALS1-12*) have been identified in the *A. thaliana* genome [130]. Among these 12 genes, *CALS5* is implicated in the normal deposition and patterning of the exine pollen grain [131,132] but opposite data are obtained concerning the pollen viability and the ability of the pollen tube to grow normally. *Na*GSL1 (*Nicotiana alata* GLUCAN SYNTHASE-LIKE1) was shown to be a callose synthase [133] involved in the control of callose synthesis during pollen tube growth [134]. In 2011, a study brought evidence that *CALS5* orthologues are expressed in pollen grains of many different angiosperms and gymnosperms but *CALS5* was only

expressed in fast-growing pollen tubes (*i.e.*, angiosperms), suggesting that CALS5 plays different but crucial roles during pollen formation and/or germination and pollen tube growth [55]. This study also supports the reports showing that the callose wall in slow-growing pollen tubes is generally transiently detected and the callose plug has so far not been observed in gymnosperm pollen tubes. Based on such variability and transient expression of callose in the pollen of *Pinus*, Pacini *et al*. [135] suggested that the callose may not have a structural function but rather serves as a reserve polysaccharide. In contrast, in fast growing pollen tubes like in *S. chacoense* and *Lilium orientalis*, callose was shown to have an important mechanical function [53].

4. Cell Wall Remodeling during Pollen Tube Growth

4.1. Cell Expansion: Xyloglucan-Cellulose Reassembly

4.1.1. Expansins

Expansins were first discovered in cucumber hypocotyls [136] and oat coleoptiles [137]. According to Sampedro and Cosgrove [138], expansins belong to a superfamily composed of four families: (1) EXPANSIN A (EXPA), also called α-expansin; (2) EXPANSIN B (EXPB), also known as β-expansin; (3) EXPANSIN-LIKE (EXLA); and (4) EXPANSIN-LIKE B (EXLB). α- and β-expansins are involved in cell expansion: EXPAs may promote separation of cellulose microfibrils by inducing local dissociation and slippage of XyG on the surface of the cellulose, whereas EXPBs work on different polymers, maybe xylan, with a similar effect [139]. The precise role of EXLA and EXLB has not been has not been established yet [138] and to date, no enzymatic activity has been detected for these proteins [140,141].

The *A. thaliana* genome contains 36 genes encoding putative EXPs [141,142]. Expression profile analyses of the transcripts reveal that two expansin genes one α-(*EXPA4*) and one β-(*EXPB5*) are strongly expressed in dry pollen grains, during pollen imbibition and pollen tube growth (Table 2). In addition, four other *EXPs* are strongly expressed in the stigma and one in the ovary of *A. thaliana* (Table 2). To date and to our knowledge, no study has pointed out the role of expansins in the remodeling of the pollen tube cell wall in eudicot plants. Most of the work on expansins comes from the Poales in which the development of pollen grains is accompanied by the expression of *EXPB*. In rice, several putative EXPBs were found in pollen grains by proteomics approach [143] and 4 isoforms were purified from the maize pollen [144]. During the maturation of wheat and triticale male gametophytes, a strong expression of two EXPB genes is detected but unlike the β-expansins from maize, they are not expressed in the mature pollen [145,146]. Even if the exact function of pollen EXPBs remains unanswered, Cosgrove *et al*. [147] suggested that they are released from the pollen grain on the pistil to soften the cell wall of the stigma thus facilitating the penetration and the growth of the pollen tube. Some others hypothesized that EXPBs are implicated in the formation of the exine wall during the male gametophyte formation [145].

Table 2. Expression of expansin and xyloglucan *endo*-transglucosylase hydrolase genes in pollen grains, pollen tubes and the pistil of *A. thaliana*. Data were collected from eFP Browser [148]. Proteins are named according to Magrane and the UniProt consortium [149] and according to Hende *et al*. [150] for the expansin family. Pollen grain and pollen tube data are from Qin *et al*. [93] and pistil data from Swanson *et al*. [151]. When the level of expression was <50, the data are not shown.

Cell wall metabolism	Locus	Protein name	Expression level					
			Pollen grain		Pollen tube		Pistil	
			Dry	Imbibed	4 h *in vitro*	Semi *in vivo*	stigma	ovary
Cell expansion								
CBMs	At1g20190	Expansin A11 (EXPA11)	<50	<50	<50	<50	1,614.7	421.6
	At1g26770	Expansin A10 (EXPA10)	<50	<50	<50	<50	1,893.9	641.8
	At2g28950	Expansin A6 (EXPA6)	<50	<50	<50	<50	1,919.8	1,614.2
	At2g39700	Expansin A4 (EXPA4)	4,069.6	3,962.1	3,950.8	2,106.8	321.3	429.6
	At3g45970	Expansin-like A1 (EXLA1)	<50	<50	<50	<50	1,462.7	322.1
	At3g60570	Expansin B5 (EXPB5)	1,020.2	1,139.5	1,347.1	3,002.9	53.9	52.7
Hemicellulose reassembly								
GH16	At2g06850	XTH4	<50	<50	<50	<50	129.8	1,174.4
	At4g03210	XTH9	<50	<50	<50	<50	785.1	2,518.8
	At4g30270	XTH24	<50	<50	<50	<50	146.5	1,975.7
	At5g65730	XTH6	<50	<50	<50	<50	752.1	1,013.4
	At1g32170	XTH30	1,286.7	346.2	354.2	378.6	167.2	86.2
	At4g18990	XTH29	1,02.2	95.8	91.7	<50	<50	<50

CBMs. Carbohydrate-Binding Modules, GH. Glycoside hydrolase, XTH. Xyloglucan *endo*-transglucosylase hydrolase. <50<500<1,000<2,000<3,000<5,000<10,000.

4.1.2. Xyloglucan *endo*-Transglucosylase Hydrolase

The two known activities of XyG *endo*-transglucosylase hydrolase proteins (XTHs) are XyG *endo*-transglucosylase (XET) and XyG *endo*-hydrolase (XEH) [152]. The XET activity consists of cleaving XyG polymers and joining the newly generated end to another XyG chain whereas XEH activity hydrolyzed XyG polymers [152]. XET activity was detected in extracts of the growing portions of various eudicots (including pea, lupin, tomato, sycamore, cow parsley, dandelion and bean), monocots (chive, maize, brome grass and Yorkshire fog) and Bryophytes (liverwort and moss) [153,154]. XTHs are believed to play a central role in the construction and the disassembly of the cell wall architecture [152]. XTHs are encoded by large gene families in land plants and *A. thaliana* and rice contain 33 and 29 *XTH* genes dispersed across their genomes, respectively [155,156]. Among the 33 *XTHs* in the *A. thaliana* genome, 4 are strongly expressed in flowers. Becnel *et al.* [157]

have studied the expression of the *XTH* genes using *XTH::GUS* constructions and they showed that *pXTH29::GUS* and *pXTH30::GUS* activities are clearly detected during the anther development and in the mature pollen grain [157]. In contrast, *pXTH1::GUS* and *pXTH33::GUS* activities are restricted to very young flowers. Microarray data extracted from EFP browser are consistent with these results (Table 2). Moreover, expression profiles of *XTH29* and *XTH30* appear to be pollen specific suggesting a specialized function during pollen development.

However, to date, no evidence demonstrates a role of XTHs in the pollen tube growth and cell wall remodeling. Only one *XTH* was linked to pollination. The loss of function of *AtXTH28* led to a dramatic decrease in seed setting due to the inability of the plants to self-pollinate. This phenotype was caused by a net reduction of the stamen filament length due presumably to a reduced capability of the filament cells to expand [158].

4.2. Pectin Methylesterase and Pectin/Xyloglucan Acetylesterase

HG is synthesized in the Golgi apparatus and deposited in the expanding tube tip in a highly methylesterified form [159]. The methylesterified HG in the apical zone is thought to provide sufficient plasticity for sustaining the pollen tube growth [15]. Upon block-wise action of PMEs, de-methylesterified HG polymers can form multimers via ionic bonds between the negatively charged carboxyl groups of several HG and Ca^{2+} ions forming a pectate gel that may provide rigidification of the pollen tube cell wall [12,58]. Therefore, the control of the cell wall plasticity by PMEs is critical to ensure a proper fertilization. Conversely, upon random action of PMEs, the partial removal of methylester groups may allow the pectin-degrading enzymes, polygalacturonases (PGs) or pectate lyases (PLs) (see lower section) to cleave the HG backbone thus affecting the rigidity of the cell wall [58,160]. This sequential action of PME and PG was demonstrated in the *quartet* mutants that release pollen grains as tetrads due to the persistence of pectic polysaccharides [161]. The *QUARTET1* gene encodes a PME that is required in association with the *QUARTET3* encoding a PG for the degradation of the HG of the tetrad resulting in the normal pollen separation during microsporogenesis [162,163].

The *A. thaliana* genome contains 66 putative *PMEs*. Most of the genes encoding PMEs display a tissue-specific expression pattern, especially for 14 of them that are specifically expressed in pollen grains or pollen tubes (Table 3) [93,164]. Moreover, proteomics studies of germinated pollen grains from maize, wheat, rice and *A. thaliana* have identified two putative PMEs in germinated maize pollen [165], one in rice [143] and at least one in *A. thaliana* pollen tubes [166]. In tobacco pollen tubes, biochemical analyses have shown the presence of seven isoforms with a wide isoelectric point range [167]. Two PME isoforms were co-localized with methylesterified HG in the cell wall and Golgi-derived vesicles suggesting that PMEs are transported to the tip under an inactive precursor form [167].

The first functional characterization of *PME* genes and their critical roles in pollen tube growth were obtained from two knock-out mutants *vanguard1(vgd1)* [168] and *atppme1* [169]. The disruption of *VGD1* resulted in the burst of pollen tubes *in vitro* and marked retardation of the *vgd1* pollen tube elongation in the pistil resulting in a strong reduction of male fertility and seed set [168]. The lack of AtPPME1 activity in knock-out mutants affects the shape and the growth rates of the pollen tubes, indicating that AtPPME1 is required for the integrity of the cell wall and for the tip-polarized

growth [169]. Moreover, when PME from orange peel is exogenously applied to pollen tubes of *Lilium formosanum* and tobacco or when PME is overexpressed, the pollen tube growth is inhibited [170].

Table 3. Analyses of the expression profile of pectin methylesterase and pectin and/or xyloglucan acetylesterase genes in pollen grains, pollen tubes and the pistil of *A. thaliana*. Data were collected from eFP Browser [148]. Proteins are named according to Magrane and the UniProt consortium [149]. Pollen grain and pollen tube data are from Qin *et al.* [93] and pistil data from Swanson *et al.* [151]. If the level of expression was <50 for all the selected tissues, data are not shown.

Cell wall metabolism	Locus	Protein name	Expression level					
			Pollen grain		Pollen tube		Pistil	
			Dry	Imbibed	4 h *in vitro*	Semi *in vivo*	stigma	ovary
Esterase								
CE8	At1g69940	PPME1	7,600.7	5,098.6	4,702.65	3,209.4	<50	<50
	At2g26450	PME13	4,168.8	4,391.9	4,361.9	4,954.5	<50	<50
	At2g47030	PME4/VGDH1	9,592.1	7,074.2	6,539.6	7,813.1	164.1	<50
	At2g47040	PME5/VGD1	9,592.2	7,074.3	6,539.6	7,813.1	164.1	<50
	At3g05610	PME21	7,557.3	4,778.3	4,618.9	5,347.8	<50	<50
	At3g06830	PME23	4,485.1	1,952.0	1,593.5	73.6	<50	<50
	At3g14310	PME3	<50	<50	<50	<50	284.2	1,047.5
	At3g17060	PME67	4,796.4	4,707.4	4,826.6	4,838.3	<50	<50
	At3g49220	PME34	<50	<50	<50	<50	1,370.3	1,408.2
	At3g62170	PME37	6,829.9	5,434.6	5,566.4	868.0	<50	<50
	At4g15980	PME43	1,930.8	905.9	592.5	<50	<50	51.5
	At4g33230	PME45	759.8	904.1	917.7	92.9	<50	<50
	At5g07410	PME48	7,600.8	5,098.7	4,702.65	3,209.4	<50	<50
	At5g07420	PME49	3,519.5	3,605.9	3,144.6	132.4	<50	<50
	At5g07430	PME50	8,606.5	7,181.6	7,258.6	7,198.7	90.3	<50
	At5g27870	PME28	2,859.6	2,817.7	2,537.8	66.6	<50	<50
	At5g47500	PME68	<50	<50	<50	<50	687.9	1,308.9
	At5g49180	PME58	<50	<50	<50	1,361.1	446.2	1,175.3
CE12	At4g19410	Putative PAE	<50	<50	<50	<50	438.9	1,095.7

CE. Carbohydrate Esterases, PAE. Pectin AcetylEsterase, PME. Pectin MethylEsterase, PPME. Pollen Pectin MethylEsterase, VGD. Vanguard, VGDH. Vanguard Homolog. <50<500<1,000<2,000<3,000<5,000<10,000.

The main regulators of PMEs are PME inhibitors (PMEIs). Sequence analyses indicate that several PMEs contain, in addition to the catalytic domain, an *N*-terminal extension domain (the PRO region) showing similarity with PMEI domains [58]. Based on this, PMEs are classified in two distinct groups depending on the presence or absence of this putative PMEI domain. Group 1 PMEs do not have the PRO region, whereas PMEs from group 2 can contain from 1 to 3 PMEI domains [169]. It is hypothesized that the PRO region is cleaved during the maturation of PME, as so far, only PMEs lacking this domain were found in the cell wall [58].

Recently, Wolf *et al.* [164] indicated that the PRO region of the group 2 PMEs might regulate the release of the mature PMEs from the Golgi apparatus. It was also suggested that the PRO region might play an auto-inhibitory role during maturation [170]. PMEIs are not only found in the PRO region of

PMEs but also exist as individual proteins sharing strong sequence similarities with invertase inhibitors (Inv inhibitors). However, there is no clear evidence of a similar function and mode of action between PMEIs/Inv inhibitors and PMEI domains of PMEs. The *A. thaliana* genome contains 76 genes coding highly putative PMEIs/Inv inhibitors. The expression patterns of *PMEIs/Inv inhibitors* are all regulated in a tissue-specific manner [171,172] and transcriptomic data reveal that *PMEIs/Inv inhibitors* are highly expressed in the *A. thaliana* pollen compared to other tissues [171,173]. As 9 out of the 14 *PMEs* specifically expressed in pollens are from the group 2 (with PMEI domains), it may suggest that PMEIs play a crucial role in regulating the activity of PMEs during pollen germination and pollen tube growth. Suppression of the expression of At1g10770 (coding for a putative PMEI) leads to a partial male sterility reducing the seed set by inhibition of pollen tube growth [174]. Moreover, treatments of pollen tubes with exogeneous PMEI also result in an abnormal germination and burst of pollen tubes in *A. thaliana* [175]. Finally, it was shown that AtPPME1 and AtPMEI2, both pollen specific, physically interact and *in vitro* assays revealed that AtPMEI2 was able to inactivate AtPPME1 [176]. The transient expression of AtPPME1 and AtPMEI2 in tobacco pollen tubes demonstrated that AtPPME1 accumulates uniformly from the tip to the shank of the pollen tube. In contrast, the localization of AtPMEI2 is restricted to the tip and in endosomal vesicles suggesting its internalization and recycling [176]. PMEs are thought to play an important role during the tip-polarized growth of the pollen tube by controlling the mechanistic properties of the cell wall. However, the function of PMEs is probably not restricted to the change of the mechanical properties of the cell wall. Weakly methylesterified HG have been implicated in other important physiological processes such as cell attachment in vegetative cells or organs [92,177,178] and in lily, associated with a stigma/style cysteine-rich adhesin (SCA), a secreted plant lipid transfer protein (LTP), in pollen tube adhesion [179,180]. Several *LTPs* are expressed in the transmitting tract of the *A. thaliana* pistil along the pollen tube path [181] that may be involved in this process. In tobacco, it was shown that TobLTP2 purified from the stigma exudates accumulate in the pistil and are able, as expansins do, to promote cell wall loosening. However, the pollen tube growth in LTP-silenced plants is similar to wild type plants, suggesting either that pollen tubes do not require this loosening protein or that other loosening agents may have act redundantly [182]. Recently, LTP5, produced in *A. thaliana* pollen tubes and in the transmitting tract, was proposed to play important roles in maintaining the cell polarity at the tube tip and adhesion-mediated guidance perhaps by interactions with pectins [183]. Direct evidence is lacking, but it appears highly probable that PMEs, by modifying the degree of methylesterification of HG, play a direct role in adhesion and guidance of the pollen tube.

Finally, one putative pectin acetylesterase was detected in rice pollen [143] and a recent report has shown that the overexpression of the *Populus PECTIN-ACETYLESTERASE1* in tobacco affected the shape of the pollen grains and their abilities to germinate [184].

4.3. Pectin lyase

PL (PECTIN LYASE) and PLL (PECTIN LYASE-LIKE) genes are also abundantly expressed in tomato, tobacco, alfalfa and arabidopsis pollen [185–187] and several pollen allergens have PLL activities [188]. Out of the 26 *PLL* genes, 14 are expressed in pollen [189]. None of these 14 genes is specifically dedicated to the male gametophyte but 4 of them are strongly expressed in pollen grains

(Table 4). To our knowledge, there is no experimental evidence of the implication of *PLL* in the remodeling of the pollen tube wall. Many promoter activities of the *PLLs* genes are similar to those exhibited by many *POLYGALACTURONASEs* (*PGs*) [190]. This may imply a close functional association between PLLs and PGs, particularly in the digestion of the pollen grain cell wall prior to germination and during pollen tube growth [190,191].

Table 4. Analyses of the expression profile of *PECTATE LYASEs* in pollen grains, pollen tubes and in the pistil of *A. thaliana*. Data were collected from eFP Browser [148]. Proteins are named according to Magrane and the UniProt consortium [149]. Pollen grain and pollen tube data are from Qin *et al*. [93] and the pistil data from Swanson *et al*. [151]. If the level of expression was <50 for all the selected tissues, data are not shown.

Cell wall metabolism	Locus	Protein name	Expression level					
			Pollen grain		Pollen tube		Pistil	
			Dry	Imbibed	4 h *in vitro*	Semi *in vivo*	stigma	ovary
Lyase								
PL1	At1g04680	Probable pectate lyase 1	<50	<50	<50	<50	681.0	1,457.2
	At1g14420	Probable pectate lyase 3	3,922.2	3,514.5	3,591.2	1,171.3	<50	<50
	At2g02720	Probable pectate lyase 6	3,608.0	3,599.7	3,533.1	4,007.9	<50	<50
	At3g01270	Probable pectate lyase 7	6,694.0	6,572.3	6,546.1	7,161.1	166.1	112.7
	At4g24780	Probable pectate lyase 18	<50	<50	<50	<50	1,969.1	1,173.3
	At5g09280	Major pollen allergen like protein	<50	<50	<50	3,192.1	<50	<50
	At5g15110	Probable pectate lyase 18	3,865.4	3,782.2	3,390.4	625.1	<50	<50

PL. Pectin Lyase. <50<500<1,000<2,000<3,000<5,000<10,000

4.4. Glycoside Hydrolases

Glycoside hydrolases (GHs) are enzymes that catalyze the hydrolysis of glycosidic linkages between two or more glycosides or between a carbohydrate and a non-carbohydrate moiety. In 1991, GHs were classified into 35 families [192] and to date they are divided into over 100 families [193]. GHs involved in the reassembly of the pollen tube cell wall belong to the GH3, 9, 10, 17, 28, 35, 43 and 51 families. Their activities as well as their possible functions during pollen tube growth are presented in Table 5.

Table 5. Summary of the main glycoside hydrolase (GH) families possibly involved in the remodeling of the pollen tube cell wall.

Family	Known activities	Possible function during pollen tube growth
GH3	β-D-xylosidase (EC 3.2.1.37) α-L-arabinofuranosidase (EC 3.2.1.55) β-glucosidase (EC 3.2.1.21)	Degradation of xylan/arabinoxylan Degradation of RG-I, arabinogalactan proteins.
GH9	*Endo*-(1→4)-β-glucanase (EC 3.2.1.4) Cellobiohydrolase (EC 3.2.1.91) β-glucosidase (EC 3.2.1.21)	Degradation of cellulose and XyG backbone May control the diameter of the pollen tube. May help to digest the cell wall of the stigma to facilitate the pollen tube penetration in the female tissues.
GH10	*Endo*-(1→4)-β-xylanase (EC 3.2.1.8)	Degradation of xylan
GH17	*Endo*-Glucan (1→3)-β-glucosidase (EC 3.2.1.39) Glucan (1→3)-β-glucosidase (EC 3.2.1.58) *Endo*-(1→3-1→4)-β-glucanase (EC 3.2.1.73) β-(1→3)-glucanosyltransglycosylase (EC 2.4.1.)	Degradation of callose or β-mixed-(1→3, 1→4) glucans. May promote pollen germination and control the mechanical properties of the pollen tube cell wall during elongation.
GH28	Polygalacturonase (EC 3.2.1.15) *Exo*-polygalacturonase (EC 3.2.1.67) *Exo*-polygalacturonosidase (EC 3.2.1.82) Rhamnogalacturonase (EC 3.2.1.171) Rhamnogalacturonan α-L-rhamnopyranohydrolase (EC 3.2.1.40) *Endo*-xylogalacturonan hydrolase (EC 3.2.1.-)	Degradation of weakly esterified HG: cell wall loosening. May control the stiffness of the tube during elongation and/or help to digest the cell wall of the stigma thus facilitating the penetration of the tube. Degradation of RG-I backbone Degradation of xylogalacturonan
GH31	α-xylosidase (EC 3.2.1.177)	Degradation of XyG or RG-II side chains
GH35	β-galactosidase (EC 3.2.1.23) *Exo*-β-(1→4)-galactanase (EC 3.2.1.-)	Degradation of RG-I, XyG and/or arabinogalactan proteins. Turn over of pollen tube cell wall. Pollen tube guidance
GH43	β-D-xylosidase (EC 3.2.1.37) α-L-arabinofuranosidase (EC 3.2.1.55)	Degradation of xylan/arabinoxylan Degradation of RG-I, arabinogalactan proteins, arabinoxylan.
GH51	α-L-arabinofuranosidase (EC 3.2.1.55)	Degradation of RG-I, arabinogalactan proteins, arabinoxylan.

Endo-(1→4)-β-glucanases and *endo*-(1→3)-β-glucosidases are members of the GH9 and GH17 families, respectively (Tables 5 and 6). In *A. thaliana*, 25 genes are encoding GH9 proteins and 49 the GH17 proteins. Among the 25 putative *CELLULASES*, two are strongly expressed in pollen grains and three in *in vitro*-grown pollen tubes (Table 6). Four members of the GH17 family are expressed in *in vitro*-grown pollen tubes (Table 6). Three and five genes encoding the GH9 and GH17 are also found in the pistil tissues, respectively. Twenty years ago, these two enzyme activities were assayed in pistils and anthers of bean and they were linked to the cell wall disruption occurring during the release of the pollen grain from the anther and during the penetration of the pollen tube through the stigma [194].

Recently, and despite its low abundance in the pollen tube cell wall, it was shown that cellulose plays a crucial role by influencing the diameter of *in vitro*-grown pollen tubes [195]. As described previously, the cell wall of fast-growing pollen tubes is enriched in callose and several studies have shown that moderate β-(1→3)-glucanase treatments are able to stimulate the germination of pollen grains [53,196]. Moreover, it was reported that *exo*-β-glucanases might play an important role in the regulation of pollen tube elongation in lily [197]. On the contrary, treatments with inhibitors of glucosidases severely inhibited the growth of pollen tubes [198]. It was hypothesized that the mechanical properties of callose and more precisely the resistance to lateral deformation of the tube was regulated by glucanases [53] (Table 5).

Table 6. Analyses of the expression profile of glycoside hydrolase (*GHs*) genes in pollen grains, pollen tubes and in the pistil of *A. thaliana*. Data were collected from eFP Browser [148]. Proteins are named according to Magrane and the UniProt consortium [149] and to Hruba *et al*. [199] for the GH3 family. Pollen grain and pollen tube data are from Qin *et al*. [93] and the pistil data from Swanson *et al*. [151]. If the level of expression was <50 for all the selected tissues, data are not shown.

Cell wall metabolism	Locus	Protein name	Expression level					
			Pollen grain		Pollen tube		Pistil	
			Dry	Imbibed	4 h *in vitro*	Semi *in vivo*	stigma	ovary
Glycoside Hydrolases								
GH3	At1g02640	β-D-xylosidase	<50	<50	<50	<50	66.1	227.3
	At1g78060	β-D-xylosidase	<50	<50	<50	<50	149.2	401.8
	At3g19620	β-D-xylosidase	<50	<50	<50	<50	388.6	76.9
	At3g47000	β-D-xylosidase	<50	<50	<50	<50	190.2	330.6
	At3g62710	β-D-xylosidase	4,780.4	4,342.3	4,813.6	6,223.6	73	51.7
	At5g09730	β-D-xylosidase 3/α-L-Arabinofuranosidase	<50	<50	<50	<50	803.5	2,807.8
	At5g10560	β-D-xylosidase	<50	<50	<50	<50	191.5	508.8
	At5g20940	β-D-xylosidase	<50	<50	<50	<50	<50	62.9
	At5g20950	β-D-xylosidase	<50	<50	<50	<50	741.4	1,468.4
	At5g49360	β-D-xylosidase 1/α-L-Arabinofuranosidase	<50	<50	<50	<50	193.9	921.4
	At5g64570	β-D-xylosidase	<50	<50	<50	<50	324.3	1,586.8
GH9	At1g70710	Endo-(1→4)-β-glucanase (CEL1)	<50	<50	<50	<50	732.8	1,921.9
	At1g71380	Endo-(1→4)-β-glucanase (CEL3)	<50	71.0	665.4	2,823.2	<50	57.8
	At2g44560	Endo-(1→4)-β-glucanase	2,345.4	2,152.9	2,492.6	1,224.1	<50	<50
	At3g43860	Endo-(1→4)-β-glucanase	5,932.2	5,925.4	5,738.7	3,735.4	<50	<50
GH9	At4g02290	Endo-(1→4)-β-glucanase (CEL4)	<50	<50	<50	<50	<50	1,223.5
	At5g49720	Endo-(1→4)-β-glucanase (RSW2/KOR1)	<50	<50	<50	<50	822.2	1,027.5

Table 6. *Cont.*

Cell wall metabolism	Locus	Protein name	Expression level					
			Pollen grain		Pollen tube		Pistil	
			Dry	Imbibed	4 h *in vitro*	Semi *in vivo*	stigma	ovary
GH10	At4g33850	GH 10 protein	1,571.9	1,369.8	1,495.2	205.7	<50	<50
	At4g33860	Endo-(1→4)-β xylanase, putative	1,571.9	1,369.8	1,495.2	205.7	<50	<50
GH17	At2g05790	Putative β-(1→3)-glucanase	<50	<50	<50	<50	1,054.1	2,723.2
	At3g07320	Putative β-(1→3)-glucanase	<50	<50	<50	<50	482.9	1,241.9
	At3g55430	Putative β-(1→3)-glucanase	3,815.6	3,499.7	3,184.8	1,146.9	504.2	824.6
	At4g26830	Putative β-(1→3)-glucanase	<50	<50	221.1	3,284.7	<50	<50
	At5g20390	Putative β-(1→3)-glucanase	3,190.6	3,251.1	3,427.8	365	<50	<50
	At5g42100	Glucan endo-(1→3)-β-glucosidase 10	<50	<50	<50	<50	726.5	1,402.3
	At5g55180	β-(1→3)-glucanase like	<50	<50	<50	<50	258.2	1,247.9
	At5g64790	β-(1→3)-glucanase	2,007.8	1,991.2	1,972.5	1,439.2	<50	<50
GH28	At1g02790	Exopolygalacturonase (PGA4)	6,048.4	5,842.1	5,885.1	5,376.4	137.3	82.5
	At2g23900	Putative polygalacturonase	3,341.6	3,090.6	3,228.7	2,308.4	<50	<50
	At3g07820	Polygalacturonase (PGA3)	6,791.1	7,077.4	6,983.5	7,731.2	137.5	63.1
	At3g07850	Exopolygalacturonase	7,694.0	7,415.6	7,187.2	3,814.6	<50	<50
	At3g14040	Exopolygalacturonase	7,694.0	7,415.6	7,187.2	3,814.6	<50	<50
	At4g23820	Putative polygalacturonase	<50	<50	<50	<50	726.1	1,214.5
	At5g48140	Putative polygalacturonase	5,423.3	5,327.8	5,417.7	5,266.6	<50	<50
GH31	At1g68560	α-xylosidase (XYL1)	<50	<50	<50	<50	500.4	765.4
	At3g45940	α-xylosidase (XYL2)	<50	<50	<50	<50	101.3	171.9
GH35	At2g16730	β-galactosidase (BGAL13)	3,753.9	3,752.6	3,219.2	550.5	<50	<50
	At2g28470	β-galactosidase (BGAL8)	<50	<50	<50	<50	2,437.4	2,075.1
	At4g35010	β-galactosidase (BGAL11)	4,248.3	4,056.9	4,264.4	5,783.1	77.7	<50
	At4g36360	β-galactosidase (BGAL3)	<50	<50	<50	<50	598.5	1,462.5
GH43	At3g49880	β-xylosidase	<50	<50	<50	<50	77.8	134.7
GH51	At3g10740	α-L-Arabinofuranosidase	<50	<50	<50	<50	184.9	402.8

GH. Glycoside Hydrolases, CEL. Cellulase, RSW.Radially Swollen, KOR. Korrigan, PGA. Polygalacturonase, BGAL. β-galactosidase, XYL. xylosidase. 50<500<1,000<2,000<3,000<5,000<10,000

Polygalacturonases (PGs) are involved in the HG degradation. They were characterized in the pollen from corn and other Poales [200] and have since been identified in various plants including rice, pea, tomato and arabidopsis [143,190,201,202]. PGs belong to the GH28 family composed of 69 genes in *A. thaliana* [203,204]. In 2000, Torki *et al*. [205] showed that 7 *PG* genes were strongly expressed in *A. thaliana* flowers. Publicly available microarray data are consistent with this result as 6 *PG* genes are strongly expressed in pollen tubes and one is expressed in the pistil (Table 6). Together with the strong expression of more than 10 *PMEs* and 4 *PLLs* in pollen tubes, these data suggest an important remodeling of the HG during pollen tube growth. PGs are involved, during pollen maturation of *Brassica campestris*, in the intine and/or exine formations [206,207] and in *Turnera subulata*, PGs are implicated in self-incompatibility [208]. PGs are released upon rehydration of triticale pollen grains [146] and are also detected in the tip region of pollen tubes in *Brassica napus* during papillar cell penetration [209] suggesting that PGs are probably involved in the loosening of the stigma cell wall during pollination. As PGs degrade weakly methylesterified HG and that the demethylesterification of methylesterified HG by PMEs at the tip of the tube is accompanied by the release of protons, it was suggested that this local change of pH in the pollen tube cell wall may promote PG activity [58,210]. This activation of PGs might then control the loosening of the pollen tube cell wall back from the tip and then promote the proper pulse growth of the tube (Table 5). Alternatively, pollen tube PGs may also affect the loosening of the stigma and transmitting tract cell wall to facilitate the penetration of the pollen tube (Table 5).

β-galactosidases (BGALs) belong to the GH35 family. BGALs can act on different substrates including arabinogalactan proteins, galactolipids, RG-I and RG-II side chains of pectin and XyG releasing galactose [211]. Eighteen genes are encoding BGALs in the *A. thaliana* genome and the functional genomics analysis reveals that *BGAL* expression levels are high in mature leaf, root, flower and silique but are low in young seedling [212]. Publicly available microarray data (Table 6) show that 2 *BGALs* are highly expressed in mature pollen grains and 2 others are highly expressed in the pistil confirming the results obtained by Ahn *et al*. [212]. Other *BGAL* genes are also strongly expressed during the microspore mitosis in developing pollen grains [199]. In rice, 35 genes are encoding BGALs; among them, two are strongly expressed in dry pollen grains [213] (Table 6). As mutants defective in BGAL have impaired fertility, it was hypothesized that BGAL may be involved in the pollen tube wall turnover in *Brassica campestris* by hydrolyzing arabinogalactan [214]. In 1995, it was suggested in tobacco that BGALs could be secreted from the pollen tube and released in the stylar transmitting tract to modify the branching pattern of arabinogalactan involved in the guidance of pollen tubes [215,216]. In tobacco, *BGAL* mRNAs are accumulated during the formation of pollen grains, presumably stored for future use during pollen germination and pollen tube growth as BGAL activities were detected in growing pollen tubes [217]. In rice, 6 isoforms of putative BGALs were detected by proteomic [143]. Finally, it was also suggested that BGALs might also be required for PME activity [218,219]. Transcriptomic data showed very strong pollen specific expression profile of one β-xylosidase gene in mature dry pollen grains [199], and in *in vitro* and semi-*in vivo* grown pollen tubes. The exact substrate of this enzyme is not known but it may degrade several cell wall polymers such as xylan, xylogalacturonan and possibly *N*-linked glycoproteins. All the other putative xylosidases (12 genes that belong to the families GH3 and GH31) are only expressed in the pistil (Table 6). In addition, transcriptomic data do not show a strong expression of arabinofuranosidase

genes in the pollen (Table 6). This is somehow surprising considering that Ara is one of the main carbohydrates present in the cell wall of *A. thaliana* pollen tubes [25]. It may suggest that the Ara containing polymers are not remodeled and/or that arabinofuranosidases originate from the female tissues (Table 6). The pattern of expression of α-xylosidase genes (GH31) is close to the one found for the arabinofuranosidase genes. α-xylosidase genes are not strongly expressed in dry pollen grains or pollen tubes. However, two α-xylosidase genes are expressed in the pistil (Table 6). Analyses of the *A. thaliana Atxyl1* mutants show reduced α-xylosidase activity, altered XyG composition and shorter siliques compared to the wild type. Moreover *pAtxyl1::GUS* expression is strong in the style [220]. It suggests that AtXYL1 may remodel the XyG of pollen tubes. However, it is difficult to directly implicate this α-xylosidase activity in pollen tube growth as seed production was apparently not affected.

By comparing the proteome of rice pollen grains and pollen tubes, Dai *et al*. [191] showed that several proteins involved in the cell wall biosynthesis and remodeling are either up- or down-regulated. Several RGP, PME, PG and EXPB isoforms are up-regulated upon pollen germination whereas others PGs, xylanases and EXPBs are down-regulated indicating that several proteins are dedicated to pollen germination and others to pollen tube growth. The authors suggested that the down-regulated proteins in the pollen tube may result from their release into the culture medium. In the *in vivo* context, the release of these proteins in the pistil tissues may facilitate the pollen tube growth. Finally, glycosylated and/or phosphorylated proteins were detected and contributed to the generation of new isoforms [191]. The activity of enzymes is commonly regulated by phosphorylation, glycosylation and/or interaction with specific inhibitors but more studies are required to assess the fine tuning and the exact function of these posttranslational modifications in pollen tube growth [191].

5. Mechanical Properties of the Cell Wall Network during Pollen Tube Growth

In recent years, A. Geitmann's lab has studied the mechanical properties of pollen tubes using micro-indentation and finite element technique [63]. In *A. thaliana*, lily and *S. chacoense*, it is observed that the tip region is elastic and the shank of the tube is rigid [26,53]. The modification of the cell wall mechanical properties using exogenous and moderate pectinase concentrations promotes pollen tube growth and the overall stiffness of the pollen tube decreased in both the apical and distal regions [53] suggesting that pectins are important components in respect to the cell wall mechanics [63]. As expected, an increase of the pectinase concentrations results at first by in apical swelling and ultimately bursting of the pollen tube. By contrast, PME treatments of pollen tubes increase the cellular stiffness at the apex and reduce the visco-elasticity. It reveals that the gradient from methylesterified (in the hemisphere-shape tip) to de-methylesterified (in the cylindrical shank) HG increases the cell wall rigidity [30] by promoting calcium cross-links with the negatively charged carboxylic groups of HG. This was also observed by Rounds *et al*. [45] using PI on pollen tubes treated with PME. A dramatic increase of the PI fluorescence at the apex of treated pollen tubes was detected due to an increase of demethylesterified HG. The authors suggested that PI interacted with demethylesterified HG by competing with calcium.

Despite its low abundance, cellulose plays an important role in stabilizing the pollen tube tip wall especially in the transition zone between the tip and the shank [13]. Cellulose microfibrils display an oblique orientation along the pollen tube wall in *Pinus* [27] whereas a more longitudinal orientation is

observed in *Lilium*, *S. chacoense* and *A. thaliana* suggesting that cellulose microfibrils are not the main stress bearing component against turgor pressure [26,195,221]. However, cellulose is of main importance in the mechanical stabilization of the tip region. Cellulase treatments or inhibition of cellulose crystal formation with drugs resulted in larger pollen tube diameters and promoted tip swelling and eventually bursting [195] as observed with the *cellulose synthase* mutants. Similar phenotypes were observed on *Petunia* and lily pollen tubes treated with 2,6-dichlorobenzonitrile (DCB), a cellulose biosynthesis inhibitor [222] or on conifer pollen tubes treated with isoxaben [56]. Recently, Derksen *et al*. [54] have shown that the cell wall structure of tobacco pollen tubes is organized both at the tip and back from the tip of 40–50 nm spaced lattice of continuous fibers that will allow intake of substantial size molecules from the surroundings.

In planta, XyGs are known to interact by hydrogen bounding with cellulose microfibrils but no information is available in pollen tubes. *O*-acetyl groups and the fucose residues of XyG do not seem to play a major role in the interaction with cellulose. *In vitro* experiments have shown that acetylated or de-acetylated XyG can cross-link similarly cellulose microfibrils [223]. In contrast, the presence of galactosyl residues appeared to be important in promoting the interaction with cellulose. XyG lacking Gal residues self-associated and did not interacted with cellulose [223]. Moreover, *A. thaliana* mutants with XyG lacking xylosyl and galactosyl residues showed a reduction of the tensile strength [224] and abnormal bulging in root hairs, possibly due to impaired cellulose-XyG assembly [225,226]. All together, these data suggests that the high levels of fucosylation and *O*-acetylation in the *A. thaliana* pollen tube XyG and perhaps in other species may prevent a strong interaction with cellulose microfibrils at the tip, promoting the fast growth of the pollen tube. Moreover, the high level of *O*-acetylation in XyG pollen tubes may also modulate the interaction between cell wall polymers and/or hinder enzymatic degradation [227] perhaps from enzymes originating from the pistil. Very recently, in root hairs of *A. thaliana*, a new branching pattern of XyG was characterized with GalA residues instead of Gal [228]. This motif was not detected in *A. thaliana* pollen tubes but it indicates clearly that tip-polarized cells can have specific XyG compositions to modulate the interaction with cellulose microfibrils and promote fast growth.

The amorphous callose is also important in the mechanical properties of the pollen tube cell wall. Treatments of pollen tubes with lyticase, an enzyme able to degrade callose, increase the diameter of the pollen tube, reduce the cellular stiffness and increase the cellular viscoelasticity in the distal part of *S. chacoense* pollen tubes suggesting that the callose wall may function in resistance to compression and/or tension stresses [53]. Using a combination of PME, pectinase and lyticase on fixed pollen tubes, Chebli *et al*. [26] suggested that cellulose and pectin are closely linked in the tip region of *A. thaliana* pollen tubes as demonstrated in the *A. thaliana* primary cell wall [229] and in the shank of the tube, a tight network of cellulose and callose is formed. Recently, using cellular force microscopy on lily pollen tubes, Vogler *et al*. [230] revealed also that the apparent stiffness of the pollen tube was lower at the tip than in the shank. However, they suggested that these differences are not originating from the distribution of the cell wall polymers or the thickness of the cell wall but solely due to the geometry of the pollen tube.

6. Conclusions

Over the last 25 years, the use of *in vitro* systems has been very valuable and a lot of information was collected concerning the distribution of the cell wall polymers in many species, but mostly focused on HG, callose, cellulose and arabinogalactan-proteins. In *A. thaliana*, functional genomics approaches have allowed the characterization of several genes implicated in the biosynthesis of pollen tube cell wall polysaccharides (mostly callose and cellulose). However, considering the large number of genes necessary to synthesize pectin, very few of them have been functionally characterized (several in the RG-II biosynthesis) and so far, none involved in the synthesis of XyG. Similarly, very few pollen genes involved in the remodeling of the pollen tube cell wall have been experimentally characterized. In addition, in the *in vitro* studies of pollen mutants, it is sometimes difficult to compare the data due to the use of different culture media and conditions, which may enhance or reduce the observed phenotypes. In many cases, a mutation completely inhibits pollen germination thus preventing the investigation of functional studies during pollen tube growth. Moreover, very little information is available on "non model" pollen tube species especially in gymnosperms and monocots. However, in recent years, the number of sequenced genomes from evolutionary divergent species has increased and will probably provide important information in the search of orthologous genes as it was done with *CALLOSE SYNTHASE5*. The development of new probes targeting the cell wall components and the improvement of the technology have also allowed more detailed studies on the cell wall biochemistry and the mechanic of the pollen tube cell wall. Finally, to increase the complexity of the system during their journey pollen tubes travel in the female tissues where additional cell wall interactions, cross-linking, modification, degradation and recycling can occur (Figure 4). The challenge will be to integrate all the parameters from protein signaling and trafficking to cell wall deposition and remodeling in the *in vivo* context in response to extracellular cues. Solving this complex network of information will unravel the secret of pollen tube tip expansion and guidance.

Figure 4. Model presenting the deposition of the main polysaccharides composing the pollen tube cell wall and its possible remodeling with proteins originating from the pollen tube or the pistil. (❶) Callose and cellulose synthases as well as XyG and pectin (HG, RG-I and RG-II) are carried within Golgi-derived vesicles. HG is synthesized in a highly methylesterified form and may or not be transported together with PME/PMEI complexes. (❷) The vesicles are directed to the plasma membrane in the sub-apical zone of the pollen tube tip where they fuse and release their contents (polysaccharides and/or remodeling proteins) in the cell wall. XyG is released under its final fucosylated form. Callose and cellulose synthases stay embedded in the membrane whereas PME/PMEI complexes and the other cell wall remodeling enzymes are released in the apoplast (❸). (❹) XyG and cellulose microfibrils probably interact loosely in the pollen tube tip and/or XTHs and expansins may facilitate the loosening process. It is not known if the RG-II borate dimer is synthesized in the Golgi and secreted under its final form or formed in the cell wall with exogenous boron coming from the culture medium or the pistil. (❺) PMEs are activated after their separations from PMEIs. PMEs are demethylesterifying the HG that promote the fixation of calcium ions between several parallel HG chains, thus reinforcing the cell wall

rigidity. PMEs are hypothesized to remain in the apoplast in the shank of the pollen tube. PMEIs may be degraded by proteases or recycled by endocytosis (❻). Similarly, it is hypothesized that the excess of cellulose and callose synthases may eventually be recycled by endocytosis. Similarly, cellulose microfibrils may also be endocytosed suggesting the action of cellulases. (❼) Comparable process might be observed with the degradation of callose with β-glucanases. The main class of enzymes (cellulases, β-glucanases, PLLs, PGs, PMEs, BGALs, α-xylosidases and α-arabinosidases, expansins and XTHs) possibly implicated in the remodeling and/or degradation of the pollen tube cell wall are presented. Numbers below the proteins correspond to the number of genes highly expressed in the pistil (♀) and the pollen tube (♂) of *A. thaliana*. BGALs, β-galactosidases; PGs, polygalacturonases; PLLs, pectate lyases-like; PMEs, pectin methylesterases; PMEIs, pectin methylesterase inhibitors; RG-I, rhamnogalacturonan-I; RG-II, rhamnogalacturonan-II; XTHs, xyloglucan *endo*-transglucosylase hydrolases; XyG, xyloglucan. Objects are not drawn to scale.

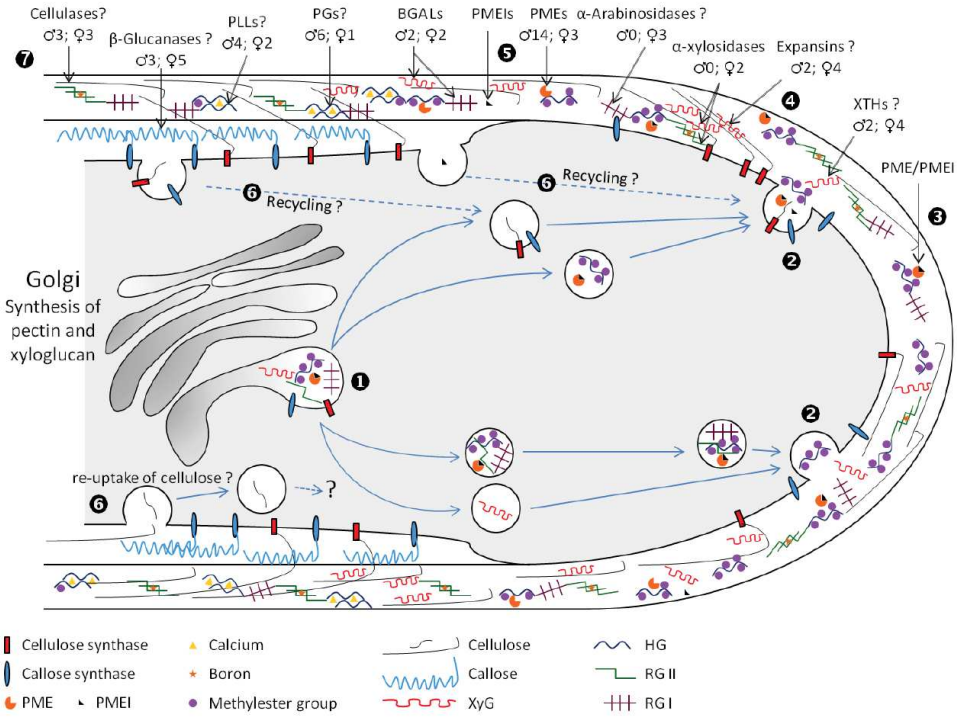

Acknowledgments

Very special thanks are due to E.M. Lord (UC Riverside) for having passionately launched JCM onto the fascinating field of pollen tube biology and plant reproduction. JCM is also grateful to all the students who have worked on pollen tubes and our colleagues for the interesting discussions during our

lab meetings. The authors wish to thank John Moore (Stellenbosch University, South Africa) and the four anonymous reviewers for their comments and suggestions for improving the quality of the manuscript. This work was partly supported by the University of Rouen and the research network VASI (Plant, Agronomy, Soils and Innovations) of the region Haute-Normandie, France. The authors are grateful to VASI for supporting FD during his PhD and the research network IRIB (Institute for Research and Innovation in Biomedicine) of the region Haute-Normandie, France for the doctoral fellowship to CL.

References

1. Lord, E.M.; Russell, S.D. The mechanisms of pollination and fertilization in plants. *Annu. Rev. Cell Dev. Biol.* **2002**, *18*, 81–105.
2. Kandasamy, M.K.; Nasrallah, J.B.; Nasrallah, M.E. Pollen-pistil interactions and developmental regulation of pollen tube growth in *Arabidopsis*. *Development* **1994**, *120*, 3405–3418.
3. Lennon, K.A.; Roy, S.; Hepler, P.K.; Lord, E.M. The structure of the transmitting tissue of *Arabidopsis thaliana* (L.) and the path of pollen tube growth. *Sex. Plant Reprod.* **1998**, *11*, 49–59.
4. Palanivelu, R.; Preuss, D. Pollen tube targeting and axon guidance: Parallels in tip growth mechanisms. *Trends Cell Biol.* **2000**, *10*, 517–524.
5. Kim, S.; Mollet, J.C.; Dong, J.; Zhang, K.; Park, S.Y.; Lord, E.M. Chemocyanin, a small basic protein from the lily stigma, induces pollen tube chemotropism. *Proc. Natl. Acad. Sci. USA* **2003**, *100*, 16125–16130.
6. McCormick, S.; Yang, H. Is there more than one way to attract a pollen tube? *Trends Plant Sci.* **2005**, *10*, 260–263.
7. Boavida, L.C.; Vieira, A.M.; Becker, J.D.; Feijò, J.A. Gametophyte interaction and sexual reproduction: How plants make a zygote. *Int. J. Dev. Biol.* **2005**, *49*, 615–632.
8. Johnson, M.A.; Lord, E.M. Extracellular guidance cues and intracellular signaling pathways that direct pollen tube growth. In *The Pollen Tube: A Cellular and Molecular Perspective*; Malho, R., Ed.; Springer: Berlin, Germany, 2006; Volume 3, pp. 223–242.
9. Mollet, J.C.; Faugeron, C.; Morvan, H. Cell adhesion, separation and guidance in compatible plant reproduction. *Annu. Plant Rev.* **2007**, *25*, 69–90.
10. Wang, H.J.; Huang, J.C.; Jauh, G.Y. Pollen germination and tube growth. *Adv. Bot. Res.* **2010**, *54*, 1–52.
11. Boisson-Dernier, A.; Kessler, S.A.; Grossniklaus, U. The walls have ears: The role of plant CrRLK1Ls in sensing and transducing extracellular signals. *J. Exp. Bot*. **2011**, *62*, 1581–1591.
12. Geitmann, A.; Steer, M. The Architecture and properties of the pollen tube cell wall. In *The Pollen Tube: A Cellular and Molecular Perspective*; Malhó, R., Ed.; Springer: Berlin, Germany, 2006; Volume 3, pp. 177–200.
13. Geitmann, A. How to shape a cylinder: Pollen tube as a model system for the generation of complex cellular geometry. *Sex. Plant Reprod.* **2010**, *23*, 63–71.
14. Nguema-Ona, E.; Coimbra, S.; Vicré-Gibouin, M.; Mollet, J.C.; Driouich, A. Arabinogalactan-proteins in root and pollen tube cells: Distribution and functional aspects. *Ann. Bot.* **2012**, *110*, 383–404.

15. Cheung, A.Y.; Wu, H.M. Structural and signalling networks for the polar cell growth machinery in pollen tubes. *Annu. Rev. Plant Biol.* **2008**, *59*, 547–572.
16. Moscatelli, A.; Ciampolini, F.; Rodigheiro, S.; Onelli, E.; Cresti, M.; Santo, N.; Idilli, A. Distinct endocytosis pathways identified in tobacco pollen tubes using charged nanogold. *J. Cell Sci.* **2007**, *120*, 3804–3819.
17. Bove, J.; Vaillancourt, B.; Kroeger, J.; Hepler, P.K.; Wiseman, P.W.; Geitmann, A. Magnitude and direction of vesicle dynamics in growing pollen tubes using spatiotemporal image correlation spectroscopy and fluorescence recovery after photobleaching. *Plant Physiol.* **2008**, *147*, 1646–1658.
18. Moscatelli, A.; Idilli, A.I. Pollen tube growth: A delicate equilibrium between secretory and endocytic pathways. *J. Integr. Plant Biol.* **2009**, *51*, 727–739.
19. Zonia, L. Spatial and temporal integration of signalling networks regulating pollen tube growth. *J. Exp. Bot.* **2010**, *61*, 1939–1957.
20. Roy, S.; Eckard, K.J.; Lancelle, S.; Hepler, P.K.; Lord, E.M. High-pressure freezing improves the ultrastructural preservation of *in vivo* grown lily pollen tubes. *Protoplasma* **1997**, *20*, 87–98.
21. Li, Y.Q.; Faleri, C.; Geitmann, A.; Zhang, H.Q.; Cresti, M. Immunogold localization of arabinogalactan proteins, unesterified and esterified pectins in pollen grains and pollen tubes of *Nicotiana tabacum* L. *Protoplasma* **1995**, *189*, 26–36.
22. Ferguson, C.; Teeri, T.T.; Siika-aho, M.; Read, S.M.; Bacic, A. Location of cellulose and callose in pollen tubes and grains of *Nicotiana tabacum*. *Planta* **1998**, *206*, 452–460.
23. Lennon, K.A.; Lord, E.M. The *in vivo* pollen tube cell of *Arabidopsis thaliana*. I. Tube cell cytoplasm and wall. *Protoplasma* **2000**, *214*, 45–56.
24. Derksen, J.; Knuiman, B.; Hoedemaekers, K.; Guyon, A.; Bonhomme, S.; Pierson, E.S. Growth and cellular organization of *Arabidopsis* pollen tubes *in vitro*. *Sex. Plant Reprod.* **2002**, *15*, 133–139.
25. Dardelle, F.; Lehner, A.; Ramdani, Y.; Bardor, M.; Lerouge, P.; Driouich, A.; Mollet, J.C. Biochemical and immunocytological characterizations of *Arabidopsis thaliana* pollen tube cell wall. *Plant Physiol.* **2010**, *153*, 1563–1576.
26. Chebli, Y.; Kaneda, M.; Zerzour, R.; Geitmann, A. The cell wall of the *Arabidopsis thaliana* pollen tube—Spatial distribution, recycling and network formation of polysaccharides. *Plant Physiol*. **2012**, *160*, 1940–1955.
27. Derksen, J.; Li, Y.Q.; Knuiman, B.; Geurts, H. The wall of *Pinus sylvestris* L. pollen tubes. *Protoplasma* **1999**, *208*, 26–36.
28. Yatomi, R.; Nakamura, S.; Nakamura, N. Immunochemical and cytochemical detection of wall components of germinated pollen of Gymnosperms. *Grana* **2002**, *41*, 21–28.
29. Qin, Y.; Chen, D.; Zhao, J. Localization of arabinogalactan proteins in anther, pollen, and pollen tube of *Nicotiana tabacum* L. *Protoplasma* **2007**, *231*, 43–53.
30. Parre, E.; Geitmann, A. Pectin and the role of the physical properties of the cell wall in pollen tube growth of *Solanum chacoense*. *Planta* **2005**, *220*, 582–592.
31. Hasegawa, Y.; Nakamura, S.; Kakizoe, S.; Sato, M.; Nakamura, N. Immunocytochemical and chemical analyses of Golgi vesicles isolated from the germinated pollen of *Camellia japonica*. *J. Plant Res.* **1998**, *111*, 421–429.

32. Wu, J.Z.; Lin, Y.; Zhang, X.L.; Pang, D.W.; Zhao, J. IAA stimulates pollen tube growth and mediates the modification of its wall composition and structure in *Torenia fournieri*. *J. Exp. Bot.* **2008**, *59*, 2529–2543.
33. Abreu, I.; Oliveira, M. Immunolocalisation of arabinogalactan proteins and pectins in *Actinidia deliciosa* pollen. *Protoplasma* **2004**, *224*, 123–128.
34. Puhlmann, J.; Bucheli, E.; Swain, M.J.; Dunning, N.; Albersheim, P.; Darvill, A.G.; Hahn, M.G. Generation of monoclonal antibodies against plant cell wall polysaccharides. I. Characterization of a monoclonal antibody to a terminal alpha-(1,2)-linked fucosyl-containing epitope. *Plant Physiol.* **1994**, *104*, 699–710.
35. Marcus, S.E.; Verhertbruggen, Y.; Herve, C.; Ordaz-Ortiz, J.J.; Farkas, V.; Pedersen, H.L.; Willats, W.G.T.; Knox, J.P. Pectic homogalacturonan masks abundant sets of xyloglucan epitopes in plant cell walls. *BMC Plant Biol.* **2008**, *8*, 60–71.
36. Clausen, M.H.; Willats, W.G.T.; Knox, J.P. Synthetic methyl hexagalacturonate hapten inhibitors of anti-homogalacturonan monoclonal antibodies LM7, JIM5 and JIM7. *Carbohydr. Res.* **2003**, *338*, 1797–1800.
37. Verhertbruggen, Y.; Marcus, S.E.; Haeger, A.; Ordaz-Ortiz, J.J.; Knox, J.P. An extended set of monoclonal antibodies to pectic homogalacturonan. *Carbohydr. Res.* **2009**, *344*, 1858–1862.
38. Willats, W.G.T.; McCartney, L.; Steele-King, C.G.; Marcus, S.E.; Mort, A.; Huisman, M.; van Alebeek, G.-J.; Schols, H.A.; Voragen, A.G.J.; Le Goff, A.; *et al*. A xylogalacturonan epitope is specifically associated with plant cell detachment. *Planta* **2004**, *218*, 673–681.
39. Jones, L.; Seymour, G.B.; Knox, J.P. Localization of pectic galactan in tomato cell walls using a monoclonal antibody specific to (1->4)-beta-D-galactan. *Plant Physiol.* **1997**, *113*, 1405–1412.
40. Willats, W.G.T.; Marcus, S.E.; Knox, J.P. Generation of a monoclonal antibody specific to (1->5)-alpha-L-arabinan. *Carbohydr. Res.* **1998**, *308*, 149–152.
41. Moller, I.; Marcus, S.E.; Haeger, A.; Verhertbruggen, Y.; Verhoef, R.; Schols, H.; Mikklesen, J.D.; Knox, J.P.; Willats, W. High-throughput screening of monoclonal antibodies against plant cell wall glycans by hierarchial clustering of their carbohydrate microarray binding profiles. *Glycoconj. J.* **2008**, *25*, 49–58.
42. Meikle, P.J.; Bonig, I.; Hoogenraad, N.J.; Clarke, A.E.; Stone, B.A. The location of (1→3)-beta-glucans in the walls of pollen tubes of *Nicotiana alata* using a (1→3)-beta-glucan-specific monoclonal antibody. *Planta* **1991**, *185*, 1–8.
43. Matoh, T.; Takasaki, M.; Takabe, K.; Kobayashi, M. Immunocytochemistry of rhamnogalacturonan II in cell walls of higher Plants. *Plant Cell Physiol.* **1998**, *39*, 483–491.
44. Johnson-Brousseau, S.A.; McCormick, S. A compendium of methods useful for characterizing *Arabidopsis* pollen mutants and gametophytically expressed genes. *Plant J.* **2004**, *39*, 761–775.
45. Rounds, C.M.; Lubeck, E.; Hepler, P.K.; Winship, L.J. Propidium iodide competes with Ca^{2+} to label pectin in pollen tubes and *Arabidopsis* root hairs. *Plant Physiol.* **2011**, *157*, 175–187.
46. Blake, A.W.; McCartney, L.; Flint, J.E.; Bolam, D.N.; Boraston, A.B.; Gilbert, H.J.; Knox, J.P. Understanding the biological rationale for the diversity of cellulose-directed carbohydrate-binding molecules in prokaryotic enzymes. *J. Biol. Chem.* **2006**, *281*, 29321–29329.
47. WallMbDB. Available online: http://glycomics.ccrc.uga.edu/wall2/jsp/abIndex.jsp/ (accessed on 6 November 2012).

48. Jauh, G.Y.; Lord, E.M. Localization of pectins and arabinogalactan-proteins in lily (*Lilium longiflorum* L.) pollen tube and style, and their possible roles in pollination. *Planta* **1996**, *199*, 251–261.
49. Mollet, J.C.; Kim, S.; Jauh, G.Y.; Lord, E.M. AGPs, pollen tube growth and the reversible effects of Yariv phenylglycoside. *Protoplasma* **2002**, *219*, 89–98.
50. Rubinstein, A.L.; Márque, J.; Cervera, M.S.; Bedinger, P.A. Extensin-like glycoproteins in the maize pollen tube wall. *Plant Cell* **1995**, *7*, 2211–2225.
51. Chen, T.; Teng, N.J.; Wu, X.Q.; Wang, Y.H.; Tang, W.; Šamaj, J.; Baluška, F.; Lin, J.X. Disruption of actin filaments by latrunculin B affects cell wall construction in *Picea meyeri* pollen tube by disturbing vesicle trafficking. *Plant Cell Physiol.* **2007**, *48*, 19–30.
52. Fernando, D.D.; Quinn, C.R.; Brenner, E.; Owens, J.N. Male gametophyte development and evolution in Gymnosperms. *Int. J. Plant Dev. Biol.* **2010**, *4*, 47–63.
53. Parre, E.; Geitmann, A. More than a leak sealant. The mechanical properties of callose in pollen tubes. *Plant Physiol.* **2005**, *137*, 274–286.
54. Derksen, J.; Janssen, G.J.; Wolters-Arts, M.; Lichtscheidl, I.; Adlassnig, W.; Ovecka, M.; Doris, F.; Steer, M. Wall architecture with high porosity is established at the tip and maintained in growing pollen tubes of *Nicotiana tabacum*. *Plant J.* **2011**, *68*, 495–506.
55. Abercrombie, J.M.; O'Meara, B.C.; Moffatt, A.R.; Williams, J.H. Developmental evolution of flowering plant pollen tube cell walls: Callose synthase (CalS) gene expression patterns. *EvoDevo* **2011**, *2*, 14.
56. Lazzaro, M.D.; Donohue, J.M.; Soodavar, F.M. Disruption of cellulose synthesis by isoxaben causes tip swelling and disorganizes cortical microtubules in elongating conifer pollen tubes. *Protoplasma* **2003**, *220*, 201–207.
57. Caffall, K.H.; Mohnen, D. The structure, function, and biosynthesis of plant cell wall pectic polysaccharides. *Carbohydr. Res.* **2009**, *344*, 1879–1900.
58. Micheli, F. Pectin methylesterases: Cell wall enzymes with important roles in plant physiology. *Trends Plant Sci.* **2001**, *6*, 414–419.
59. Stepka, M.; Ciampolini, F.; Charzynska, M.; Cresti, M. Localization of pectins in the pollen tube wall of *Ornithogalum virens* L. Does the pattern of pectin distribution depend on the growth rate of the pollen tube? *Planta* **2000**, *210*, 630–635.
60. Li, Y.Q.; Chen, F.; Linskens, H.F.; Cresti, M. Distribution of unesterified and esterified pectins in cell walls of pollen tubes of flowering plants. *Sex. Plant Reprod.* **1994**, *7*, 145–152.
61. Chen, K.M.; Wu, G.L.; Wang, Y.H.; Tian, C.T.; Samaj, J.; Baluska, F.; Lin, J.X. The block of intracellular calcium release affects the pollen tube development of *Picea wilsonii* by changing the deposition of cell wall components. *Protoplasma* **2008**, *233*, 39–49.
62. Willats, W.G.T.; Orfila, C.; Limberg, G.; Buchholt, H.C.; van Alebeek, G.-J.; Voragen, A.G.J.; Marcus, S.E.; Christensen, T.M.; Mikkelsen, J.D.; Murray, B.S.; *et al*. Modulation of the degree and pattern of methyl-esterification of pectic homogalacturonan in plant cell walls: implications for pectin methyl esterase action, matrix properties, and cell adhesion. *J. Biol. Chem*. **2001**, *276*, 19404–19413.
63. Fayant, P.; Girlanda, O.; Chebli, Y.; Aubin, C.; Villemure, I.; Geitmann, A. Finite element model of polar growth in pollen tubes. *Plant Cell* **2010**, *22*, 2579–2593.

64. APGIII. Angiosperm Phylogeny Group. An update of the Angiosperm phylogeny group classification for the orders and families of flowering plants. *Bot. J. Linn. Soc.* **2009**, *161*, 105–121.
65. Fry, S.C. Cell wall polysaccharide composition and covalent crosslinking. *Annu. Plant Rev.* **2011**, *41*, 1–42.
66. Scheller, H.V.; Ulvskov, P. Hemicelluloses. *Annu. Rev. Plant Biol.* **2010**, *61*, 263–289.
67. Cosgrove, D.J. Enzymes and other agents that enhance cell wall extensibility. *Annu. Rev. Plant Physiol. Plant Mol. Biol.* **1999**, *50*, 391–417.
68. Freshour, G.; Bonin, C.P.; Reiter, W.D.; Albersheim, P.; Darvill, A.G.; Hahn, M.G. Distribution of fucose-containing xyloglucans in cell walls of the *mur1* mutant of *Arabidopsis*. *Plant Physiol.* **2003**, *131*, 1602–1612.
69. Williams, J.H. Novelties of the flowering plant pollen tube underlie diversification of a key life history stage. *Proc. Natl. Acad. Sci. USA* **2008**, *105*, 11259–11263.
70. Laughlin, S.T.; Bertozzi, C.R. Imaging the glycome. *Proc. Natl. Acad. Sci. USA* **2009**, *106*, 12–17.
71. Anderson, C.T.; Wallace, I.S. Illuminating the wall: Using click chemistry to image pectins in Arabidopsis cell walls. *Plant Signal. Behav.* **2012**, *7*, 661–663.
72. Anderson, C.T.; Wallace, I.S.; Somerville, C.R. Metabolic click-labeling with a fucose analog reveals pectin delivery, architecture, and dynamics in Arabidopsis cell walls. *Proc. Natl. Acad. Sci. USA* **2012**, *109*, 1329–1334.
73. Rae, A.L.; Harris, P.J.; Bacic, A.; Clarke, A.E. Composition of the cell walls of *Nicotiana alata* Link et Otto pollen tubes. *Planta* **1985**, *166*, 128–133.
74. Nakamura, N.; Suzuki, H. Sugar composition of pollen grain and pollen tube cell walls. *Phytochemistry* **1981**, *20*, 981–984.
75. Fry, S.C.; York, W.S.; Albersheim, P.; Darvill, A.; Hayashi, T.; Joseleau, J.P.; Seitz, H.U.; Kato, Y.; Pérez Lorences, E.; Maclachlan, G.A.; *et al*. An unambiguous nomenclature for xyloglucan-derived oligosaccharides. *Physiol. Plant* **1993**, *89*, 1–3.
76. Cavalier, D.M.; Lerouxel, O.; Neumetzler, L.; Yamauchi, K.; Reinecke, A.; Freshour, G.; Zabotina, O.A.; Hahn, M.G.; Burgert, I.; Pauly, M.; *et al*. Disrupting two *Arabidopsis thaliana* xylosyltransferase genes results in plants deficient in xyloglucan, a major primary cell wall component. *Plant Cell* **2008**, *20*, 1519–1537.
77. Günl, M.; Kraemer, F.; Pauly, M. Oligosaccharide Mass Profiling (OLIMP) of Cell Wall Polysaccharides by MALDI-TOF/MS. In *The Plant Cell Wall: Methods and Protocols, Methods in Molecular Biology*; Popper, Z.A., Ed.; Springer, Humana Press: New York, NY, USA, 2011; Volume 715, pp. 43–54.
78. Lerouxel, O.; Choo, T.S.; Seveno, M.; Usadel, B.; Faye, L.; Lerouge, P.; Pauly, M. Rapid structural phenotyping of plant cell wall mutants by enzymatic oligosaccharide fingerprinting. *Plant Physiol.* **2002**, *130*, 1754–1763.
79. Copyright American Society of Plant Biologists. Available online: http://www.plantphysiol.org/ (accessed on 19 February 2013).

80. Sekkal, M.; Huvenne, J.-P.; Legrand, P.; Sombret, B.; Mollet, J.-C.; Mouradi-Givernaud, A.; Verdus, M.-C. Direct structural identification of polysaccharides from red algae by FTIR microspectrometry. I. Localization of agar in *Gracilaria verrucosa* sections. *Microchim. Acta* **1993**, *112*, 1–10.
81. Chen, L.; Carpita, N.C.; Reiter, W.D.; Wilson, R.H.; Jeffries, C.; McCann, M.C. A rapid method to screen for cell-wall mutants using discriminant analysis of Fourier transform infrared spectra. *Plant J.* **1998**, *16*, 385–392.
82. Mouille, G.; Robin, S.; Lecomte, M.; Pagant, S.; Höfte, H. Classification and identification of *Arabidopsis* cell wall mutants using Fourier-Transform InfraRed (FT-IR) microspectroscopy. *Plant J.* **2003**, *35*, 393–404.
83. Wang, Q.; Lu, L.; Wu, X.; Li, Y.; Lin, J. Boron influences pollen germination and pollen tube growth in *Picea meyeri*. *Tree Physiol.* **2003**, *23*, 345–351.
84. Wang, Q.L.; Kong, L.A.; Hao, H.Q.; Wang, X.H.; Lin, J.X.; Samaj, J.; Baluska, F. Effects of brefeldin A on pollen germination and tube growth: Antagonistic effects on endocytosis and secretion. *Plant Physiol.* **2005**, *139*, 1692–1703.
85. Wang, Y.; Chen, T.; Zhang, C.; Hao, H.; Liu, P.; Zheng, M.; Baluska, F.; Samaj, J.; Lin, J. Nitric oxide modulates the influx of extracellular Ca^{2+} and actin filament organization during cell wall construction in *Pinus bungeana* pollen tubes. *New Phytol.* **2009**, *182*, 851–862.
86. Mohnen, D. Pectin structure and biosynthesis. *Curr. Opin. Plant Biol.* **2008**, *11*, 266–277.
87. Driouich, A.; Follet-Gueye, M.L.; Bernard, S.; Kousar, S.; Chevalier, L.; Vicré-Gibouin, M.; Lerouxel, O. Golgi-mediated synthesis and secretion of matrix polysaccharides of the primary cell wall of higher plants. *Front. Plant Sci.* **2012**, *3*, doi:10.3389/fpls.2012.00079.
88. Akita, K.; Ishimizu, T.; Tsukamoto, T.; Ando, T.; Hase, S. Successive glycosyltransfer activity and enzymatic characterization of pectic polygalacturonate 4-alpha-galacturonosyltransferase solubilized from pollen tubes of *Petunia axillaris* using pyridylaminated oligogalacturonates as substrates. *Plant Physiol.* **2002**, *130*, 374–379.
89. Caffall, K.H.; Pattathil, S.; Phillips, S.; Hahn, M.G.; Mohnen, D. *Arabidopsis thaliana* T-DNA mutants implicate GAUT genes in the biosynthesis of pectin and xylan in cell walls and seed testa. *Mol. Plant* **2009**, *2*, 1000–1014.
90. Kong, Y.; Zhou, G.; Yin, Y.; Xu, Y.; Pattathil, S.; Hahn, M.G. Molecular analysis of a family of *Arabidopsis* genes related to galacturonosyltransferases. *Plant Physiol.* **2011**, *155*, 1791–1805.
91. Sterling, J.D.; Atmodjo, M.A.; Inwood, S.E.; Kumar Kolli, V.S.; Quigley, H.F.; Hahn, M.G.; Mohnen, D. Functional identification of an *Arabidopsis* pectin biosynthetic homogalacturonan galacturonosyltransferase. *Proc. Natl. Acad. Sci. USA* **2006**, *103*, 5236–5241.
92. Bouton, S.; Leboeuf, E.; Mouille, G.; Leydecker, M.T.; Talbotec, J.; Granier, F.; Lahaye, M.; Höfte, H.; Truong, H.N. QUASIMODO1 encodes a putative membrane-bound glycosyltransferase required for normal pectin synthesis and cell adhesion in *Arabidopsis*. *Plant Cell* **2002**, *14*, 2577–2590.
93. Qin, Y.; Leydon, A.R.; Manziello, A.; Pandey, R.; Mount, D.; Denic, S.; Vasic, B.; Johnson, M.A.; Palanivelu, R. Penetration of the stigma and style elicits a novel transcriptome in pollen tubes, Pointing to genes critical for growth in a pistil. *PLoS Genet.* **2009**, *5*, e1000621.

94. Jensen, J.K.; Sørensen, S.O.; Harholt, J.; Geshi, N.; Sakuragi, Y.; Møller, I.; Zandleven, J.; Bernal, A.J.; Jensen, N.B.; Sørensen, C.; *et al*. Identification of a xylogalacturonan xylosyltransferase involved in pectin biosynthesis in *Arabidopsis*. *Plant Cell* **2008**, *20*, 1289–1302.
95. Harholt, J.; Suttangkakul, A.; Scheller, H.V. Biosynthesis of pectin. *Plant Physiol.* **2010**, *153*, 384–395.
96. Konishi, T.; Takeda, T.; Miyazaki, Y.; Ohnishi-Kameyama, M.; Hayashi, T.; O'Neill, M.A.; Ishii, T. A plant mutase that interconverts UDP-arabinofuranose and UDP-arabinopyranose. *Glycobiology* **2007**, *17*, 345–354.
97. Drakakaki, G.; Zabotina, O.; Delgado, I.; Robert, S.; Keegstra, K.; Raikhel, N. *Arabidopsis* reversibly glycosylated polypeptides 1 and 2 are essential for pollen development. *Plant Physiol.* **2006**, *142*, 1480–1492.
98. Rautengarten, C.; Ebert, B.; Herter, T.; Petzold, C.J.; Ishii, T.; Mukhopadhyay, A.; Usadel, B.; Scheller, H.V. The interconversion of UDP-arabinopyranose and UDP-arabinofuranose is indispensable for plant development in *Arabidopsis*. *Plant Cell* **2011**, *23*, 1373–1390.
99. Iwai, H.; Hokura, A.; Oishi, M.; Chida, H.; Ishii, T.; Sakai, S.; Satoh, S. The gene responsible for borate cross-linking of pectin Rhamnogalacturonan-II is required for plant reproductive tissue development and fertilization. *Proc. Natl. Acad. Sci. USA* **2006**, *103*, 16592–16597.
100. Wu, A.M.; Rihouey, C.; Seveno, M.; Hörnblad, E.; Singh, S.; Matsunaga, T.; Ishii, T.; Lerouge, P.; Marchant, A. The *Arabidopsis* IRX10 and IRX10-LIKE glycosyltransferases are critical for glucuronoxylan biosynthesis during secondary cell wall formation. *Plant J.* **2009**, *57*, 718–731.
101. Brown, D.M.; Zhang, Z.; Stephens, E.; Dupree, P.; Turner, S.R. Characterization of IRX10 and IRX10-like reveals an essential role in glucuronoxylan biosynthesis in *Arabidopsis*. *Plant J.* **2009**, *57*, 732–746.
102. Delmas, F.; Séveno, M.; Northey, J.G.; Hernould, M.; Lerouge, P.; McCourt, P.; Chevalier, C. The synthesis of the rhamnogalacturonan II component 3-deoxy-D-manno-2-octulosonic acid (Kdo) is required for pollen tube growth and elongation. *J. Exp. Bot.* **2008**, *59*, 2639–2647.
103. Liu, X.L.; Liu, L.; Niu, Q.K.; Xia, C.; Yang, K.Z.; Li, R.; Chen, L.Q.; Zhang, X.Q.; Zhou, Y.; Ye, D. Male gametophyte defective 4 encodes a rhamnogalacturonan II xylosyltransferase and is important for growth of pollen tubes and roots in *Arabidopsis*. *Plant J.* **2011**, *65*, 647–660.
104. Deng, Y.; Wang, W.; Li, W.Q.; Xia, C.; Liao, H.Z.; Zhang, X.Q.; Ye, D. MALE GAMETOPHYTE DEFECTIVE 2, encoding a sialyltransferase-like protein, is required for normal pollen germination and pollen tube growth in *Arabidopsis*. *J. Integr. Plant Biol.* **2010**, *52*, 829–843.
105. Kobayashi, M.; Kouzu, N.; Inami, A.; Toyooka, K.; Konishi, Y.; Matsuoka, K.; Matoh, T. Characterization of *Arabidopsis* CTP:3-deoxy-D-manno-2-octulosonate cytidylyltransferase (CMP-KDO synthetase), the enzyme that activates KDO during rhamnogalacturonan II biosynthesis. *Plant Cell Physiol.* **2011**, *52*, 1832–1843.
106. Goubet, F.; Mohnen, D. Solubilization and partial characterization of homogalacturonan-methyltransferase from microsomal membranes of suspension-cultured tobacco cells. *Plant Physiol.* **1999**, *121*, 281–290.

107. Pauly, M.; Scheller, H.V. *O*-Acetylation of plant cell wall polysaccharides: Identification and partial characterization of a rhamnogalacturonan *O*-acetyl-transferase from potato suspension-cultured cells. *Planta* **2000**, *210*, 659–667.
108. Mouille, G.; Ralet, M.C.; Cavelier, C.; Eland, C.; Effroy, D.; Hématy, K.; McCartney, L.; Truong, H.N.; Gaudon, V.; Thibault, J.F.; *et al*. Homogalacturonan synthesis in *Arabidopsis thaliana* requires a Golgi-localized protein with a putative methyltransferase domain. *Plant J.* **2007**, *50*, 605–614.
109. Miao, Y.; Li, H.Y.; Shen, J.; Wang, J.; Jiang, L. QUASIMODO 3 (QUA3) is a putative homogalacturonan methyltransferase regulating cell wall biosynthesis in *Arabidopsis* suspension-cultured cells. *J. Exp. Bot.* **2011**, *62*, 5063–5078.
110. Manabe, Y.; Nafisi, M.; Verhertbruggen, Y.; Orfila, C.; Gille, S.; Rautengarten, C.; Cherk, C.; Marcus, S.E.; Somerville, S.; Pauly, M.; *et al*. Loss-of-function mutation of REDUCED WALL ACETYLATION2 in *Arabidopsis* leads to reduced cell wall acetylation and increased resistance to *Botrytis cinerea*. *Plant Physiol.* **2011**, *155*, 1068–1078.
111. Zabotina, O.A. Xyloglucan and its biosynthesis. *Front. Plant Sci.* **2012**, *3*, doi:10.3389/fpls.2012.00134.
112. Cocuron, J.C.; Lerouxel, O.; Drakakaki, G.; Alonso, A.P.; Liepman, A.H.; Keegstra, K.; Raikhel, N.; Wilkerson, C.G. A gene from the cellulose synthase-like C family encodes a beta-1,4 glucan synthase. *Proc. Natl. Acad. Sci. USA* **2007**, *104*, 8550–8555.
113. Cavalier, D.M.; Keegstra, K. Two xyloglucan xylosyltransferases catalyze the addition of multiple xylosyl residues to cellohexaose. *J. Biol. Chem.* **2006**, *281*, 34197–34207.
114. Vuttipongchaikij, S.; Brocklehurst, D.; Steele-King, C.; Ashford, D.A.; Gomez, L.D.; McQueen-Mason, S.J. *Arabidopsis* GT34 family contains five xyloglucan α-1,6-xylosyltransferases. *New Phytol.* **2012**, *195*, 585–595.
115. Madson, M.; Dunand, C.; Li, X.; Verma, R.; Vanzin, G.F.; Caplan, J.; Shoue, D.A.; Carpita, N.C.; Reiter, W.D. The MUR3 gene of *Arabidopsis* encodes a xyloglucan galactosyltransferase that is evolutionarily related to animal exostosins. *Plant Cell* **2003**, *15*, 1662–1670.
116. Jensen, J.K.; Schultink, A.; Keegstra, K.; Wilkerson, C.G.; Pauly, M. RNA-Seq analysis of developing nasturtium seeds (*Tropaeolum majus*): Identification and characterization of an additional galactosyltransferase involved in xyloglucan biosynthesis. *Mol. Plant* **2012**, *5*, 984–992.
117. Perrin, R.M.; DeRocher, A.E.; Bar-Peled, M.; Zeng, W.; Norambuena, L.; Orellana, A.; Raikhel, N.V.; Keegstra, K. Xyloglucan fucosyltransferase, an enzyme involved in plant cell wall biosynthesis. *Science* **1999**, *284*, 1976–1979.
118. Vanzin, G.F.; Madson, M.; Carpita, N.C.; Raikhel, N.V.; Keegstra, K.; Reiter, W.D. The *mur2* mutant of *Arabidopsis thaliana* lacks fucosylated xyloglucan because of a lesion in fucosyltransferase AtFUT1. *Proc. Natl. Acad. Sci. USA* **2002**, *99*, 3340–3345.
119. Guerriero, G.; Fugelstad, J.; Bulone, V. What do we really know about cellulose biosynthesis in Higher Plants? *J. Integr. Plant Biol.* **2010**, *52*, 161–175.
120. Richmond, T. Higher plant cellulose synthases. *Genome Biol.* **2000**, *1*, reviews3001.1–reviews3001.6.
121. Doblin, M.S.; Kurek, I.; Jacob-Wilk, D.; Delmer, D.P. Cellulose biosynthesis in plants: From genes to rosettes. *Plant Cell Physiol.* **2002**, *43*, 1407–1420.

122. Richmond, T.A.; Somerville, C.R. Integrative approaches to determining Csl function. *Plant Mol. Biol.* **2001**, *47*, 131–143.
123. Bernal, A.J.; Yoo, C.M.; Mutwil, M.; Jensen, J.K.; Hou, G.; Blaukopf, C.; Sørensen, I.; Blancaflor, E.B.; Scheller, H.V.; Willats, W.G. Functional analysis of the cellulose synthase-like genes CSLD1, CSLD2, and CSLD4 in tip-growing *Arabidopsis* cells. *Plant Physiol.* **2008**, *148*, 1238–1253.
124. Wang, L.; Guo, K.; Li, Y.; Tu, Y.; Hu, H.; Wang, B.; Cui, X.; Peng, L. Expression profiling and integrative analysis of the CESA/CSL superfamily in rice. *BMC Plant Biol.* **2010**, *10*, 282.
125. Doblin, M.S.; de Melis, L.; Newbigin, E.; Bacic, A.; Read, S.M. Pollen tubes of *Nicotiana alata* express two genes from different β-Glucan synthase families. *Plant Physiol.* **2001**, *125*, 2040–2052.
126. Cai, G.; Faleri, C.; Del Casino, C.; Emons, A.M.C.; Cresti, M. Distribution of callose synthase, cellulose synthase, and sucrose synthase in tobacco pollen tube is controlled in dissimilar ways by actin filaments and microtubules. *Plant Physiol.* **2011**, *155*, 1169–1190.
127. Wang, W.; Wang, L.; Chen, C.; Xiong, G.; Tan, X.Y.; Yang, K.Z.; Wang, Z.C.; Zhou, Y.; Ye, D.; Chen, L.Q. *Arabidopsis* CSLD1 and CSLD4 are required for cellulose deposition and normal growth of pollen tubes. *J. Exp. Bot.* **2011**, *62*, 5161–5177.
128. Persson, S.; Paredez, A.; Carroll, A.; Palsdottir, H.; Doblin, M.; Poindexter, P.; Khitrov, N.; Auer, M.; Somerville, C.R. Genetic evidence for three unique components in primary cell-wall cellulose synthase complexes in Arabidopsis. *Proc. Natl. Acad. Sci. USA* **2007**, *104*, 15566–15571.
129. Boavida, L.C.; Shuai, B.; Yu, H.J.; Pagnussat, G.C.; Sundaresan, V.; McCormick, S. A collection of Ds insertional mutants associated with defects in male gametophyte development and function in *Arabidopsis thaliana*. *Genetics* **2009**, *181*, 1369–1385.
130. Verma, D.P.; Hong, Z. Plant callose synthase complexes. *Plant Mol. Biol.* **2001**, *47*, 693–701.
131. Nishikawa, S.; Zinkl, G.M.; Swanson, R.J.; Maruyama, D.; Preuss, D. Callose (beta-1,3 glucan) is essential for *Arabidopsis* pollen wall patterning, but not tube growth. *BMC Plant Biol.* **2005**, *5*, 15.
132. Dong, X.; Hong, Z.; Sivaramakrishnan, M.; Mahfouz, M.; Verma, D.P. Callose synthase (CalS5) is required for exine formation during microgametogenesis and for pollen viability in *Arabidopsis*. *Plant J.* **2005**, *42*, 315–328.
133. Brownfield, L.; Ford, K.; Doblin, M.S.; Newbigin, E.; Read, S.; Bacic, A. Proteomic and biochemical evidence links the callose synthase in *Nicotiana alata* pollen tubes to the product of the NaGSL1 gene. *Plant J.* **2007**, *52*, 147–156.
134. Brownfield, L.; Wilson, S.; Newbigin, E.; Bacic, A.; Read, S. Molecular control of the glucan synthase-like protein NaGSL1 and callose synthesis during growth of *Nicotiana alata* pollen tubes. *Biochem. J.* **2008**, *414*, 43–52.
135. Pacini, E.; Franchi, G.G.; Ripaccioli, M. Ripe pollen structure and histochemistry of some Gymnosperms. *Plant Syst. Evol.* **1999**, *217*, 81–99.
136. McQueen-Mason, S.; Durachko, D.M.; Cosgrove, D.J. Two endogenous proteins that induce cell wall extension in plants. *Plant Cell* **1992**, *4*, 1425–1433.
137. Li, Z.-C.; Durachko, D.M.; Cosgrove, D.J. An oat coleoptile wall protein that induces wall extension *in vitro* and that is antigenically related to a similar protein from cucumber hypocotyls. *Planta* **1993**, *191*, 349–356.

138. Sampedro, J.; Cosgrove, D.J. The expansin superfamily. *Genome Biol.* **2005**, *6*, 1–11.
139. McQueen-Mason, S.; Cosgrove, D.J. Disruption of hydrogen bonding between plant cell wall polymers by proteins that induce wall extension. *Proc. Natl. Acad. Sci. USA* **1994**, *91*, 6574–6578.
140. McQueen-Mason, S.; Cosgrove, D.J. Expansin mode of action on cell walls. Analysis of wall hydrolysis, stress relaxation, and binding. *Plant Physiol.* **1995**, *107*, 87–100.
141. Sharova, E.I. Expansins: Proteins involved in cell wall softening during plant growth and morphogenesis. *Russ. J. Plant Physiol.* **2007**, *54*, 713–727.
142. Arabidopsis genes. Available online: https://homes.bio.psu.edu/expansins/arabidopsis.htm/ (accessed on 6 November 2012).
143. Dai, S.; Li, L.; Chen, T.; Chong, K.; Xue, Y.; Wang, T. Proteomic analyses of *Oryza sativa* mature pollen reveal novel proteins associated with pollen germination and tube growth. *Proteomics* **2006**, *6*, 2504–2529.
144. Li, L.C.; Bedinger, P.A.; Volk, C.; Jones, A.D.; Cosgrove, D.J. Purification and characterization of four β-expansins (*Zea* m 1 Isoforms) from maize pollen. *Plant Physiol.* **2003**, *132*, 2073–2085.
145. Jin, Y.; Tashpulatov, A.S.; Katholnigg, H.; Heberle-Bors, E.; Touraev, A. Isolation and characterization of two wheat β-expansin genes expressed during male gametophyte development. *Protoplasma* **2006**, *228*, 13–19.
146. Zaidi, M.A.; O'Leary, S.; Wu, S.; Gleddie, S.C.; Eudes, F.; Laroche, A.; Robert, L.S. A molecular and proteomic investigation of proteins rapidly released from triticale pollen upon hydration. *Plant Mol Biol.* **2012**, *79*, 101–121.
147. Cosgrove, D.J.; Bedinger, P.; Durachko, D.M. Group 1 allergens of grass pollen as cell wall-loosening agents. *Proc. Natl. Acad. Sci. USA* **1997**, *94*, 6559–6564.
148. Winter, D.; Vinegar, B.; Nahal, H.; Ammar, R.; Wilson, G.V.; Provart, N.J. An "Electronic fluorescent pictograph" browser for exploring and analyzing large-scale biological data sets. *PLoS One* **2007**, *2*, e718.
149. Magrane, M.; UniProt Consortium. UniProt Knowledgebase: A hub of integrated protein data. *Database* **2011**, doi:10.1093/database/bar009.
150. Hende, H.; Bradford, K.J.; Brummel, D.A.; Cho, H.T.; Cosgrove, D.J.; Fleming, A.J.; Gehring, C.; Lee, Y.; McQuenn-Mason, S.; Rose, J.K.C.; *et al*. Nomenclature for members of the expansin superfamily of genes and proteins. *Plant Mol. Biol.* **2004**, *55*, 311–314.
151. Swanson, R.; Clark, T.; Preuss, D. Expression profiling of *Arabidopsis* stigma tissue identifies stigma-specific genes. *Sex. Plant Reprod.* **2005**, *18*, 163–171.
152. Rose, J.K.C.; Braam, J.; Fry, S.C.; Nishitani, K. The XTH family of enzymes involved in xyloglucan endotransglucosylation and endohydrolysis: Current perspectives and a new unifying nomenclature. *Plant Cell Physiol.* **2002**, *43*, 1421–1435.
153. Fry, S.C.; Smith, R.C.; Renwick, K.F.; Martin, D.J.; Hodge, S.K.; Matthews, K.J. Xyloglucan endotransglycosylase, a new wall-loosening enzyme activity from plants. *Biochem. J.* **1992**, *282*, 821–828.
154. Nishitani, K.; Tominaga, R. Endo-xyloglucan transferase, a novel class of glycosyltransferase that catalyzes transfer of a segment of xyloglucan molecule to another xyloglucan molecule. *J. Biol. Chem.* **1992**, *267*, 21058–21064.

155. Yokoyama, R.; Nishitani, K. A comprehensive expression analysis of all members of a gene family encoding cell-wall enzymes allowed us to predict *cis*-regulatory regions involved in cell wall construction in specific organs of *Arabidopsis*. *Plant Cell Physiol.* **2001**, *42*, 1025–1033.
156. Yokoyama, R.; Rose, J.K.C.; Nishitani, K. A surprising diversity and abundance of xyloglucan endotransglucosylase/hydrolases in rice. Classification and expression analysis. *Plant Physiol.* **2004**, *134*, 1088–1099.
157. Becnel, J.; Natarajan, M.; Kipp, A.; Braam, J. Developmental expression patterns of *Arabidopsis* XTH genes reported by transgenes and Genevestigator. *Plant Mol. Biol.* **2006**, *61*, 451–467.
158. Kurasawa, K.; Matsui, A.; Yokoyama, R.; Kuriyama, T.; Yoshizumi, T.; Matsui, M.; Suwabe, K.; Watanabe, M.; Nishitani, K. The *AtXTH28* gene, a xyloglucan endotransglucosylase/hydrolase, is involved in automatic self-pollination in *Arabidopsis thaliana*. *Plant Cell Physiol.* **2009**, *50*, 413–422.
159. Zhang, G.F.; Staehelin, L.A. Functional compartmentation of the Golgi apparatus of plant cells: Immunocytochemical analysis of high-pressure frozen- and freeze-substituted sycamore maple suspension culture cells. *Plant Physiol.* **1992**, *99*, 1070–1083.
160. Gaffe, J.; Tieman, D.M.; Handa, A.K. Pectin methylesterase isoforms in tomato (*Lycopersicon esculentum*) tissues (effects of expression of a pectin methylesterase antisense gene). *Plant Physiol.* **1994**, *105*, 199–203.
161. Rhee, S.Y.; Somerville, C.R. Tetrad pollen formation in quartet mutants of *Arabidopsis thaliana* is associated with persistence of pectic polysaccharides of the pollen mother cell wall. *Plant J.* **1998**, *15*, 79–88.
162. Rhee, S.Y.; Osborne, E.; Poindexter, P.D.; Somerville, C.R. Microspore separation in the *quartet 3* mutants of Arabidopsis is impaired by a defect in a developmentally regulated polygalacturonase required for pollen mother cell-wall degradation. *Plant Physiol.* **2003**, *133*, 1170–1180.
163. Francis, K.E.; Lam, S.Y.; Copenhaver, G.P. Separation of Arabidopsis pollen tetrads is regulated by QUARTET1, a pectin methyl-esterase gene. *Plant Physiol.* **2006**, *142*, 1004–1013.
164. Wolf, S.; Mouille, G.; Pelloux, J. Homogalacturonan methyl-esterification and plant development. *Mol. Plant* **2009**, *2*, 851–860.
165. Zhu, Y.; Zhao, P.; Wu, X.; Wang, W.; Scali, M.; Cresti, M. Proteomic identification of differentially expressed proteins in mature and germinated maize pollen. *Acta Physiol. Plant* **2011**, *33*, 1467–1474.
166. Ge, W.; Song, Y.; Zhang, C.; Zhang, Y.; Burlingame, A.L.; Guo, Y. Proteomic analyses of apoplastic proteins from germinating *Arabidopsis thaliana* pollen. *Biochim. Biophys. Acta* **2011**, *1814*, 1964–1973.
167. Li, Y.Q.; Mareck, A.; Faleri, C.; Moscatelli, A.; Liu, Q.; Cresti, M. Detection and localization of pectin methylesterase isoforms in pollen tubes of *Nicotiana tabacum* L. *Planta* **2002**, *214*, 734–740.
168. Jiang, L.; Yang, S.L.; Xie, L.F.; Puah, C.S.; Zhang, X.Q.; Yang, W.C.; Sundaresan, V.; Ye, D. VANGUARD1 encodes a pectin methylesterase that enhances pollen tube growth in the *Arabidopsis* style and transmitting tract. *Plant Cell* **2005**, *17*, 584–596.
169. Tian, G.W.; Chen, M.H.; Zaltsman, A.; Citovsky, V. Pollen-specific pectin methylesterase involved in pollen tube growth. *Dev. Biol.* **2006**, *294*, 83–91.

170. Bosch, M.; Cheung, A.Y.; Hepler, P.K. Pectin methylesterase, a regulator of pollen tube growth. *Plant Physiol.* **2005**, *138*, 1334–1346.
171. Wolf, S.; Grsic-Rausch, S.; Rausch, T.; Greiner, S. Identification of pollen-expressed pectin methylesterase inhibitors in *Arabidopsis*. *FEBS Lett.* **2003**, *555*, 551–555.
172. Raiola, A.; Camardella, L.; Giovane, A.; Mattei, B.; de Lorenzo, G.; Cervone, F.; Bellincampi, D. Two *Arabidopsis thaliana* genes encode functional pectin methylesterase inhibitors. *FEBS Lett.* **2004**, *557*, 199–203.
173. Pina, C.; Pinto, F.; Feijó, J.A.; Becker, J.D. Gene family analysis of the *Arabidopsis* pollen transcriptome reveals biological implications for cell growth, division control, and gene expression regulation. *Plant Physiol.* **2005**, *138*, 744–756.
174. Zhang, G.Y.; Feng, J.; Wu, J.; Wang, X.W. BoPMEI1, a pollen-specific pectin methylesterase inhibitor, has an essential role in pollen tube growth. *Planta* **2010**, *231*, 1323–1334.
175. Lehner, A.; Leroux, C.; Mollet, J.C. University of Rouen, Mont Saint-Aignan, France. Unpublished work, 2013.
176. Röckel, N.; Wolf, S.; Kost, B.; Rausch, T.; Greiner, S. Elaborate spatial patterning of cell-wall PME and PMEI at the pollen tube tip involves PMEI endocytosis, and reflects the distribution of esterified and de-esterified pectins. *Plant J.* **2008**, *53*, 133–143.
177. Leboeuf, E.; Guillon, F.; Thoiron, S.; Lahaye, M. Biochemical and immunohistochemical analysis of pectic polysaccharides in the cell walls of *Arabidopsis* mutant QUASIMODO 1 suspension-cultured cells: Implications for cell adhesion. *J. Exp. Bot.* **2005**, *56*, 3171–3182.
178. Durand, C.; Vicre-Gibouin, M.; Follet-Gueye, M.L.; Duponchel, L.; Moreau, M.; Lerouge, P.; Driouich, A. The organization pattern of root border-likes cells of *Arabidopsis thaliana* is dependent on cell wall homogalacturonan. *Plant Physiol.* **2009**, *150*, 1411–1421.
179. Mollet, J.C.; Park, S.Y.; Nothnagel, E.A.; Lord, E.M. A lily stylar pectin is necessary for pollen tube adhesion to an *in vitro* stylar matrix. *Plant Cell* **2000**, *12*, 1737–1749.
180. Park, S.Y.; Jauh, G.Y.; Mollet, J.C.; Eckard, K.J.; Nothnagel, E.A.; Walling, L.L.; Lord, E.M. A lipid transfer-like protein is necessary for lily pollen tube adhesion to an *in vitro* stylar matrix. *Plant Cell* **2000**, *12*, 151–164.
181. Tung, C.W.; Dwyer, K.G.; Nasrallah, M.E.; Nasrallah, J.B. Genome-wide identification of genes expressed in *Arabidopsis* pistils specifically along the path of pollen tube growth. *Plant Physiol.* **2005**, *138*, 977–989.
182. Nieuwland, J.; Feron, R.; Huisman, B.A.H.; Fasolino, A.; Hilbers, C.W.; Derksen, J.; Mariani, C. Lipid transfer proteins enhance cell wall extension in tobacco. *Plant Cell* **2005**, *17*, 2009–2019.
183. Chae, K.; Kieslich, C.A.; Morikis, D.; Kim, S.C.; Lord, E.M. A gain-of-function mutation of *Arabidopsis* lipid transfer protein 5 disturbs pollen tube tip growth and fertilization. *Plant Cell* **2009**, *21*, 3902–3914.
184. Gou, J.Y.; Miller, L.M.; Hou, G.; Yu, X.H.; Chen X.Y.; Liu, C.J. Acetylesterase-mediated deacetylation of pectin impairs cell elongation, pollen germination and Plant reproduction. *Plant Cell* **2012**, *24*, 50–65.
185. Wing, R.A.; Yamaguchi, J.; Larabell, S.K.; Ursin, V.M.; McCormick, S. Molecular and genetic characterization of two pollen−expressed genes that have sequence similarity to pectate lyases of the plant pathogen *Erwinia*. *Plant Mol. Biol.* **1989**, *14*, 17–28.

186. Wu, Y.; Qiu, X.; Du, S.; Erickson, L. PO149, a new member of pollen pectate lyase-like gene family from alfalfa. *Plant Mol. Biol*. **1996**, *32*, 1037–1042.
187. Kulikauskas, R.; McCormick, S. Identification of the tobacco and *Arabidopsis* homologues of the pollen-expressed LAT59 gene of tomato. *Plant Mol. Biol.* **1997**, *34*, 809–814.
188. Marin-Rodriguez, M.V.; Orchard, J.; Seymour, G.B. Pectate lyases, cell wall degradation and fruit softening. *J. Exp. Bot.* **2002**, *53*, 2115–2119.
189. Palusa, S.G.; Golovkin, M.; Shin, S.B.; Richardson, D.N.; Reddy, A.S. Organ-specific, developmental, hormonal and stress regulation of expression of putative pectate lyase genes in *Arabidopsis*. *New Phytol.* **2007**, *174*, 537–550.
190. Sun, L.; van Nocker, S. Analysis of promoter activity of members of the PECTATE LYASE-LIKE (PLL) gene family in cell separation in *Arabidopsis*. *BMC Plant Biol.* **2010**, *10*, 152.
191. Dai, S.; Chen, T.; Chong, K.; Xue, Y.; Liu, S.; Wang, T. Proteomics identification of differentially expressed proteins associated with pollen germination and tube growth reveals characteristics of germinated *Oryza sativa* pollen. *Mol. Cell. Proteomics* **2007**, *6*, 207–230.
192. Henrissat, B. A classification of glycosyl hydrolases based on amino acid sequence similarities. *Biochem J.* **1991**, *280*, 309–316.
193. Glycoside Hydrolase Family Classification. Available online: http://www.cazy.org/Glycoside-Hydrolases.html/ (accessed on 23 October 2012).
194. Del Campillo, E.; Lewis, L.N. Occurrence of 9.5 cellulase and other hydrolases in flower reproductive organs undergoing major cell wall disruption. *Plant Physiol.* **1992**, *99*, 1015–1020.
195. Aouar, L.; Chebli, Y.; Geitmann, A. Morphogenesis of complex plant cell shapes: The mechanical role of crystalline cellulose in growing pollen tubes. *Sex. Plant Reprod*. **2010**, *23*, 15–27.
196. Roggen, H.P.J.; Stanley, R.G. Cell-wall-hydrolysing enzymes in wall formation as measured by pollen-tube extension. *Planta* **1969**, *84*, 295–303.
197. Takeda, H.; Yoshikawa, T.; Liu, X.Z.; Nakagawa, N.; Li, Y.Q.; Sakurai, N. Molecular cloning of two exo-beta-glucanases and their *in vivo* substrates in the cell walls of lily pollen tubes. *Plant Cell Physiol.* **2004**, *45*, 436–444.
198. Kotake, T.; Li, Y.Q.; Takahashi, M.; Sakurai, N. Characterization and function of wall-bound exo-beta-glucanases of *Lilium longiflorum* pollen tubes. *Sex. Plant Reprod.* **2000**, *13*, 1–9.
199. Hruba, P.; Honys, D.; Twell, D.; Capkova, V.; Tupy, J. Expression of beta-galactosidase and beta-xylosidase genes during microspore and pollen development. *Planta* **2005**, *220*, 931–940.
200. Pressey, R.; Reger, B.J. Polygalacturonase in pollen from corn and other grasses. *Plant Sci.* **1969**, *59*, 57–62.
201. Hadfield, K.A.; Bennett, A.B. Polygalacturonases: Many genes in search of a function. *Plant Physiol.* **1998**, *117*, 337–343.
202. Arabidopsis Genome Initiative. Analysis of the genome sequence of the flowering plant *Arabidopsis thaliana*. *Nature* **2000**, *408*, 796–815.
203. González-Carranza, Z.H.; Elliott, K.A.; Roberts, J.A. Expression of polygalacturonases and evidence to support their role during cell separation processes in *Arabidopsis thaliana*. *J. Exp. Bot.* **2007**, *58*, 3719–3730.

204. Kim, J.; Shiu, S.H.; Thoma, S.; Li, W.H.; Patterson, S.E. Patterns of expansion and expression divergence in the plant polygalacturonase gene family. *Genome Biol.* **2007**, *7*, R87.
205. Torki, M.; Mandaron, P.; Mache, R.; Falconet, D. Characterization of a ubiquitous expressed gene family encoding polygalacturonase in *Arabidopsis thaliana*. *Gene* **2000**, *242*, 427–436.
206. Huang, L.; Ye, Y.; Zhang, Y.; Zhang, A.; Liu, T.; Cao, J. BcMF9, a novel polygalacturonase gene, is required for both *Brassica campestris* intine and exine formation. *Ann. Bot.* **2009**, *104*, 1339–1351.
207. Huang, L.; Cao, J.; Zhang, A.; Ye, Y.; Zhang, Y.; Liu, T. The polygalacturonase gene BcMF2 from *Brassica campestris* is associated with intine development. *J. Exp. Bot.* **2009**, *60*, 301–313.
208. Tamari, F.; Shore, J.S. Allelic variation for a short-specific polygalacturonase in *Turnera subulata*: Is it associated with the degree of self-compatibility? *Int. J. Plant Sci.* **2006**, *167*, 125–133.
209. Dearnaley, J.D.W.; Daggard, G.A. Expression of a polygalacturonase enzyme in germinating pollen of *Brassica napus*. *Sex. Plant Reprod.* **2001**, *13*, 265–271.
210. Bosch, M.; Hepler, P.K. Pectin methylesterases and pectin dynamics in pollen tubes. *Plant Cell* **2005**, *17*, 3219–3226.
211. Dey, P.M.; del Campillo, E. Biochemistry of the multiple forms of glycosidases in plants. *Adv. Enzymol. Relat. Areas Mol. Biol.* **1984**, *56*, 141–249.
212. Ahn, Y.O.; Zheng, M.; Bevan, D.R.; Esen, A.; Shiu, S.H.; Benson, J.; Peng, H.P.; Miller, J.T.; Cheng, C.L.; Poulton, J.E.; *et al*. Functional genomic analysis of *Arabidopsis thaliana* glycoside hydrolase family 35. *Phytochemistry* **2007**, *68*, 1510–1520.
213. Tanthanuch, W.; Chantarangsee, M.; Maneesan, J.; Ketudat-Cairns, J. Genomic and expression analysis of glycosyl hydrolase family 35 genes from rice (*Oryza sativa* L.). *BMC Plant Biol.* **2008**, *8*, 84.
214. Singh, M.B.; Knox, R.B. Grass pollen allergens: Antigenic relationships detected using monoclonal antibodies and dot blotting immunoassay. *Int. Arch. Allergy Appl. Immunol.* **1985**, *78*, 300–304.
215. Cheung, A.Y.; Wang, H.; Wu, H.M. A floral transmitting tissue-specific glycoprotein attracts pollen tubes and stimulates their growth. *Cell* **1995**, *82*, 383–393.
216. Wu, H.M.; Wang, H.; Cheung, A.Y. A pollen tube growth stimulatory glycoprotein is deglycosylated by pollen tubes and displays a glycosylation gradient in the flower. *Cell* **1995**, *82*, 395–403.
217. Rogers, H.J.; Maund, S.L.; Johnson, L.H. A β-galactosidase-like gene is expressed during tobacco pollen development. *J. Exp. Bot.* **2001**, *52*, 67–75.
218. Walker, M.; Tehseen, M.; Doblin, M.S.; Pettolino, F.A.; Wilson, S.M.; Bacic, A.; Golz, J.F. The transcriptional regulator LEUNIG_HOMOLOG regulates mucilage release from the *Arabidopsis* testa. *Plant Physiol.* **2011**, *156*, 46–60.
219. Western, T.L.; Burn, J.; Tan, W.L.; Skinner, D.J.; Martin-McCaffrey, L.; Moffatt, B.A.; Haughn, G.W. Isolation and characterization of mutants defective in seed coat mucilage secretory cell development in *Arabidopsis*. *Plant Physiol.* **2001**, *127*, 998–1011.
220. Sampedro, J.; Pardo, B.; Gianzo, C.; Guitian, E.; Revilla, G.; Zarra, I. Lack of alpha-xylosidase activity in *Arabidopsis* alters xyloglucan composition and results in growth defects. *Plant Physiol*. **2010**, *154*, 1105–1115.

221. Lehner, A.; Dardelle, F.; Soret-Morvan, O.; Lerouge, P.; Driouich, A.; Mollet, J.C. Pectins in the cell wall of *Arabidopsis thaliana* pollen tube and pistil. *Plant Signal. Behav*. **2010**, *5*, 1282–1285.
222. Anderson, J.R.; Barnes, W.S.; Bedinger, P. 2,6-Dichlorobenzonitrile, a cellulose biosynthesis inhibitor, affects morphology and structural integrity of petunia and lily pollen tubes *J. Plant Physiol.* **2002**, *159*, 61–67.
223. Whitney, S.E.C.; Wilson, E.; Webster, J.; Bacic, A.; Reid, J.S.G.; Gidley, M.J. Effects of structural variation in xyloglucan polymers on interactions with bacterial cellulose. *Am. J. Bot.* **2006**, *93*, 1402–1414.
224. Pena, M.J.; Ryden, P.; Madson, M.; Smith, A.C.; Carpita, N.C. The galactose residues of xyloglucan are essential to maintain mechanical strength of the primary cell walls in *Arabidopsis* during growth. *Plant Physiol.* **2004**, *134*, 443–451.
225. Nguema-Ona, E.; Andeme-Onzighi, C.; Aboughe-Angone, S.; Bardor, M.; Ishii, T.; Lerouge, P.; Driouich, A. The reb1-1 mutation of *Arabidopsis*: Effect on the structure and localization of galactose-containing cell wall polysaccharides. *Plant Physiol*. **2006**, *140*, 1406–1417.
226. Zabotina, O.A.; van de Ven, W.T.; Freshour, G.; Drakakaki, G.; Cavalier, D.; Mouille, G.; Hahn, M.G.; Keegstra, K.; Raikhel, N.V. *Arabidopsis XXT5* gene encodes a putative alpha-1,6-xylosyltransferase that is involved in xyloglucan biosynthesis. *Plant J.* **2008**, *56*, 101–115.
227. Gille, S.; Pauly, M. *O*-acetylation of plant cell wall polysaccharides. *Front. Plant Sci.* **2012**, *3*, doi:10.3389/fpls.2012.00012.
228. Pena, P.J.; Kong, Y.; York, W.S.; O'Neill, M.A. A galacturonic acid-containing xyloglucan is involved in *Arabidopsis* root hair tip growth. *Plant Cell* **2012**, *24*, 1–14.
229. Wang, T.; Zabotina, O.; Hong, M. Pectin-cellulose interactions in the *Arabidopsis* primary cell wall from two-dimensional magic-angle-spinning solid-state nuclear magnetic resonance. *Biochemistry* **2012**, *51*, 9846–9856.
230. Vogler, H.; Draeger, C.; Weber, A.; Felekis, D.; Eichenberger, C.; Routier-Kierzkowska, A.L.; Boisson-Dernier, A.; Ringli, C.; Nelson, B.J.; Smith, R.S.; *et al*. The pollen tube: A soft shell with a hard core. *Plant J.* **2012**, doi:10.1111/tpj.12061.

Annals of Botany Page 1 of 12
doi:10.1093/aob/mcu093, available online at www.aob.oxfordjournals.org

ANNALS OF BOTANY
Founded 1887

RESEARCH IN CONTEXT: PART OF A SPECIAL ISSUE ON PLANT CELL WALLS

The cell wall pectic polymer rhamnogalacturonan-II is required for proper pollen tube elongation: implications of a putative sialyltransferase-like protein

Marie Dumont[1], Arnaud Lehner[1], Sophie Bouton[2], Marie Christine Kiefer-Meyer[1], Aline Voxeur[1,3], Jérôme Pelloux[2], Patrice Lerouge[1] and Jean-Claude Mollet[1,*]

[1]*Laboratoire de Glycobiologie et Matrice Extracellulaire Végétale (Glyco-MEV) EA4358, Normandy University, University of Rouen, Institut de Recherche et d'Innovation Biomédicale, 76821 Mont-Saint-Aignan, France,* [2]*Laboratoire Biologie des Plantes & Innovation (BIOPI) EA3900, University of Picardie Jules Verne, 80039 Amiens, France and* [3]*Institut Jean-Pierre Bourgin UMR1318 INRA-AgroParisTech, 78026 Versailles Cedex, France*
** For correspondence. E-mail jean-claude.mollet@univ-rouen.fr*

Received: 31 October 2013 Returned for revision: 16 December 2013 Accepted: 1 April 2014

• **Background and Aims** Rhamnogalacturonan-II (RG-II) is one of the pectin motifs found in the cell wall of all land plants. It contains sugars such as 2-keto-3-deoxy-D-*lyxo*-heptulosaric acid (Dha) and 2-keto-3-deoxy-D-*manno*-octulosonic acid (Kdo), and within the wall RG-II is mostly found as a dimer via a borate diester cross-link. To date, little is known regarding the biosynthesis of this motif. Here, after a brief review of our current knowledge on RG-II structure, biosynthesis and function in plants, this study explores the implications of the presence of a Golgi-localized sialyltransferase-like 2 (SIA2) protein that is possibly involved in the transfer of Dha or Kdo in the RG-II of *Arabidopsis thaliana* pollen tubes, a fast-growing cell type used as a model for the study of cell elongation.
• **Methods** Two heterozygous mutant lines of arabidopsis (*sia2-1+/−* and *qrt1* × *sia2-2+/−*) were investigated. *sia2-2+/−* was in a *quartet1* background and the inserted T-DNA contained the reporter gene β-glucuronidase (GUS) under the pollen-specific promoter LAT52. Pollen germination and pollen tube phenotype and growth were analysed both *in vitro* and *in vivo* by microscopy.
• **Key Results** Self-pollination of heterozygous lines produced no homozygous plants in the progeny, which may suggest that the mutation could be lethal. Heterozygous mutants displayed a much lower germination rate overall and exhibited a substantial delay in germination (20 h of delay to reach 30 % of pollen grain germination compared with the wild type). In both lines, mutant pollen grains that were able to produce a tube had tubes that were either bursting, abnormal (swollen or dichotomous branching tip) or much shorter compared with wild-type pollen tubes. *In vivo*, mutant pollen tubes were restricted to the style, whereas the wild-type pollen tubes were detected at the base of the ovary.
• **Conclusions** This study highlights that the mutation in arabidopsis *SIA2* encoding a sialyltransferase-like protein that may transfer Dha or Kdo on the RG-II motif has a dramatic effect on the stability of the pollen tube cell wall.

Key words: Rhamnogalacturonan-II, RG-II, Dha, Kdo, pollen tube, plant cell wall, sialyltransferase-like protein, pectin motif, *Arabidopsis thaliana*.

INTRODUCTION

The pollen tube is a fast tip-growing cell carrying the two sperm cells to the ovule, allowing the double fertilization process and seed setting (Johnson and Lord, 2006; Mollet *et al.*, 2007; Palanivelu and Tsukamoto, 2012). It requires a massive deposition of polymers in the cell wall, including pectins, hemicelluloses and cellulose, to promote the fast pollen tube elongation, and a tight control of cell wall remodelling to modify the mechanical properties (Mollet *et al.*, 2013). As a consequence, the most highly expressed genes in *Arabidopsis thaliana* (arabidopsis) pollen encode enzymes involved in cell wall remodelling (Pina *et al.*, 2005). This research in context focuses on our current knowledge of the role of rhamnogalacturonan-II (RG-II), one of the cell wall pectic polymers with homogalacturonan (HG) and rhamnogalacturonan-I (RG-I), in pollen tube growth. Moreover, new results regarding the characterization of mutant lines impaired in a sialyltransferase-like protein that is possibly involved in RG-II synthesis are presented.

Rhamnogalacturonan-II is a highly complex polysaccharide representing between 1 and 4 % of the pectin-rich primary cell wall of eudicots (O'Neill *et al.*, 2004). RG-II was primarily characterized from the sycamore cell wall in the late 1970s (Darvill *et al.*, 1978). Since then, RG-II has also been isolated from the cell walls of gymnosperms (Edashige and Ishii, 1998; Shimokawa *et al.*, 1999), lycopodiophytes and pteridophytes (Matsunaga *et al.*, 2004). To date, RG-II has been identified in all vascular plants, with a highly conserved glycosyl sequence. This low molecular weight polysaccharide (5–10 kDa) solubilizes when subjected to an *endo*-polygalacturonase treatment, and contains 13 different glycosyl residues linked together by >20 different linkages, requiring 22 specific glycosyltransferases (GTs) (Bar-Peled *et al.*, 2012). RG-II has an HG backbone made up of seven to nine α-(1,4)-D-galacturonic acid (GalA) residues that is substituted with different side chains (A–E) (Whitcombe *et al.*, 1995; Pérez *et al.*, 2003). Chain E is made of only one arabinosyl residue and is not always considered as a side chain. Therefore, it is usually considered that RG-II is

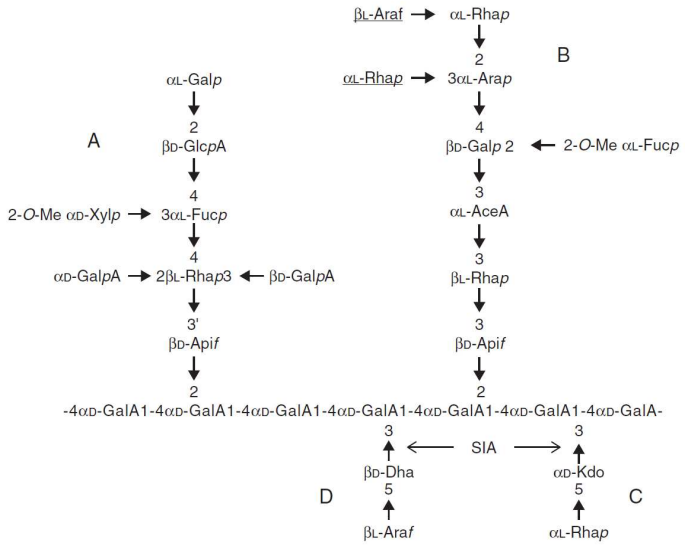

FIG. 1. Structure of RG-II. The sugars underlined are absent in arabidopsis RG-II. Arrows indicate the glycosyl linkages that are postulated to result from the action of sialyltransferase-like SIA1 (At1g08660) and SIA2 (At3g48820) proteins.

decorated with only four oligosaccharide side chains (Fig. 1; O'Neill *et al.*, 2004; Bar-Peled *et al.*, 2012). The A and B side chains are composed of octa- and hepta- to nonasaccharide, respectively, whereas chains C and D are disaccharides. The glycosyl sequences of these oligosaccharide chains are conserved among vascular plant species, except for the lycophytes and several pterydophytes that show some degrees of variability on the terminal extension of the B side chain (Matsunaga *et al.*, 2004). Nevertheless, RG-II's originality resides in the presence of sugars such as D-apiose (Api), L-aceric acid (3-*C*-carboxy-5-deoxy-L-xylose; AceA), 2-*O*-methyl L-fucose (2-*O*-Me-Fuc), 2-*O*-methyl D-xylose (2-*O*-Me-Xyl), L-galactose (L-Gal), 2-keto-3-deoxy-D-*lyxo*-heptulosaric acid (Dha) and 2-keto-3-deoxy-D-*manno*-octulosonic acid (Kdo). Until recently, RG-II's structure within a given plant species was considered to be unique and no modulation of the RG-II composition was thought to occur. Recently, Pabst *et al.* (2013) reported variations of the RG-II structure within a single individual plant concerning either the length of chain B or the monosaccharide substitution and methylation of uronic acids in chain A. However, the biological significance of structural variations of the RG-II side chains is not known.

Even if very little is known about its biosynthesis, RG-II is believed to be synthesized in the Golgi apparatus (Mohnen, 2008). Because of its structural complexity, the synthesis requires a large number of different activated sugars, many specific GTs and also additional enzymes required for methylation and acetylation of the side chain residues (Bar-Peled *et al.*, 2012). So far, only one GT has been fully characterized. This enzyme, named RGXT (rhamnogalacturonan-specific xylosyltransferase), is involved in the synthesis of the A side chain of RG-II by transferring an α-(1,3)-D-xylose on the internal L-fucose (Egelund *et al.*, 2006, 2008). Recently, a bioinformatic study has listed an additional 26 putative GTs including ten sequences belonging to the GT4, 8, 29, 31, 68 and 92 CAZy families and 16 non-CAZy GTs (Voxeur *et al.*, 2012).

Boron is an essential micronutrient, and plant boron deficiency has been known for a long time to be responsible for many anatomical, physiological and biochemical defects (Blevins and Lukaszewski, 1998). The first definitive evidence of boron requirement for the growth of higher plants was described by Warrington (1923) in legumes. To date, in agriculture, to avoid boron deficiency, calcium or sodium borate, also called borax, is commonly applied directly to the soil to promote plant growth or sprayed at the flowering stage to improve fruit and seed set or reduce fruit drop (Ganie *et al.*, 2013). To date, the exact functions of boron in plant development have not been clearly determined (Goldbach and Wimmer, 2007), but structural studies have shown that the cell wall is a sink for boron and that it is involved in RG-II dimerization (O'Neill *et al.*, 1996, 2004). *In planta*, at least 90 % of RG-II exists as a dimer that is cross-linked by a borate di-ester bond between two apiosyl residues of the A side chain. This dimer was shown to be present in angiosperms, gymnosperms, lycophytes and pteridophytes (Ishii and Matsunaga, 1996; O'Neill *et al.*, 1996; Kaneko *et al.*, 1997; Shimokawa *et al.*, 1999; Vidal *et al.*, 2001; Matsunaga *et al.*, 2004). This dimer of RG-II is thought to play a crucial role in cell wall integrity by strengthening the pectic network, and defects in boron dimerization result in notable growth alterations (Noguchi *et al.*, 1997; O'Neill *et al.*, 2001; Voxeur *et al.*, 2011).

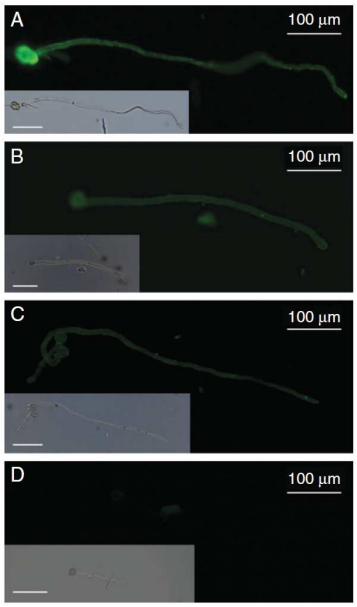

FIG. 2. Immunolocalization of RG-II in the cell wall of pollen tubes using the anti-RG-II antibody described by Matoh *et al.* (1998). (A) *Arabidopsis thaliana* Col-0, (B) *Nicotiana benthamiana* and (C) *Solanum lycopersicum* var. *cerasiforme* WVA 106. (D) Negative control of *A. thaliana* pollen tubes. Inserts are the bright field images of the same pollen tubes. Scale bars = 100 µm.

The pollen tube wall is mainly composed of cellulose, hemicellulose, callose and pectins together with HG and RG-I (Dardelle *et al.*, 2010; Lehner *et al.*, 2010; Chebli *et al.*, 2012), but very little information has been reported concerning RG-II. RG-II has been localized in the cell wall of *Lilium longiflorum* pollen tubes using a polyclonal antibody directed against both the borate–RG-II complex and monomeric RG-II (Matoh *et al.*, 1998). Using this antibody, we also observed staining along the cell walls of *Arabidopsis thaliana*, *Solanum lycopersicum* var. *cerasiforme* WVA 106 (tomato) and *Nicotiana benthamiana* (tobacco) pollen tubes and pollen grains (Fig. 2), suggesting that RG-II is a common structural feature of pollen tube cell walls. Moreover, this is supported by biochemical analysis. The monosaccharide composition of a hot water extract isolated from *in vitro* grown arabidopsis pollen tubes revealed the main sugars found in pectins (rhamnose, arabinose, galactose and GalA) as previously described by Dardelle *et al.* (2010). In addition, xylose, probably originating from xyloglucan, and glucose, probably arising from xyloglucan, callose and/or starch of pollen tubes (Fig. 3A), were also present. Gas chromatography coupled to electron impact mass spectrometry (GC-EIMS) has allowed the detection of specific RG-II monosaccharides. Traces of methylated sugars were detected in minor peaks eluting before the arabinose residue. Furthermore, Kdo was detected (Fig. 3A) and its structure was confirmed by analysing its electron impact (EI) mass spectrum (Fig. 3B, C) (Doco *et al.*, 2001). The results indicate that RG-II is undoubtedly present in pollen tube cell walls of *A. thaliana* and other species, although in a low amount.

Even though the RG-II structure and dimerization within the wall have not been investigated in pollen tubes, we postulate that boron-induced RG-II cross-linking is crucial for pollen tube germination and/or elongation. Pollen of most plant species requires boron to germinate both *in vivo* and *in vitro* (Table 1; García-Hernández and López, 2005) and boron is essential to control the mechanical properties of the cell wall and the oscillatory pulses during pollen tube elongation (Holdaway-Clarke *et al.*, 2003). Wang *et al.* (2003) have shown that the culture of *Picea meyeri* pollen in a boron-deficient medium affected pollen germination and resulted in the abnormal accumulation of callose and acidic pectin in the tip region of pollen tubes compared with pollen tubes grown in optimum conditions. Moreover, Li *et al.* (2011) have characterized an anther-specific boric acid transporter of the aquaporin superfamily regulating the transport of this critical nutrient to the male gametophyte. However, too high concentrations of boron reduce pollen germination, slightly increase the rate of burst pollen tubes and decrease the final fruit set (Potts and Marsden-Smedley, 1989; Wang *et al.*, 2003; Lee *et al.*, 2009). As a consequence, the boron concentration is critical *in planta* and *in vitro* for optimal pollen germination. According to the basal Brewbaker and Kwack (1963) pollen germination medium, the boric acid concentration routinely used for *in vitro* germination assays of many species including arabidopsis, tobacco and tomato is 0·01 % (Table 1). Other species such as maize or rice required the supply of much less boron to promote pollen germination.

Further evidence of the importance of the borate–RG-II complex in pollen tube development was deduced from the analysis of arabidopsis mutants. Alteration of the expression of genes involved in RG-II biosynthesis was reported to impair male fertility (Delmas *et al.*, 2008; Deng *et al.*, 2010; Kobayashi *et al.*, 2011; Liu *et al.*, 2011) and consequently no homozygous lines can be obtained. Two mutants affected in genes encoding the Kdo-8-P synthase (*AtkdsA1* and *AtkdsA2*) have been characterized (Delmas *et al.*, 2008). These mutants affected in the synthesis of this cytosolic monosaccharide are probably impaired in RG-II because Kdo is exclusively present in this pectic polymer (Fig. 1). A single mutation in the *KDSA1* or *KDSA2* gene did not display any phenotype, but the generation of a double knockout mutant *AtkdsA1/AtkdsA2* failed. In order to test whether this was due to a gametophytic or sporophytic defect, the authors generated *AtkdsA* mutants in the *quartet* (*qrt*) mutant background. Analysis of pollen tetrads revealed that a maximum of two out of the four pollen grains from the *quartet 1-2* × *AtkdsA1*−/− *AtkdsA2*+/− were able to germinate and form a proper pollen tube. These results showed that the absence of Kdo biosynthesis in arabidopsis pollen impairs pollen tube growth.

To date, the α-(1,3)-xylosyltransferase RGXT is the only reported GT that has been demonstrated to be involved in RG-II biosynthesis. This type II enzyme belongs to the CAZy GT77 family and is involved in the synthesis of chain A by transferring an α-D-xylose residue on the internal α-L-fucose (Egelund *et al.*, 2006). Four isoforms, RGXT1–RGXT4, are expressed in arabidopsis. The biological function of the last one (RGXT4) was investigated in arabidopsis. The mutant line

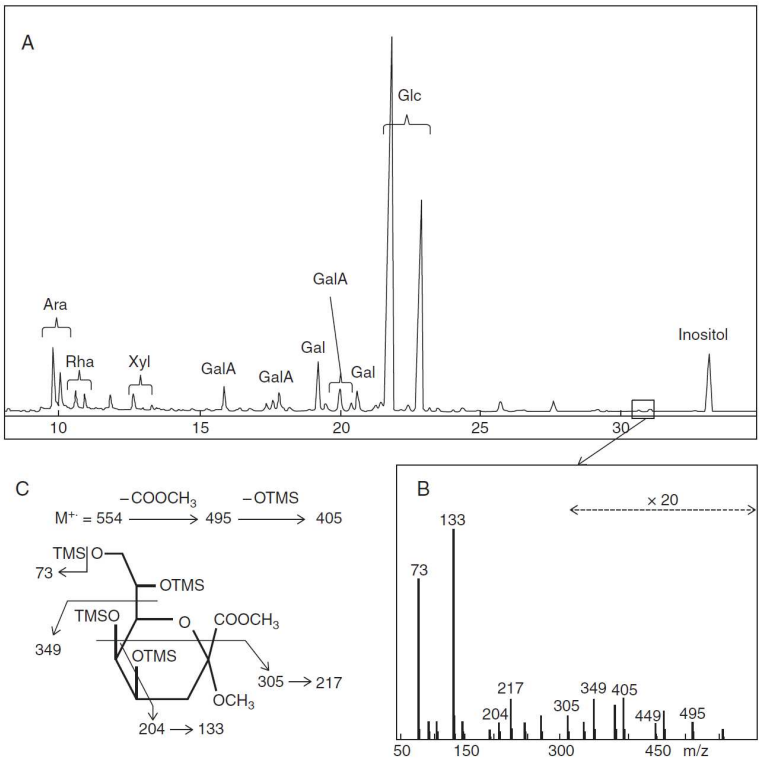

FIG. 3. Identification of Kdo in a hot water extract from 6-hour-old arabidopsis pollen tubes. (A) Gas chromatogram of trimethylsilyl (TMS) derivatives of the methyl glycosides, (B) electron impact mass spectrum (EIMS) of the minor peaks boxed in the chromatogram and (C) assignment of EIMS fragmentation ions showing that the minor peaks are Kdo derivatives. Ara, arabinose; Gal, galactose; GalA, galacturonic acid; Glc, glucose; Rha, rhamnose; Xyl, xylose.

TABLE 1. *Examples of species that required boron for optimum* in vitro *pollen germination and pollen tube growth*

Plant species	H_3BO_3 (%)	Reference
Areca catechu	0·04–0·06	Liu *et al.* (2013)
Cajanus cajan	0·025	Jayaprakash and Sarla (2001)
Cucumis sativus	0·025	Vižintin and Bohanec (2004)
Arabidopsis thaliana	0·01	Boavida and McCormick (2007)
Solanum lycopersicum	0·01	Covey *et al.* (2010)
Solanum chacoense	0·01	Parre and Geitmann (2005*b*)
Nicotiana tabacum	0·01	Persia *et al.* (2008)
Gossypium hirsutum	0·01	Kakani *et al.* (2005)
Triticum aestivum	0·01	Cheng *et al.* (1992)
Lilium longiflorum	0·01	Rounds *et al.* (2011)
Pinus sylvestris	0·01	Fang *et al.* (2008)
Pinus bungeana	0·01	Wang *et al.* (2003)
Picea meyeri	0·01	McKenna *et al.* (2009)
Luffa aegyptica	0·005	Prajapati and Jain (2010)
Zea mays	0·005	Schreiber and Dresselhaus (2003)
Oryza sativa	0·004	Dai *et al.* (2006)
Pisum sativum	0·002	McGee and Baggett (1992)
Brassica oleracea	0·001	Roberts *et al.* (1983)

was called *mgp4* for *male gametophyte defective4* because of the severe defect observed in pollen tube growth (Liu *et al.*, 2011). Genetic analyses indicated that *mgp4* completely suppressed the genetic transmission of the male gametophyte without affecting the female function. Pollen grain formation was not affected in the mutant, but *in vitro* germination revealed short or burst pollen tubes by comparison with the wild type. Homozygous *mgp4*−/− plants were generated by introducing into the heterozygous line the full-length cDNA of *MGP4* under the control of a pollen-specific promoter. The seedlings harvested from the pollen-rescued *mgp4* homozygous plants exhibited severe defects in root growth and swollen root cells. These growth defects were partially suppressed by supplying the plants with exogenous boric acid. Restoration of wild-type phenotypes in RG-II mutants by supplementation with borate was previously reported and supports the crucial role of borate-induced RG-II dimerization in plant cell wall elongation (O'Neill *et al.*, 2001; Voxeur *et al.*, 2011). Together with the study of Kdo mutants, this work on RGXT transferase demonstrated that RG-II biosynthesis is crucial for proper pollen tube growth.

Two sialyltransferase-like sequences that belong to the GT29 family were selected in a bioinformatic screening recently reported by Voxeur and co-workers (2012). These two proteins encoded by At1g08660 and At3g48820 contain the four conserved sialyl motifs (Audry *et al.*, 2011) of mammalian sialyltransferases and are located in the Golgi apparatus (Dunkley *et al.*, 2006; Daskalova *et al.*, 2009). While At1g08660 is found in the Affimetrix ATH1 microarray chips, At3g48820 is not, but is present in the Complete Arabidopsis Transcriptome Microarray (CATMA, http://www.catma.org/). Moreover, RNA-seq analyses have detected RNA fragments from At3g48820 in arabidopsis pollen, although not with an extensive coverage (Loraine *et al.*, 2013). Sialic acid is a nine-carbon acidic sugar that is involved in a large variety of structural and biological roles in mammalian cells. This monosaccharide has not been detected in plants (Séveno *et al.*, 2004). However, sialic acid, Kdo and Dha share common features; for example, they result from the condensation in the cytosol of phosphoenol pyruvate to a monosaccharide phosphate, and GTs of the GT29 family use CMP-activated nucleotide sugars as substrates. As a consequence, we have previously proposed that these two plant sialyltransferase-like GTs may be involved in the transfer of Kdo and/or Dha on the HG backbone of RG-II (Fig. 1) (Voxeur *et al.*, 2012). Deng *et al.* (2010) have investigated one of these two putative sialyltransferase-like proteins encoded by At1g08660 in pollen tube growth. The isolated heterozygous *mgp2* (*male gametophyte defective2*) mutant had a loss of male gametophytic function without affecting the female gametophyte. While *mgp2* pollen grains did not show any morphological abnormality, *in vivo* analysis revealed that *mgp2* pollen tubes were restricted to the stigmatic tissues and were not able to reach and fertilize the ovules in comparison with the wild-type pollen tubes. Moreover, introduction of the *MGP2* genomic fragment into *mgp2*+/− plants could restore the genetic transmission of the *mgp2* mutation through the male gametophyte.

Herein, we report on the effect of inactivation of the At3g48820 gene, predicted to encode the second sialyltransferase-like protein, on pollen tube development. We hypothesized that, as postulated for its homologue At1g08660, At3g48820 may be involved in the transfer of Kdo and/or Dha on the HG backbone of RG-II and that this protein is important for efficient pollen grain germination and pollen tube elongation in arabidopsis. For a better understanding, the two sialyltransferase-like proteins were named SIA1 (sialyltransferase-like 1, MGP2, At1g08660) and SIA2 (sialyltransferase-like 2, At3g48820).

MATERIALS AND METHODS

Plant material and growth conditions

The *Arabidopsis thaliana* plant lines were from the Columbia (Col) ecotype. The T-DNA At3g48820 insertion lines SALK_059690 and SAIL_259_H07, named *sia2-1* and *qrt1* × *sia2-2* respectively, were obtained from the Nottingham Arabidopsis Stock Centre. The *sia2-2* (SAIL_259_H07) mutant line has a *quartet1* (*qrt1*, At5g55590) background and the T-DNA vector pCSA110 encodes a β-glucuronidase (GUS) reporter gene under the control of the post-meiotic pollen-specific LAT52 promoter. The *qrt1* line expressing LAT52::GUS was from Mark Johnson's lab (Brown University, USA). Wild-type and mutant seeds were spread on the surface of sterile soil and cultured in a growth chamber with a photoperiod of 16 h light/8 h dark cycle at 20 °C during the light phase and 16 °C in the dark phase, with 60 % relative humidity.

For comparison of RG-II distribution in pollen tubes, *Nicotiana benthamiana* and *Solanum lycopersicum* var. *cerasiforme* WVA 106 were grown in soil with a photoperiod of 16 h light/8 h dark cycle at 25 °C and 22 °C during the light and dark phase, respectively. Relative humidity was maintained at 60 % and plants were watered every 2 d.

Genetic analysis of sia2-1+/− *and* qrt1 × sia2-2+/− *mutants*

Genotypes of the *sia2-1*+/− arabidopsis plants were confirmed by PCR using the combination of the gene-specific primers (P1, 5′-GCAAATGGTTTGGGACTACAA-3′; and P2, 5′-TGTTTCAGGAAGCACCAATG-3′) and a T-DNA-pecific primer (LBb1·3: 5′-ATTTTGCCGATTTCGGAAC-3′). Similarly, the genotypes of the *qrt1* × *sia2-2*+/− plants were identified with gene-specific primers (P3, 5′-CGCAGCGTTTTATAAAGTGAAA-3′; and P4, 5′-ACAAGCATGGGACAATGATG-3′) and a T-DNA-specific primer (LB2: 5′-GCTTCCTATTATATCTTCCCAAATTACCAATACA-3′).

Pollen tube growth conditions

Arabidopsis pollen germination was performed in liquid medium [5 mM $CaCl_2$, 0·01 % H_3BO_3, 1 mM $MgSO_4$, 5 mM KCl, 10 % (w/v) sucrose, pH 7·5] as described by Boavida and McCormick (2007). *Nicotiana benthamiana* and *S. lycopersicum* var. *cerasiforme* WVA 106 pollen grains were grown in BK medium [1·62 mM H_3BO_3, 1·25 mM $Ca(NO_3)_2{\cdot}4H_2O$, 2·97 mM KNO_3 and 1·65 mM $MgSO_4{\cdot}7H_2O$, pH 7] (Brewbaker and Kwack, 1963) containing 10 % (w/v) sucrose at 22 °C in the dark for 6 h under agitation.

In vitro *phenotypic characterization of pollen tubes*

The *sia2-1*+/− germinating pollen grains were scored after 4, 6, 8 and 24 h of incubation at 22 °C. A pollen grain was considered germinated if the pollen tube length was greater than the pollen grain diameter. To discriminate the *sia2-2*+/− pollen grains from wild-type pollen grains within the tetrads by GUS staining, the germinated pollen grains from *qrt1* × *sia2-2*+/− plants were fixed for 15 min in 80 % acetone and washed twice with GUS buffer (2 mM potassium ferrocyanide, 2 mM potassium ferricyanide, 50 mM $NaPO_4$ pH 7, 0·2 % Triton X-100). Pollen grains were incubated at 37 °C overnight in GUS staining solution [1 mM 5-bromo-4-chloro-3-indolyl-β-D-glucuronic acid (X-Gluc)] and observed.

In vivo *phenotypic characterization of pollen tubes*

To investigate the growth of pollen tubes *in vivo*, a double staining was performed on self-pollinated flowers. Flowers were fixed in 80 % acetone for 30 min, washed twice with GUS buffer and incubated overnight at 37 °C in GUS staining solution. Samples were rinsed several times with 70 % ethanol (EtOH) at room temperature and successively treated with 50 and 30 % EtOH and distilled water. The flowers were deposited on a glass slide and treated with 8 m NaOH overnight at room temperature in a wet chamber.

After careful washing in distilled water, the flowers were incubated in decolorized aniline blue solution (Johnson-Brousseau and McCormick, 2004) for at least 2 h in the dark.

Immunolabelling of pollen tubes

Pollen tubes were fixed and immunolabelled as described by Dardelle *et al.* (2010) Briefly, pollen tubes were mixed (v/v) with a fixation solution containing 100 mM PIPES buffer pH 6·9, 4 mM $MgSO_4 \cdot 7H_2O$, 4 mM EGTA, 10 % (w/v) sucrose and 5 % (v/v) formaldehyde, and incubated for 1 h at room temperature. Pollen tubes were rinsed three times by centrifugation (1 min, 3000 g) with CMF-DPBS (calcium- and magnesium-free Dulbecco's phosphate-buffered saline: 137 mM NaCl, 2·7 mM KCl, 7 mM $Na_2HPO_4 \cdot 7H_2O$, 1·5 mM KH_2PO_4). A saturation step was carried out for 30 min in CMF-DPBS supplemented with 3 % fat-free milk. After three washes, pollen tubes were incubated overnight at 4 °C in the dark in the anti-RG-II antibody (Matoh *et al.*, 1998) diluted 1:20 with CMF-DPBS. Pollen tubes were rinsed with the buffer and incubated for 2 h at 30 °C with a goat secondary antibody anti-rabbit IgG (whole molecule) combined with fluorescein isothiocyanate (FITC; Sigma) diluted 1:50. Controls were carried out by incubation of the pollen tubes without the primary antibody.

Microscope observation and image acquisition

Pollen grains, pollen tubes or pistils were observed under bright field using an inverted Leica DMI6000B microscope or an upright Leica DLMB microscope equipped with a Leica DFC300FX camera. For immunolocalization of RG-II epitopes, pollen tubes were observed under fluorescence with an FITC filter (absorption, 485–520 nm; emission, 520–560 nm). The UV illumination was used to detect the aniline blue-stained pollen tubes. Pollen grain germination and pollen tube length were measured from the images using the ImageJ program (Abramoff *et al.*, 2004). Images were assembled using the program GIMP (GNU Image Manipulation Program; http://www.gimp.org/).

Sugar composition of a hot water extract from arabidopsis pollen tubes

Six-hour-old pollen tubes from 3800 arabidopsis flowers were pooled after addition of 3 vols of 95 % EtOH to the germination medium. The EtOH-insoluble residue was then prepared as previously reported (Dardelle *et al.*, 2010) and pectins were then extracted in boiling water. The monosaccharide composition of the pectin-enriched extract was determined by gas chromatography coupled to an electron impact mass spectrometer (GC-EIMS). The extract was first hydrolysed with 2 m trifluoroacetic acid (TFA) for 2 h at 110 °C and then submitted to a methanolysis for 16 h at 80 °C with 500 µL of dried 1 m methanolic-HCl (Supelco). After evaporation of the methanol, the methyl glycosides were converted into their trimethylsilyl (TMS) derivatives at 110 °C for 20 min with 200 µL of the silylation reagent (HMDS:TMCS:pyridine, 3:1:9, Supelco). Monosaccharides were then separated by GC (HP6890 series) on a Zebron Z5-MSi capillary column (length 30 m, i.d. 0·25 mm) (Macherey-Nagel) and analysed by EIMS using an Autospec GC-MS (Micromass, Manchester, UK) equipped with an Opus 3·1 data system.

RT-qPCR analysis

Total RNA was extracted from inflorescences of 6-week-old wild-type, *quartet1*, *sia2-1+/–* and *qrt1* × *sia2-2+/–* plants using the NucleoSpin® RNA Plant kit (Macherey-Nagel) as described by the supplier. After RNA quantification using NanoDrop spectrophotometry, and a DNase treatment, 400 ng of RNA were converted into single cDNAs with a QuantiTect Reverse Transcription Kit (Qiagen, Valencia, CA, USA) following the instructions of the supplier. Real-time quantitative PCR (RT-qPCR) analyses were performed on 1/2 diluted cDNA. For RT-qPCR, the LightCycler® 480 SYBR Green I Master (Roche, Cat. No. 04887352001) was used in 384-well plates in the LightCycler® 480 Real-Time PCR System (Roche). The CT values for each sample (crossing threshold values are the number of PCR cycles required for the accumulated fluorescence signal to cross a threshold above the background) were acquired with the LightCycler 480 software (Roche) using the second derivative maximum method. Primers used are shown in Supplementary Data Table S1. Stably expressed reference genes (At3g28750, At3g57690 and At5g59370), selected using GeNorm software (Vandesompele *et al.*, 2002), were used as internal controls to calculate the relative expression of target genes, according to the method described in Gutierrez *et al.* (2009). Each amplicon was first sequenced to ensure the specificity of the amplified sequence.

Statistical analysis

The data were analysed statistically by Student's *t*-test (GraphPad Software, La Jolla, CA, USA; www.graphpad.com).

RESULTS

Phenotypic characterization of the sia2-1 *mutant*

sia2-1 (SALK_059690) is a T-DNA insertion mutant in the At3g48820 gene. The T-DNA insertion is located in the fourth intron, 809 bp downstream of the start codon (Fig. 4A). PCR analyses of the progeny from the self-pollinated heterozygous *sia2-1+/–* plants showed a 1:1 segregation ratio between the heterozygous *sia2-1+/–* (308/609 plants, 50·6 %) and the wild-type (301/609, 49·4 %) plants. Of the 609 plants analysed in the progeny, no homozygous *sia2-1–/–* plant was identified, which may suggest that the mutation is lethal. However, we cannot rule out that the number of screened plants may not be enough to obtain homozygous lines. On the other hand, the heterozygous plants did not show any obvious visible phenotype compared with wild-type plants. The RT-qPCR analysis revealed that the expression level of *SIA2* in the inflorescences of *sia2-1+/–* plants was reduced by about 70 % in comparison with Col-0 plants (Fig. 4B). Similar results were reported for *SIA1* in the *mgp2–1* mutant (Deng *et al.*, 2010).

In order to investigate how the mutation in At3g48820 was affecting male gametophyte function, we compared the pollen tube phenotypes of the heterozygous *sia2-1+/–* plants (which contain a population of 50 % mutant and 50 % wild-type pollen grains) with those of wild-type plants. In *in vitro* conditions, 64 % of *sia2-1+/–* pollen tubes had burst (Fig. 4C, E) and 6 % were short or had an abnormal shape (swollen or dichotomous branching tip) (Fig. 4C, E, F). In contrast, 70 % of pollen tubes from wild-type plants were normal (Fig. 4C, D), 27 % had

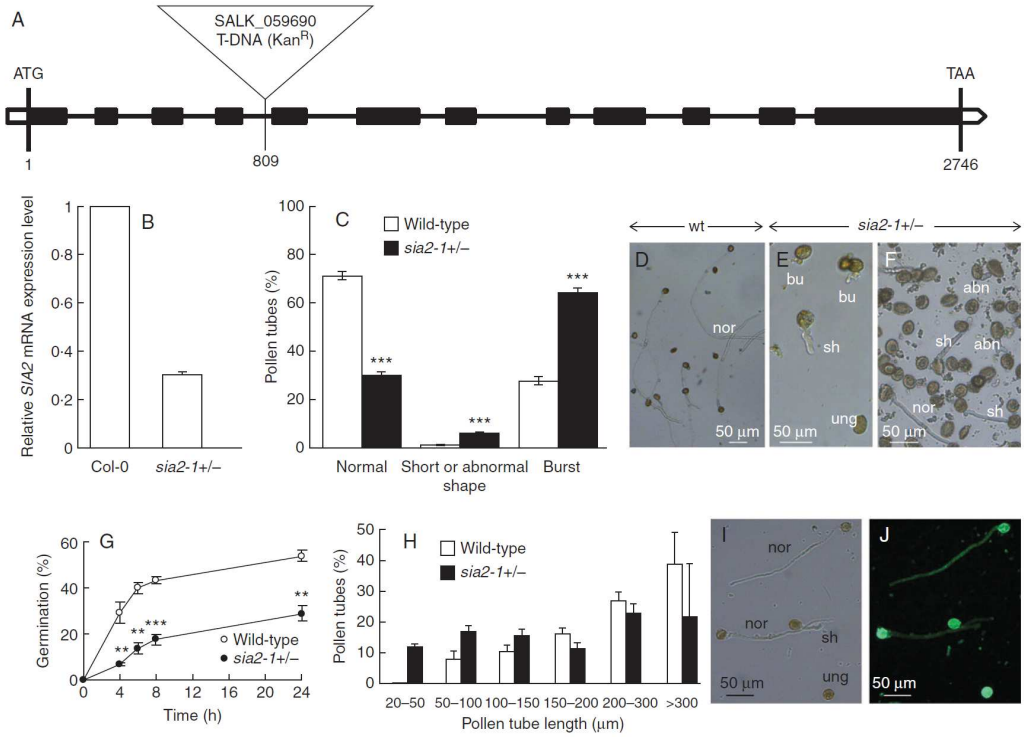

FIG. 4. Characterization of the *sia2-1* mutant. (A) Genomic organization of the *SIA2–1* gene and location of the T-DNA insertion site. The black boxes indicate the exons. (B) Relative expression levels of *SIA2* in Col-0 and *sia2-1+/–* quantified in inflorescences using three references genes (At3g28750, At3g57690 and At5g59370). Similar variations were observed with the three references genes and the three biological replicates. Only the results obtained with At3g28750 are shown using the *SIA2–1*-flanking primer pair. (C) *In vitro* germination of pollen grains from *sia2-1+/–* and wild-type plants (see key) showing the percentage of normal and abnormal pollen tubes ($n > 2000$) after 6 h of culture. (D) *In vitro* culture of wild-type pollen tubes. Pollen grains were cultured for 6 h at 22 °C. (E, F) *In vitro* culture of 6-hour-old *sia2-1+/–* pollen tubes showing ungerminated pollen grains (ung), normal (nor), short (sh), burst (bu) and abnormal (abn) pollen tubes. (G) Time course of pollen germination from *sia2-1+/–* and wild-type plants ($n > 3000$). (H) Comparison of *sia2-1+/–* and wild-type pollen tube length after 6 h of culture ($n > 300$). (I, J) Bright field (I) and epifluorescent (J) images of *sia2-1+/–* pollen tubes labelled with the anti-RG-II antibody. $^{**}P < 0{\cdot}01$; $^{***}P < 0{\cdot}001$.

burst and 1 % displayed short or abnormal tubes. Time course analyses over a 24 h period revealed an important delay in germination of pollen grains from *sia2-1+/–* plants (Fig. 4G). After 6 h of growth, 12 % of the *sia2-1+/–* pollen grains were germinated compared with 43 % of the wild-type pollen grains. With the same culture period, only 20 % of the *sia2-1+/–* pollen tubes reached 300 µm compared with 38 % for the wild-type pollen tubes (Fig. 4H), and 3 0 % of the *sia2-1+/–* pollen tubes were <100 µm in length. For wild-type pollen tubes, only 8 % were <100 µm in length. These data suggest that the differences observed between wild-type and *sia2-1+/–* pollen may be due to the disruption of *SIA2* expression in the mutant pollen grains. Immunolabelling of pollen tubes from the *sia2-1+/–* plants with the RG-II-specific antibody showed no visible difference between the short and normal pollen tubes (Fig. 4I, J), which may suggest that the epitopes recognized by the antibody are still synthesized and incorporated in the cell wall. However, we cannot rule out that the short pollen tubes were wild type. To assess the function of *SIA2* more precisely, another mutant, *sia2-2+/–* in the *qrt1* background with a GUS reporter gene, was studied which allowed the discrimination between wild-type and mutant pollen grains within a tetrad.

Phenotypic characterization of in vitro *grown* qrt1 × sia2-2 *pollen*

The *sia2-2* mutant (SAIL_259_H07) has a T-DNA insertion in the first intron (53 bp downstream of the start codon) in the arabidopis *qrt* background (Fig. 5A). Surprisingly, in contrast to data obtained in *sia2-1+/–*, overexpression of *SIA2* in the inflorescences of *qrt1* × *sia2-2+/–* plants compared with the *qrt1* plants was observed by RT-qPCR. This could be due to the pCSA110 vector used to generate the SAIL lines, which contains

a 1′2′ bidirectional promoter at the left border of the T-DNA leading to overexpression or antisense RNA production (Ülker *et al.*, 2008). Moreover, insertion near the transcription start site, as in *qrt1* × *sia2*-2+/−, can create alternative transcripts (Missihoun *et al.*, 2012) which have a lower stability and undergo a post-transcriptional degradation that prevents their translation into protein. It is noteworthy that, as described by Wang (2008), the transcript level may not be correlated with the protein level.

At the mature stage, the *qrt1* mutant releases tetrads as the microspores fail to separate during pollen development (Rhee and Somerville, 1998) without affecting pollen tube growth considerably (Boavida and McCormick, 2007). As the T-DNA contains a GUS reporter gene under the pollen LAT-52 promoter,

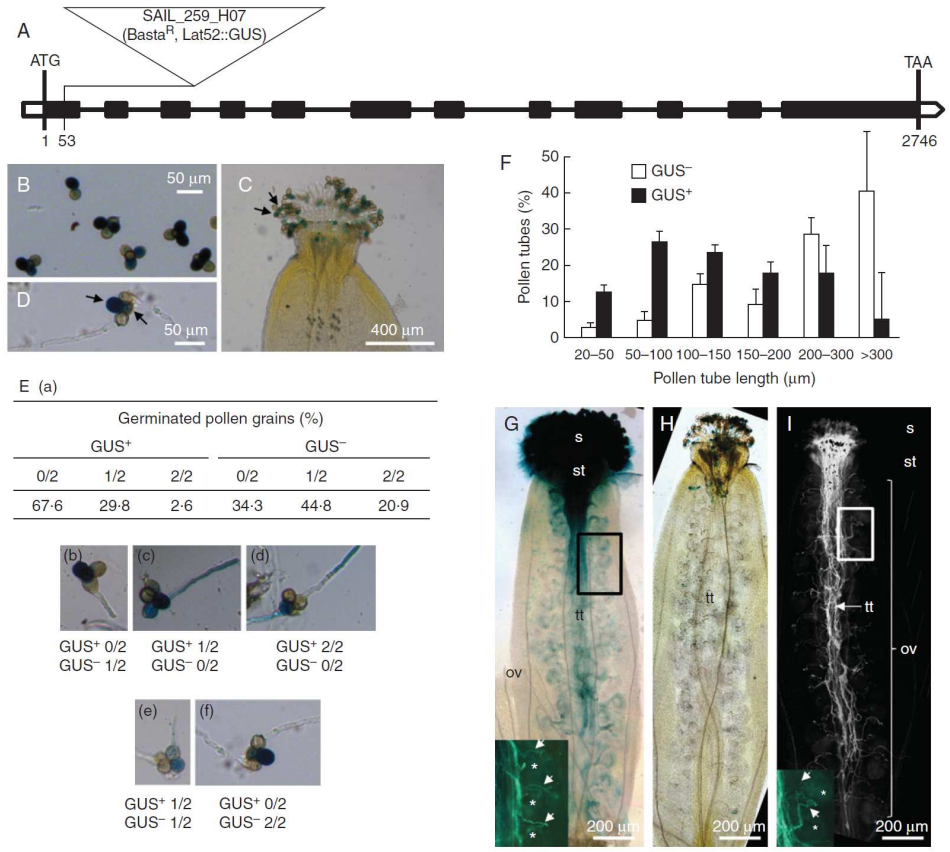

FIG. 5. Characterization of the *qrt1* × *sia2-2* mutant. (A) Genomic organization of the *SIA2–2* gene and location of the T-DNA insertion site. The black boxes indicate the exons. (B) GUS staining of the *qrt1* × *sia2*-2+/− tetrads showing two GUS$^+$ and two GUS$^-$ pollen grains. (C) GUS staining of the *qrt1* × *sia2*-2+/− pollen grains on the stigma. Arrows show the two GUS$^+$ pollen grains in the tetrad. (D) GUS staining of the *qrt1* × *sia2*-2+/− pollen grains and pollen tubes grown for 6 h. Arrows show the two GUS$^+$ pollen grains. (E) Percentages of GUS$^+$ and GUS$^-$ germinated pollen grains in *qrt1* × *sia2*-2+/− tetrads (n >800 grains). (a) Table summarizing the percentages of pollen tubes growing from the two GUS$^+$ and the two GUS$^-$ pollen grains of the tetrads. (b–f) Images representing the different cases summarized in the table (a). (F) Distribution of the pollen tube length between the GUS$^+$ and GUS$^-$ in *qrt1* × *sia2*-2+/− tetrads after 6 h of culture (n >200). (G) GUS staining of a self-pollinated *qrt1* plant showing pollen grains on the stigma and the *in vivo* growth of pollen tubes in the transmitting tract. Pollen tubes have reached the base of the ovary. The close-up picture at the bottom left shows the aniline blue staining of the same pistil. Arrows indicate pollen tubes, and asterisks indicate ovules. (H, I) GUS (H) and aniline blue (I) staining of a self-pollinated *qrt1* × *sia2*-2+/− plant showing GUS$^+$ and GUS$^-$ pollen grains on the stigma (H). No GUS$^+$ pollen tubes were visible in the transmitting tract (H) but GUS$^-$ pollen tubes were stained with aniline blue and able to produce pollen tubes that reached the base of the ovary (I). The close-up image at the bottom left in (I) shows pollen tubes (arrows) and ovules (asterisks). ov, ovary; s, stigma; st, style; tt, transmitting tract.

mutant pollen can be discriminated from the wild-type pollen within a single tetrad after GUS staining (Fig. 5B, C). This allows the unambiguous *in vitro* and *in vivo* phenotypic study of the *qrt1* × *sia2-2+/−* mutant pollen tubes (Fig. 5D). About 67 % of the GUS^+ pollen failed to germinate (Fig. 5Ea, b, f) whereas only 2·6 % of the tetrads produced two GUS^+ pollen tubes (Fig. 5Ea, d). Of the two GUS^- pollen grains (wild type) in the tetrads, 65·7 % had produced one or two tubes (Fig. 5Ea, b, e, f). When the GUS^+ pollen grains had produced a pollen tube, the tubes were much shorter than the GUS^- pollen tubes (Fig. 5F). Approximately 50 % of the GUS^+ pollen tubes were 50–150 μm long after 6 h of growth whereas 40 % of the wild-type pollen tubes (GUS^-) were >300 μm long.

In vivo *study of pollen tube elongation in* qrt1 × sia2-2

The GUS staining of the self-pollinated *qrt1* plants revealed that the pollen tubes were able to grow normally inside the transmitting tract, to reach the base of the ovary and allow double fertilization (Fig. 5G). On the other hand, the GUS^+ *qrt1* × *sia2-2+/−* pollen grains and pollen tubes were restricted to the stigma and style (Fig. 5H) and no pollen tubes were detected in the transmitting tract of the ovary. However, aniline blue staining of the same pistil revealed that pollen tubes were growing in the transmitting tract and have reached the base of the ovary (Fig. 5I), indicating that the GUS^- pollen tubes (wild type) were able to perform the fertilization but the GUS^+ *qrt1* × *sia2-2* pollen tubes were not.

DISCUSSION

Sialyltransferase-like sequences belonging to the GT29 family are predicted to occur in plant genomes. These proteins contain the four conserved sialyl motifs of mammalian sialyltransferases (Audry *et al.*, 2011). Sialic acids are acidic sugars involved in multiple functions in mammals. Since endogenous sialyltransferase activity has not been detected in plants (Séveno *et al.*, 2004), it was postulated that these transferases could be involved in the transfer of Kdo and/or Dha on the HG backbone of RG-II, considering that sialic acid and Kdo transferases share common features such as the use of CMP-activated nucleotide sugars as substrates (Voxeur *et al.*, 2012). Studying the biological function of Kdo transferases is not achievable through an enzymatic assay since the nucleotide sugar CMP-Kdo, required for the bioassay, is an unstable compound (Belunis *et al.*, 1995). The activated form of Dha is as yet unidentified, although it is likely to be CMP-Dha as for other phosphoenolpyruvate-derived monosaccharides.

In arabidopsis, two sialyltransferase-like sequences, encoded by At1g08660 and At3g48820, are predicted. These two transferases were found in the Golgi apparatus, as expected for GTs involved in the biosynthesis of non-cellulosic cell wall polysaccharides (Dunkley *et al.*, 2006; Daskalova *et al.*, 2009). Furthermore, these two candidate genes were selected from a bioinformatic study based on the selection of candidate GT genes that are tightly co-expressed in rice and arabidopsis with previously characterized genes encoding enzymes involved in the synthesis of RG-II (Voxeur *et al.*, 2012). Deng *et al.* (2010) have investigated the pollen growth features in one of these two putative sialyltransferase-like proteins encoded by At1g08660. The isolated heterozygous *mgp2* mutant (named *sia1+/−* in this study) had a loss of male gametophytic function without any effect on the female gametophyte. *In vitro*, the mutant pollen grains failed to germinate or the pollen tubes either burst, were short or had an abnormal shape. *In vivo*, the mutant pollen tubes were restricted to the stigma 24 h after pollination and could not reach the ovules, whereas wild-type pollen tubes had already grown to the base of the ovary (Deng *et al.*, 2010). In our study, the same conclusions are drawn for the two *sia2* mutant lines. Mutation in the *SIA2* gene has a dramatic effect *in vitro* on the stability of the pollen tube cell wall. This results in a large number of pollen tubes that burst in the tip region or showed a significantly reduced length. This effect was correlated *in vivo* with the inability of the pollen tubes to grow further down than the style, possibly explaining the lack of homozygous line.

From the conclusions on both the *sia1+/−* and *qrt1* × *sia2+/−* mutants, it is worth noting that no functional compensation was observed between the two SIA1 and SIA2 sequences, which may suggest that the two enzymes are responsible for either Kdo or Dha transfers. The strong homology between the two transferases does not allow the discrimination between the two biosynthetic pathways. Furthermore, two CMP-sialic acid transporter-like proteins are predicted in plant genomes (Bakker *et al.*, 2008; Daskalova *et al.*, 2009) one of which was shown to complement the transport of CMP-sialic acid in CHO Lec2 mutant cells which were unable to transport CMP-sialic acid to the Golgi lumen (Bakker *et al.*, 2008). As a consequence, plant CMP-sialic acid transporter-like proteins are probably able to transport other CMP-nucleotide sugars such as CMP-Kdo. As observed for *SIA1* and *SIA2*, T-DNA insertion lines of *A. thaliana* targeting these genes exhibited a lethal phenotype (Takashima *et al.*, 2009). Based on these observations, we postulate that Kdo and Dha are synthesized, transported and integrated into the RG-II side chains through two independent pathways.

Many studies have shown that the integrity of the cell wall is important for pollen tube growth and for the tube to resist the turgor pressure. Studies on single or double pollen mutants affected in the biosynthesis of more abundant polymers than RG-II such as cellulose (Wang *et al.*, 2011) and HG (Wang *et al.*, 2013) resulted in abnormal pollen tube shape with a swollen tip and/or bursting of the pollen tubes in the tip region. The same phenotypes were observed on mutant pollen tubes impaired in cell wall remodelling enzymes such as pectin methylesterases (PMEs) (Jiang *et al.*, 2005; Tian *et al.*, 2006) or by exogenous application to pollen grains or pollen tubes of moderate concentrations of pectinase, cellulase, lyticase, PME (Parre and Geitmann, 2005*a*, *b*), a PME inhibitor (Woriedh *et al.*, 2013; Paynel *et al.*, 2014) or drugs such as the cellulose inhibitor isoxaben (Lazzaro *et al.*, 2003). All these data indicate that the proper biosynthesis, assembly and remodelling of the polymers in the pollen tube cell wall need to be tightly controlled and are required to create a network sufficiently rigid to support internal pressure but with adequate plasticity at the tip to promote fast growth.

Conclusions

Our study and three others (Delmas *et al.*, 2008; Deng *et al.*, 2010; Liu *et al.*, 2011) have indicated that mutations in genes coding for proteins possibly implicated in the machinery of

building RG-II have a dramatic effect on the integrity of the cell wall and correct pollen tube elongation. However, more studies are required to verify if the RG-II structure is impaired in the mutant pollen tubes, but the low abundance of this motif in the cell wall of pollen tubes, the high levels of burst tubes and short pollen tubes, and the mixture of mutant and wild-type pollen tubes will make this task very difficult. Finally, we lack conclusive evidence for Dha or Kdo transferase activity of SIA. It will require the setting up of an appropriate bioassay by incubating the catalytic domains of SIA1 and SIA2 proteins with short HG chains harbouring or not the A, the B or both side chains, and CMP-Kdo synthesized *in vitro* by incubating Kdo, CTP and a bacterial CMP-Kdo synthase as reported in the study of the biosynthesis of bacterial lipopolysaccharides (White *et al*., 1997).

SUPPLEMENTARY DATA

Supplementary data are available online at www.aob.oxfordjournals.org and consist of Table S1: list of primers used for the RT-qPCR.

ACKNOWLEDGEMENTS

This work was supported by the University of Rouen and the 'Trans Channel Wallnet' project that was selected by the INTERREG IVA program France (Channel)–England European cross-border co-operation programme, which is co-financed by the ERDF. The authors are grateful to the Grand Réseau de Recherche VASI de Haute Normandie for the use of equipment, to Mark Johnson (Brown University, USA) for the seeds of the pLAT-52::GUS *quartet* mutant line, to Corinne Loutelier-Bourhis for the GC-EIMS analysis to Hélène Dauchel for her advice on bioinformatic, and to Gaëtan Vannier for preliminary results. We also thank the Molecular Biology Platform (CRRBM) of the UPJV for scientific and technical support with the RT-qPCR.

LITERATURE CITED

Abramoff MD, Magalhães PJ, Ram SJ. 2004. Image processing with ImageJ. *Biophotonics International* **11**: 36–42.

Audry M, Jeanneau C, Imberty A, Harduin-Lepers A, Delannoy P, Breton C. 2011. Current trends in the structure–activity relationships of sialyltransferases. *Glycobiology* **21**: 716–726.

Bakker H, Routier F, Ashikov A, Neumann D, Bosch D, Gerardy-Schahn R. 2008. A CMP-sialic acid transporter cloned from *Arabidopsis thaliana*. *Carbohydrate Research* **343**: 2148–2152.

Bar-Peled M, Urbanowicz BR, O'Neill MA. 2012. The synthesis and origin of the pectic polysaccharide rhamnogalacturonan II – Insights from nucleotide sugar formation and diversity. *Frontiers in Plant Science* **3**: 1–12.

Belunis CJ, Clementz T, Carty SM, Raetz CRH. 1995. Inhibition of lipopolysaccharide biosynthesis and cell growth following inactivation of the kdtA gene in *Escherichia coli*. *Journal of Biological Chemistry* **270**: 27646–27652.

Blevins DG, Lukaszewski KM. 1998. Boron in plant structure and function. *Annual Review of Plant Physiology and Plant Molecular Biology* **49**: 481–500.

Boavida LC, McCormick S. 2007. Temperature as a determinant factor for increased and reproducible *in vitro* pollen germination in *Arabidopsis thaliana*. *The Plant Journal* **52**: 570–582.

Brewbaker JL, Kwack BH. 1963. The essential role of calcium ion in pollen germination and pollen tube growth. *American Journal of Botany* **50**: 859.

Chebli Y, Kaneda M, Zerzour R, Geitmann A. 2012. The cell wall of the *Arabidopsis* pollen tube – spatial distribution, recycling, and network formation of polysaccharides. *Plant Physiology* **160**: 1940–1955.

Cheng C, McComb JA, Rerkasem B. 1992. Techniques to study the anther in wheat. In: Mann CE, Rerkasem B, eds. *Wheat Special Report No. 11. Boron deficiency in wheat*. Mexico: CIMMYT, 32–33.

Covey PA, Subbaiah CC, Parsons RL, *et al*. 2010. A pollen-specific RALF from tomato that regulates pollen tube elongation. *Plant Physiology* **153**: 703–715.

Dai S, Chen T, Chong K, Xue Y, Liu S, Wang T. 2006. Proteomics identification of differentially expressed proteins associated with pollen germination and tube growth reveals characteristics of germinated *Oryza sativa* pollen. *Molecular and Cellular Proteomics* **6**: 207–230.

Dardelle F, Lehner A, Ramdani Y, *et al*. 2010. Biochemical and immunocytological characterizations of *Arabidopsis* pollen tube cell wall. *Plant Physiology* **153**: 1563–1576.

Darvill AG, McNeil M, Albersheim P. 1978. Structure of plant cell walls. *Plant Physiology* **62**: 418–422.

Daskalova SM, Pah AR, Baluch DP, Lopez LC. 2009. The *Arabidopsis thaliana* putative sialyltransferase resides in the Golgi apparatus but lacks the ability to transfer sialic acid. *Plant Biology* **11**: 284–299.

Delmas F, Séveno M, Northey JGB, *et al*. 2008. The synthesis of the rhamnogalacturonan II component 3-deoxy-d-manno-2-octulosonic acid (Kdo) is required for pollen tube growth and elongation. *Journal of Experimental Botany* **59**: 2639–2647.

Deng Y, Wang W, Li W-Q, *et al*. 2010. *MALE GAMETOPHYTE DEFECTIVE 2*, encoding a sialyltransferase-like protein, is required for normal pollen germination and pollen tube growth in *Arabidopsis*. *Journal of Integrative Plant Biology* **52**: 829–843.

Doco T, O'Neill MA, Pellerin P. 2001. Determination of the neutral and acidic glycosyl-residue compositions of plant polysaccharides by GC-EI-MS analysis of the trimethylsilyl methyl glycoside derivatives. *Carbohydrate Polymers* **46**: 249–259.

Dunkley TPJ, Hester S, Shadforth IP, *et al*. 2006. Mapping the *Arabidopsis* organelle proteome. *Proceedings of the National Academy of Sciences, USA* **103**: 6518–6523.

Edashige Y, Ishii T. 1998. Rhamnogalacturonan II from cell walls of *Cryptomeria japonica*. *Phytochemistry* **49**: 681–690.

Egelund J, Petersen BL, Motawia MS, *et al*. 2006. *Arabidopsis thaliana RGXT1* and *RGXT2* encode Golgi-localized (1,3)-alpha-d-xylosyltransferases involved in the synthesis of pectic rhamnogalacturonan-II. *The Plant Cell* **18**: 2593–2607.

Egelund J, Damager I, Faber K, Olsen C-E, Ulvskov P, Petersen BL. 2008. Functional characterisation of a putative rhamnogalacturonan II specific xylosyltransferase. *FEBS Letters* **582**: 3217–3222.

Fang K, Wang Y, Yu T, *et al*. 2008. Isolation of de-exined pollen and cytological studies of the pollen intines of *Pinus bungeana* Zucc. Ex Endl. and *Picea wilsonii* Mast. *Flora* **203**: 332–340.

Ganie MA, Akhter F, Bhat MA, *et al*. 2013. Boron – a critical nutrient element for plant growth and productivity with reference to temperate fruits. *Current Science* **104**: 76–85.

García-Hernández ER, Cassab López GI. 2005. Structural cell wall proteins from five pollen species and their relationship with boron. *Brazilian Journal of Plant Physiology* **17**: 375–381.

Goldbach HE, Wimmer MA. 2007. Boron in plants and animals: is there a role beyond cell wall structure? *Journal of Plant Nutrition and Soil Science* **170**: 39–48.

Gutierrez L, Bussell JD, Pacurar DI, Schwambach J, Pacurar M, Bellini C. 2009. Phenotypic plasticity of adventitious rooting in *Arabidopsis* is controlled by complex regulation of AUXIN RESPONSE FACTOR transcripts and microRNA abundance. *The Plant Cell* **21**: 3119–3132.

Holdaway-Clarke TL, Weddle NM, Kim S, *et al*. 2003. Effect of extracellular calcium, pH and borate on growth oscillations in *Lilium formosanum* pollen tubes. *Journal of Experimental Botany* **54**: 65–72.

Ishii T, Matsunaga T. 1996. Isolation and characterization of a boron–rhamnogalacturonan-II complex from cell walls of sugar beet pulp. *Carbohydrate Research* **284**: 1–9.

Jayaprakash P, Sarla N. 2001. Development of an improved medium for germination of *Cajanus cajan* (L.) Millsp. pollen *in vitro*. *Journal of Experimental Botany* **52**: 851–855.

Jiang L, Yang S-L, Xie L-F, *et al*. 2005. *VANGUARD1* encodes a pectin methylesterase that enhances pollen tube growth in the *Arabidopsis* style and transmitting tract. *The Plant Cell* **17**: 584–596.

Johnson MA, Lord E. 2006. Extracellular guidance cues and intracellular signalling pathways that direct pollen tube growth. In: Malhó R, ed. *Plant Cell Monographs. The pollen tube*. Berlin: Springer, 223–242.

Johnson-Brousseau SA, McCormick S. 2004. A compendium of methods useful for characterizing *Arabidopsis* pollen mutants and gametophytically-expressed genes. *The Plant Journal* **39**: 761–775.

Kakani VG, Reddy KR, Koti S, *et al.* 2005. Differences in *in vitro* pollen germination and pollen tube growth of cotton cultivars in response to high temperature. *Annals of Botany* **96**: 59–67.

Kaneko S, Ishii T, Matsunaga T. 1997. A boron–rhamnogalacturonan-II complex from bamboo shoot cell walls. *Phytochemistry* **44**: 243–248.

Kobayashi M, Kouzu N, Inami A, *et al.* 2011. Characterization of *Arabidopsis* CTP:3-deoxy-d-manno-2-octulosonate cytidylyltransferase (CMP-KDO synthetase), the enzyme that activates KDO during rhamnogalacturonan II biosynthesis. *Plant and Cell Physiology* **52**: 1832–1843.

Lazzaro MD, Donohue JM, Soodavar FM. 2003. Disruption of cellulose synthesis by isoxaben causes tip swelling and disorganizes cortical microtubules in elongating conifer pollen tubes. *Protoplasma* **220**: 201–207.

Lee S-H, Kim W-S, Han T-H. 2009. Effects of post-harvest foliar boron and calcium applications on subsequent season's pollen germination and pollen tube growth of pear (*Pyrus pyrifolia*). *Scientia Horticulturae* **122**: 77–82.

Lehner A, Dardelle F, Soret-Morvan O, Lerouge P, Driouich A, Mollet J-C. 2010. Pectins in the cell wall of *Arabidopsis thaliana* pollen tube and pistil. *Plant Signaling and Behavior* **5**: 1282–1285.

Li T, Choi W-G, Wallace IS, Baudry J, Roberts DM. 2011. *Arabidopsis thaliana* NIP7.1: an anther-specific boric acid transporter of the aquaporin superfamily regulated by an unusual tyrosine in helix 2 of the transport pore. *Biochemistry* **50**: 6633–6641.

Liu L, Huang L, Li Y. 2013. Influence of boric acid and sucrose on the germination and growth of *Areca* pollen. *American Journal of Plant Sciences* **4**: 1669–1674.

Liu X-L, Liu L, Niu Q-K, *et al.* 2011. *MALE GAMETOPHYTE DEFECTIVE 4* encodes a rhamnogalacturonan II xylosyltransferase and is important for growth of pollen tubes and roots in *Arabidopsis*. *The Plant Journal* **65**: 647–660.

Loraine AE, McCormick S, Estrada A, Patel K, Qin P. 2013. RNA-Seq of *Arabidopsis* pollen uncovers novel transcription and alternative splicing. *Plant Physiology* **162**: 1092–1109.

Matoh T, Takasaki M, Takabe K, Kobayashi M. 1998. Immunocytochemistry of rhamnogalacturonan II in cell walls of higher plants. *Plant and Cell Physiology* **39**: 483–491.

Matsunaga T, Ishii T, Matsumoto S, *et al.* 2004. Occurrence of the primary cell wall polysaccharide rhamnogalacturonan II in pteridophytes, lycophytes, and bryophytes. Implications for the evolution of vascular plants. *Plant Physiology* **134**: 339–351.

McGee RJ, Baggett JR. 1992. Unequal growth rate of pollen tubes from normal and stringless pea genotypes. *HortScience* **27**: 833–834.

McKenna ST, Kunkel JG, Bosch M, *et al.* 2009. Exocytosis precedes and predicts the increase in growth in oscillating pollen tubes. *The Plant Cell* **21**: 3026–3040.

Missihoun TD, Kirch H-H, Bartels D. 2012. T-DNA insertion mutants reveal complex expression patterns of the *aldehyde dehydrogenase 3H1* locus in *Arabidopsis thaliana*. *Journal of Experimental Botany* **63**: 3887–3898.

Mohnen D. 2008. Pectin structure and biosynthesis. *Current Opinion in Plant Biology* **11**: 266–277.

Mollet J-C, Faugeron C, Morvan H. 2007. Cell adhesion, separation and guidance in compatible plant reproduction. *Annual Plant Reviews* **25**: 69–90.

Mollet J-C, Leroux C, Dardelle F, Lehner A. 2013. Cell wall composition, biosynthesis and remodelling during pollen tube growth. *Plants* **2**: 107–147.

Noguchi K, Yasumori M, Imai T, *et al.* 1997. *bor1–1*, an *Arabidopsis thaliana* mutant that requires a high level of boron. *Plant Physiology* **115**: 901–906.

O'Neill MA, Warrenfeltz D, Kates K, *et al.* 1996. Rhamnogalacturonan-II, a pectic polysaccharide in the walls of growing plant cell, forms a dimer that is covalently cross-linked by a borate ester. *In vitro* conditions for the formation and hydrolysis of the dimer. *Journal of Biological Chemistry* **271**: 22923–22930.

O'Neill MA, Eberhard S, Albersheim P, Darvill AG. 2001. Requirement of borate cross-linking of cell wall rhamnogalacturonan II for *Arabidopsis* growth. *Science* **294**: 846–849.

O'Neill MA, Ishii T, Albersheim P, Darvill AG. 2004. Rhamnogalacturonan II: structure and function of a borate cross-linked cell wall pectic polysaccharide. *Annual Review of Plant Biology* **55**: 109–139.

Pabst M, Fischl RM, *et al.* 2013. Rhamnogalacturonan II structure shows variation in the side chains monosaccharide composition and methylation status within and across different plant species. *The Plant Journal* **76**: 61–72.

Palanivelu R, Tsukamoto T. 2012. Pathfinding in angiosperm reproduction: pollen tube guidance by pistils ensures successful double fertilization. *Developmental Biology* **1**: 96–113.

Parre E, Geitmann A. 2005*a*. More than a leak sealant. The mechanical properties of callose in pollen tubes. *Plant Physiology* **137**: 274–286.

Parre E, Geitmann A. 2005*b*. Pectin and the role of the physical properties of the cell wall in pollen tube growth of *Solanum chacoense*. *Planta* **220**: 582–592.

Paynel F, Leroux C, Surcouf O, Schaumann A, Pelloux J, Driouich A, Mollet JC, Lerouge P, Lehner A, Mareck A. 2014. Kiwi fruit PMEI inhibits PME activity, modulates root elongation and induces pollen tube burst in *Arabidopsis thaliana*. *Plant Growth Regulation*. doi:10.1007/s10725-014-9919-7.

Pérez S, Rodríguez-Carvajal MA, Doco T. 2003. A complex plant cell wall polysaccharide: rhamnogalacturonan II. A structure in quest of a function. *Biochimie* **85**: 109–121.

Persia D, Cai G, Casino CD, Faleri C, Willemse MTM, Cresti M. 2008. Sucrose synthase is associated with the cell wall of tobacco pollen tubes. *Plant Physiology* **147**: 1603–1618.

Pina C. 2005. Gene family analysis of the *Arabidopsis* pollen transcriptome reveals biological implications for cell growth, division control, and gene expression regulation. *Plant Physiology* **138**: 744–756.

Potts B, Marsden-Smedley J. 1989. *In vitro* germination of Eucalyptus pollen: response to variation in boric acid and sucrose. *Australian Journal of Botany* **37**: 429–441.

Prajapati PP, Jain BK. 2010. Effect of sucrose, boron, calcium, magnesium and nitrate during *in vitro* pollen germination in *Luffa aegyptica* Mill. *Prajna* **18**: 5–8

Rhee SY, Somerville CR. 1998. Tetrad pollen formation in *quartet* mutants of *Arabidopsis thaliana* is associated with persistence of pectic polysaccharides of the pollen mother cell wall. *The Plant Journal* **15**: 79–88.

Roberts IN, Gaude TC, Harrod G, Dickinson HG. 1983. Pollen–stigma interactions in *Brassica oleracea*; a new pollen germination medium and its use in elucidating the mechanism of self incompatibility. *Theoretical and Applied Genetics* **65**: 231–238.

Rounds CM, Winship LJ, Hepler PK. 2011. Pollen tube energetics: respiration, fermentation and the race to the ovule. *AoB Plants* **2011**: plr019.

Schreiber DN, Dresselhaus T. 2003. *In vitro* pollen germination and transient transformation of *Zea mays* and other plant species. *Plant Molecular Biology Reporter* **21**: 31–41.

Séveno M, Bardor M, Paccalet T, Gomord V, Lerouge P, Faye L. 2004. Glycoprotein sialylation in plants? *Nature Biotechnology* **22**: 1351–1352.

Shimokawa T, Ishii T, Matsunaga T. 1999. Isolation and structural characterization of rhamnogalacturonan II–borate complex from *Pinus densiflora*. *Journal of Wood Science* **45**: 435–439.

Takashima S, Seino J, Nakano T, *et al.* 2009. Analysis of CMP-sialic acid transporter-like proteins in plants. *Phytochemistry* **70**: 1973–1981.

Tian G-W, Chen M-H, Zaltsman A, Citovsky V. 2006. Pollen-specific pectin methylesterase involved in pollen tube growth. *Developmental Biology* **294**: 83–91.

Ülker B, Peiter E, Dixon DP, *et al.* 2008. Getting the most out of publicly available T-DNA insertion lines. *The Plant Journal* **56**: 665–677.

Vandesompele J, De Preter K, Pattyn F, *et al.* 2002. Accurate normalization of real-time quantitative RT-PCR data by geometric averaging of multiple internal control genes. *Genome Biology* **3**: research0034.

Vidal S, Williams P, O'Neill MA, Pellerin P. 2001. Polysaccharides from grape berry cell walls. Part I : tissue distribution and structural characterization of the pectic polysaccharides. Carbohydrate Polymers **45**: 315–323.

Vižintin L, Bohanec B. 2004. *In vitro* manipulation of cucumber (*Cucumis sativus* L.) pollen and microspores: isolation procedures, viability tests, germination, maturation. *Acta Biologica Cracoviensia Series Botanica* **46**: 177–183.

Voxeur A, Gilbert L, Rihouey C, *et al.* 2011. Silencing of the GDP-d-mannose 3,5-epimerase affects the structure and cross-linking of the pectic polysaccharide rhamnogalacturonan II and plant growth in tomato. *Journal of Biological Chemistry* **286**: 8014–8020.

Voxeur A, André A, Breton C, Lerouge P. 2012. Identification of putative rhamnogalacturonan-II specific glycosyltransferases in *Arabidopsis* using a combination of bioinformatics approaches. *PLoS One* **7**: e51129.

Wang L, Wang W, Wang Y-Q, *et al.* 2013. *Arabidopsis* galacturonosyltransferase (GAUT) 13 and GAUT14 have redundant functions in pollen tube growth. *Molecular Plant* **6**: 1131–1148.

Wang Q, Lu L, Wu X, Li Y, Lin J. 2003. Boron influences pollen germination and pollen tube growth in *Picea meyeri*. *Tree Physiology* **23**: 345–351.

Wang W, Wang L, Chen C, *et al*. 2011. *Arabidopsis CSLD1* and *CSLD4* are required for cellulose deposition and normal growth of pollen tubes. *Journal of Experimental Botany* **62**: 5161–5177.

Wang YH. 2008. How effective is T-DNA insertional mutagenesis in *Arabidopsis*? *Journal of Biochemical Technology* **1**: 11–20.

Warrington K. 1923. The effect of boric acid and borax on the broad bean and certain other plants. *Annals of Botany* **37**: 629–672.

Whitcombe AJ, O'Neill MA, Steffan W, Albersheim P, Darvill AG. 1995. Structural characterization of the pectic polysaccharide, rhamnogalacturonan-II. *Carbohydrate Research* **271**: 15–29.

White KA, Kaltashov IA, Cotter RJ, Raetz CR. 1997. A mono-functional 3-deoxy-d-manno-octulosonic acid (Kdo) transferase and a Kdo kinase in extracts of *Haemophilus influenzae*. *Journal of Biological Chemistry* **272**: 16555–16563.

Woriedh M, Wolf S, Márton ML, *et al*. 2013. External application of gametophyte-specific ZmPMEI1 induces pollen tube burst in maize. *Plant Reproduction* **26**: 255–266.

SUPPLEMENTARY DATA

TABLE S1. List of primers used for the RT-qPCR.

Primer name	Forward primers	Reverse primers
SIA2-1-flanking	5'-CAAATGGAAAGATCCCAAGTCTGG-3'	5'-CCCATCCATTTGGTAAGGCA-3'
SIA2-2-flanking	5'-CCTGGAAATCACGAAGCTGA-3'	5'-GACTCGTAGAGATTAGAGACGC-3'
SIA2-3'UTR	5'-GCGCCATTGTTAGGAGTTGA-3'	5'-GCTTTGTTCTCTTTCAGTCCTCT-3'
At3g28750	5'-AGGCGATGGTTATTGCACAAGC-3'	5'-TGCCCAACTTAACAGCGAGGTC-3'
At3g57690	5'-AAGAAGATTGCTTGCGGTGTGC-3'	5'-AAAGAGCCAAGAGCTGGCAACG-3'
At5g59370	5'-GCAGATGTGGATTGCGAAAGCAG-3'	5'-CCGTCTTCGTTTGGTGATCTTAGG-3'

PECTIN METHYLESTERASE48 Is Involved in Arabidopsis Pollen Grain Germination[1][OPEN]

Christelle Leroux, Sophie Bouton, Marie-Christine Kiefer-Meyer, Tohnyui Ndinyanka Fabrice, Alain Mareck, Stéphanie Guénin, Françoise Fournet, Christoph Ringli, Jérôme Pelloux, Azeddine Driouich, Patrice Lerouge, Arnaud Lehner[2], and Jean-Claude Mollet[2]*

Laboratoire Glycobiologie et Matrice Extracellulaire, Normandie Université, Institute for Research and Innovation in Biomedicine, Végétal, Agronomie, Sol, et Innovation, 76821 Mont-Saint-Aignan, France (C.L., M.-C.K.-M., A.M., A.D., P.L., A.L., J.-C.M.); Unité Biologie des Plantes et Innovation (S.B., S.G., F.F., J.P.) and Centre de Ressources Régionales en Biologie Moléculaire (S.G.), Université de Picardie Jules Verne, 80039 Amiens, France; and Institute of Plant Biology, University of Zürich, 8008 Zurich, Switzerland (T.N.F., C.R.)

Germination of pollen grains is a crucial step in plant reproduction. However, the molecular mechanisms involved remain unclear. We investigated the role of PECTIN METHYLESTERASE48 (PME48), an enzyme implicated in the remodeling of pectins in Arabidopsis (*Arabidopsis thaliana*) pollen. A combination of functional genomics, gene expression, in vivo and in vitro pollen germination, immunolabeling, and biochemical analyses was used on wild-type and *Atpme48* mutant plants. We showed that *AtPME48* is specifically expressed in the male gametophyte and is the second most expressed *PME* in dry and imbibed pollen grains. Pollen grains from homozygous mutant lines displayed a significant delay in imbibition and germination in vitro and in vivo. Moreover, numerous pollen grains showed two tips emerging instead of one in the wild type. Immunolabeling and Fourier transform infrared analyses showed that the degree of methylesterification of the homogalacturonan was higher in *pme48−/−* pollen grains. In contrast, the PME activity was lower in *pme48−/−*, partly due to a reduction of PME48 activity revealed by zymogram. Interestingly, the wild-type phenotype was restored in *pme48−/−* with the optimum germination medium supplemented with 2.5 mM calcium chloride, suggesting that in the wild-type pollen, the weakly methylesterified homogalacturonan is a source of Ca^{2+} necessary for pollen germination. Although pollen-specific PMEs are traditionally associated with pollen tube elongation, this study provides strong evidence that PME48 impacts the mechanical properties of the intine wall during maturation of the pollen grain, which, in turn, influences pollen grain germination.

Sexual plant reproduction requires the growth of tip-polarized pollen tubes through the female tissues in order to deliver the two sperm cells to the embryo sac. Despite the importance of this crucial step that leads to seed production, the molecular mechanisms implicated in the spatial and temporal controls of pollen tube growth are not fully known (Johnson and Lord, 2006; Palanivelu and Tsukamoto, 2012). However, it has been proposed that the modulation of the stiffness of the pollen tube was important during pollen tube growth (Parre and Geitmann, 2005a; Fayant et al., 2010; Vogler et al., 2013). Pollen tube elongation is highly polarized, with the growth area being restricted to the apex of the tube. New membranes and cell wall materials are rapidly secreted at the tip, providing the building material necessary to sustain the fast pollen tube growth (Bove et al., 2008; Guan et al., 2013). The pollen tube cell wall of many species, including tobacco (*Nicotiana tabacum*; Li et al., 1995; Ferguson et al., 1998), lily (*Lilium longiflorum*; Roy et al., 1997), and Arabidopsis (*Arabidopsis thaliana*; Lennon and Lord, 2000; Dardelle et al., 2010), is characterized by one layer in the tip region and two distinguishable layers back in the shank. Back from the tip, the inner layer is mainly composed of callose, a (1,3)-β-glucan, which is not detectable in the tip region in normal growth conditions (Ferguson et al., 1998; Derksen et al., 2002; Parre and Geitmann, 2005b; Dardelle et al., 2010; Chebli et al., 2012). Moreover, callose is also deposited periodically within the pollen tube to form plugs that maintain the tube cell in the expanding apical region. The outer cell wall in the tip and back from the tip is mostly composed of pectins, xyloglucan, cellulose, and proteoglycans such as arabinogalactan proteins (Geitmann and Steer, 2006; Dardelle et al., 2010; Chebli et al., 2012; Nguema-Ona et al., 2012).

In eudicot species, pectins constitute a major portion of the primary cell wall. Pectins are complex polysaccharides consisting of homogalacturonan (HG), rhamnogalacturonan I,

[1] This work was supported by the Institute for Research and Innovation in Biomedicine of the region Haute-Normandie, France (to C.L.), by the University of Rouen, and by the Trans Channel Wallnet project that was selected by the INTERREG IVA program, France (Channel)-England European cross-border cooperation program, financed by the European Regional Development Fund.

[2] These authors contributed equally to the article.

* Address correspondence to jean-claude.mollet@univ-rouen.fr.

The author responsible for distribution of materials integral to the findings presented in this article in accordance with the policy described in the Instructions for Authors (www.plantphysiol.org) is: Jean-Claude Mollet (jean-claude.mollet@univ-rouen.fr).

[OPEN] Articles can be viewed without a subscription.

www.plantphysiol.org/cgi/doi/10.1104/pp.114.250928

rhamnogalacturonan II, and xylogalacturonan (Vincken et al., 2003; Dardelle et al., 2010; Fry, 2011; Dumont et al., 2014). HG is a polymer consisting of repeating units of (1,4)-α-D-galacturonic acid (GalUA) that is synthesized in the Golgi apparatus and may be deposited in the cell wall in a highly methylesterified form (Zhang and Staehelin, 1992).

Immunolabeling of HG on Arabidopsis pollen tubes showed a dominant localization of the highly methylesterified HG in the tip and of partially methylesterified HG behind the tip region (Dardelle et al., 2010; Chebli et al., 2012). This labeling pattern is also observed in pollen tubes from plants possessing a solid style, such as species in the Solanaceae (potato [*Solanum tuberosum*], tobacco, and petunia [*Petunia hybrida*]), the Oleaceae (jasmine [*Jasmium* spp.]), and the Poaceae (maize [*Zea mays*]; Li et al., 1994; Qin et al., 2007; for review, see Mollet et al., 2013), and those with a hollow style, such as lily (Jauh and Lord, 1996). The methylesterified HG in the apical dome of the pollen tube is thought to provide sufficient plasticity of the cell wall to sustain pollen tube growth (Chebli and Geitmann, 2007). In the subapical region, methylesterified HG is processed by pectin methylesterases (PMEs). Two modes of action have been described for PMEs (Micheli, 2001). If PMEs remove contiguous methylester groups, the mode of action is named the block-wise mode of action. In that case, demethylesterified HG can form ionic bonds between the negatively charged carboxyl groups of several HG chains and Ca^{2+} ions, forming a pectate gel that may provide sufficient stiffness to the pollen tube cell wall (Micheli, 2001; Geitmann and Steer, 2006; Chebli et al., 2012). Alternatively, the partial removal of noncontiguous methylester groups by PMEs, which is named the random mode of action, may allow pectin-degrading enzymes (such as polygalacturonases [PGases] and pectate lyases [PLs]) to cleave the HG backbone, thus affecting the rigidity of the cell wall (Micheli, 2001; Bosch and Hepler, 2005; Parre and Geitmann, 2005a; Sénéchal et al., 2014). Therefore, the fine control of the modulation of the degree of methylesterification (DM) of the HG by PMEs is of main importance (Wolf et al., 2009a) in the pollen tube growth dynamics. The Arabidopsis genome contains 66 putative PMEs. Most of them display a specific expression pattern, especially for 14 of them that are specifically expressed in pollen grains or pollen tubes (Qin et al., 2009; Wolf et al., 2009a). PMEs are classified in two distinct groups depending on the presence/absence of an N-terminal extension domain (the PRO region) showing similarity with the pectin methylesterase inhibitor (PMEI) domain (Micheli, 2001). PMEs from group 1 do not have a PMEI domain but can be inhibited by PMEIs (Röckel et al., 2008), whereas PMEs from group 2 can contain from one to three PMEI domains (Tian et al., 2006). It is hypothesized that the PRO region is cleaved during maturation of the PME, as so far, only PMEs lacking this domain were found in the cell wall (Micheli, 2001). Wolf et al. (2009b) have shown that the PRO region of the group 2 PMEs could regulate the release of the mature PME from the Golgi apparatus. It has also been reported that the PRO region could play an autoinhibitory role during maturation (Bosch et al., 2005).

The first direct evidence for the crucial roles of PMEs during pollen tube growth was described in two knockout mutants, *vanguard1* (*vgd1*; Jiang et al., 2005) and *Atppme1* (Tian et al., 2006). *VGD1* (At2g47040) encodes a pollen-specific group 2 PME. The functional disruption of *VGD1* resulted in the bursting of pollen tubes in vitro and the marked retardation of *vgd1* pollen tube elongation in the pistil, resulting in a strong reduction of male fertility and seed set. *AtPPME1* (At1g69940), coding for a pollen-specific group 1 PME, also was identified to play an important role in pollen tube growth (Tian et al., 2006). The lack of *AtPPME1* transcripts in the knockout mutant affected the shape and growth rate of pollen tubes, indicating that AtPPME1 is required for the integrity of the cell wall and the tip-polarized growth of the pollen tube (Tian et al., 2006).

Here, we report the study of a homozygous knockdown mutant for *AtPME48* during the imbibition and germination of pollen grains and pollen tube growth. We have investigated in vitro and in vivo pollen germination, pollen tube morphology and growth, as well as the level of PME activity and the DM of the HG by immunolabeling and Fourier transform infrared (FT-IR) spectroscopy in mutant and wild-type plants. Our results show that the group 1 PME48, the second most expressed *PME* gene in pollen, plays a major role in remodeling the HG of the intine cell wall during Arabidopsis pollen grain maturation, resulting, after rehydration, in normal pollen grain germination.

RESULTS

Expression of Pollen-Specific PMEs Assessed by Quantitative Reverse Transcription-PCR

The expression of the 14 pollen-specific PME genes was analyzed by quantitative reverse transcription (qRT)-PCR on total RNA extracted from dry and imbibed (for 1 h in liquid germination medium [GM]) pollen grains and 6-h-old pollen tubes. Most PME genes were expressed in dry pollen grains, with a strong expression of PME4 (VGD1 homolog), PME5 (VGD1), PME37, and PME48 (Fig. 1A). During imbibition and in in vitro-grown pollen tubes, PME4, PME5, PME50, as well as PME48 were strongly expressed compared with the 10 other PMEs (Fig. 1, B and C). PME48 and PME50 belong to the group 1 PMEs, whereas PME4 and PME5, known as VGD1 homolog and VGD1 (Jiang et al., 2005), belong to the group 2 PMEs.

Tissue-Specific Expression of *AtPME48*

In order to check whether *PME48* is specifically expressed in pollen, the activity of the promoter of *PME48* was assessed using the *pPME48*::*GUS* and *pPME48*::*YFP* constructs. Fluorescence of the yellow fluorescent protein (YFP) was observed in dry (Fig.

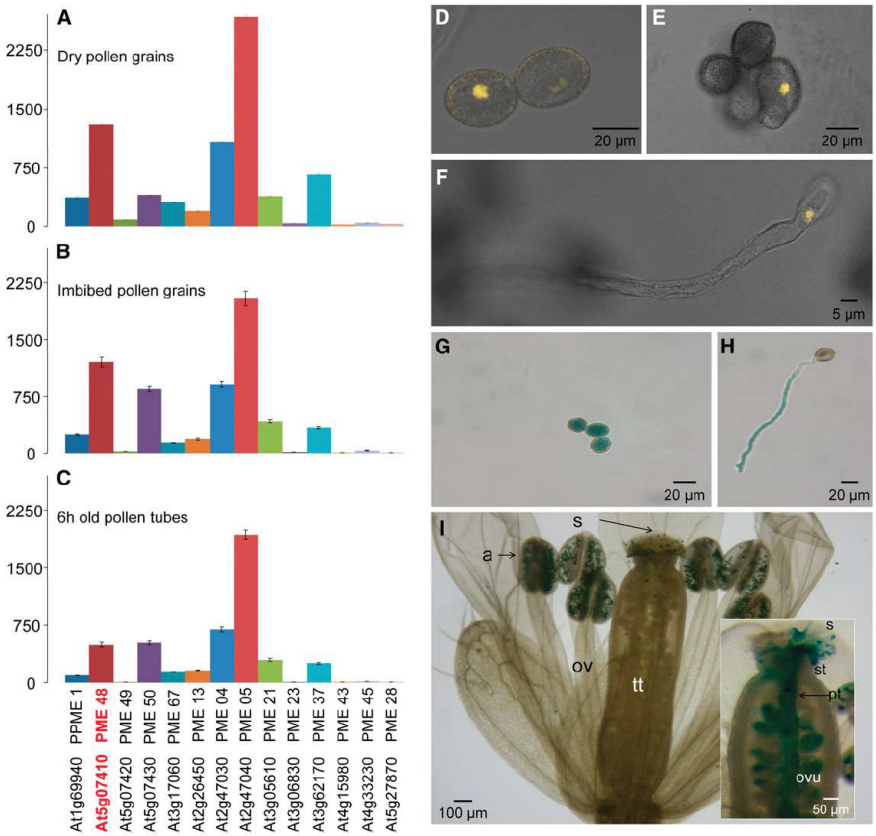

Figure 1. A to C, Relative gene expression of the 14 pollen-specific *PMEs* in wild-type dry pollen grains (A), 1-h imbibed pollen grains (B), and 6-h-old pollen tubes (C) measured using stably expressed reference genes (At3g28750, At3g57690, and At5g59370) in three biological samples with similar results. Only the results obtained with At3g28750 are shown. The locus and the corresponding UniProt name of each protein are indicated. The data correspond to means ± SD of three technical replicates of a biological sample. D to F, Analyses of the expression of the promoter of *PME48* using the *pPME48*::YFP construct by confocal microscopy in dry pollen grains (D), 1-h imbibed pollen grains (E), and during pollen tube growth (F). Images shown are overlays of the bright-field and fluorescent images. G to I, Analyses of the expression of the promoter of *PME48* using the *pPME48*::GUS construct in dry pollen grains (G), 3-h-old pollen tube (H), anthers (I), and self-pollinated pistil (inset in I). a, Anther; ov, ovary; ovu, ovule; pt, pollen tube; s, stigma; st, style; tt, transmitting tract.

1D) and imbibed (Fig. 1E) pollen grains and in 6-h-old in vitro-grown pollen tubes (Fig. 1F). GUS staining showed that the promoter activity of *PME48* was restricted to the male gametophyte (Fig. 1, G–I). GUS activity was detected in dry pollen grains (Fig. 1G) and in 6-h-old in vitro-grown pollen tubes (Fig. 1H). In vivo staining also showed a strong GUS activity in pollen grains within the anther and in germinated pollen grains deposited on the stigma (Fig. 1I). GUS staining was also clearly visible in pollen tubes growing through the transmitting tract (Fig. 1I, inset). Staining was observed neither in the vegetative organs of the transformed plants nor in pollen grains or pollen tubes from wild-type plants (data not shown).

Isolation and Characterization of the *pme48−/−* Homozygous Mutant Line

We selected a transfer DNA (T-DNA) insertion line from the Salk library. SALK_122970 contained a T-DNA insert in the *PME48* coding sequence. The T-DNA insertion was predicted to be located in the last exon of the sequence (Supplemental Fig. S1A). The homozygous

mutant line (*pme48−/−*) has been isolated, two copies of the insert were amplified with the genomic DNA (Supplemental Fig. S1B), and the *PME48* transcript was not detectable by reverse transcription (RT)-PCR (Supplemental Fig. S1C). The vegetative organs of *pme48−/−* did not display any visible phenotype or growth defect compared with wild-type plants (data not shown).

The level of the *PME48* transcript was then analyzed by qRT-PCR in dry, imbibed pollen grains and 6-h-old pollen tubes. Unlike the data obtained by RT-PCR (Supplemental Fig. S1C), qRT-PCR revealed that *pme48−/−* was not a knockout but a knockdown mutant (Fig. 2). *PME48* was lightly expressed in dry (9%; Fig. 2A) and imbibed (10%; Fig. 2B) pollen grains and in 6-h-old pollen tubes (19%; Fig. 2C) compared with wild-type pollen grains and pollen tubes. 4′,6-Diamidino-2-phenylindole (DAPI) staining showed that *pme48−/−* pollen grains contained the two sperm cells and the vegetative nucleus as observed in wild-type pollen grains (Supplemental Fig. S2A). Using fluorescein diacetate (FDA), the viability assays showed that most *pme48−/−* pollen grains were viable (72.3% ± 3.7%), but slightly less than wild-type pollen grains (79% ± 4.6%; $P < 0.0001$, $n > 1{,}000$ for each sample; Supplemental Fig. S2, B and C). In addition, the length of wild-type dry pollen grains was also slightly higher (29.8 ± 0.15 μm) than that of *pme48−/−* pollen grains (28.8 ± 0.12 μm; $P < 0.0001$, $n = 550$ for each sample; Supplemental Fig. S2, D and E). Similarly, the length of the siliques of the mutant was 1.4 mm shorter than that of the wild type ($P < 0.0001$, $n = 210$ for each sample; Supplemental Fig. S2F). The silique of the mutant contained a reduced number of seeds (40.3 ± 1.33 seeds per silique) compared with the wild-type silique (48.6 ± 0.5 seeds per silique; $P < 0.0001$, $n = 210$ for each sample; Supplemental Fig. S2G).

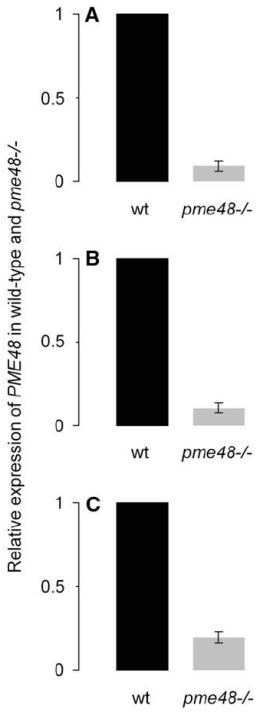

Figure 2. Relative gene expression of *PME48* in *pme48−/−* dry pollen grains (A), 1-h imbibed pollen grains (B), and 6-h-old pollen tubes (C) was measured using stably expressed reference genes (At3g28750, At3g57690, and At5g59370) in three biological samples with similar results. Only the results obtained with At3g28750 are shown. The data correspond to the ratio of expression in the wild type (wt) or *pme48−/−* compared with the wild type and are means ± SD of three technical replicates of a biological sample.

In Vitro and in Vivo Pollen Grain Germination and Pollen Tube Growth of *pme48−/−*

In the optimal solid GM described by Boavida and McCormick (2007), 65% and 90% of wild-type pollen grains were germinated after 6 and 24 h of culture, respectively (Fig. 3A). In contrast, the percentage of germinated *pme48−/−* pollen grains was reduced drastically, as only 10% of the pollen grains were germinated after 24 h of culture ($P < 0.0001$, $n > 10{,}000$ for each sample; Fig. 3A). In liquid medium, 71% and 73% germination was observed after 6 and 24 h of culture for the wild-type pollen grains (Supplemental Fig. S3A). In contrast, the level of *pme48−/−* pollen grain germination did not exceed 43.8% after 6 h of culture and reached only 60% after 24 h ($P < 0.0001$, $n > 10{,}000$ for each sample; Supplemental Fig. S3A). As *pme48−/−* pollen grains displayed a delay in germination, the speed of imbibition of the pollen grains was assessed by calculating the ratio of length to width. Dry pollen grains have ellipsoid shapes, and the length is approximately twice as much as the width. During imbibition, pollen grains become spherical and the length is nearly equal to the width; the length:width ratio is then approximately 1. On the optimal solid medium, the imbibition was faster for the wild-type pollen grains compared with the mutant. The smallest ratio was obtained after 24 h, with 1.16 and 1.39 for the wild-type and *pme48−/−*, respectively (Fig. 3B). After 24 h of culture, pollen grains from the mutant lines were less imbibed than the wild-type pollen grains imbibed for 6 h ($P < 0.0001$, $n > 500$ for each sample). The same result was observed in liquid medium ($P < 0.0001$, $n > 500$ for each sample; Supplemental Fig. S3B). Based on these observations, it appeared that the ability of the pollen grain to rehydrate was affected in *pme48−/−* mutant lines. The delay in germination was also observed in vivo. Hand pollination of emasculated wild-type pistils with wild-type or *pme48−/−* pollen grains showed that the wild-type

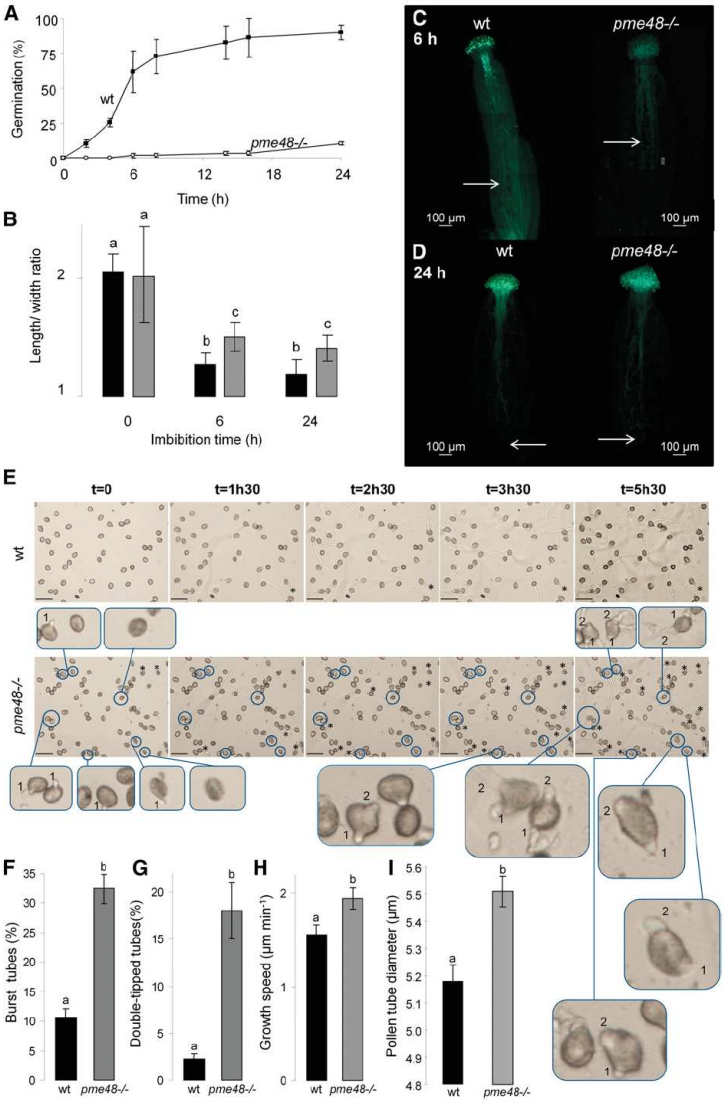

Figure 3. In vitro and in vivo germination of wild-type and *pme48−/−* pollen grains. A, Germination rate of wild-type (wt; black squares) and *pme48−/−* (white circles) pollen grains in the optimum solid medium. Pollen grains were considered germinated when the length of the tube was equal to the diameter of the pollen grain. B, Estimation of the imbibition rate by measuring the ratio of length to width of wild-type (black bars) and *pme48−/−* (gray bars) pollen grains. C and D, In vivo growth of wild-type and *pme48−/−* pollen tubes in wild-type pistil at 6 h (C) and 24 h (D) after hand pollination revealed by Aniline Blue staining. Arrows indicate the locations that most of the pollen tubes have reached in the transmitting tissue. Bars = 100 μm. E, Time-lapse images of wild-type and *pme48−/−* pollen germination in liquid medium showing two emerging tips from the pollen grain (blue circles) and burst tubes (asterisks). Numbers in the closeup images indicate which tubes emerged first. Closeup images of abnormal phenotypes were observed in the mutant line compared with the wild type. Bars = 50 μm. F, Estimation of the rate of burst pollen tubes in the wild type (black bar) and *pme48−/−* (gray bar). G, Estimation of the rate of pollen grains with two emerging tips in the wild type (black bar) and *pme48−/−* (gray bar). H, Estimation of the growth speed of wild-type (black bar) and *pme48−/−* (gray bar) germinated pollen tubes. I, Comparison of the pollen tube diameters between the wild type (black bar) and *pme48−/−* (gray bar) grown in liquid GM for 4 h. Different letters indicate statistically significant differences between the wild-type and *pme48−/−* lines, as determined by Student's *t* test ($P < 0.0001$); $n >$ 10,000 in A; $n > 500$ in B, F, and G; $n > 35$ in H; $n = 126$ for the wild type and $n = 172$ for *pme48−/−* from four independent experiments in I.

pollen tubes had traveled two-thirds of the transmitting tract after 6 h (Fig. 3C, left) and completed their journey by reaching the bottom of the ovary after 24 h (Fig. 3D, left). In contrast, *pme48−/−* pollen tubes had reached only one-half of the transmitting tract after 6 h (Fig. 3C, right), but after 24 h, *pme48−/−* pollen tubes also had reached the base of the ovary (Fig. 3D, right).

In addition to lower germination rates, *pme48−/−* displayed a remarkable phenotype, as shown on the representative images obtained by time-lapse video during the germination of pollen grains and the growth of pollen tubes (Fig. 3E). Wild-type pollen grains had already germinated 90 min after immersion in the liquid medium (Fig. 3E, top), the proportion of burst tubes was around 10% (Fig. 3F), the growth rate was about 1.5 μm min^{-1} during the first 90 min of growth (Fig. 3H; Supplemental Fig. S4), and pollen tubes displayed a normal phenotype (Fig. 3E; Supplemental Movie S1).

On the other hand, *pme48−/−* pollen tubes appeared to be more unstable, with 32% of burst tubes ($P < 0.0001$, $n > 500$ for each sample; Fig. 3F). Moreover, a significant number of *pme48−/−* pollen grains (18%) displayed two tips emerging from the same pollen grain ($P < 0.0001$, $n > 500$ for each sample; Fig. 3, E and G, bottom closeup images). The first tip emerged from pollen grains, and after 4 to 5 h of culture, a second tip emerged from the same pollen grain (pollen grains circled in blue; Fig. 3E, bottom closeup images; Supplemental Movie S2). Once germinated and if pollen tubes were produced, the growth speed of *pme48−/−* pollen tubes was slightly faster compared with wild-type pollen tubes ($P < 0.0001$, $n > 35$ for each sample; Fig. 3H; Supplemental Fig. S4). Another consequence of the *PME48* mutation was that pollen tubes growing in liquid GM displayed larger diameters than wild-type pollen tubes (Figs. 3I and 4, A and H). The *pme48−/−* pollen tube diameters were significantly wider (5.51 ± 0.05 μm) compared with wild-type pollen tubes (5.18 ± 0.06 μm; $P < 0.0001$, $n = 126$ for wild-type pollen tubes and $n = 172$ for *pme48−/−* pollen tubes; Fig. 3I).

Immunolabeling of Highly Methylesterified HG in Pollen Grains and Pollen Tubes

Cell surface immunolocalization of highly methylesterified HG with the monoclonal antibody LM20 revealed that the epitopes were almost exclusively restricted to the tip region of wild-type pollen tubes (Fig. 4, A–E). Pollen grains from wild-type plants showed a very weak, almost no, labeling of the intine wall (Fig. 4, C–E). Similar results were obtained on semithin sections (Fig. 4, F and G). In contrast, the labeling of *pme48−/−* pollen tubes was not restricted to the tube tip but extended to the subapical region of the tube, but with the strongest fluorescence at the tip (Fig. 4, H–K). Finally, *pme48−/−* pollen grains displayed a more intense fluorescence of the intine wall by cell surface immunolabeling (Fig. 4, J–L) and on semithin sections (Fig. 4, M and N) compared with the wild type.

Immunolabeling with the monoclonal antibody LM19 that recognizes weakly methylesterified HG epitopes did not reveal any noticeable difference between the wild type and *pme48−/−* (data not shown). LM19 and LM20 show overlapping binding capabilities to different levels of methylesterification, except for totally deesterified HG epitopes that are only recognized by LM19 (Verhertbruggen et al., 2009). Therefore, these results suggest that highly methylesterified HG epitopes were more abundant in the intine wall of *pme48−/−* pollen grains compared with the wild type.

PME Activity and DM of HG in *pme48−/−*

In order to assess further the biochemical differences between the wild type and *pme48−/−*, we investigated the total PME activity in pollen grains by using enzymatic assays. The data showed a 50% reduction of total PME activity in *pme48−/−* pollen grains compared with the wild type (Fig. 5A). Moreover, a zymogram after isoelectric focalization (IEF) of total proteins extracted from pollen grains revealed the disappearance of a diffuse band in the pI range between 8.2 and 9 in *pme48−/−* (Fig. 5B) that may correspond at least in part to PME48, which has a predicted pI of 8.3. Two spots, at pI ranging from 9.8 to 10.2 and from 9.5 to 9.7, in the range of predicted pIs of other pollen PMEs did not show any visible change in activity (Fig. 5B). These

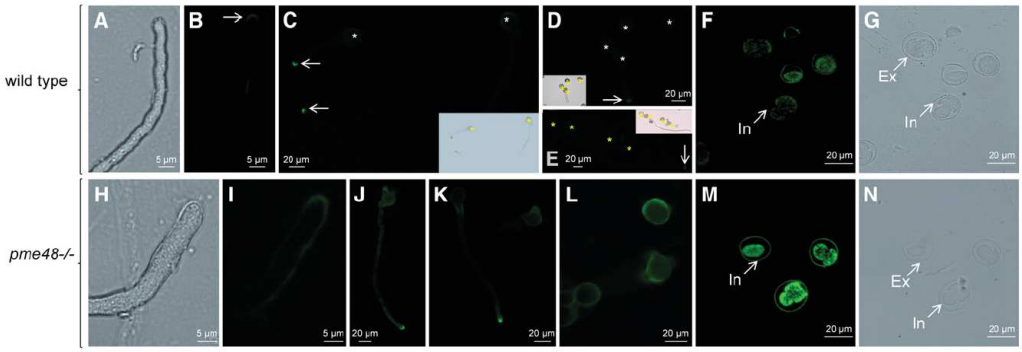

Figure 4. Immunolocalization of highly methylesterified HG epitopes probed with LM20 in wild-type and *pme48−/−* pollen grains and pollen tubes. A to E, Cell surface immunolabeling in wild-type pollen grains and pollen tubes. F and G, Immunolabeling on semithin sections of wild-type dry pollen grains. H to L, Cell surface immunolabeling in *pme48−/−* pollen grains and pollen tubes. M and N, Immunolabeling on semithin sections of *pme48−/−* dry pollen grains. Asterisks indicate pollen grains, and arrows point to pollen tube tips. Ex, Exine; In, intine.

biochemical data support the qRT-PCR results that clearly showed a significant reduction of *PME48* expression. Finally, the DM of HG was estimated by FT-IR spectroscopy in hot water-soluble pectin-enriched fractions extracted from dry pollen grains (Fig. 5, C and D). A marked difference was observed at 1,740 cm^{-1} assigned to the vibration of methylester groups of HG (Fig. 5C). The relative absorbance at this wave number was higher in *pme48−/−* pollen grains. The DM of the HG was consistently higher in the *pme48−/−* (32.5% ± 1.7%) compared with the wild-type (13.4% ± 1.1%) pollen grains (Fig. 5D). As deesterified HG binds more Ca^{2+} than esterified HG, our data may suggest that HGs in the intine wall of *pme48−/−* are less associated with Ca^{2+} compared with wild-type pollen grains.

Supplementation of Ca^{2+} to the GM Restores the Phenotype of *pme48−/−*

To assess if the germination defect of *pme48−/−* pollen grains was related to the possible lower Ca^{2+} sink in the intine wall due to the higher DM of the HG, the optimum culture medium containing 5 mM $CaCl_2$ was supplemented with 2.5 mM $CaCl_2$ to reach a final concentration of 7.5 mM or with the Ca^{2+} chelator, EDTA. In the presence of 1 mM EDTA, none of the wild-type and *pme48−/−* pollen grains germinated, even after 24 h of culture ($n > 1,000$; Fig. 6, A and B). In the medium supplemented with Ca^{2+}, *pme48−/−* pollen grain germination rates were restored, reaching levels similar to those observed with wild-type pollen grains ($n > 1,000$). The percentage of pollen germination reached 52% and 90% after 6 and 24 h, respectively (Fig. 6, A and B). Moreover, the speed of imbibition of *pme48−/−* pollen grains was as fast as that of the wild-type pollen grains (Fig. 6C). In addition, a significant reduction of the abnormal phenotypes, such as burst tubes (from 33% to 13%; Figs. 3F and 6D) and double-tipped tubes (from 18% to 2%; Figs. 3G and 6E), was observed in *pme48−/−* pollen grains cultured in the supplemented GM. Finally, in the $CaCl_2$-supplemented medium, the rates of burst tubes increased in wild-type pollen grains (32%; Fig. 6D) compared with those observed when pollen grains were grown in the optimum GM (approximately 10%; Fig. 3F).

DISCUSSION

The regulation of the DM of HG has been implicated in many aspects of plant development (Wolf et al., 2009a), including cell adhesion (Tieman and Handa, 1994; Wen et al., 1999; Mollet et al., 2000; Bouton et al., 2002; Mouille et al., 2007; Durand et al., 2009), adventitious rooting (Guénin et al., 2011), primordia emergence at the shoot apical meristem (Peaucelle et al., 2008, 2011), fruit ripening (Brummell and Harpster, 2001; Phan et al., 2007), and plant defense (Bethke et al., 2014). Although data have shown an important role for

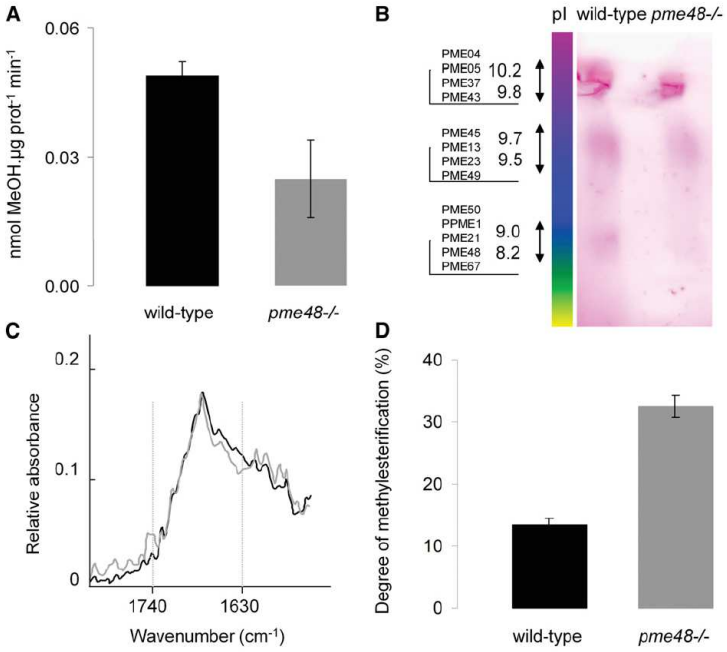

Figure 5. Biochemical analyses of wild-type and *pme48−/−* dry pollen grains. A, Enzymatic assay of the total PME activity contained in wild-type (black bar) and *pme48−/−* dry (gray bar) pollen grains. MeOH, Methanol. B, Zymogram after IEF of PMEs contained in wild-type and *pme48−/−* dry pollen grains. A diffuse band corresponding to the pI (8.2) of PME48 is lacking in *pme48−/−* dry pollen grains. C and D, Determination of the DM of the HG in dry pollen grains by FT-IR spectroscopy. C, Representative FT-IR spectra of pectin-enriched fractions extracted from wild-type (black trace) and *pme48−/−* (gray trace) dry pollen grains. D, Quantification of the DM of HG in wild-type (black bar) and *pme48−/−* (gray bar) pollen grains. Data are means of three biological replicates ± SD.

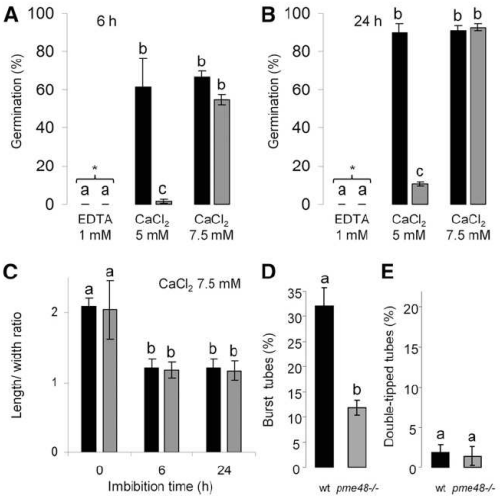

Figure 6. Effect of calcium on the germination and phenotype of pollen tubes. A and B, Germination percentage of wild-type (black bars) and *pme48−/−* (gray bars) pollen grains in the optimal solid medium (5 mM $CaCl_2$), in the optimal solid medium supplemented with 1 mM EDTA, and in the optimal medium supplemented with 2.5 mM calcium (i.e. final concentration of $CaCl_2$, 7.5 mM) after 6 h (A) and 24 h (B) of growth. Pollen grains were considered germinated when the length of the tube was equal to the diameter of the pollen grain. C, Estimation of the imbibition rate by measuring the ratio of length to width of wild-type (black bars) and *pme48−/−* (gray bars) pollen grains in the solid medium containing 7.5 mM $CaCl_2$. D, Estimation of the rate of burst pollen tubes in the wild type (wt; black bar) and *pme48−/−* (gray bar) in solid medium containing 7.5 mM $CaCl_2$. E, Estimation of the rate of pollen grains with two emerging tips in the wild type (black bar) and *pme48−/−* (gray bar) in solid medium containing 7.5 mM $CaCl_2$. Different letters indicate statistically significant differences between the wild-type and *pme48−/−* lines, as determined by Student's *t* test ($P < 0.0001$); $n > 1{,}000$ in A and B; $n > 500$ in C; and $n > 250$ in D and E.

the pectin demethylesterification process in pollen tetrad separation (Francis et al., 2006) and pollen tube growth (Jiang et al., 2005; Tian et al., 2006), the involvement of PMEs during pollen germination is still poorly understood. Among the 66 predicted *PME* genes in the genome of Arabidopsis, 14 are specifically expressed in the male gametophyte (data from Genevestigator [Hruz et al., 2008] and EFP Browser [Winter et al., 2007]). Two of them have already been studied using functional genomics approaches. The first one is VGD1 (At2g47040), the alteration of which led to unstable pollen tubes and retarded growth of the pollen tube in the style and transmitting tract, resulting in a significant reduction of male fertility (Jiang et al., 2005). The second pollen-specific PME characterized to date is PPME1 (At1g69940; Tian et al., 2006). The homozygous mutant *Atppme1* displayed reduced growth and irregular shape of pollen tubes grown in vitro. In this study, we show that alteration of the expression of *PME48*, the second most expressed *PME* in pollen grains, results in a strong delay in imbibition and in germination both in vivo and in vitro, as well as altered phenotypes with abnormal rates of burst tubes and two pollen tube tips emerging from the same pollen grain. The phenotype is rescued by supplementing the optimum GM (Boavida and McCormick, 2007) with 2.5 mM $CaCl_2$ to reach 7.5 mM. In 7.5 mM $CaCl_2$, *pme48−/−* pollen grains imbibed and germinated normally. These data suggest that PME48 is mainly involved in the remodeling of the intine cell wall during maturation of the pollen grain. The reduction of PME48 activity also has consequences later on pollen tube morphology. The pollen tubes are slightly wider in the mutant, which may reflect the role of HG in the mechanical properties of the cell wall (Parre and Geitmann, 2005a; Palin and Geitmann, 2012) and corroborates the predictions made by mechanical simulations (Chebli and Geitmann, 2007; Zerzour et al., 2009; Fayant et al., 2010). The more abundant highly methylesterified HG in the intine wall of *pme48−/−* pollen grains and at the tip and in the subapical region of *pme48−/−* pollen tubes provides more viscoelasticity and less rigidity of the cell wall, thus promoting several tips emerging from the pollen grain and wider diameters of pollen tubes, probably due to the internal turgor pressure (Parre and Geitmann, 2005a; Winship et al., 2010).

Mature pollen grains are surrounded by two cell walls: the outer exine and the inner intine. In many species, such as tobacco (Li et al., 1995), Arabidopsis (Van Aelst and Van Went, 1992; Rhee and Somerville, 1998), *Lilium hybrida* (Aouali et al., 2001), *Euphorbia peplus* (Suárez-Cervera et al., 2002), *Zygophyllum fabago* (Castells et al., 2003), and *Larix decidua* (Rafińska et al., 2014), the intine of mature pollen grains is mostly composed of weakly methylesterified HG or a mix of highly and weakly methylesterified HGs, the latter being more abundant. The almost absent labeling of weakly methylesterified HG with John Innes Monoclonal5 at the pollen mother cell and tetrad stages (Rhee and Somerville, 1998) but its strong detection in the intine at the late microspore stage and mature dry Arabidopsis pollen grains (Van Aelst and Van Went, 1992; Rhee and Somerville, 1998) indicate an early action of PMEs during pollen formation and maturation. HG polymers are synthesized in the Golgi apparatus and may be secreted under a highly methylesterified form and then processed in the cell wall by PMEs (Zhang and Staehelin, 1992; Caffall and Mohnen, 2009; Harholt et al., 2010). This is consistent with our qRT-PCR results showing that pollen-specific PMEs, including *PME48*, are strongly expressed in dry pollen grains. A similar pattern of expression of these *PMEs* was obtained previously in two transcriptomic analyses of dry pollen grains and pollen tubes (Wang et al., 2008; Qin et al., 2009). Moreover, proteomic analyses of Arabidopsis revealed the presence of at least three PMEs in mature pollen grains: PME37, PPME1, and PME48 (Holmes-Davis et al., 2005; Ge et al., 2011). Similarly, at least two PMEs were found in the

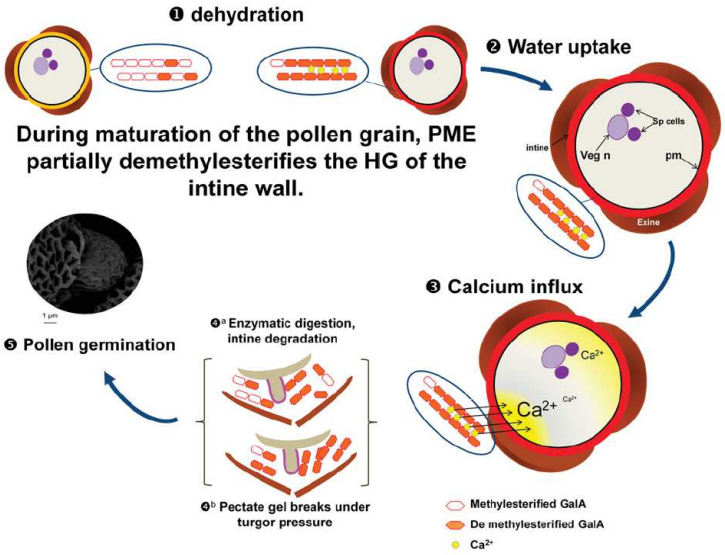

Figure 7. Model showing the possible mode of action of PME48 during pollen dehydration, imbibition, and germination. 1, PME48 may be secreted in the intine wall during the maturation of the pollen grain and start to act on the methylesterified form of the HG by random or block-wise actions. Methylesterified HG of the intine (black) is then transformed in weakly methylesterified HG (orange). The dry pollen grain contains mostly weakly esterified HG that could form pectate gel with calcium. 2, Imbibition of the pollen grain is enhanced by the presence of the more hydrophilic weakly methylesterified HG. 3, The source of calcium creating the calcium influx in the pollen grain may originate, at least partially, from the release of Ca^{2+} from the pectate gel, thus weakening the mechanical properties of the intine. 4, The intine may be degraded by PGases and/or PLs (a) and/or break under the turgor pressure (b). 5, These processes may promote the emergence of the pollen tube tip and allow the germination of the pollen grain. GalA, (1,4)-α-D-GalUA; pm, plasma membrane; Sp, sperm cells; Veg n, vegetative nucleus.

proteome of rice (*Oryza sativa*; Dai et al., 2006) and maize (Zhu et al., 2011) dry pollen grains.

The early demethylesterification of HG by PME48 during pollen formation and maturation (Fig. 7) may have three major consequences. First, the removal of hydrophobic methylester groups can enhance the hydrophilic properties of the cell wall, thus promoting pollen grain hydration (Fig. 7). The DM of HG can affect the water-holding capacity of the pectate gel (Willats et al., 2001), leading to water loss and changes of the physical properties of the pectate gel, which appeared to collapse under pressure (Willats et al., 2001). The *mucilage modified2* (*mum2*) mutant (impaired in the expression of a β-galactosidase) failed to properly hydrate the seed mucilage (Macquet et al., 2007). Interestingly, in the mucilage of *mum2*, the content of methylesterified HG increased compared with the wild type, suggesting that (1) β-galactosidase may be required for PME activity (Western et al., 2001; Walker et al., 2011) and (2) PME activity is required for the hydration of HGs. This observation may explain why, in the *pme48−/−* mutant lines, the imbibition and germination of pollen grains were strongly delayed, as the DM of the HG in the intine of *pme48−/−* is almost 2.5-fold higher than in the wild type. Second, upon the block-wise action of PMEs, deesterified blocks of HG chains can be cross-linked with calcium (Micheli, 2001). During wild-type pollen grain formation and maturation, the activity of PME48 promotes the release of negative charges of the carboxylic groups, allowing the interaction of calcium with the HG chains. The main Ca^{2+} sink in the plant cell wall is the demethylesterified HG (Wolf et al., 2009a; Hepler et al., 2012). Thus, the unesterified HG in the maturing pollen grain may act as a reservoir of Ca^{2+} that will be used later during rehydration and germination (Fig. 7). The reduction of PME activity in *pme48−/−* may locally affect the binding capacity of calcium ions by HGs. This possibly may explain the reverse phenotype observed in the calcium-supplemented GM. In vitro pollen germination of many species requires Ca^{2+} (Brewbaker and Kwack, 1963; Ge et al., 2007), and Ca^{2+} plays a central role during pollen germination (Brewbaker and Kwack, 1963; Ge et al., 2007; Hepler et al., 2012), acting putatively as a signal to activate the germination process and/or acting directly on the physical property of the intine. Ca^{2+} dynamics have been investigated in Arabidopsis pollen grains during germination (Iwano et al., 2004).

Those authors have shown that, during pollen grain hydration, cytoplasmic Ca^{2+} increased at the future site of protrusion of the pollen tube tip but not exclusively, as, often, an increase also was observed at the opposite site (Fig. 7). The early action of PME48 during the maturation and dehydration of pollen grains and the accumulation of Ca^{2+} in the intine may help to prepare the future protrusion of the pollen tube tip by weakening the intine wall (Fig. 7). Recently, Rafińska et al. (2014) suggested that the cell wall of the female tissues also can act as a reservoir of Ca^{2+} in order to ensure correct germination and pollen tube growth in *L. decidua*. Upon pollination, an increase of Ca^{2+} concentration also was observed in the stigma and transmitting tract of lily (Zhao et al., 2004) and tobacco (Ge et al., 2009). This observation may explain why the impact of the *PME48* mutation on in vivo pollen germination and tube growth was not as dramatic as that in vitro in the optimum solid GM. However, we cannot rule out that PMEs originating from the stigma also may participate in this process or that pollen grains cultured in in vitro and semi-in vivo conditions display a different gene expression pattern (Qin et al., 2009).

As discussed by Jolie et al. (2010), the pH, the DM, and the pattern of methylesterification are known to modify the mode of action of PMEs (Catoire et al., 1998; Denès et al., 2000; Sénéchal et al., 2014). Thus, we can also hypothesize that, upon random action of the PME (PME48 or others from the 13 other pollen-specific PMEs), the partial removal of methylester groups may allow other pectin-degrading enzymes such as PGases and/or PLs to cleave the HG, affecting the rigidity of the cell wall (Micheli, 2001; Sénéchal et al., 2014). In the Arabidopsis genome, 69 annotated genes can be classified as putative PGases (González-Carranza et al., 2007). A semiquantitative RT-PCR analysis investigating 66 among the 69 genes coding for PGases showed that 32 genes were strongly expressed in flower tissues (Kim et al., 2006). Other studies also have shown that PGases were present in ungerminated pollen grains of *Brassica napus* (Dearnaley and Daggard, 2001) and during hydration of *Platanus acerifolia* pollen grains (Suárez-Cervera et al., 2005). In addition, in *Brassica campestris*, alteration of the expression of *B. campestris MALE FERTILITY2* (coding for a putative PGase) resulted in an overdeveloped intine and abnormal germination (Huang et al., 2009). The transcriptome analysis of Arabidopsis pollen grains has revealed that six genes coding for putative PGases and four genes encoding putative PLs are strongly expressed in dry pollen grains and pollen tubes (for review, see Mollet et al., 2013). Taken together, these observations suggest that the early action of PME48 during maturation of the pollen grain also may be required to ensure the future degradation of the intine by PGases and PLs (Fig. 7). Enzymes originating from the stigma also may participate in the degradation of HGs in the intine. Such enzymes, including PGases, have been found in the exudates from lily and olive (*Olea europaea*) stigmas (Rejón et al., 2013).

Although pollen-specific PMEs are traditionally associated with pollen tube elongation, this study provides substantial evidence that PMEs, especially PME48, also are directly implicated in changes of the mechanical properties of the intine wall during maturation, promoting the correct germination of mature pollen grains.

MATERIALS AND METHODS

Plant Materials, Growth Conditions, and Mutant Genotyping

Arabidopsis (*Arabidopsis thaliana* ecotype Columbia-0) wild-type and mutant seeds, stored at 4°C, were spread on the surface of sterile soil and cultured in a growth chamber with a photoperiod of 16 h of light/8 h of dark at 20°C during the light phase and at 16°C in the dark phase with 60% humidity with daily watering.

pme48−/− (mutant of the *PME48* gene; At5g07410) seeds originated from the Arabidopsis Biological Resource Center and corresponded to SALK_122970 (T-DNA 1,403 bp downstream of ATG). Homozygous plants for the T-DNA insertion in the *PME48* gene were identified by PCR. Genotyping PCR was performed with primer pair PME48-F1 (5′-TGACAAGACCGTGTTCTACG-3′)/PME48-R1 (5′-GAAGAGAGGATTTCTGGAAATTGA-3′) and LB (5′-GCGTGGACCGCTTGCTGCAACT-3′) matching with the left border of the T-DNA.

qRT-PCR Analyses

Gene Expression of Pollen-Specific PMEs

Total RNA was extracted from pollen of 6-week-old wild-type and *pme48−/−* plants using the NucleoSpin RNA Plant Kit (Macherey-Nagel) as described by the supplier. After RNA quantification using NanoDrop spectrophotometry and a DNase treatment, 100 ng of RNA was converted into single complementary DNAs (cDNAs) with the QuantiTect Reverse Transcription Kit (Qiagen) following the instructions of the supplier.

Real-time quantitative PCR analyses were performed on 1:5 diluted cDNA. For real-time quantitative PCR, the LightCycler 480 SYBR Green I Master (Roche; catalog no. 04887352001) was used on 384-well plates in the LightCycler 480 Real-Time PCR System (Roche). The crossing threshold values for each sample (the number of PCR cycles required for the accumulated fluorescence signal to cross a threshold above the background) were acquired with the LightCycler 480 software (Roche) using the second derivative maximum method. Primers used are shown in Supplemental Table S1. Stably expressed reference genes (At3g28750, At3g57690, and At5g59370), specifically designed for this study on pollen grains, were selected using GeNorm software (Vandesompele et al., 2002). They were used as internal controls to calculate the relative expression of target genes according to the method described by Gutierrez et al. (2009). Each amplicon was first sequenced to ensure the specificity of the amplified sequence.

Analysis of PME48 Transcripts in Mutant Lines

The lack of *PME48* transcript in *pme48−/−* was checked by RT-PCR using PME48-F2 (5′-CTGGAACTGGAGGAGGAACT-3′) and PME48-R2 (5′-CATAAATCTCAACTCCTCCATG-3′). PCR was performed on the cDNA generated from total RNA extracted from 6-h-old pollen tubes grown in vitro. Primers used for the RT-PCR are in boldface and underlined in Supplemental Figure S1D.

Analysis of Promoter Activity

GUS Staining

Mutant seeds containing 1 kb of the promoter of At5g07410 upstream of the GUS coding sequence were generated as described by Louvet et al., (2006).

GUS staining was performed on dry pollen grains, in vitro-grown pollen tubes, and in vivo on self-pollinated flowers. Flower and dry pollen grain samples were fixed in cold acetone for 20 min and rinsed three times in 50 mM phosphate buffer, pH 7, containing 2 mM potassium ferricyanide, 2 mM

potassium ferrocyanide, and 0.2% (v/v) Triton X-100. In vitro-grown pollen tube samples were not incubated in acetone. Samples were then incubated for 16 h in the dark at 37°C in 50 mM phosphate buffer, pH 7, containing 1 mM 5-bromo-4-chloro-3-indolyl-β-glucuronic acid, 2 mM potassium ferricyanide, 2 mM potassium ferrocyanide, and 0.2% (v/v) Triton X-100. Flower samples were then cleared with several washes in 70% (v/v) ethanol.

Analysis of the Activity of the Promoter of PME48 Using YFP

The promoter of the PME48 gene (At5g07410) was PCR amplified from a plasmid construct containing this sequence cloned upstream of the GUS coding sequence in the pBI101.3 binary vector (Louvet et al., 2006). A ligation-independent cloning method was used to insert the promoter of the *PME48* gene (*pPME48*) upstream of the super YFP (Kremers et al., 2006) in a ligation-independent cloning binary vector, named pPLV06 (GenBank accession no. JF909459) and belonging to the set of plant ligation-independent cloning vectors made by De Rybel et al. (2011). This vector also contains the Simian Virus40 nuclear localization signal. The PCR-amplified promoter insert contained in the plasmid construct was subsequently verified by sequencing, and the plasmid was used to transform *Agrobacterium tumefaciens* GV3101::pSOUP (Hellens et al., 2000). Arabidopsis plants were transformed by floral dip as described by Zhang et al. (2006) and selected on kanamycin (25 mg L^{-1}).

In Vitro Pollen Tube Growth

Pollen grains were grown in vitro in a liquid medium according to the method described by Boavida and McCormick (2007). Briefly, flowers (40 per 1.5-mL tube) were submerged in 1 mL of GM (pH 7.5) containing 5 mM $CaCl_2$•$2H_2O$, 0.01% (w/v) H_3BO_3, 5 mM KCl, 1 mM $MgSO_4$•$7H_2O$, and 10% (w/v) Suc. Tubes were shaken with a vortex to release the pollen grains from the anthers. Flowers were removed with a pair of tweezers, and the pollen suspension was then centrifuged at 4,000*g* for 7 min. New GM (250 μL) was added to the pellet, and pollen grains were transferred into glass vials (14 × 45 mm) and grown in a growth chamber in the dark at 22°C. For solid medium culture, 1.5% agarose (Sigma) was added to the GM and deposited on a microscope slide. After polymerization, wild-type or mutant open flowers were gently brushed on the surface of the agarose pad to release the pollen grains. Glass slides were then placed in a growth chamber in the dark at 22°C under 100% relative humidity. Before any further manipulation, pollen germination and pollen tube growth were assessed with a microscope.

Twenty images per sample were acquired after 2, 4, 6, 8, 14, 16, and 24 h of culture, and the percentage of germination ($n > 10{,}000$) and the speed of growth of pollen tubes ($n > 35$) were measured using ImageJ software (Abràmoff et al., 2004). Germination assays and the speed of growth of pollen tubes were repeated six times. For measurement of the diameter of pollen tubes, wild-type and *pme48−/−* pollen grains were harvested by dabbing flowers onto silane-coated microscope slides. Slides were incubated at 30°C for 30 min in a moist chamber, subsequently covered with liquid GM, and grown for 4 h in a growth chamber in the dark at 22°C. The diameter of pollen tubes was determined on the images with ImageJ ($n = 126$ and $n = 172$ for wild-type and *pme48−/−* pollen tubes, respectively, from four independent experiments).

Pollen grains were also cultured in the GM supplemented with 1 mM EDTA or 2.5 mM $CaCl_2$•$2H_2O$ to reach the final concentration of 7.5 mM $CaCl_2$.

In Vivo Pollen Tube Growth

Emasculated mature flowers from wild-type plants were hand pollinated with wild-type or mutant (*pme48−/−*) pollen grains. The pollinated pistils were collected 6, 12, and 24 h after pollination and fixed in an ethanol:acetic acid (3:1, v/v) solution. The fixed pistils were rehydrated with successive baths of ethanol (70%, 50%, and 30% [v/v]), washed three times with distilled water, and treated overnight in a softening solution composed of 8 M NaOH. After several washes with distilled water, the pistil tissues were stained with decolorized Aniline Blue solution (0.1% [w/v] Aniline Blue in 100 mM K_2PO_4 buffer, pH 11) for 2 h in the dark (Johnson-Brousseau and McCormick, 2004).

Viability Test and DAPI Staining

The viability of pollen grains was assessed using FDA dissolved in acetone at 10 mg mL^{-1} and stored at −20°C. Prior to each experiment, FDA was diluted in a 10% Suc solution to a final concentration of 0.2 mg mL^{-1}. Hydrated pollen grains were dipped in 250 μL of the FDA solution on a glass slide and kept in the dark for 5 min. A minimum of 1,000 pollen grains were analyzed.

The nuclei of the pollen grains were stained with 10 μg mL^{-1} DAPI for 15 min in the dark at room temperature. At least 250 pollen grains were analyzed for each mutant or the wild type.

Immunolocalization of Highly Methylesterified HG Epitopes

Immunolocalization was performed by cell surface labeling as described previously by Dardelle et al. (2010) or on semithin sections. For the cell surface immunolabeling, pollen grains or pollen tubes in GM were mixed (v/v) with a fixation medium containing 100 mM PIPES buffer, pH 6.9, 4 mM $MgSO_4$•$7H_2O$, 4 mM EGTA, 10% (w/v) Suc, and 5% (w/v) formaldehyde and incubated for 90 min at room temperature. Pollen grains or pollen tubes were rinsed three times by centrifugation with 50 mM PIPES buffer, pH 6.9, 2 mM $MgSO_4$•$7H_2O$, and 2 mM EGTA and three times with phosphate-buffered saline (PBS; 100 mM potassium phosphate, pH 7.4, 138 mM NaCl, and 2.7 mM KCl).

For immunolocalization on semithin sections, dry pollen grains were fixed in ethanol:acetic acid (3:1, v/v) and rinsed in 75% (v/v) ethanol. After centrifugation, the pellet of pollen grains was embedded in a block of 2% (w/v) agarose. The block was then incubated in 75%, 95%, and 100% (v/v) ethanol for 1.5 h each at room temperature. Pollen grains were then transferred in increasing concentrations of methacrylate (25%, 50%, 75%, and 100%) according to Baskin et al. (1992). The resin was polymerized at 4°C for 24 h under UV light. Semithin sections (1 μm) were obtained with the EM UC6 ultramicrotome (Leica) and deposited on poly-L-Lys-coated microscope slides.

Samples were then incubated overnight at 4°C with the LM20 antibody that recognizes methylesterified HG epitopes (Verhertbruggen et al., 2009; diluted 1:5 with PBS + 3% [w/v] milk). Samples were rinsed three times with PBS and incubated for 3 h at 30°C with the secondary antibody, a goat anti-rat IgG (whole molecule)-fluorescein isothiocyanate, diluted 1:100. Controls were carried out by incubation of pollen grains or pollen tubes with the secondary antibody only.

Image Acquisition

Pollen grains and pollen tubes were observed under bright-field and fluorescence illumination on a Leica DLMB microscope equipped with the FDA filter (absorption, 470; emission, 520–560 wavelength) under UV illumination for DAPI and decolorized Aniline Blue staining (absorption, 358; emission, 461 wavelength) or fluorescein isothiocyanate filter (absorption, 490; emission, 520 wavelength). Images were acquired with the Leica DFC300FX camera. Pollen grains and pollen tubes expressing *pPME48::YFP* were observed with a laser scanning confocal microscope (Leica TCS SP2 AOBS). YFP was visualized using the 488-nm laser line of an argon laser with a 510- to 530-nm band-pass filter. Pollen grains were also observed using the Hitachi TM3000 tabletop scanning electron microscope in analytical mode. Time-lapse imaging was performed with the inverted Leica DMI 6000B microscope equipped with the Leica DFC450C camera.

FT-IR Spectroscopy

Eight milligrams of pollen grains from wild-type or mutant plants was collected with the vacuum-pollen method described by Johnson-Brousseau and McCormick (2004). After removing the flower debris with tweezers, pollen grains were placed into microcentrifuge tubes containing 96% ethanol. After several washes, the samples were dried overnight under a fume hood. Pollen grains were then incubated for 1 h in 200 μL of sterilized water at 100°C. After a speed vacuum treatment to eliminate water, samples were oven dried for 48 h to obtain a pectin-enriched fraction. This fraction was stored in a sealed container with silica gel prior to FT-IR analysis. Dry samples were analyzed with an OMNI-Sampler FT-IR spectroscope (version 5.2a) at 4 cm^{-1} resolution. The DM was calculated using the absorbance intensities at 1,630 and 1,740 cm^{-1} assigned to the vibration of carboxyl groups of (1,4)-α-D-GalUA and its methylester form, respectively (Gribaa et al., 2013), using the equation described by Gnanasambandam and Proctor (2000) and Manrique and Lajolo (2002): $DM = A_{1,740} / (A_{1,740} + A_{1,630})$. Commercial pectins with determined DM were used as controls. Using this method, the DM of pectin from citrus (*Citrus*

spp.) fruit with 85% DM (Sigma) gave 75.1% ± 2.5% DM, pectin from citrus fruit with 55% to 70% DM (Sigma) gave 60.5% ± 1.5% DM, pectin from citrus fruit with 20% to 30% DM (Sigma) gave 26.9% ± 3.4% DM, and pectate sodium pectin from citrus fruit with DM of 8.6% (Sigma) gave 10.8% ± 0.9% DM. Three biological replicates for the wild type and the mutant were analyzed, and 10 acquisitions were acquired per biological sample.

Protein Extraction and Enzymatic Assay

Total proteins were extracted by grinding 2 mg of dry pollen grains in 50 mM sodium phosphate buffer, pH 7.5, 12.5 mM citric acid, 1 M NaCl, 0.2% (w/v) polyvinylpolypyrrolidone, and 0.01% (w/v) Tween 20 plus one tablet of protease inhibitor cocktail (Roche) for one night at 4°C. Cellular fragments were discarded by centrifugation at 10,000*g* for 45 min. The crude protein extract was concentrated by ultrafiltration on Amicon PM10 membranes (Millipore) in 50 mM sodium phosphate buffer, pH 7.5. Proteins were quantified by the micromethod of Bradford (1976), with the Bio-Rad kit and bovine serum albumin as a standard. PME activity was measured using the alcohol oxidase method according to Klavons and Bennett (1986). One international unit of PME activity induces the production of 1 μmol of methanol per min.

IEF and Zymography

IEF and zymography were performed as described by Paynel et al. (2014). Briefly, IEF of native proteins was performed on ultrathin polyacrylamide gels with a 6 to 10.5 pH range (Pharmalytes) in 5% acrylamide according to the manufacturer's procedure with the Multiphor II system (LKB Pharmacia). The pH gradient was measured with a contact electrode (pH Inlab 426; VWR International) along a central gel strip. Samples (20 μL) were loaded at the anodic side. After IEF, gels were washed for 15 to 30 min in 20 mM Tris-HCl, pH 8.5, and 5 mM EDTA. Activity of PME was then monitored in gel (zymogram) by using a sandwich of 1% (w/v) citrus pectin with a DM of 85% (Sigma) and 1% (w/v) agar according to Bertheau et al. (1984). The gel was incubated for 1 h at 25°C, and the demethylated pectins resulting from PME activities were precipitated with 0.1 M malic acid and stained with 0.02% (w/v) Ruthenium Red.

Statistical Analysis

Data were statistically treated using the GraphPad software (www.graphpad.com).

Supplemental Data

The following supplemental materials are available.

Supplemental Figure S1. Genomic organization of the *PME48* gene, location of the T-DNA, *PME48* expression in the mutant, and transcript sequence of *PME48*.

Supplemental Figure S2. Viability and phenotypic characteristics of wild-type and mutant lines.

Supplemental Figure S3. Germination rates of wild-type and *pme48−/−* pollen grains in liquid medium.

Supplemental Figure S4. Estimation of the growth speed in liquid medium of wild-type and *pme48−/−* pollen tubes.

Supplemental Table S1. List of primer pairs used for the qRT-PCR analyses.

Supplemental Movie S1. Time-lapse imaging of germination and tube growth of wild-type pollen grains.

Supplemental Movie S2. Time-lapse imaging of germination and tube growth of *pme48−/−* pollen grains.

ACKNOWLEDGMENTS

We thank the Research Network Végétal, Agronomie, Sol, et Innovation, PRIMACEN (Regional Platform for Cell Imaging), part of the Institute for Research and Innovation in Biomedicine of the Region Haute-Normandie, and the Fonds Européen de Développement Régional for the use of equipment. We also thank Dr. Claudine Morvan (Polymères, Biopolymères Surfaces, University of Rouen) for help on FT-IR analyses; Gaëlle Lucas and Carole Plasson (Glycobiologie et Matrice Extracellulaire Végétale, University of Rouen) for technical contributions in molecular biology and plant culture; and Dr. Bert De Rybel and Dolf Weijers (Laboratory of Biochemistry, Wageningen University) for the gift of the pPLV06 plasmid.

Received September 22, 2014; accepted December 16, 2014; published December 18, 2014.

LITERATURE CITED

Abràmoff MD, Magalhães PJ, Ram SJ (2004) Image processing with ImageJ. Biophotonics Int **11:** 36–42

Aouali N, Laporte P, Clément C (2001) Pectin secretion and distribution in the anther during pollen development in *Lilium*. Planta **213:** 71–79

Baskin TI, Busby CH, Fowke LC, Sammut M, Gubler F (1992) Improvements in immunostaining samples embedded in methacrylate: localization of microtubules and other antigens throughout developing organs in plants of diverse taxa. Planta **187:** 405–413

Bertheau Y, Madgidi-Hervan E, Kotoujansky A, Nguyen-The C, Andro T, Coleno A (1984) Detection of depolymerase isoenzymes after electrophoresis or electrofocusing, or in titration curves. Anal Biochem **139:** 383–389

Bethke G, Grundman RE, Sreekanta S, Truman W, Katagiri F, Glazebrook J (2014) Arabidopsis PECTIN METHYLESTERASEs contribute to immunity against *Pseudomonas syringae*. Plant Physiol **164:** 1093–1107

Boavida LC, McCormick S (2007) Temperature as a determinant factor for increased and reproducible *in vitro* pollen germination in *Arabidopsis thaliana*. Plant J **52:** 570–582

Bosch M, Cheung AY, Hepler PK (2005) Pectin methylesterase, a regulator of pollen tube growth. Plant Physiol **138:** 1334–1346

Bosch M, Hepler PK (2005) Pectin methylesterases and pectin dynamics in pollen tubes. Plant Cell **17:** 3219–3226

Bouton S, Leboeuf E, Mouille G, Leydecker MT, Talbotec J, Granier F, Lahaye M, Höfte H, Truong HN (2002) *QUASIMODO1* encodes a putative membrane-bound glycosyltransferase required for normal pectin synthesis and cell adhesion in *Arabidopsis*. Plant Cell **14:** 2577–2590

Bove J, Vaillancourt B, Kroeger J, Hepler PK, Wiseman PW, Geitmann A (2008) Magnitude and direction of vesicle dynamics in growing pollen tubes using spatiotemporal image correlation spectroscopy and fluorescence recovery after photobleaching. Plant Physiol **147:** 1646–1658

Bradford MM (1976) A rapid and sensitive method for the quantitation of microgram quantities of protein utilizing the principle of protein-dye binding. Anal Biochem **72:** 248–254

Brewbaker JL, Kwack BH (1963) The essential role of calcium ion in pollen germination and pollen tube growth. Am J Bot **50:** 859–865

Brummell DA, Harpster MH (2001) Cell wall metabolism in fruit softening and quality and its manipulation in transgenic plants. Plant Mol Biol **47:** 311–340

Caffall KH, Mohnen D (2009) The structure, function, and biosynthesis of plant cell wall pectic polysaccharides. Carbohydr Res **344:** 1879–1900

Castells T, Seoane-Camba JA, Suárez-Cervera M (2003) Intine wall modifications during germination of *Zygophyllum fabago* (Zygophyllaceae) pollen grains. Can J Bot **81:** 1267–1277

Catoire L, Pierron M, Morvan C, du Penhoat CH, Goldberg R (1998) Investigation of the action patterns of pectinmethylesterase isoforms through kinetic analyses and NMR spectroscopy: implications in cell wall expansion. J Biol Chem **273:** 33150–33156

Chebli Y, Geitmann A (2007) Mechanical principles governing pollen tube growth. Funct Plant Sci Biotech **1:** 232–245

Chebli Y, Kaneda M, Zerzour R, Geitmann A (2012) The cell wall of the Arabidopsis pollen tube: spatial distribution, recycling, and network formation of polysaccharides. Plant Physiol **160:** 1940–1955

Dai S, Li L, Chen T, Chong K, Xue Y, Wang T (2006) Proteomic analyses of *Oryza sativa* mature pollen reveal novel proteins associated with pollen germination and tube growth. Proteomics **6:** 2504–2529

Dardelle F, Lehner A, Ramdani Y, Bardor M, Lerouge P, Driouich A, Mollet JC (2010) Biochemical and immunocytological characterizations of Arabidopsis pollen tube cell wall. Plant Physiol **153:** 1563–1576

Dearnaley JD, Daggard GA (2001) Expression of a polygalacturonase enzyme in germinating pollen of *Brassica napus*. Sex Plant Reprod **13:** 265–271

Denès JM, Baron A, Renard CM, Péan C, Drilleau JF (2000) Different action patterns for apple pectin methylesterase at pH 7.0 and 4.5. Carbohydr Res **327:** 385–393

Derksen J, Knuiman B, Hoedemaekers K, Guyon A, Bonhomme S, Pierson ES (2002) Growth and cellular organization of *Arabidopsis* pollen tubes *in vitro*. Sex Plant Reprod **15:** 133–139

De Rybel B, van den Berg W, Lokerse A, Liao CY, van Mourik H, Möller B, Peris CL, Weijers D (2011) A versatile set of ligation-independent cloning vectors for functional studies in plants. Plant Physiol **156:** 1292–1299

Dumont M, Lehner A, Bouton S, Kiefer-Meyer MC, Voxeur A, Pelloux J, Lerouge P, Mollet JC (2014) The cell wall pectic polymer rhamnogalacturonan-II is required for proper pollen tube elongation: implications of a putative sialyltransferase-like protein. Ann Bot (Lond) **114:** 1177–1188

Durand C, Vicré-Gibouin M, Follet-Gueye ML, Duponchel L, Moreau M, Lerouge P, Driouich A (2009) The organization pattern of root border-like cells of Arabidopsis is dependent on cell wall homogalacturonan. Plant Physiol **150:** 1411–1421

Fayant P, Girlanda O, Chebli Y, Aubin CE, Villemure I, Geitmann A (2010) Finite element model of polar growth in pollen tubes. Plant Cell **22:** 2579–2593

Ferguson C, Teeri TT, Siika-Aho M, Read SM, Bacic A (1998) Location of cellulose and callose in pollen tubes and grains of *Nicotiana tabacum*. Planta **206:** 452–460

Francis KE, Lam SY, Copenhaver GP (2006) Separation of Arabidopsis pollen tetrads is regulated by *QUARTET1*, a pectin methylesterase gene. Plant Physiol **142:** 1004–1013

Fry SC (2011) Cell wall polysaccharide composition and covalent cross-linking. Annu Plant Rev **41:** 1–42

Ge LL, Tian HQ, Russell SD (2007) Calcium function and distribution during fertilization in angiosperms. Am J Bot **94:** 1046–1060

Ge LL, Xie CT, Tian HQ, Russell SD (2009) Distribution of calcium in the stigma and style of tobacco during pollen germination and tube elongation. Sex Plant Reprod **22:** 87–96

Ge W, Song Y, Zhang C, Zhang Y, Burlingame AL, Guo Y (2011) Proteomic analyses of apoplastic proteins from germinating *Arabidopsis thaliana* pollen. Biochim Biophys Acta **1814:** 1964–1973

Geitmann A, Steer M (2006) The architecture and properties of the pollen tube cell wall. In **R Malho**, ed, The Pollen Tube: Plant Cell Monographs, **Vol 3**. Springer-Verlag, Berlin, pp 177–200

Gnanasambandam R, Proctor A (2000) Determination of pectin degree of esterification by diffuse reflectance Fourier transform infrared spectroscopy. Food Chem **68:** 327–332

González-Carranza ZH, Elliott KA, Roberts JA (2007) Expression of polygalacturonases and evidence to support their role during cell separation processes in *Arabidopsis thaliana*. J Exp Bot **58:** 3719–3730

Gribaa A, Dardelle F, Lehner A, Rihouey C, Burel C, Ferchichi A, Driouich A, Mollet JC (2013) Effect of water deficit on the cell wall of the date palm (Phoenix dactylifera 'Deglet nour', Arecales) fruit during development. Plant Cell Environ **36:** 1056–1070

Guan Y, Guo J, Li H, Yang Z (2013) Signaling in pollen tube growth: crosstalk, feedback, and missing links. Mol Plant **6:** 1053–1064

Guénin S, Mareck A, Rayon C, Lamour R, Assoumou Ndong Y, Domon JM, Sénéchal F, Fournet F, Jamet E, Canut H, et al (2011) Identification of pectin methylesterase 3 as a basic pectin methylesterase isoform involved in adventitious rooting in *Arabidopsis thaliana*. New Phytol **192:** 114–126

Gutierrez L, Bussell JD, Păcurar DI, Schwambach J, Păcurar M, Bellini C (2009) Phenotypic plasticity of adventitious rooting in *Arabidopsis* is controlled by complex regulation of AUXIN RESPONSE FACTOR transcripts and microRNA abundance. Plant Cell **21:** 3119–3132

Harholt J, Suttangkakul A, Vibe Scheller H (2010) Biosynthesis of pectin. Plant Physiol **153:** 384–395

Hellens RP, Edwards EA, Leyland NR, Bean S, Mullineaux PM (2000) pGreen: a versatile and flexible binary Ti vector for Agrobacterium-mediated plant transformation. Plant Mol Biol **42:** 819–832

Hepler PK, Kunkel JG, Rounds CM, Winship LJ (2012) Calcium entry into pollen tubes. Trends Plant Sci **17:** 32–38

Holmes-Davis R, Tanaka CK, Vensel WH, Hurkman WJ, McCormick S (2005) Proteome mapping of mature pollen of *Arabidopsis thaliana*. Proteomics **5:** 4864–4884

Hruz T, Laule O, Szabo G, Wessendorp F, Bleuler S, Oertle L, Widmayer P, Gruissem W, Zimmermann P (2008) Genevestigator v3: a reference expression database for the meta-analysis of transcriptomes. Adv Bioinformatics **2008:** 420747

Huang L, Cao J, Zhang A, Ye Y, Zhang Y, Liu T (2009) The polygalacturonase gene *BcMF2* from *Brassica campestris* is associated with intine development. J Exp Bot **60:** 301–313

Iwano M, Shiba H, Miwa T, Che FS, Takayama S, Nagai T, Miyawaki A, Isogai A (2004) Ca^{2+} dynamics in a pollen grain and papilla cell during pollination of Arabidopsis. Plant Physiol **136:** 3562–3571

Jauh GY, Lord EM (1996) Localization of pectins and arabinogalactan-proteins in lily (*Lilium longiflorum* L.) pollen tube and style, and their possible roles in pollination. Planta **199:** 251–261

Jiang L, Yang SL, Xie LF, Puah CS, Zhang XQ, Yang WC, Sundaresan V, Ye D (2005) *VANGUARD1* encodes a pectin methylesterase that enhances pollen tube growth in the *Arabidopsis* style and transmitting tract. Plant Cell **17:** 584–596

Johnson MA, Lord EM (2006) Extracellular guidance cues and intracellular signaling pathways that direct pollen tube growth. In **R Malho**, ed, The Pollen Tube: A Cellular and Molecular Perspective, **Vol 3**. Springer, Heidelberg, pp 223–242

Johnson-Brousseau SA, McCormick S (2004) A compendium of methods useful for characterizing Arabidopsis pollen mutants and gametophytically-expressed genes. Plant J **39:** 761–775

Jolie RP, Duvetter T, Van Loey AM, Hendrickx ME (2010) Pectin methylesterase and its proteinaceous inhibitor: a review. Carbohydr Res **345:** 2583–2595

Kim J, Shiu SH, Thoma S, Li WH, Patterson SE (2006) Patterns of expansion and expression divergence in the plant polygalacturonase gene family. Genome Biol **7:** R87

Klavons JA, Bennett AD (1986) Determination of methanol using alcohol oxidase and its application to methyl ester content of pectins. J Agric Food Chem **34:** 597–599

Kremers GJ, Goedhart J, van Munster EB, Gadella TW Jr (2006) Cyan and yellow super fluorescent proteins with improved brightness, protein folding, and FRET Förster radius. Biochemistry **45:** 6570–6580

Lennon KA, Lord EM (2000) In vivo pollen tube cell of *Arabidopsis thaliana*. I. Tube cell cytoplasm and wall. Protoplasma **214:** 45–56

Li YQ, Chen F, Linskens HF, Cresti M (1994) Distribution of unesterified and esterified pectins in cell walls of pollen tubes of flowering plants. Sex Plant Reprod **7:** 145–152

Li YQ, Faleri C, Geitmann A, Zhang HQ, Cresti M (1995) Immunogold localization of arabinogalactan proteins, unesterified and esterified pectins in pollen grains and pollen tubes of *Nicotiana tabacum* L. Protoplasma **189:** 26–36

Louvet R, Cavel E, Gutierrez L, Guénin S, Roger D, Gillet F, Guerineau F, Pelloux J (2006) Comprehensive expression profiling of the pectin methylesterase gene family during silique development in *Arabidopsis thaliana*. Planta **224:** 782–791

Macquet A, Ralet MC, Loudet O, Kronenberger J, Mouille G, Marion-Poll A, North HM (2007) A naturally occurring mutation in an *Arabidopsis* accession affects a β-D-galactosidase that increases the hydrophilic potential of rhamnogalacturonan I in seed mucilage. Plant Cell **19:** 3990–4006

Manrique GD, Lajolo FM (2002) FT-IR spectroscopy as a tool for measuring degree of methyl esterification in pectins isolated from ripening papaya fruit. Postharvest Biol Technol **25:** 99–107

Micheli F (2001) Pectin methylesterases: cell wall enzymes with important roles in plant physiology. Trends Plant Sci **6:** 414–419

Mollet JC, Leroux C, Dardelle F, Lehner A (2013) Cell wall composition, biosynthesis and remodeling during pollen tube growth. Plants **2:** 107–147

Mollet JC, Park SY, Nothnagel EA, Lord EM (2000) A lily stylar pectin is necessary for pollen tube adhesion to an in vitro stylar matrix. Plant Cell **12:** 1737–1750

Mouille G, Ralet MC, Cavelier C, Eland C, Effroy D, Hématy K, McCartney L, Truong HN, Gaudon V, Thibault JF, et al (2007) Homogalacturonan synthesis in *Arabidopsis thaliana* requires a Golgi-localized protein with a putative methyltransferase domain. Plant J **50:** 605–614

Nguema-Ona E, Coimbra S, Vicré-Gibouin M, Mollet JC, Driouich A (2012) Arabinogalactan proteins in root and pollen-tube cells: distribution and functional aspects. Ann Bot (Lond) **110:** 383–404

Palanivelu R, Tsukamoto T (2012) Pathfinding in angiosperm reproduction: pollen tube guidance by pistils ensures successful double fertilization. Wiley Interdiscip Rev Dev Biol **1:** 96–113

Palin R, Geitmann A (2012) The role of pectin in plant morphogenesis. Biosystems **109:** 397–402

Parre E, Geitmann A (2005a) Pectin and the role of the physical properties of the cell wall in pollen tube growth of *Solanum chacoense*. Planta **220:** 582–592

Parre E, Geitmann A (2005b) More than a leak sealant: the mechanical properties of callose in pollen tubes. Plant Physiol **137:** 274–286

Paynel F, Leroux C, Surcouf O, Schaumann A, Pelloux J, Driouich A, Mollet JC, Lerouge P, Lehner A, Mareck A (2014) Kiwi fruit PMEI inhibits PME activity, modulates root elongation and induces pollen tube burst in *Arabidopsis thaliana*. Plant Growth Regul **74:** 285–297

Peaucelle A, Braybrook SA, Le Guillou L, Bron E, Kuhlemeier C, Höfte H (2011) Pectin-induced changes in cell wall mechanics underlie organ initiation in *Arabidopsis*. Curr Biol **21:** 1720–1726

Peaucelle A, Louvet R, Johansen JN, Höfte H, Laufs P, Pelloux J, Mouille G (2008) Arabidopsis phyllotaxis is controlled by the methyl-esterification status of cell-wall pectins. Curr Biol **18:** 1943–1948

Phan TD, Bo W, West G, Lycett GW, Tucker GA (2007) Silencing of the major salt-dependent isoform of pectinesterase in tomato alters fruit softening. Plant Physiol **144:** 1960–1967

Qin Y, Chen D, Zhao J (2007) Localization of arabinogalactan proteins in anther, pollen, and pollen tube of *Nicotiana tabacum* L. Protoplasma **231:** 43–53

Qin Y, Leydon AR, Manziello A, Pandey R, Mount D, Denic S, Vasic B, Johnson MA, Palanivelu R (2009) Penetration of the stigma and style elicits a novel transcriptome in pollen tubes, pointing to genes critical for growth in a pistil. PLoS Genet **5:** e1000621

Rafińska K, Świdziński M, Bednarska-Kozakiewicz E (2014) Homogalacturonan deesterification during pollen-ovule interaction in *Larix decidua* Mill.: an immunocytochemical study. Planta **240:** 195–208

Rejón JD, Delalande F, Schaeffer-Reiss C, Carapito C, Zienkiewicz K, de Dios Alché J, Rodríguez-García MI, Van Dorsselaer A, Castro AJ (2013) Proteomics profiling reveals novel proteins and functions of the plant stigma exudate. J Exp Bot **64:** 5695–5705

Rhee SY, Somerville CR (1998) Tetrad pollen formation in *quartet* mutants of *Arabidopsis thaliana* is associated with persistence of pectic polysaccharides of the pollen mother cell wall. Plant J **15:** 79–88

Röckel N, Wolf S, Kost B, Rausch T, Greiner S (2008) Elaborate spatial patterning of cell-wall PME and PMEI at the pollen tube tip involves PMEI endocytosis, and reflects the distribution of esterified and de-esterified pectins. Plant J **53:** 133–143

Roy S, Eckard KJ, Lancelle S, Hepler PK, Lord EM (1997) High-pressure freezing improves the ultrastructural preservation of *in vivo* grown lily pollen tubes. Protoplasma **200:** 87–98

Sénéchal F, Wattier C, Rustérucci C, Pelloux J (2014) Homogalacturonan-modifying enzymes: structure, expression, and roles in plants. J Exp Bot **65:** 5125–5160

Suárez-Cervera M, Arcalis E, Le Thomas A, Seoane-Camba JA (2002) Pectin distribution pattern in the apertural intine of *Euphorbia peplus* L. (Euphorbiaceae) pollen. Sex Plant Reprod **14:** 291–298

Suárez-Cervera M, Asturias JA, Vega-Maray A, Castells T, López-Iglesias C, Ibarrola I, Arilla MC, Gabarayeva N, Seoane-Camba JA (2005) The role of allergenic proteins Pla a1 and Pla a2 in the germination of *Platanus acerifolia* pollen grains. Sex Plant Reprod **18:** 101–112

Tian GW, Chen MH, Zaltsman A, Citovsky V (2006) Pollen-specific pectin methylesterase involved in pollen tube growth. Dev Biol **294:** 83–91

Tieman DM, Handa AK (1994) Reduction in pectin methylesterase activity modifies tissue integrity and cation levels in ripening tomato (*Lycopersicon esculentum* Mill.) fruits. Plant Physiol **106:** 429–436

Van Aelst AC, Van Went JL (1992) Ultrastructural immuno-localization of pectins and glycoproteins in *Arabidopsis thaliana* pollen grains. Protoplasma **168:** 14–19

Vandesompele J, De Preter K, Pattyn F, Poppe B, Van Roy N, De Paepe A, Speleman F (2002) Accurate normalization of real-time quantitative RT-PCR data by geometric averaging of multiple internal control genes. Genome Biol **3:** research0034

Verhertbruggen Y, Marcus SE, Haeger A, Ordaz-Ortiz JJ, Knox JP (2009) An extended set of monoclonal antibodies to pectic homogalacturonan. Carbohydr Res **344:** 1858–1862

Vincken JP, Schols HA, Oomen RJ, McCann MC, Ulvskov P, Voragen AG, Visser RG (2003) If homogalacturonan were a side chain of rhamnogalacturonan I: implications for cell wall architecture. Plant Physiol **132:** 1781–1789

Vogler H, Draeger C, Weber A, Felekis D, Eichenberger C, Routier-Kierzkowska AL, Boisson-Dernier A, Ringli C, Nelson BJ, Smith RS, et al (2013) The pollen tube: a soft shell with a hard core. Plant J **73:** 617–627

Walker M, Tehseen M, Doblin MS, Pettolino FA, Wilson SM, Bacic A, Golz JF (2011) The transcriptional regulator LEUNIG_HOMOLOG regulates mucilage release from the Arabidopsis testa. Plant Physiol **156:** 46–60

Wang Y, Zhang WZ, Song LF, Zou JJ, Su Z, Wu WH (2008) Transcriptome analyses show changes in gene expression to accompany pollen germination and tube growth in Arabidopsis. Plant Physiol **148:** 1201–1211

Wen F, Zhu Y, Hawes MC (1999) Effect of pectin methylesterase gene expression on pea root development. Plant Cell **11:** 1129–1140

Western TL, Burn J, Tan WL, Skinner DJ, Martin-McCaffrey L, Moffatt BA, Haughn GW (2001) Isolation and characterization of mutants defective in seed coat mucilage secretory cell development in Arabidopsis. Plant Physiol **127:** 998–1011

Willats WGT, Orfila C, Limberg G, Buchholt HC, van Alebeek GJ, Voragen AG, Marcus SE, Christensen TM, Mikkelsen JD, Murray BS, et al (2001) Modulation of the degree and pattern of methyl-esterification of pectic homogalacturonan in plant cell walls: implications for pectin methyl esterase action, matrix properties, and cell adhesion. J Biol Chem **276:** 19404–19413

Winship LJ, Obermeyer G, Geitmann A, Hepler PK (2010) Under pressure, cell walls set the pace. Trends Plant Sci **15:** 363–369

Winter D, Vinegar B, Nahal H, Ammar R, Wilson GV, Provart NJ (2007) An "Electronic Fluorescent Pictograph" browser for exploring and analyzing large-scale biological data sets. PLoS ONE **2:** e718

Wolf S, Mouille G, Pelloux J (2009a) Homogalacturonan methyl-esterification and plant development. Mol Plant **2:** 851–860

Wolf S, Rausch T, Greiner S (2009b) The N-terminal pro region mediates retention of unprocessed type-I PME in the Golgi apparatus. Plant J **58:** 361–375

Zerzour R, Kroeger J, Geitmann A (2009) Polar growth in pollen tubes is associated with spatially confined dynamic changes in cell mechanical properties. Dev Biol **334:** 437–446

Zhang GF, Staehelin LA (1992) Functional compartmentation of the Golgi apparatus of plant cells: immunocytochemical analysis of high-pressure frozen- and freeze-substituted sycamore maple suspension culture cells. Plant Physiol **99:** 1070–1083

Zhang X, Henriques R, Lin SS, Niu QW, Chua NH (2006) Agrobacterium-mediated transformation of *Arabidopsis thaliana* using the floral dip method. Nat Protoc **1:** 641–646

Zhao J, Yang HY, Lord EM (2004) Calcium levels increase in the lily stylar transmitting tract after pollination. Sex Plant Reprod **16:** 259–263

Zhu Y, Zhao P, Wu X, Wang W, Scali M, Cresti M (2011) Proteomic identification of differentially expressed proteins in mature and germinated maize pollen. Acta Physiol Plant **33:** 1467–1474

Supplemental data

Table S1. List of primer pairs used for the qRT-PCR analyses.

Primer name	Forward primers	Reverse primers
PME1	5'-CCAGGATCACACAAAGCCAAG-3'	5'-GAGTTTACAAAGCGGGTGGTG-3'
PME48	5'-AGACTCCCGCACATGACAAGAC-3'	5'-CACTCTCTTGGCTTTGTGTGACC-3'
PME49	5'-AAACACTTCTCCAATGCCAAAGCC-3'	5'-GAAAGCAGCCTTATCGCCGTTG-3'
PME50	5'-CGAAGTTACGCCTTTCCTCACTC-3'	5'-GAGGAGGAAGTAGCCATGTGGA-3'
PME67	5'-TCGATGCTGTCCCTGTTGGTAAC-3'	5'-CGGAATGTGCACTCTCTCCTTG-3'
PME13	5'-GGTCATAAACAAGGAGGAGGCTTT-3'	5'-AGCCTGAGGCACTGATCCAA-3'
PME04	5'-ACAACAGAAGTGTTGCTCTCAGC-3'	5'-AACCTGAACTGTGGCACTGAGG-3'
PME05	5'-TTCCCTTAGTGGCACAGTCCAG-3'	5'-CGTTCACTCTGATAGCCACAGC-3'
PME21	5'-CCATGTCGCATCTTGTGTTCATCG-3'	5'-AGTAGTTTCCAACAATGGCGACAG-3'
PME23	5'-GACCTTCCTAACAGCCACAATCAC-3'	5'-TCCAGCTGTGTTCTCGATTCCG-3'
PME37	5'-ACCGTTCAGGTCGAATCTGAGG-3'	5'-TCCCAATGGACCAGCAGTGTTC-3'
PME43	5'-TCTTCCCGTGAAAGCCAAGAAC-3'	5'-CGCAAACGTCTCGTTCCACTTC-3'
PME45	5'-TGCCAAGTACCAAGGAAGGTACAC-3'	5'-TGTTTCCCGTCACGATCGTCTTC-3'
PME28	5'-GCGAGAATCCACGGGATTTGTTC-3'	5'-ACTGCCAAGTAATCCGGTTCGC-3'
At3g28750	5'-AGGCGATGGTTATTGCACAAGC-3'	5'-TGCCCAACTTAACAGCGAGGTC-3'
At3g57690	5'-AAGAAGATTGCTTGCGGTGTGC-3'	5'-AAAGAGCCAAGAGCTGGCAACG-3'
At5g59370	5'-GCAGATGTGGATTGCGAAAGCAG-3'	5'-CCGTCTTCGTTTGGTGATCTTAGG-3'

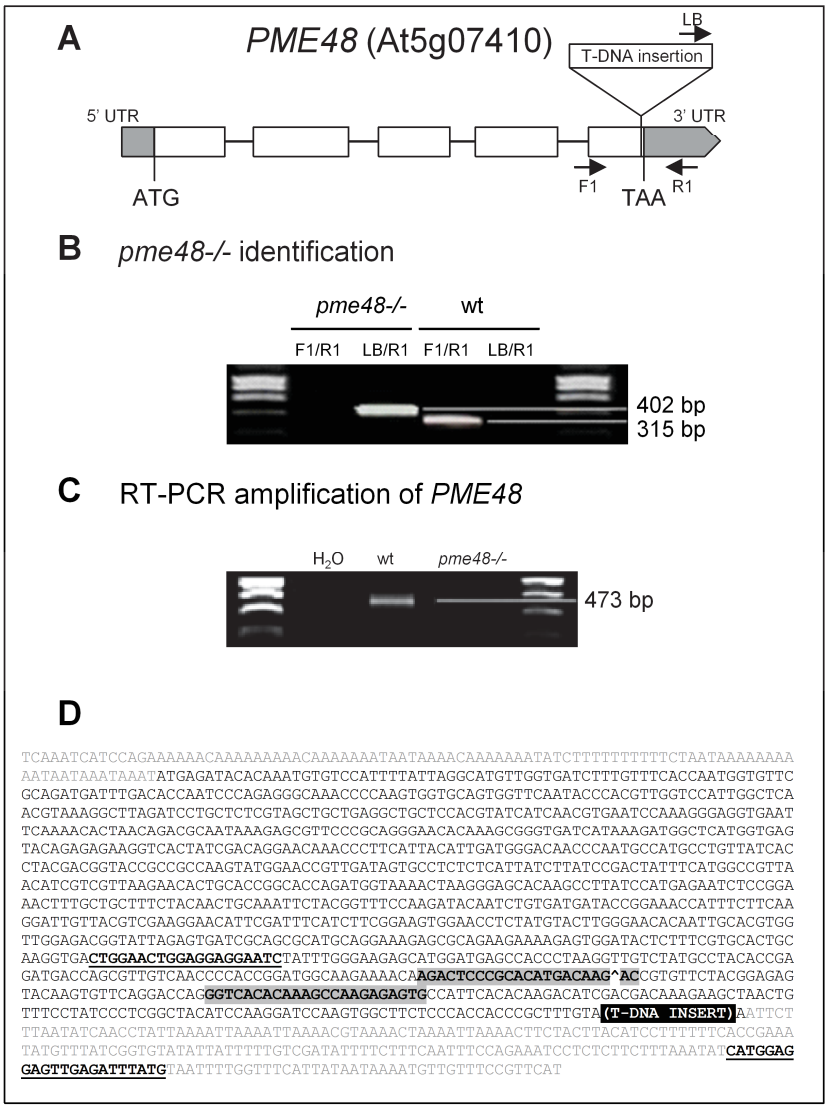

Figure S1. A, Genomic organization of the *PME48* (At5g07410) gene and location of the T-DNA insertion of *pme48-/-* mutant line. The white boxes indicate the positions of the exons and the line the position of the introns (both exons and introns are drawn to scale). Grey boxes indicate the untranslated regions (UTR) in 3' and 5'. Primers used for the genotyping are marked with arrows and labelled F1, R1 and LB. B, Amplification of the T-DNA insert in the homozygous *pme48-/-* mutant line. gDNA was extracted from leaves of wild-type and mutant plants. C, RT-PCR amplification products of *PME48* mRNA transcripts in 6 h-old pollen tubes from wild-type and *pme48-/-*. D, Transcript sequence of *PME48*. Primers used for the RT-PCR are in bold and underlined, primers used for the qRT-PCR are highlighted in grey. The T-DNA is located in a black box. Letters in grey are UTR. ^ Location of an intron in the genomic DNA.

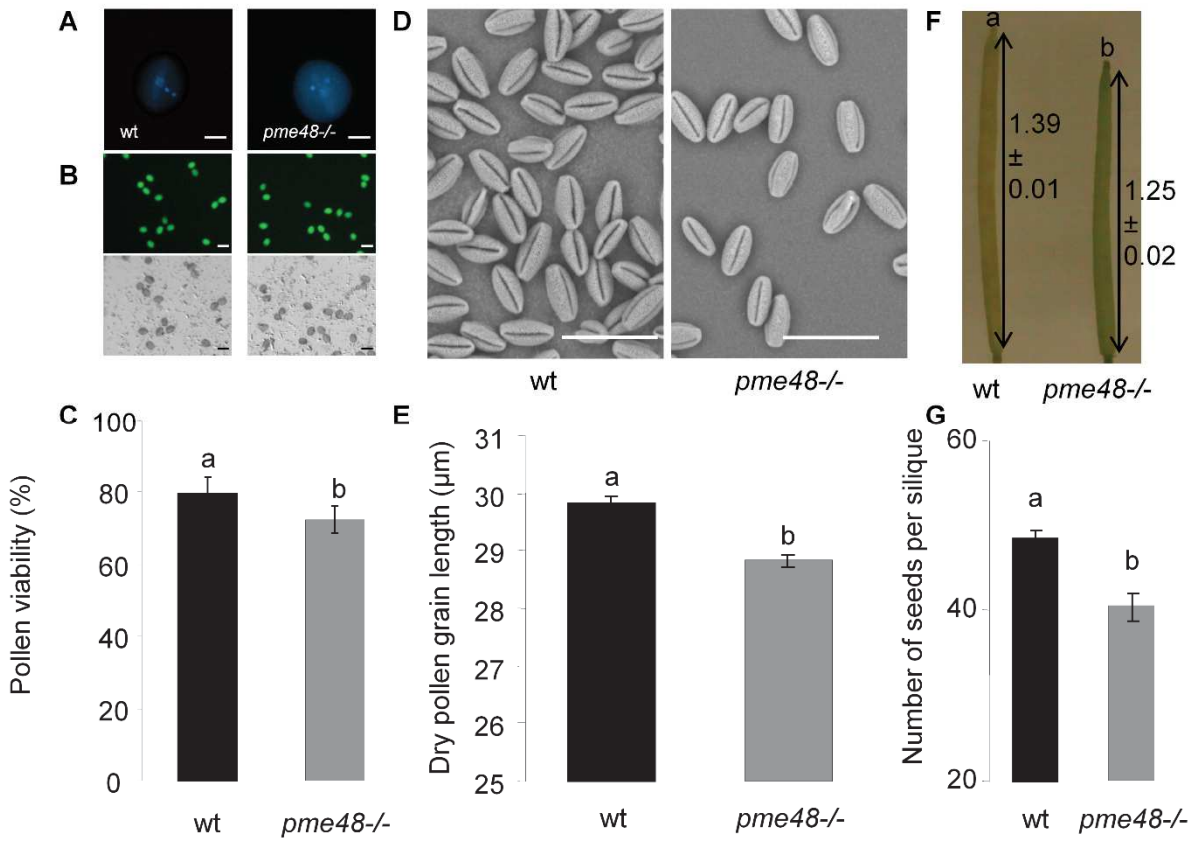

Figure S2. Viability and phenotypic characteristics of wild-type and mutant lines. A, DAPI staining of pollen grains showing the nuclei of the two sperm cells and the vegetative nucleus. Scale bars = 10 µm. B, C, Pollen viability test using FDA. Viable pollen grains fluoresce under UV. Scale bars = 30 µm. D, SEM of wild-type and *pme48-/-* dry pollen grains. Scale bars = 30 µm. E, Measurements of the length of wild-type and *pme48-/-* dry pollen grains. F, G, Quantification of the size of the siliques and the number of seeds per silique in wild-type and *pme48-/-* plants. Different letters indicate statistically significant differences as determined by the Student's t-test ($P<0.0001$). n> 1000 (B,C), n=550 (D,E), n=210 (F,G).

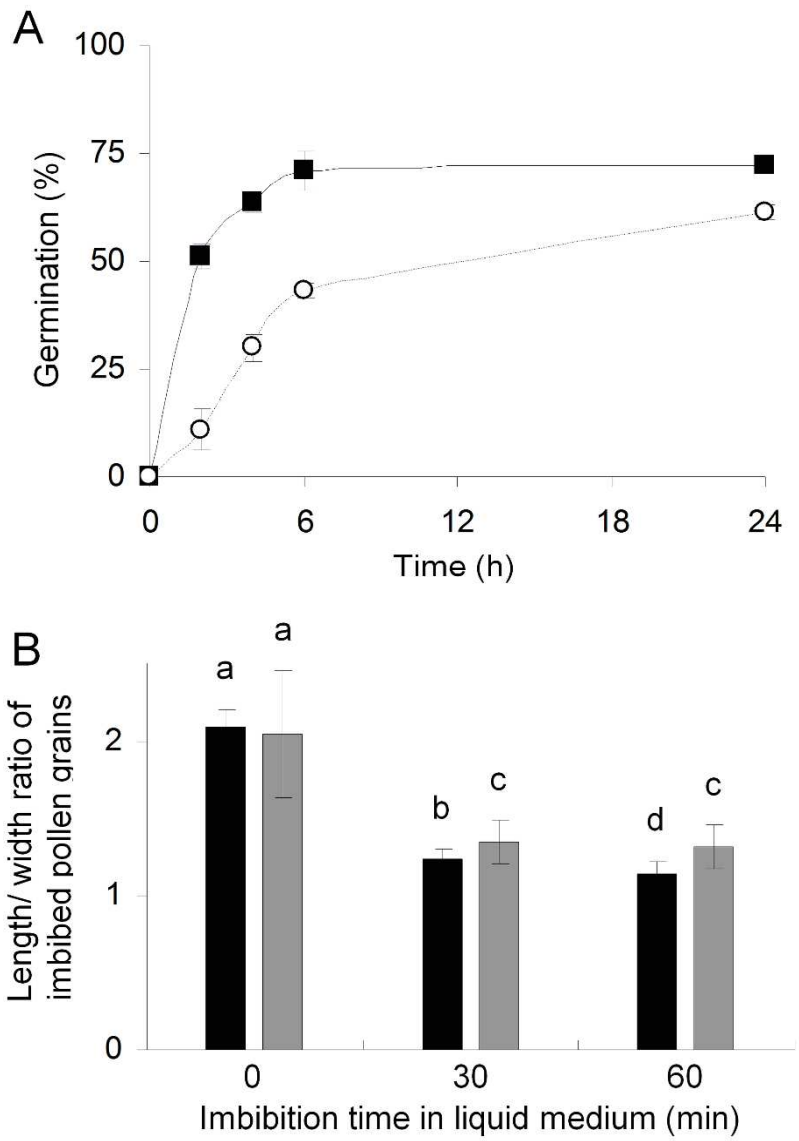

Figure S3. A, Germination rate of wild-type (black square) and *pme48-/-* (white circle) pollen grains in the optimum liquid GM. Pollen grains were considered germinated when the length of the tube was equal to the diameter of the pollen grain. B, Estimation of the imbibition rate by measuring the ratio length/width of wild-type (black bars) and *pme48-/-* (grey bars) pollen grains. Different letters indicate statistically significant differences among the wild-type and *pme48-/-* lines, as determined by the Student's t-test ($P<0.0001$; $n>10\,000$ in A; $n>500$ in B).

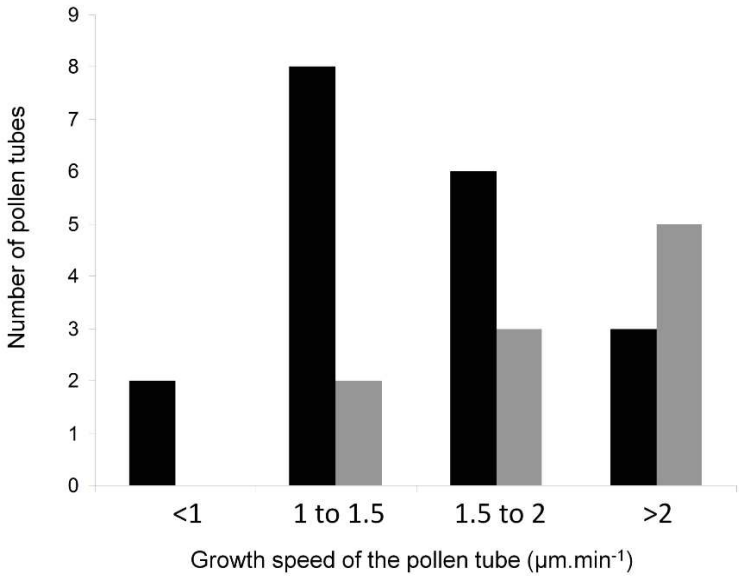

Figure S4. Estimation of the growth speed of wild-type (black bars) and *pme48-/-* (grey bars) pollen tubes in liquid medium.

the plant journal

SEB Society for Experimental Biology

The Plant Journal (2015) **84,** 1137–1151 doi: 10.1111/tpj.13071

Inhibition of fucosylation of cell wall components by 2-fluoro 2-deoxy-L-fucose induces defects in root cell elongation

Marie Dumont[1], Arnaud Lehner[1], Muriel Bardor[1], Carole Burel[1], Boris Vauzeilles[2,3,4], Olivier Lerouxel[5], Charles T. Anderson[6], Jean-Claude Mollet[1] and Patrice Lerouge[1,*]

[1]*Laboratoire Glycobiologie et Matrice Extracellulaire Végétale, EA 4358, IRIB, VASI, Normandie Université, 76821 Mont-Saint-Aignan, France,*

[2]*Institut de Chimie Moléculaire et des Matériaux d'Orsay (ICMMO) UMR CNRS 8182, Université de Paris Sud, 91405 Orsay, France,*

[3]*Institut de Chimie des Substances Naturelles (ICSN) UPR CNRS 2301, 91198 Gif-sur-Yvette, France,*

[4]*Click4Tag, Zone Luminy Biotech, Case 922, 163 Avenue de Luminy, 13009 Marseille, France,*

[5]*Centre de Recherches sur les Macromolécules Végétales (CERMAV) – CNRS BP 53, 38041 Grenoble Cedex 9, France, and*

[6]*Department of Biology and Center for Lignocellulose Structure and Formation, Pennsylvania State University, University Park, Pennsylvania, USA*

Received 21 September 2015; revised 26 October 2015; accepted 3 November 2015; published online 13 November 2015.
*For correspondence (e-mail patrice.lerouge@univ-rouen.fr).

SUMMARY

Screening of commercially available fluoro monosaccharides as putative growth inhibitors in *Arabidopsis thaliana* revealed that 2-fluoro 2-L-fucose (2F-Fuc) reduces root growth at micromolar concentrations. The inability of 2F-Fuc to affect an *Atfkgp* mutant that is defective in the fucose salvage pathway indicates that 2F-Fuc must be converted to its cognate GDP nucleotide sugar in order to inhibit root growth. Chemical analysis of cell wall polysaccharides and glycoproteins demonstrated that fucosylation of xyloglucans and of *N*-linked glycans is fully inhibited by 10 μM 2F-Fuc in Arabidopsis seedling roots, but genetic evidence indicates that these alterations are not responsible for the inhibition of root development by 2F-Fuc. Inhibition of fucosylation of cell wall polysaccharides also affected pectic rhamnogalacturonan-II (RG-II). At low concentrations, 2F-Fuc induced a decrease in RG-II dimerization. Both RG-II dimerization and root growth were partially restored in 2F-Fuc-treated seedlings by addition of boric acid, suggesting that the growth phenotype caused by 2F-Fuc was due to a deficiency of RG-II dimerization. Closer investigation of the 2F-Fuc-induced growth phenotype demonstrated that cell division is not affected by 2F-Fuc treatments. In contrast, the inhibitor suppressed elongation of root cells and promoted the emergence of adventitious roots. This study further emphasizes the importance of RG-II in cell elongation and the utility of glycosyltransferase inhibitors as new tools for studying the functions of cell wall polysaccharides in plant development. Moreover, supplementation experiments with borate suggest that the function of boron in plants might not be restricted to RG-II cross-linking, but that it might also be a signal molecule in the cell wall integrity-sensing mechanism.

Keywords: *Arabidopsis thaliana*, 2-fluoro 2-deoxy-L-fucose, cell elongation, rhamnogalacturonan-II, boron, root.

INTRODUCTION

Analyses of a wide range of plant species have revealed that all plant cell walls contain three classes of structural polysaccharides: cellulose, hemicelluloses and pectins, which together form a complex extracellular matrix (Albersheim *et al.*, 2010). The synthesis of cell wall polysaccharides is performed by membrane-localized polysaccharide synthetases and glycosyltransferases (GTs). Glycosyltransferases are enzymes that allow the transfer of single sugars from nucleotide sugar donors onto specific acceptors. Reverse genetic experiments targeting GT sequences have provided numerous data concerning the function of cell wall polysaccharides in plant development (Bouton *et al.*, 2002; Vanzin *et al.*, 2002). However, for some cell wall polymers such as rhamnogalacturonan II (RG-II), mutations

affecting GTs or enzymes involved in the biosynthesis of RG-II-specific monosaccharides are lethal or induce very strong developmental phenotypes (O'Neill *et al.*, 2001; Ahn *et al.*, 2006; Delmas *et al.*, 2008; Deng *et al.*, 2010; Dumont *et al.*, 2014). The lack of information available from these knock-out phenotypes can be partially addressed by studying RNA interference (RNAi) lines (Voxeur *et al.*, 2011). Rhamnogalacturonan II is a low-molecular-weight complex polysaccharide that is composed of at least 12 types of residues that are linked by at least 22 distinct glycosidic bonds (Bar-Peled *et al.*, 2012). Rhamnogalacturonan II contains four side chains linked to a homogalacturonan backbone made of seven to nine α-1,4-galacturonic acid residues (Figure S1 in supporting information). Despite its complex structure, RG-II is evolutionarily conserved in the plant kingdom (Matsunaga *et al.*, 2004). It is present in the primary cell walls of all higher plants, predominantly in the form of a dimer that is cross-linked by a borate di-ester between the apiosyl residues of two side chains (Figure S1) (Kobayashi *et al.*, 1996; O'Neill *et al.*, 1996). The lethality of knock-out lines affecting RG-II biosynthesis makes the study of its biosynthesis and function challenging. To date, only one α-1,3-xylosyltransferase, named RGXT, has been fully characterized. This GT is involved in the transfer of a xylose onto a fucose residue (Egelund *et al.*, 2006, 2008). Other GTs, such as sialyl-like transferases, have been postulated to attach 3-deoxy-D-*lyxo*-hept-2-ulosaric acid (Dha) and 3-deoxy-D-*manno*-oct-2-ulosonic acid (Kdo) to the homogalacturonan backbone (Deng *et al.*, 2010; Dumont *et al.*, 2014). Nevertheless, despite numerous efforts to determine why plants need such a complex molecule to ensure efficient cell wall formation and cell elongation, the precise function of RG-II remains unclear.

The use of modified monosaccharides, such as deoxy or fluorinated sugars, has been reported as a powerful pharmacological approach for studying carbohydrate metabolism and physiology in prokaryotic and eukaryotic organisms (Som *et al.*, 1980; Edmonds and Peddie, 2006). After uptake from the culture medium, the sugar analogue can either compete with endogenous metabolites or inhibit enzymes. The analogue 2-deoxy-D-glucose inhibits protein glycosylation (Schwarz and Datema, 1980) and, in plants, inhibits callose production and delays gravitropism (Jaffe and Leopold, 1984). In *Prototheca zopfii,* a unicellular alga, deoxy-glucose also inhibits β-1,4-glucan formation (Datema *et al.*, 1983). A recent study reported the effects of 2β-deoxy-Kdo, a deoxy analogue of Kdo, which is found in RG-II (Figure S1) (Smyth *et al.*, 2013). This deoxy sugar was demonstrated to inhibit cytosolic CMP-Kdo synthase and, as a consequence, to affect RG-II biosynthesis and cause severe root growth phenotypes (Smyth *et al.*, 2013).

Replacement of hydroxyl groups by fluorine atoms makes deoxy fluoro sugars useful probes for the study of enzyme mechanisms (Burkart *et al.*, 2000). The fluorine atom has a small atomic radius with high electronegativity and ionization potential. After conversion into nucleotide sugars, fluorinated analogues can form stable complexes with enzyme-binding sites. These molecules have been used in several studies as probes to elucidate the mechanisms and functions of GT (Burkart *et al.*, 2000; Brown *et al.*, 2012). Recently, Rillahan *et al.* (2012) investigated two fucosyltransferase inhibitors [2-fluoro 2-deoxy-L-fucose (2F-Fuc) and 6-fluoro-L-fucose (6F-Fuc)] and one sialyltransferase inhibitor [3-fluoro 3-deoxy-*N*-acetyl-neuraminic acid (3F-Neu5Ac)], which hamper the fucosylation and sialylation of protein *N*-linked glycans, respectively, in mammalian cells. The 2F-Fuc inhibitor has been demonstrated to inhibit both fucosyltransferase enzymes and the *de novo* cytosolic synthesis of GDP-Fuc in mammalian cells (Okeley *et al.*, 2013). In plants, the use of fluorinated sugars has received relatively little attention to date. 2-[^{18}F] fluoro 2-deoxy-D-glucose has been applied to study both the real-time translocation of photosynthetic products in living plants (Hattori *et al.*, 2008) and plant defence (Ferrieri *et al.*, 2012), while UDP 2-fluoro 2-deoxy-D-glucuronic acid has also been used to study the enzyme mechanism of plant UDP-α-D-apiose/UDP-α-D-xylose synthase (Choi *et al.*, 2011).

In this work, we report the effects of commercially available fluoro monosaccharides on seedling growth in Arabidopsis. Among the compounds tested, 2F-Fuc was the most effective growth inhibitor and arrested root elongation at micromolar concentrations. Biochemical analyses of cell wall polysaccharides showed that the fucosylation of xyloglucan and of *N*-glycosylated proteins was suppressed by 2F-Fuc. Moreover, defects in RG-II biosynthesis were found to be responsible for the growth phenotype observed in plants treated with 2F-Fuc.

RESULTS

Screening of fluoro sugar analogues for effects on cell elongation

Arabidopsis seeds were sown on solid growth medium containing commercially available fluorinated sugar analogues. Seedling root and shoot elongation were measured in the presence of fluoro deoxy-D-glucose isomers differing in the position of the fluorine atom (2F-Glc, 3F-Glc and 4F-Glc), 2-fluoro 2-deoxy-L-fucose (2F-Fuc) and 3-fluoro 3-deoxy-*N*-acetyl D-neuraminic acid (3F-Neu5Ac) at concentrations ranging from 2.5 to 200 μM (Figure S2). Considering the structural similarity between Neu5Ac and Kdo, 3F-Neu5Ac was tested as a possible Kdo transferase inhibitor. Peracetylated and non-acetylated fluoro sugars were tested, but effects were only observed with peracetylated sugars, indicating that the peracetylated molecules are likely to be entering the cell by passive diffusion through the plasma membrane. Four-day-old Arabidopsis

seedlings exhibited various susceptibilities to these fluorinated sugars, with growth defects being observed primarily in roots rather than shoots (Figure S2). Treatment with 3F-Neu5Ac did not induce any root growth inhibition even at a high concentration (200 μM). Growth inhibition was observed with fluoro glucose analogues in the 25–100 μM range, with the inhibitory effect depending on the position of the fluorine atom: the most effective glucose analogue was 2F-Glc, which inhibited root growth by 75% at a concentration of 25 μM (Figure S2). The strongest growth effect of all of the inhibitors was observed with 2F-Fuc, since the lowest concentration of this compound tested (2.5 μM) was sufficient to reduce root elongation by 70%. Moreover, this effect was observed in a dose-dependent manner (Figure 1a) and was not suppressed by supplementation with an excess amount of fucose (10 mM) (Figure S3). Considering the strong inhibition of root growth observed with 2F-Fuc treatment, we decided to focus on the biochemical and physiological effects induced by this sugar analogue.

2F-Fuc is a potent inhibitor of the fucosylation of cell wall polysaccharides

To investigate the effects of 2F-Fuc on the fucosylation of cell wall polysaccharides or glycoconjugates, we first carried out a click-mediated labelling experiment. Anderson *et al.* (2012) have recently shown that an alkynylated L-fucose analogue (Fuc-Al) is a useful probe for imaging fucose-containing cell wall polysaccharides in Arabidopsis. Figure 1(b)–(f) shows that the cell walls of 4-day-old seedlings were efficiently labelled after incorporation of Fuc-Al and coupling to an Alexa Fluor 488 azide probe via copper-catalysed azide–alkyne cyclooaddition. In contrast, labelling was strongly reduced in seedlings treated with 25 μM 2F-Fuc, indicating that this fluoro analogue inhibits the transfer of Fuc-Al to cell wall polysaccharides (Figure 1e,f).

The fucose content in shoot and root cell walls of 10-day-old Arabidopsis seedlings treated with 2.5–25 μM 2F-Fuc were measured by gas chromatography (Figure 1g). In comparison with control seedlings (DMSO), the fucose content in root cell walls was reduced by about 50% in seedlings treated with 2.5 μM 2F-Fuc whereas only traces of fucose were detected in the root cell walls of seedlings treated with 10 or 25 μM 2F-Fuc. Beyond its effect on fucose content, 2F-Fuc treatment did not strongly affect the overall sugar composition of root cell walls in seedlings (Figure 2). For instance, the galacturonic acid (GalA) content in roots was about 25% of total cell wall sugars regardless of the 2F-Fuc concentration. Some limited [2F-Fuc]-dependent changes in sugar composition were observed, such as decreases in relative xylose content and increases in rela-

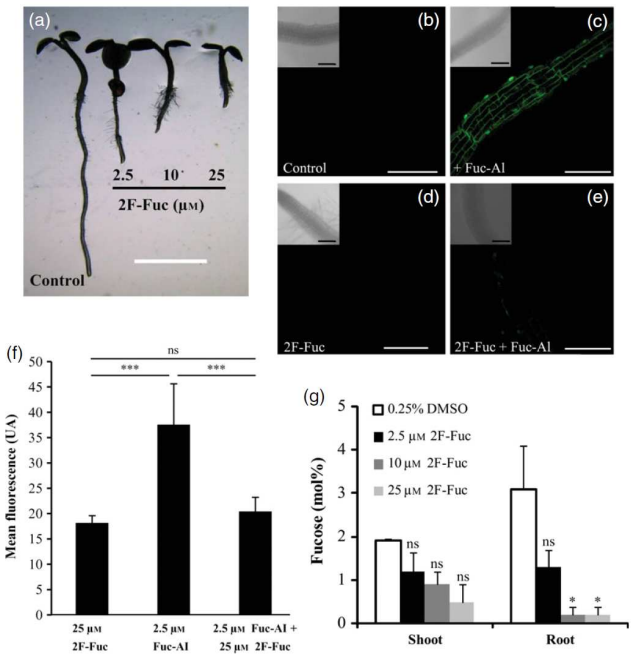

Figure 1. Effect of 2-fluoro 2-L-fucose (2F-Fuc) on plant growth and on fucose incorporation into root cell walls.
(a) Four-day-old Arabidopsis seedlings grown on medium supplemented with peracetylated 2F-Fuc or DMSO (control). Scale bar = 0.3 cm. (b)–(e) Click-mediated labelling of Arabidopsis seedling cell walls using the alkynylated fucose analogue Fuc-Al. Four-day-old seedlings grown on MS were incubated in liquid MS medium ± Fuc-Al (b, c) for 16 h and 4-day-old seedlings grown on MS supplemented with 25 μM 2F-Fuc were incubated in liquid MS medium ± Fuc-Al + 25 μM 2F-Fuc (d, e) for 16 h and labelled. Scale bars = 100 μm. (f) Quantification of the root-tip fluorescence in (c)–(e). Data are the mean ± SEM ($n > 6$) from three experiments. Mann–Whitney test, ***$P < 0.001$. (g) Fucose contents (mol%) determined by gas phase chromatography analysis of cell walls isolated from 10-day-old Arabidopsis seedlings grown with 2.5–25 μM 2F-Fuc or DMSO (control). $n > 300$ seedlings per replicate. Data are the mean ± SEM of three biological replicates.

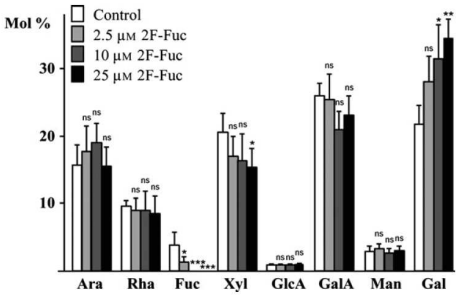

Figure 2. Effect of 2-fluoro 2-L-fucose (2F-Fuc) on the sugar composition of root cell walls.
Monosaccharide composition of root cell walls of control (0.25% DMSO) and seedlings treated with 2.5–25 µM 2F-Fuc. Data are mean ± SEM of three biological replicates. Unpaired *t*-test: ns, not significant; $*P < 0.05$, $**P < 0.01$;$***P < 0.001$.

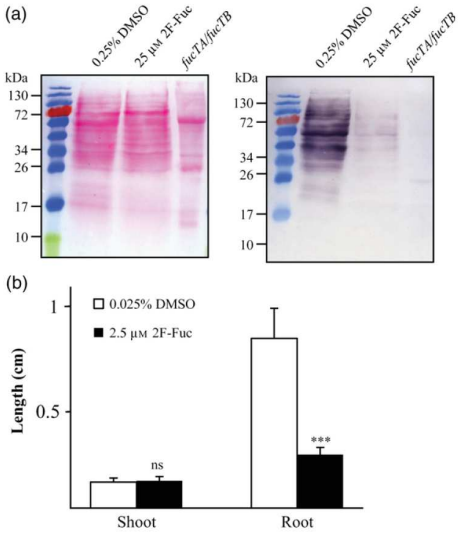

Figure 3. Effect of 2-fluoro 2-L-fucose (2F-Fuc) on the fucosylation of *N*-glycoproteins.
(a) Ponceau S staining (left) and Western blot (right) using antibody directed against the core α-1,3-fucose *N*-glycans. *fucTA*/*fucTB*, double *fucTA*/*fucTB* mutant impaired in *N*-linked glycan fucosylation.
(b) Shoot and root lengths of 4-day-old *cgl* seedlings grown in the presence of 0.025% DMSO (control) or 2.5 µM 2F-Fuc ($n > 20$ seedlings). Mann–Whitney test.

tive galactose content (Figure 2). In contrast to roots, the effect of 2F-Fuc on shoots was less severe. Twenty-five per cent of the fucose content in shoot cell walls was still detected in 25 µM 2F-Fuc-treated seedlings in comparison with the negative control (DMSO) (Figure 1g). Taken together, these data suggest that 2F-Fuc acts as a potent inhibitor of the fucosylation of cell wall polysaccharides at concentrations as low as 10 µM in root tissues.

To begin to probe the mechanism of 2F-Fuc inhibition, the effects of 2F-Fuc on a mutant defective in the fucose salvage pathway (Kotake *et al.*, 2008) were investigated. This mutant, *Atfkgp*, is impaired in cytosolic L-fucokinase and GDP-L-fucose pyrophosphorylase activities that convert exogenously supplied L-fucose to its GDP-activated form (Kotake *et al.*, 2008). *Atfkgp* seedlings were insensitive to 2F-Fuc (Figure S4), strongly suggesting that 2F-Fuc must be activated into its GDP nucleotide sugar in order to exert its inhibitory effects.

Decreased fucosylation of xyloglucan and glycoproteins in Arabidopsis seedlings after 2F-Fuc treatment is not responsible for defects in root growth

Plant cell walls possess several fucose-containing polysaccharides and glycoconjugates such as xyloglucan (Perrin *et al.*, 2003), *N*-glycosylated proteins (Rayon *et al.*, 1998), pectic rhamnogalacturonan-I (RG-I) (Nakamura *et al.*, 2001) and RG-II (Glushka *et al.*, 2003), as well as arabinogalactan proteins (AGPs) (Tryfona *et al.*, 2012). To investigate whether the fucosylation of *N*-glycosylated proteins is affected by treatment with 2F-Fuc, we extracted proteins from Arabidopsis root seedlings treated with 25 µM 2F-Fuc. Protein *N*-linked glycan fucosylation was detected using a specific antibody directed against the core α-1,3-fucose epitope (Faye *et al.*, 1993). A shown in Figure 3(a), glycoproteins were detected at much lower amounts in 2F-Fuc treated-roots compared with control roots. The specificity of the primary antibody was confirmed as glycoproteins were not detected in *fucTA*/*fucTB* Arabidopsis double mutant seedlings impaired in *N*-glycan α-1,3-fucosyltransferases (Strasser *et al.*, 2004). Moreover, the effect of 2F-Fuc on the growth of the *cgl* (*complex glycan-deficient*) mutant was investigated. This Arabidopsis mutant is impaired in its Golgi *N*-acetyl glucosaminyltransferase I, preventing the synthesis of fucosylated complex-type *N*-linked glycans, but does not exhibit obvious growth phenotypes when grown in standard conditions (von Schaewen *et al.*, 1993). The root growth of *cgl* seedlings was affected by 2.5 µM 2F-Fuc treatment as observed for Col-0 seedlings (Figure 3b), indicating that the decrease in *N*-glycoprotein fucosylation induced by 2F-Fuc treatment is not responsible for the observed inhibition of root growth.

Arabidopsis xyloglucan consists of a β-1,4-glucan backbone substituted with α-1,6-xylosyl residues (side chain X; Fry *et al.*, 1993). Terminal Gal (side chain L; Fry *et al.*, 1993) or Fucα-1,2-Gal disaccharides (side chain F; Fry *et al.*, 1993) can also be β-1,2-linked to xylosyl residues. Xyloglucan fingerprints from the cell walls of shoots and roots of

Arabidopsis seedlings treated with DMSO (control) or 2.5–25 μM 2F-Fuc were investigated according to Lerouxel *et al.* (2002). Cell walls were isolated and subjected to endoglucanase digestion, and the resulting fragments were analysed by matrix-assisted laser desorption ionization time-of-flight mass spectrometry MALDI-TOF MS (Figure 4a). Comparison of fingerprints obtained from seedlings treated with 2.5–25 μM 2F-Fuc with the fingerprint of the negative control (DMSO) showed a dose-dependent decrease in the levels of fucosylated fragments (XXFG and XLFG) together with an increase in the levels of non-fucosylated fragments. No novel fragments were detected by comparison with control MS profiles. Quantification of xyloglucan fragments detected in the MALDI-TOF MS experiments indicated a 60% decrease in xyloglucan fucosylation for roots treated with 2.5 μM 2F-Fuc and only trace amounts of fucosylated fragments at higher 2F-Fuc concentrations (Figure 4b). In agreement with total fucose contents detected in shoot cell walls (Figure 1g), the fucosylation of xyloglucan in Arabidopsis shoots was only slightly affected by treatments with 2.5 and 10 μM 2F-Fuc. Only treatment with 25 μM 2F-Fuc was sufficient to induce a detectable decrease of xyloglucan fucosylation in cell walls derived from shoot tissues (Figure 4b).

AtFUT1 is a Golgi-localized fucosyltransferase that can add α-1,2-Fuc residues onto xyloglucan (Perrin *et al.*, 1999). The effect of 2F-Fuc on Arabidopsis AtFUT1 was investigated *in vitro* using radiolabelled GDP-Fuc and tamarind xyloglucan as an acceptor. The transferase capacity of recombinant AtFUT1 produced in insect cells was monitored in the presence of 1 mM 2F-Fuc. A weak inhibitory activity was observed (Figure S5), again suggesting that 2F-Fuc might need to be converted into a GDP nucleotide sugar to effectively inhibit the activity of AtFUT1 (Burkart *et al.*, 2000; Okeley *et al.*, 2013).

Next, Arabidopsis *mur2* (*murus2*) and *xxt1 xxt2* (*xyloglucan xylosyltransferase*) mutants, as well as tobacco seedlings, were grown in presence of 2.5 μM 2F-Fuc. Arabidopsis *mur2* lacks functional AtFUT1 and its cell walls contain less than 2% of the wild-type amount of fucosylated xyloglucan without affecting root growth (Vanzin *et al.*, 2002). The *xxt1 xxt2* double mutant is impaired in xyloglucan xyloxyltransferase activity and lacks detectable xyloglucan (Cavalier *et al.*, 2008). *Nicotiana benthamiana*, like all Solanaceae, accumulates non-fucosylated xyloglucan in its cell walls (York *et al.*, 1996; Hoffman *et al.*, 2005), with the exception of pollen (Lampugnani *et al.*, 2013; Dardelle *et al.*, 2015). In both Arabidopsis mutants and tobacco seedlings, root elongation was strongly affected by 2F-Fuc treatment (Figure 4c). Again, this suggests that the inhibition of root growth by 2F-Fuc is not related to a deficiency in xyloglucan fucosylation. The same conclusion can be drawn for AGPs, since the root growth of Arabidopsis *fut4 fut6* double mutants, which lack normal AGP fucosylation (Liang *et al.*, 2013), was also inhibited by 2F-Fuc treatment (Figure 4c).

Arabidopsis seedlings treated with 2F-Fuc are impaired in RG-II biosynthesis

Boron is responsible for the RG-II dimerization that is required for plant growth (O'Neill *et al.*, 2001). Thus, the

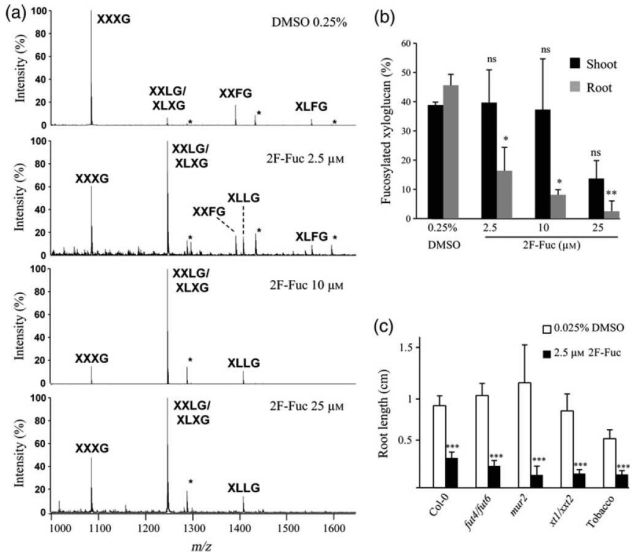

Figure 4. Effect of 2-fluoro 2-L-fucose (2F-Fuc) on xyloglucan fucosylation.
(a) Matrix-assisted laser desorption ionization time-of-flight mass spectra of endoglucanase-generated xyloglucan fragments from 10-day-old Arabidopsis root seedlings grown on medium supplemented with 2.5–25 μM 2F-Fuc or DMSO (control). Xyloglucan fragments are XXXG to XLFG according to the nomenclature reported by Fry *et al.* (1993). Asterisks indicate acetylated xyloglucan fragments.
(b) Relative ratio of fucosylated xyloglucan fragments in roots and shoots detected in the enzyme fingerprints. $n > 200$ seedlings per replicate. Data are the mean ± SEM of at least two replicates. Non-parametric *t*-test.
(c) Root length of 4-day-old Arabidopsis Col-0, *fut4 fut6*, *mur2*, *xxt1 xxt2* seedlings and 7-day-old tobacco (*Nicotiana benthamiana*) seedlings grown on medium supplemented with DMSO (control) or with 2.5 μM 2F-Fuc. The results are given as mean ± SEM ($n > 20$ seedlings). Asterisks indicate significant difference between negative control (0.025% DMSO), Mann–Whitney test, $P < 0.001$.

effect of boron on 2F-Fuc-treated seedlings was investigated. Supplementation of culture medium containing 2.5 or 25 μM 2F-Fuc with 0.75 mM boric acid was able to partially restore root growth in 4-day-old Arabidopsis seedlings, suggesting that the growth inhibition caused by 2F-Fuc is likely attributable to RG-II defects (Figure 5a).

To directly assess RG-II dimerization in 2F-Fuc-treated seedlings, we used the polyacrylamide gel electrophoresis method described by Chormova *et al.* (2014) for the separation of monomeric RG-II (mRG-II) and dimeric RG-II (dRG-II). Cell walls were prepared from roots of 10-day-old seedlings grown with 0.25% DMSO or 2F-Fuc at concentrations of 2.5, 10 and 25 μM. Then RG-II was solubilized by treatment of cell walls with endo-polygalacturonase and submitted to polyacrylamide gel electrophoresis (Figure 5b). The relative amount of cell wall sugars for each RG-II-enriched fraction was assessed by gas chromatography and identical cell wall quantities were loaded on the gel. Lemon mRG-II and dRG-II were used as standards. As reported previously (O'Neill *et al.*, 2004), RG-II extracted from untreated Arabidopsis root seedlings existed mainly in a dimeric form. Treatment of seedlings with 2.5 μM 2F-Fuc induced a major decrease in dRG-II together with an increase in mRG-II and the appearance of a RG-II fragment. At 10 and 25 μM, 2F-Fuc greatly diminished *in muro* accumulation of RG-II (Figure 5b). Although the small RG-II fragment was still detectable by PAGE after treatment with 10 or 25 μM 2F-Fuc, these data suggest that inhibition of fucosylation results in defects in the biosynthesis of mRG-II and dRG-II. In the presence of 0.75 mM boric acid, PAGE of RG-II fractions isolated from seedlings treated with 2.5 μM 2F-Fuc showed an increase in the relative amount of dRG-II, suggesting that boron promoted RG-II dimerization even in the absence of normal fucosylation (Figure 5c). However, the abnormal small RG-II fragment was still detected under these conditions, indicating that its processing or dimerization was not restored in the presence of boric acid. In seedlings treated with high concentration of 2F-Fuc (25 μM), borate had no major effect on the PAGE RG-II profile, with the small RG-II fragment being the main band detected (Figure 5c).

Incubation of Arabidopsis light-grown seedlings with 8-azido 8-deoxy-Kdo (Kdo-N_3) followed by click-mediated coupling to an alkyne-containing fluorescent probe through a copper-catalysed azide–alkyne cycloaddition provides an efficient method for imaging RG-II in cell walls without the need for RG-II-specific antibodies (Patrice Lerouge et al. Unpublished data). Figure 6(a) shows that incubation of seedlings with 50 μM Kdo-N_3 induced a robust labelling of their cell walls by Alexa 488 alkyne. In contrast, this labelling was suppressed by treatment with 25 μM 2F-Fuc (Figure 6b,c), further confirming that high concentrations of 2F-Fuc inhibit biosynthesis of RG-II.

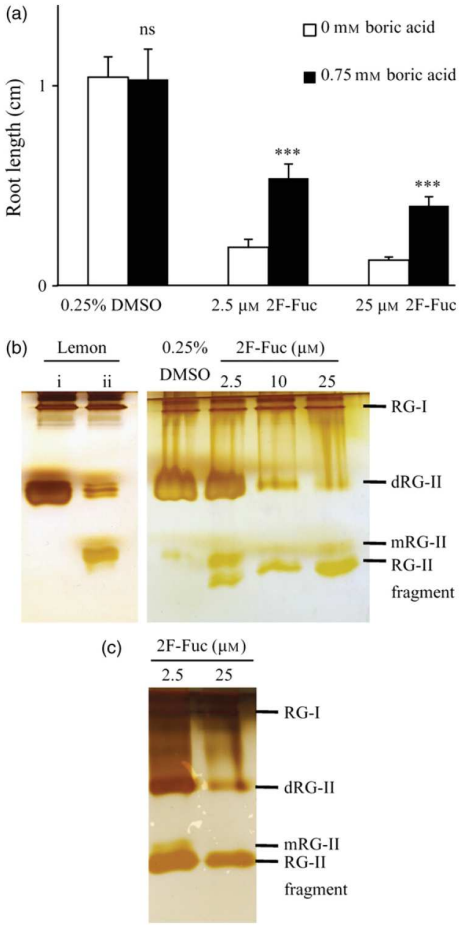

Figure 5. Effect of 2-fluoro 2-L-fucose (2F-Fuc) on rhamnogalacturonan-II (RG-II) dimerization.
(a) Root length of 4-day-old Arabidopsis seedlings treated with 2.5 or 25 μM 2F-Fuc, 0.75 mM boric acid or both. DMSO, negative control. Data are mean ± SEM ($n > 18$ seedlings). Mann–Whitney test.
(b) Polyacrylamide gel electrophoresis: RG-II was extracted from 10-day-old Arabidopsis roots grown on medium supplemented with 2.5, 10 or 25 μM 2F-Fuc. RG-II extracted from lemon was used as control (i), additional 16-h incubation with 0.1 M HCl treatment leads to a partial monomerization of RG-II (ii). RG-I, Rhamnogalacturonan I; mRG-II, monomeric RG-II; dRG-II, dimeric RG-II.
(c) The same experiment as in (b) with 2.5 and 25 μM 2F-Fuc-treated seedlings grown in a medium complemented with 0.75 mM boric acid.

Analysis of root architecture in 2F-Fuc-treated Arabidopsis seedlings

The Arabidopsis root is organized into an apical meristem where cells divide, an elongation zone where cells expand

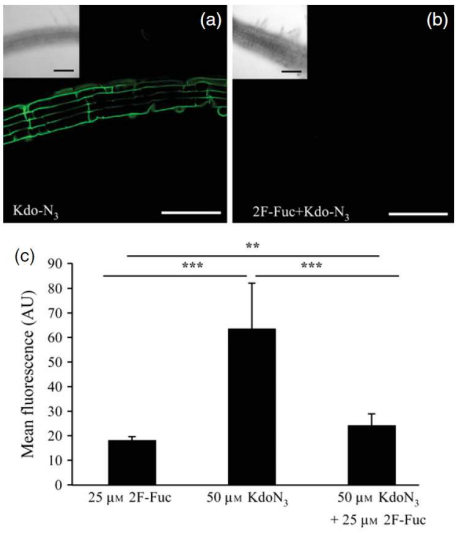

Figure 6. Effect of 2-fluoro 2-L-fucose (2F-Fuc) on incorporation of azido 3-deoxy-D-*manno*-oct-2-ulosonic acid (Kdo) analogue (Kdo-N_3).
(a), (b) Click-mediated labelling of Arabidopsis seedling using Kdo-N_3. Four-day-old seedlings were grown on MS medium supplemented without (a) or with (b) 25 μM 2F-Fuc. Seedlings were then incubated in liquid MS medium containing 50 μM Kdo-N_3. Scale bars = 100 μm. (a), (b) Click-mediated labelling of Arabidopsis seedling using Kdo-N_3. Four-day-old seedlings were grown on MS medium supplemented without (a) or with (b) 25 μM 2F-Fuc. Seedlings were then incubated in liquid MS medium containing 50 μM Kdo-N_3. Scale bars = 100 μm.
(c) Quantification of the root-tip fluorescence. Data are the mean ± SEM (n > 10 seedlings from three experiments). Unpaired t-test with Welch's correction: $^{**}P < 0.01$;$^{***}P < 0.001$.

and a differentiation zone where cells acquire their determined sizes, shapes and functions. As reported in Figure 1(a), Arabidopsis seedlings treated with 2F-Fuc exhibit a strong root growth defect. Observation of the root tips of seedlings treated with 2.5 μM 2F-Fuc revealed that the entire elongation zone was strongly diminished, with differentiated cells closer to the root tip than in control seedlings (Figures 7a–e and S6). This resulted in a hairy root phenotype in 2F-Fuc-treated seedlings that is characterized by the appearance of densely packed root hairs (Figure 7f). Staining of cell walls with the glucan-binding fluorescent dye calcofluor white revealed defects in cellulose organization and cell wall integrity in 2F-Fuc-treated root epidermal cells in the elongation zone. In contrast to control cells, where calcofluor staining was relatively evenly distributed along the cell wall, the cell wall network of 2F-Fuc-treated Arabidopsis roots appeared disorganized, as previously described for cellulose-deficient mutants (Anderson *et al.*, 2010). Moreover the presence of gaps in the 2F-Fuc-treated cell walls suggests the existence of points of weakness in the wall (Figure 7g,h).

Closer investigation of the root tips of seedlings treated with 2.5 μM 2F-Fuc did not reveal disorganization in the meristematic zone of Arabidopsis roots in comparison with control roots with similar cell numbers, types and shapes (Figure 7c). Actively dividing cells were visualized in Arabidopsis seedlings expressing the GUS reporter gene under the control of the cyclin-dependent protein kinase 1 (CYCB1) promoter. Staining of seedlings expressing the *pCYCB1::*GUS fusion protein in 2F-Fuc-treated roots did not reveal any reduction in cell division activity in the apical meristem compared with control seedlings (Figure 7i,j), suggesting that 2F-Fuc does not dramatically affect cell division. For confirmation, the cell division rate of suspension-cultured BY-2 tobacco cells was monitored in the presence of 2F-Fuc. No significant effect was observed on BY-2 cell growth even at 100 μM 2F-Fuc (Figure S7).

After 2 weeks of growth in the presence of 2.5 μM 2F-Fuc, in addition to the densely packed root hair phenotype, Arabidopsis seedlings exhibited multiple adventitious roots, with an average of 2.2 adventitious roots per treated plant (Figure S8); these were not observed in control plants or in plants supplemented with 0.75 mM boric acid (Figure S8). These data suggest that 2F-Fuc induces important changes in Arabidopsis root architecture at micromolar concentrations.

DISCUSSION

2F-Fuc is a potent inhibitor of glycoconjugate and polysaccharide fucosylation and inhibits cell elongation

Screening of commercially available fluoro monosaccharide analogues as putative growth inhibitors revealed that 2F-Fuc is able to reduce root growth at micromolar concentrations. In contrast, 3F-Neu5Ac has no effects on root growth, whereas 2F-Glc, the most active fluorinated glucose molecule we tested, caused growth phenotypes at 25 μM. Growth effects were less severe on shoots for all of the analogues tested, possibly due to poor uptake of the fluoro monosaccharides into shoot tissues, which are surrounded by a waterproof cuticle, or due to differences in shoot cell walls compared with those of root tissues. The impacts of fluoro glucose analogues on either glucosyltransferase inhibition or glucose cytosolic metabolism were not investigated further. Several lines of evidence demonstrate that 2F-Fuc is an efficient inhibitor of glycoconjugate and polysaccharide fucosylation. First, a 50% decrease in the fucose content of root cell walls was observed after treatment with 2.5 μM 2F-Fuc, and only traces of fucose were detected after treatment with higher concentrations of 2F-Fuc. Analysis of *N*-glycoprotein and xyloglucan fucosylation (Figures 3 and 4) led to the same conclusions. This indicates that at 2F-Fuc

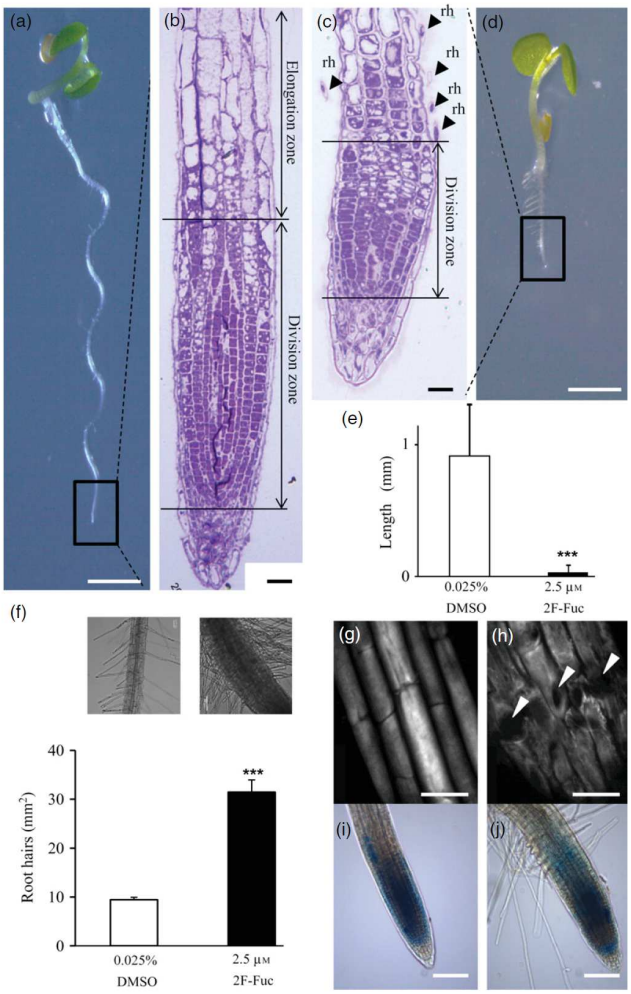

Figure 7. Effect on Arabidopsis root architecture. (a)–(d) Four-day-old Arabidopsis seedlings grown with 0.025% DMSO (a, b) or 2.5 µM 2-fluoro 2-L-fucose (2F-Fuc) (c, d). The frames at the apex of the root (a, d) indicate the zone shown in (b, c). (b), (c) Longitudinal sections showing the root cell organization in the division and the elongation zones. Arrows indicate the presence of root hairs (rh). (e) Distance measured between the apex and the early differentiation zone of 4-day-old Arabidopsis seedlings grown with 0.025% DMSO or 2.5 µM 2F-Fuc. Data are mean ± SEM ($n > 15$ roots). Mann–Whitney test, $^{***}P < 0.001$. (f) Root hair density of Arabidopsis seedlings grown with 0.025% DMSO or 2.5 µM 2F-Fuc ($n > 25$ roots). Data are mean ± SEM. Mann–Whitney test, $^{***}P < 0.001$. (g), (h) Calcofluor staining of Arabidopsis roots grown with 0.025% DMSO (g) or 2.5 µM 2F-Fuc (h). Arrowheads point out cell wall defects in the elongation zone. (i), (j) Analysis of root meristem activity of 4-day-old Arabidopsis *pCYCB1:*:GUS seedlings grown with 0.025% DMSO (i) or 2.5 µM 2F-Fuc (j). *pCYCB1:*:GUS line were used to visualize the division zone in non-treated and treated plants. Scale bars = 1 mm (a)–(d); 20 µm (b), (c); 25 µm (g), (h); 100 µm (i), (j).

concentrations as low as 10 µM, the fucosylation of polysaccharides and glycoconjugates is almost entirely inhibited in Arabidopsis seedling roots. As observed for the growth phenotypes, less severe underfucosylation was found in shoots. In addition to the possibilities listed above, the less severe effects in shoots might also reflect minimal transport of the sugar analogue from roots to the aerial parts of the plant, possibly due to the diffusion barrier presented by the endodermis. Similar results were published by Villalobos *et al.* (2015) while this article was under review.

Atfkgp mutant seedlings impaired in L-fucokinase and GDP-L-fucose pyrophosphorylase activities of the salvage pathway (Kotake *et al.*, 2008) grew normally in the presence of 2F-Fuc (Figure S4). This demonstrated that 2F-Fuc must probably be converted into its GDP-nucleotide form to inhibit root growth. Moreover, enzymatic assays performed on AtFUT1 also suggested that the 2F-Fuc must be converted into GDP-2F-Fuc to mimic the transition state and bind tightly to the active site of fucosyltransferases, leading to competitive inhibition (Burkart *et al.*, 2000; Rillahan *et al.*, 2012; Okeley *et al.*, 2013). In mammals, the

GDP-activated 2F-Fuc inhibitor inhibits mammalian Golgi-resident fucosyltransferases. This inhibitor also depletes mammalian cells of GDP-Fuc through the feedback inhibition of its *de novo* synthesis (Okeley *et al.*, 2013), thus depriving the cytosol of the activated form of fucose that is required by Golgi fucosyltransferases. In future work, experiments using recombinant enzymes and synthetic GDP-activated 2F-Fuc will be required to determine which inhibition mechanism occurs in plants treated with 2F-Fuc and is responsible for the underfucosylation of glycoconjugates and polysaccharides observed here.

Root growth is strongly affected by 2F-Fuc at micromolar concentrations. Using genetic and biochemical analyses, we investigated the relationship between the underfucosylation of cell wall fucose-containing polymers and the root growth phenotype. Arabidopsis xyloglucan and *N*-linked glycoproteins contain terminal fucose residues. However, these sugar motifs are not crucial for plant growth, since mutants impaired in xyloglucan and *N*-glycoprotein fucosylation do not exhibit visible phenotypes when grown in standard conditions (von Schaewen *et al.*, 1993; Vanzin *et al.*, 2002). The *fut4 fut6* double mutant deficient in AGP fucosylation also appears to be healthy (Liang *et al.*, 2013). Moreover, in the presence of 2F-Fuc, xyloglucan-, AGP- and *N*-glycan-deficient mutants (*mur2, xxt1*/*xxt2, fut*/*fut6* and *cgl*) exhibited growth inhibition phenotypes similar to those observed in wild-type plants, further suggesting that defects in glycoprotein, AGP and xyloglucan fucosylation are not responsible for the observed root developmental phenotypes.

The inhibition of fucosylation of cell wall polysaccharides would also be expected to affect RG-II, which contains fucose residues on two of its side chains (Figure S1). At low concentrations, PAGE experiments showed that 2F-Fuc induced a decrease in RG-II dimerization in root seedlings and the formation of a small RG-II fragment of unknown structure (Figure 5b). This fragment may result from the absence of the internal fucose residue in side chain A in 2F-Fuc-treated seedlings, as reported by Pabst *et al.* (2013) for the Arabidopsis *mur1* mutant, which is defective in fucose biosynthesis. At higher concentrations of 2F-Fuc, dimers of RG-II were greatly diminished, but this was not counterbalanced by a relative increase in the level of monomeric RG-II (Figure 5b), suggesting that deposition of RG-II and/or its stability in plant cell walls is strongly affected by 2F-Fuc. Disruption of RG-II biosynthesis at 25 μM 2F-Fuc was confirmed by the inability of plants treated with 25 μM 2F-Fuc to incorporate Kdo-N_3 in a click-mediated labelling experiment (Figure 6). We postulate that the synthesis and dimerization of RG-II within the Golgi apparatus involve enzyme complexes that cannot produce normal RG-II when side chain biosynthesis is affected. It is worth noting that the GalA content in root cell walls was not disturbed by 2F-Fuc treatment, indicating that impairment of RG-II biosynthesis does not affect the overall synthesis of pectins. Sugar composition analyses of 2F-Fuc-treated roots also indicated a decrease in relative xylose content and an increase in relative galactose content. However, it is highly speculative to conclude whether these changes in cell wall composition are a direct result of the absence of fucosylation of cell wall polysaccharides or are adaptive modifications in cell wall biosynthesis in response to 2F-Fuc-induced growth defects.

To date, several mutations affecting RG-II structure have been demonstrated to affect both RG-II dimerization and plant development. This has been mainly deduced from the study of mutants defective in the biosynthesis of monosaccharides contained in RG-II (O'Neill *et al.*, 2001; Ahn *et al.*, 2006; Delmas *et al.*, 2008; Voxeur *et al.*, 2012). For instance, depletion of UDP-D-apiose/UDP-D-xylose synthase, the enzyme responsible for the synthesis of the RG-II-specific apiose residue, results in cell wall abnormalities, including wall thickening and gaps. These phenotypes are probably due to the synthesis of abnormal RG-II in this mutant (Ahn *et al.*, 2006). We observed similar altered cell wall patterns using calcofluor staining in 2.5 μM 2F-Fuc-treated seedlings (Figure 7g,h). Among other Arabidopsis mutants defective in RG-II biosynthesis, *mur1* is impaired in fucose biosynthesis and is thus unable to properly fucosylate its cell wall polysaccharides and glycoproteins (Zablackis *et al.*, 1996; Rayon *et al.*, 1999; O'Neill *et al.*, 2001). The fucosylation defects of cell wall polysaccharides and proteins observed in this study upon treatment with 2F-Fuc are similar to those observed in fucose-deficient *mur1* mutants (Zablackis *et al.*, 1996; Rayon *et al.*, 1999; O'Neill *et al.*, 2001). Both *mur1* and 2F-Fuc-treated plants exhibit growth defects, cell wall weakness and decreased RG-II dimerization, demonstrating a relationship between RG-II biosynthesis and plant development. Although *mur1* mutants and 2F-Fuc-treated seedlings exhibit similar underfucosylation and altered growth phenotypes, they differ in several aspects. In *mur1*, fucose is partially replaced in cell wall polysaccharides and glycoproteins by the structurally similar sugar L-Gal (Zablackis *et al.*, 1996; Rayon *et al.*, 1999; Reuhs *et al.*, 2004). In MALDI-MS profiles of 2F-Fuc-treated plants, ions that could be assigned to L-Gal-containing xyloglucan fragments or to their acetylated forms were not detected. Thus, we conclude that L-Fuc is probably not replaced by L-Gal in the xyloglucan of Arabidopsis seedlings upon treatment with 2F-Fuc. Furthermore, the *MUR1* gene encodes a GDP-D-mannose-4,6-dehydratase that catalyses the first step in the *de novo* synthesis of GDP-L-fucose (Bonin *et al.*, 1997). This mutant can be rescued by supplying exogenous L-Fuc, which is converted into GDP-Fuc through the salvage pathway (Bonin *et al.*, 1997; O'Neill *et al.*, 2001). In contrast, addition of fucose to the culture medium did not reverse the growth phenotype induced by 2F-Fuc (Figure S3).

Together, this information suggests that one or more fucosyltransferases are likely to be inhibited by 2F-Fuc. However, we cannot rule out that GDP-Fuc biosynthesis is also affected by this inhibitor.

Root cell elongation is strongly affected by 2F-Fuc treatment (Figure S6), which results in a high density of root hairs and the presence of differentiated cells close to the root tip (Figure 7f). This growth phenotype was previously reported in plants treated with 2β-deoxy-Kdo, which inhibits CMP-Kdo synthesis that is required for RG-II biosynthesis (Smyth *et al.*, 2013). Defects in cell elongation in RG-II mutants have previously been reported to be responsible for impairment of pollen tube growth and fertilization (Delmas *et al.*, 2008; Deng *et al.*, 2010; Liu *et al.*, 2011; Dumont *et al.*, 2014). In our study, close inspection of the root tip and monitoring of cell division activity suggest that cell division was not affected by 2F-Fuc (Figure 7i,j). This was confirmed by investigation of the rate of division of suspension-cultured BY-2 cells in the presence of the inhibitor (Figure S7). These data, together with previous studies showing that suspension-cultured plant cells are capable of continuous and long-term growth on a boron-deficient medium (Fleischer *et al.*, 1999; Chormova *et al.*, 2014), indicate that RG-II dimerization is required for cell elongation but not for cell division. In addition to the inhibition of cell elongation, 2F-Fuc induces the formation of multiple adventitious roots (Figure S7). These changes in root architecture caused by 2F-Fuc treatment are possibly due to a dysregulation of hormone-mediated signalling, since root growth is closely related to the synthesis, distribution and transport of auxin and ethylene (Blilou *et al.*, 2005; Gutierrez *et al.*, 2012; Abreu *et al.*, 2014).

Boron is required for RG-II cross-linking in plant cell walls, but is likely to serve other functions in cell expansion

It is known that RG-II is the main boron-binding site in the cell walls of plants, enabling this pectic polymer to dimerize. Supplementation of RG-II-deficient mutants with boron has been shown to partially restore wild-type growth phenotypes and the wild-type accumulation of RG-II dimers, demonstrating that RG-II dimerization is required for proper cell elongation (O'Neill *et al.*, 2001; Voxeur *et al.*, 2012; Smyth *et al.*, 2013). For instance, supplementation of *mur1* plants with borate partially restores RG-II cross-linking and wild-type growth patterns (O'Neill *et al.*, 2001). The ability of borate to partially rescue root growth that we observed in seedlings treated with 2.5 μM 2F-Fuc (Figure 5a) is comparable with observations previously reported for RG-II-deficient mutants. The PAGE analysis of RG-II of 2.5 μM 2F-Fuc-treated plants supplemented with boric acid indicated an increase in the relative amount of dRG-II, suggesting that boric acid was able to restore the dimerization of RG-II in inhibitor-treated roots. These data are in agreement with previous studies demonstrating a link between proper RG-II cross-linking and efficient cell elongation.

Boron was also shown to partially restore cell elongation in roots treated with high concentrations of 2F-Fuc (Figure 5a). At such concentrations, RG-II biosynthesis is strongly affected without modification of the overall pectin content of roots (Figure 2). In the PAGE experiment, the relative amounts of loaded cell wall fractions were identical. Thus, the disappearance of RG-II bands is probably a result of inhibition of RG-II biosynthesis rather than an overall decrease of pectic materials in the fractions isolated from the treated roots. Disruption of RG-II biosynthesis was confirmed by a metabolic click-labelling experiment using an azido Kdo analogue. As a consequence, partial rescue of cell elongation by borate supplementation in roots treated with 2F-Fuc might not be solely attributable to the restoration of appropriate RG-II dimerization. It is known that rapidly expanding cells respond dramatically to defects in cell wall integrity. Several studies have reported that this response is mediated by a cell wall integrity-sensing mechanism involving cell wall sensors and receptors, such as receptor kinases (Humphrey *et al.*, 2007; Hematy and Hofte, 2008; Boisson-Dernier *et al.*, 2011; Engelsdorf and Hamann, 2014). These membrane-bound proteins allow for the maintenance of cell wall integrity and the coordination of plant development. We postulate that, in response to 2F-Fuc treatments, these 'sentinels' act as sensors that detect impairment of RG-II and in turn induce arrest of elongation. Since borate is able to partially restore elongation in cells that lack normal levels of RG-II, it might also function as a signalling molecule in the cell wall integrity-sensing mechanism. Boron could either act as free borate or be linked to the *cis*-diol motifs of metabolites, as reported for the bacterial boron-containing quorum-sensing signal (Chen *et al.*, 2002). Partial restoration of wild-type elongation by borate supplementation has previously been reported in mutants exhibiting growth phenotypes and structural cell wall defects that are not related to RG-II. For instance, structural alteration of cell wall xyloglucans and pectins in *mur3* and *mur4* mutants causes a hypersensitive sugar-responsive phenotype that is also rescued by supplementation with boric acid (Li *et al.*, 2007). The *mur3* and *mur4* mutants are affected in the synthesis of xyloglucan and RG-I, respectively, and the growth restoration effects are probably not related to borate cross-linking of cell wall RG-II in these plant mutants. Some authors have postulated that borate might also be involved in cross-linking of monosaccharide residues in xyloglucan and RG-I, as recently reported for glycosylinositol phosphoceramides of lipid rafts (Wimmer *et al.*, 2009; Voxeur and Fry, 2014). However, no biochemical evidence for RG-I and xyloglucan borate-mediated cross-linking in cell walls has been reported thus far. As a consequence, the data reported by Li *et al.* (2007), together

with data presented here, suggest that borate might be perceived as a positive signal for cell wall elongation. As recently speculated by Funakawa and Miwa (2015), the roles of boron in the primary cell wall might not be restricted to the physical cross-linking of the pectic network but might also include its activity as a direct regulator of cell elongation and/or cell wall integrity sensing. As a consequence, beyond their structural functions in cell walls, RG-II dimers may also play a crucial role as *in muro* sequestration sites for boron, as has been reported for deesterified homogalacturonan and calcium (Braccini and Pérez, 2001; Wolf *et al.*, 2009; Leroux *et al.*, 2015).

In conclusion, this study further emphasizes the importance of RG-II and its borate-mediated dimerization in cell elongation. It also highlights the potential of glycosyltransferase inhibitors as new tools for studying the function of cell wall polysaccharides in plant development. The use of these inhibitors enables the control of timing and the dose-dependent inhibition of glycosyltransferases, two aspects that are not easily achievable by studying genetic mutants alone. By combining chemical and genetic tools, we can hope to better understand the complexity of cell wall synthesis, structure and dynamics.

EXPERIMENTAL PROCEDURES

Plant material and growth conditions

Arabidopsis thaliana lines were derived from the Columbia ecotype (Col). Seeds were surface sterilized and sown onto Arabidopsis medium (Duchefa Biochemie no. DUO0742.0025, https://www.duchefa-biochemie.com/) supplemented with 2 mM Ca $(NO_3)_2$ and 0.8% (w/v) Bacto Agar, pH 5.8. Plates with seeds were placed for 2 days at 4°C in the dark, then submitted to 16-h day/8-h night cycles (120 μE m^{-2} s^{-1}, 21°C) in a vertical position. For click chemistry experiments, sterilized seeds were sown on Murashige and Skoog (MS; 2.2 g L^{-1}) mineral medium containing 1% sucrose and 0.8% plant agar (see below). *mur2* seeds were from the Nottingham Arabidopsis Stock Centre (NASC), the *pCYCB1::*GUS line was from A. Marchant (Southampton University, UK) and the *Atfkgp* mutant from T. Kotake (Saitama University, Japan). Suspension-cultured cells of *Nicotiana tabacum* cv. Bright Yellow 2 (BY-2) were cultured in MS liquid medium 4.3 g L^{-1} supplemented with 3% sucrose (w/v), 100 mg L^{-1} KH_2PO_4, 51 mg L^{-1} myo-inositol, 1 mg L^{-1} thiamine, 0.22 mg L^{-1} 2.4 dichlorophenoxyacetic acid, pH 5.6, in the dark at 22°C and shaking at 140 r.p.m. BY-2 cells were sub-cultured every week by transferring 10 ml of suspension cells into 150 ml of fresh medium.

Chemical compounds

Peracetylated 2-fluoro 2-deoxy-l-fucose was purchased from Calbiochem® (Merck Millipore, http://www.merckmillipore.com/). 2-Fluoro 2-deoxy-D-glucopyranose (2F-Glc), 3F-Glc and the 4F-Glc were from LC Scientific Inc. (http://www.lcsci.com/). Deoxy fluoro glucose analogues (5 mg) were peracetylated in 150 μl of 2:1 pyridine:acetic anhydride overnight at 20°C. Excess reagent was co-evaporated with toluene under a stream of air. Fluoro sugar analogues were then dissolved in DMSO (10 mM). To assess the effect of each sugar analogue on plant growth, the inhibitor was added directly to the growth medium at the desired concentration. To assess effects on cell division, peracetylated 2F-Fuc was added to the medium of tobacco BY-2 suspension-cultured cells 4 days after subculture. For boron experiments, 0.75 mM boric acid was used because higher concentrations of borate had a negative effect on Arabidopsis root length.

Metabolic click labelling of cell walls

Click chemistry experiments were performed as described in Anderson *et al.* (2012). *Arabidopsis thaliana* Col-0 sterilized seeds were sown on MS (2.2 g L^{-1}) mineral medium containing 1% sucrose and 0.8% plant agar. After 2 days at 4°C, the plates were placed vertically in a growth chamber for 4 days at 22°C under a 16-h light/8-h dark cycle. Four-day-old light-grown seedlings were transferred from MS mineral medium plates to 1 ml of liquid MS containing 2.5 μM Fuc-Al (Invitrogen, http://www.invitrogen.com/) for 16 h at 22°C in the growth chamber (16-h light/8-h dark). Seedlings were then washed three times with liquid MS and then transferred to 1 ml of 0.1 μM Alexa Fluor® 488 azide (Invitrogen) solution in liquid MS containing 1 mM $CuSO_4$ and freshly made 1 mM ascorbic acid. The solution was incubated for 1 h at room temperature (22°C) in the dark. Seedlings were then washed once with liquid MS, then for 5 min with liquid MS supplemented with 0.01% (v/v) Tween 20 and three additional times in liquid MS. Control experiments were carried out by omitting either the Fuc-Al or the fluorescent probe in click-mediated labelling assays. Inhibition of fucosyl transferases was carried out by adding 25 μM 2F-Fuc in the growth medium and then by supplementing the liquid MS with 25 μM 2F-Fuc during the Fuc-Al incorporation step. Fuc-Al labelling was examined using a confocal laser-scanning microscope (Leica TCS SP2 AOBS, excitation filter 488 nm, barrier filter 495–550 nm, http://www.leica.com/). For the click chemistry experiment using Kdo-N_3, the same protocol was carried out using 50 μM of the Kdo analogue and Alexa Fluor® 488 alkyne (Invitrogen). The fluorescence intensity of the root was calculated with ImageJ by thresholding (pixel intensity > 16) to select the root boundary and measuring the mean of pixel intensity inside the area defined by the threshold.

Histochemical GUS staining

Six-day-old pCYCB1::GUS seedlings were incubated for 3 h in the dark, at 37°C, in the reaction solution containing 2 mM potassium ferrocyanide, 2 mM potassium ferricyanide, 50 mM sodium phosphate pH 7, 0.2% Triton X100 and 1 mM 5-bromo-4-chloro-3-indolyl-β-D-glucuronic acid (X-Gluc). Arabidopsis plants were observed under bright field using a Leica M125 stereomicroscope equipped with a DFC295 camera. At least 10 seedlings per treatment were observed and photographed.

Histochemical calcofluor staining

Roots were incubated with 0.001% calcofluor white M2R (Sigma, http://www.sigmaaldrich.com/) for 5 min in the dark. Then, the roots were mounted on glass microscope slides in a drop of water and observed by spinning disk confocal microscopy (Zeiss Observer Z1, http://www.zeiss.com/) equipped with UV fluorescence (excitation filter 359 nm, barrier filter 461 nm). Root length and fluorescence were measured from images using the ImageJ program (Abramoff *et al.*, 2004).

Plant cell wall preparation

The roots and shoots of 10-day-old seedlings grown on Arabidopsis medium supplemented or not with peracetylated 2F-Fuc were

manually separated and then heated for 15 min in 70% ethanol at 70°C. The tissues were then ground in a potter homogenizer and the homogenate was washed with 70% ethanol at 70°C and then with water. The remaining alcohol-insoluble residue was dried and was considered as representative of the cell walls.

Sugar composition analysis by gas phase chromatography

Alcohol-insoluble residues from shoot and root of about 400 seedlings were hydrolysed using trifluoroacetic acid (2 M, 2 h at 110°C) and then submitted to a methanolysis for 16 h at 80°C with 500 µl of dried 1 M methanolic-HCl (Supelco, SigmaAldrich; http://www.sigmaaldrich.com/analytical-chromatography/supelco-analytical/about-supelco.html). After evaporation of the methanol, the methyl glycosides were converted into their trimethylsilyl derivatives at 110°C for 20 min with 200 µl of the silylation reagent (HMDS:TMCS:pyridine, 3:1:9; Supelco). After drying, derivatives were dissolved in 1 ml of cyclohexane and analysed using a 3800 GC system equipped with a CP-Sil5-CB column (Agilent Technologies, http://www.agilent.com/) and a flame ionization detector. The gradient temperature was from 120 to 160°C at 10°C min^{-1}, 160 to 220°C at 1.5°C min^{-1} and 220 to 280°C at 20°C min^{-1}. Quantification was carried out using inositol as the internal standard and response factors previously determined for cell wall monosaccharides. Due to contamination with starch, the glucose contents were rejected from the sugar composition of root extracts.

Extraction of proteins

Two hundred to 800 roots from 10-day-old Arabidopsis seedlings grown on Arabidopsis medium supplemented with 0.25% DMSO or 25 µM 2F-Fuc were ground on ice in a 1-ml potter homogenizer in 2-amino-2-(hydroxymethyl)-1,3-propanediol (TRIS) 0.1 M pH 8 buffer containing 0.1% of SDS. The extract was then freeze-dried. Proteins extracts were then resuspended in 300 µl of TRIS-SDS buffer.

Immunoblotting

Protein extracts were separated by SDS-PAGE using a 12% polyacrylamide gel. The proteins were transferred onto nitrocellulose membrane and stained with Ponceau Red to control the transfer efficiency and to ensure that the same protein quantities were loaded for the two conditions. Before the immunoblotting, the free binding sites on nitrocellulose were blocked overnight with TRIS-buffered saline (TBS; 50 mM TRIS, 150 mM NaCl, pH 7.5) complemented with 0.1% Tween by gentle agitation. The membrane was incubated in a 1/10 000 PBS–Tween solution of antibodies directed against the core α-1,3-fucose (anti-Fuc) epitope for 2 h (Faye *et al.*, 1993) and washed three times with 0.1% TBS–Tween for 10 min. The membrane was next incubated for 2 h in alkaline phosphatase-conjugated goat anti-rabbit IgG (Sigma) diluted 1/1000 in 0.1% PBS–Tween. The membrane was finally washed six times in 0.1% TBS–Tween and three times in TBS for 5 min. The substrate of the alkaline phosphatase (Western Blue® Stabilized substrate for alkaline phosphatase; Promega, http://www.promega.com/) was applied on the membrane until the staining appeared. The reaction was stopped by rinsing in water.

Xyloglucan fingerprinting

Xyloglucan fragments were generated by treating the alcohol-insoluble residues isolated from 200 to 500 seedlings with 4 U of endoglucanase (endo-1,4-β-D-glucanase from *Trichoderma longibrachiatum*, E-CELTR; Megazyme, https://www.megazyme.com/) in 100 µl of 10 mM sodium acetate buffer, pH 5, for 18 h at 37°C. Mass spectra were acquired on a Voyager DE-Pro MALDI-TOF (Ab Sciex, http://sciex.com/) instrument equipped with a 337-nm nitrogen laser. Mass spectra were performed in the reflector-delayed extraction mode using 2,5-dihydroxybenzoic acid as the matrix (Sigma-Aldrich). This matrix, dissolved at 5 mg ml^{-1} in a 70/30 acetonitrile/0.1% trifluoroacetic acid solution, was mixed onto the target with the digests in a 1:1 (v/v) ratio. Spectra were recorded in a positive mode, using an acceleration voltage of 20 000 V with a delay time of 100 ns. They were externally calibrated using commercially available mixtures of peptides (ProteoMass™ Peptide MALDI-MS Calibration Kit, Sigma-Aldrich). A thousand laser shots were accumulated for each spectrum. The main ions detected were assigned to $[M+Na]^+$ adducts from XXXG to XLFG on the basis of their molecular weight and literature data (Zablackis *et al.*, 1995; Lerouxel *et al.*, 2002). Relative quantification of the different oligosaccharide species was performed using their *m/z* ion intensity in MALDI-TOF spectra.

Fucosyltransferase activity assay

Fucosyltransferase activity assays were carried out using Δ_{68}-AtFuT1 (deletion of 68 amino acids at the N-terminus for protein solubility) construct amplified from the U10760 clone (TAIR, https://www.arabidopsis.org/) and cloned into the pVT-Bac-His vector for expression in insect cells. *Spodoptera frugiperda* (Sf9, Invitrogen) cells used for the transfection were cultured in Grace medium (Invitrogen) supplemented with 10% fetal bovine serum (Sigma) and 50 µg ml^{-1} gentamycin (Sigma) at 27°C and cultured in monolayer flask at 27°C. Culture medium was collected by centrifugation at 13 000 ***g*** for 30 min in order to pellet major impurities and supernatant containing recombinant protein was either stored at −80°C or used immediately. Enzymatic testing was performed as follows: Δ_{68}-AtFuT1 (134 ng of protein) was incubated in 100 µl of 10 mM HEPES-KOH buffer pH 7 containing 10 mM $MgCl_2$, 10 mM $MnCl_2$, 30 µM of GDP-Fuc and 1.5 µM (20 nCi) of GDP-[^{14}C]-Fuc with or without 2F-Fuc at 1 mM. Tamarind xyloglucan supplied by rhodia; www.rhodia.com was used at various concentrations (0.5, 1, 2 and 4 mg ml^{-1}) to determine the apparent K_m value of recombinant HisΔ_{68}-AtFuT1 for this acceptor in the presence or not of 2F-Fuc. As tamarind xyloglucan is a polymer with a mass distribution centred at about M_w = 582500 Da, mass concentration of xyloglucan were used to express K_m values accurately. After incubation at 30°C for 30 min, the reaction was stopped by the addition of 1 ml of anion exchange resin AG 1x8 (200–400 mesh) at 25% (p/v) in water. After centrifugation, 2 min at 5000 ***g***, the supernatant was collected, mixed with 3.8 ml of scintillation liquid and then the radioactivity was counted for 1 min using a Packard Bell instrument. Apparent K_m values of AtFUT1 towards xyloglucan were read on the double-reciprocal plots and thereafter referred to as K_m for data in absence of 2F-Fuc (triangle plot) and K_m' in the presence of 2F-Fuc (square plot). K_i was calculated as follows: $K_i = K_m[2F\text{-}Fuc]/(K_m' - K_m)$.

Isolation of RG-II

Roots from 200 to 1000 seedlings were ground in a 1 ml potter homogenizer in 70% ethanol. The homogenate was centrifuged at 14 000 ***g*** for 10 min and the pellet was washed with 70% ethanol until the supernatant was clear. Additional washing was performed in 100% acetone. The resulting alcohol-insoluble residue was dried and was treated with 1 M Na_2CO_3 at 4°C for 16 h, then rinsed with water until neutral pH was achieved. The pellet was suspended in 500 µl ammonium acetate buffer (0.05 M, pH 4.8) with 5 U endo-polygalacturonase from *Aspergillus niger* (Megazyme) and incubated at 37°C for 16 h. Solubilized material was

concentrated in a centrifugal vacuum concentrator. The RG-II was suspended in 25 μl of ammonium acetate buffer. The relative amount of cell wall sugars for each RG-II-enriched fraction was assessed by quantification of monosaccharides by gas chromatography analysis before running on PAGE.

Polyacrylamide gel electrophoresis of RG-II

Polyacrylamide gel electrophoresis was performed according to Chormova *et al.* (2014) with few changes. A 10% polyacrylamide stacking gel was added to a 26% polyacrylamide gel. Eight-microlitre RG-II samples were mixed with 2 μl of sample buffer [0.63 M TRIS-HCl containing 0.25% (w/v) bromophenol blue and 50% (v/v) glycerol, pH 8.8]. Eighty micrograms of RG-II extracted from lemon was used as control. For monomerization, lemon RG-II was incubated for 16 h at room temperature in 0.1 M HCl (v/v). Before loading, the sample was neutralized with 0.1 M NaOH (v/v). Electrophoresis was conducted at 220 V for 130 min. The gel was then fixed in ethanol/acetic acid/water (4:1:5) for 30 min and washed three times in 30% ethanol for 10 min and three times in water for 10 min each. Silver staining was performed as described by Chormova *et al.* (2014).

Statistical analysis

The data were analysed statistically by using GraphPad software (http://www.graphpad.com/). Differences were considered statistically significant when $P \leq 0.05$ (*), highly significant when $P < 0.01$ (**) and very highly significant when $P < 0.001$ (***).

ACKNOWLEDGEMENTS

This work was supported by the University of Rouen, the French Agency for Research (grant no. ANR-11-BSV5-0007) and the 'Trans Channel Wallnet' project that has been selected in the context of the INTERREG IVA France (Channel)–England European cross-border cooperation programme, which is co-financed by the ERDF. Work at Pennsylvania State University was supported by the Center for Lignocellulose Structure and Formation, an Energy Frontier Research Center funded by the DOE, Office of Science, BES under award no. DE-SC0001090. Images were obtained on PRIMACEN (http://www.primacen.fr), the Cell Imaging Platform of Normandy, IRIB, Faculty of Sciences, University of Rouen, 76821 Mont-Saint-Aignan, France. The authors thank Alan Marchant (University of Southampton, UK) for providing pCYCB1::GUS Arabidopsis seeds, Marie-Christine Ralet (INRA, Nantes, France) for the gift of lemon RG-II, T. Kotake (Saitama University, Japan) for providing the *Atfkgp* mutant and Aline Voxeur for technical advice.

SUPPORTING INFORMATION

Additional Supporting Information may be found in the online version of this article.

Figure S1. Structure of rhamnogalacturonan II.

Figure S2. Effects of fluoro monosaccharide analogues on plant growth.

Figure S3. Excess of fucose did not restore the inhibitory effect of 2-fluoro 2-L-fucose.

Figure S4. Cytosolic L-fucokinase and GDP-L-fucose pyrophosphorylase activities are not affected by 2-fluoro 2-L-fucose.

Figure S5. Inhibition of AtFUT1 fucosyltransferase activity by 2-fluoro 2-L-fucose.

Figure S6. Effect of 2-fluoro 2-L-fucose on cell elongation.

Figure S7. Effect of 2-fluoro 2-L-fucose on BY-2 cell division.

Figure S8. Emergence of adventitious roots in 14-day-old treated Arabidopsis seedlings.

REFERENCES

Abramoff, M.D., Magalhães, P.J. and Ram, S.J. (2004) Image processing with imageJ. *Biophotonics Int.* **11**, 36–42.

Abreu, I., Poza, L., Bonilla, I. and Bolaños, L. (2014) Boron deficiency results in early repression of a cytokinin receptor gene and abnormal cell differentiation in the apical root meristem of *Arabidopsis thaliana*. *Plant Physiol. Biochem.* **77**, 117–121.

Ahn, J.-W., Verma, R., Kim, M., Lee, J.-Y., Kim, Y.-K., Bang, J.-W., Reiter, W.-D. and Pai, H.-S. (2006) Depletion of UDP-D-apiose/UDP-D-xylose synthases results in rhamnogalacturonan-II deficiency, cell wall thickening, and cell death in higher plants. *J. Biol. Chem.* **281**, 13708–13716.

Albersheim, P., Darvill, A., Roberts, K., Sederoff, R. and Staehelin, A. (2010) *Plant Cell Walls: From Chemistry to Biology*. New York: Garland Science.

Anderson, C.T., Carroll, A., Akhmetova, L. and Somerville, C. (2010) Real-time imaging of cellulose reorientation during cell wall expansion in Arabidopsis roots. *Plant Physiol.* **152**, 787–796.

Anderson, C.T., Wallace, I.S. and Somerville, C.R. (2012) Metabolic click-labeling with a fucose analog reveals pectin delivery, architecture, and dynamics in Arabidopsis cell walls. *Proc. Natl. Acad. Sci. U. S. A.* **109**, 1329–1334.

Bar-Peled, M., Urbanowicz, B.R. and O'Neill, M.A. (2012) The synthesis and origin of the pectic polysaccharide rhamnogalacturonan II – insights from nucleotide sugar formation and diversity. *Front. Plant Sci.* **3**, 92.

Blilou, I., Xu, J., Wildwater, M., Willemsen, V., Paponov, I., Friml, J., Heidstra, R., Aida, M., Palme, K. and Scheres, B. (2005) The PIN auxin efflux facilitator network controls growth and patterning in Arabidopsis roots. *Nature*, **433**, 39–44.

Boisson-Dernier, A., Kessler, S.A. and Grossniklaus, U. (2011) The walls have ears: the role of plant CrRLK1Ls in sensing and transducing extracellular signals. *J. Exp. Bot.* **62**, 1581–1591.

Bonin, C.P., Potter, I., Vanzin, G.F. and Reiter, W.D. (1997) The MUR1 gene of Arabidopsis thaliana encodes an isoform of GDP-D-mannose-4, 6-dehydratase, catalyzing the first step in the *de novo* synthesis of GDP-L-fucose. *Proc. Natl. Acad. Sci. U. S. A.* **94**, 2085–2090.

Bouton, S., Leboeuf, E., Mouille, G., Leydecker, M.-T., Talbotec, J., Granier, F., Lahaye, M., Höfte, H. and Truong, H.-N. (2002) QUASIMODO1 encodes a putative membrane-bound glycosyltransferase required for normal pectin synthesis and cell adhesion in Arabidopsis. *Plant Cell*, **14**, 2577–2590.

Braccini, I. and Pérez, S. (2001) Molecular basis of Ca^{2+}-induced gelation in alginates and pectins: the egg-box model revisited. *Biomacromolecules*, **2**, 1089–1096.

Brown, C.D., Rusek, M.S. and Kiessling, L.L. (2012) Fluorosugar chain termination agents as probes of the sequence specificity of a carbohydrate polymerase. *J. Am. Chem. Soc.* **134**, 6552–6555.

Burkart, M.D., Vincent, S.P., Düffels, A., Murray, B.W., Ley, S.V. and Wong, C.-H. (2000) Chemo-enzymatic synthesis of fluorinated sugar nucleotide: useful mechanistic Probes for glycosyltransferases. *Bioorg. Med. Chem.* **8**, 1937–1946.

Cavalier, D.M., Lerouxel, O., Neumetzler, L. *et al.* (2008) Disrupting two Arabidopsis thaliana xylosyltransferase genes results in plants deficient in xyloglucan, a major primary cell wall component. *Plant Cell*, **20**, 1519–1537.

Chen, X., Schauder, S., Potier, N., Van Dorsselaer, A., Pelczer, I., Bassler, B.L. and Hughson, F.M. (2002) Structural identification of a bacterial quorum-sensing signal containing boron. *Nature*, **415**, 545–549.

Choi, S., Ruszczycky, M.W., Zhang, H. and Liu, H. (2011) A fluoro analogue of UDP-α-D-glucuronic acid is an inhibitor of UDP-α-D-apiose/UDP-α-D-xylose synthase. *Chem. Commun. (Camb. Engl.)* **47**, 10130–10132.

Chormova, D., Messenger, D.J. and Fry, S.C. (2014) Boron bridging of rhamnogalacturonan-II, monitored by gel electrophoresis, occurs during

polysaccharide synthesis and secretion but not post-secretion. *Plant J.* **77**, 534–546.

Dardelle, F., Le Mauff, F., Lehner, A., Loutelier-Bourhis, C., Bardor, M., Rihouey, C., Causse, M., Lerouge, P., Driouich, A. and Mollet, J.C. (2015) Pollen tube cell walls of wild and domesticated tomatoes contain arabinosylated and fucosylated xyloglucan. *Ann. Bot.* **115**, 55–66.

Datema, R., Schwarz, R.T., Rivas, L.A. and Lezica, R.P. (1983) Inhibition of beta-1,4-glucan biosynthesis by deoxyglucose : the effect on the glucosylation of lipid intermediates. *Plant Physiol.* **71**, 76–81.

Delmas, F., Séveno, M., Northey, J.G.B., Hernould, M., Lerouge, P., McCourt, P. and Chevalier, C. (2008) The synthesis of the rhamnogalacturonan II component 3-deoxy-D-manno-2-octulosonic acid (Kdo) is required for pollen tube growth and elongation. *J. Exp. Bot.* **59**, 2639–2647.

Deng, Y., Wang, W., Li, W.-Q., Xia, C., Liao, H.-Z., Zhang, X.-Q. and Ye, D. (2010) MALE GAMETOPHYTE DEFECTIVE 2, encoding a sialyltransferase-like protein, is required for normal pollen germination and pollen tube growth in Arabidopsis. *J. Integr. Plant Biol.* **52**, 829–843.

Dumont, M., Lehner, A., Bouton, S., Kiefer-Meyer, M.C., Voxeur, A., Pelloux, J., Lerouge, P. and Mollet, J.-C. (2014) The cell wall pectic polymer rhamnogalacturonan-II is required for proper pollen tube elongation: implications of a putative sialyltransferase-like protein. *Ann. Bot.* **114**, 1177–1188.

Dumont, M., Lehner, A., Vauzeilles, B. *et al.* (Accepted) Plant cell wall imaging by metabolic click-mediated labelling of rhamnogalacturonan II using azido 3-deoxy-D-manno-oct-2-ulosonic acid analogue. *Plant J.*

Edmonds, M.K. and Peddie, V. (2006) Fluorinated analogues of biological molecules: accessing new chemical, physical and biological properties. *Chem. N.Z.* **70**, 85–87.

Egelund, J., Petersen, B.L., Motawia, M.S., Damager, I., Faik, A., Olsen, C.E., Ishii, T., Clausen, H., Ulvskov, P. and Geshi, N. (2006) *Arabidopsis thaliana* RGXT1 and RGXT2 encode Golgi-localized (1,3)-alpha-D-xylosyltransferases involved in the synthesis of pectic rhamnogalacturonan-II. *Plant Cell*, **18**, 2593–2607.

Egelund, J., Damager, I., Faber, K., Olsen, C.-E., Ulvskov, P. and Petersen, B.L. (2008) Functional characterisation of a putative rhamnogalacturonan II specific xylosyltransferase. *FEBS Lett.* **582**, 3217–3222.

Engelsdorf, T. and Hamann, T. (2014) An update on receptor-like kinase involvement in the maintenance of plant cell wall integrity. *Ann. Bot.* **114**, 1339–1347.

Faye, L., Gomord, V., Fitchette-Lainé, A.C. and Chrispeels, M.J. (1993) Affinity purification of antibodies specific for Asn-linked glycans containing alpha 1–>3 fucose or beta 1–>2 xylose. *Anal. Biochem.* **209**, 104–108.

Ferrieri, A.P., Appel, H., Ferrieri, R.A. and Schultz, J.C. (2012) Novel application of 2-[18F]fluoro-2-deoxy-d-glucose to study plant defenses. *Nucl. Med. Biol.* **39**, 1152–1160.

Fleischer, A., O'Neill, M.A. and Ehwald, R. (1999) The pore size of non-graminaceous plant cell walls is rapidly decreased by borate ester cross-linking of the pectic polysaccharide rhamnogalacturonan II. *Plant Physiol.* **121**, 829–838.

Fry, S.C., York, W.S., Albersheim, P. *et al.* (1993) An unambiguous nomenclature for xyloglucan-derived oligosaccharides. *Physiol. Plant.* **89**, 1–3.

Funakawa, H. and Miwa, K. (2015) Synthesis of borate cross-linked rhamnogalacturonan II. *Front. Plant Sci.* **6**, 223.

Glushka, J.N., Terrell, M., York, W.S., O'Neill, M.A., Gucwa, A., Darvill, A.G., Albersheim, P. and Prestegard, J.H. (2003) Primary structure of the 2-O-methyl-α-l-fucose-containing side chain of the pectic polysaccharide, rhamnogalacturonan II. *Carbohydr. Res.* **338**, 341–352.

Gutierrez, L., Mongelard, G., Floková, K. *et al.* (2012) Auxin controls Arabidopsis adventitious root initiation by regulating jasmonic acid homeostasis. *Plant Cell.* **24**(6), 2515–2527.

Hattori, E., Uchida, H., Harada, N., Ohta, M., Tsukada, H., Hara, Y. and Suzuki, T. (2008) Incorporation and translocation of 2-deoxy-2-[18F] fluoro-d-glucose in *Sorghum bicolor* (L.) Moench monitored using a planar positron imaging system. *Planta* **227**, 1181–1186.

Hematy, K. and Hofte, H. (2008) Novel receptor kinases involved in growth regulation. *Curr. Opin. Plant Biol.* **11**, 321–328.

Hoffman, M., Jia, Z., Peña, M.J., Cash, M., Harper, A., Blackburn, A.R. II, Darvill, A. and York, W.S. (2005) Structural analysis of xyloglucans in the primary cell walls of plants in the subclass Asteridae. *Carbohydr. Res.* **340**, 1826–1840.

Humphrey, T.V., Bonetta, D.T. and Goring, D.R. (2007) Sentinels at the wall: cell wall receptors and sensors. *New Phytol.* **176**, 7–21.

Jaffe, M.J. and Leopold, A.C. (1984) Callose deposition during gravitropism of *Zea mays* and *Pisum sativum* and its inhibition by 2-deoxy-D-glucose. *Planta* **161**, 20–26.

Kobayashi, M., Matoh, T. and Azuma, J.I. (1996) Two chains of rhamnogalacturonan II are cross-linked by borate-diol ester bonds in higher plant cell walls. *Plant Physiol.* **110**, 1017–1020.

Kotake, T., Hojo, S., Tajima, N., Matsuoka, K., Koyama, T. and Tsumuraya, Y. (2008) A bifunctional enzyme with L-fucokinase and GDP-L-fucose pyrophosphorylase activities salvages free L-fucose in Arabidopsis. *J. Biol. Chem.* **283**, 8125–8135.

Lampugnani, E.R., Moller, I.E., Cassin, A., Jones, D.F., Koh, P.L., Ratnayake, S., Beahan, C.T., Wilson, S.M., Bacic, A. and Newbigin, E. (2013) *In vitro* grown pollen tubes of *Nicotiana alata* actively synthesise a fucosylated xyloglucan. *PLoS ONE*, **8**, e77140.

Leroux, C., Bouton, S., Kiefer-Meyer, M.C. *et al.* (2015) PECTIN METHYLESTERASE48 is involved in Arabidopsis pollen grain germination. *Plant Physiol.* **167**, 367–380.

Lerouxel, O., Choo, T.S., Séveno, M., Usadel, B., Faye, L., Lerouge, P. and Pauly, M. (2002) Rapid structural phenotyping of plant cell wall mutants by enzymatic oligosaccharide fingerprinting. *Plant Physiol.* **130**, 1754–1763.

Li, Y., Smith, C., Corke, F., Zheng, L., Merali, Z., Ryden, P., Derbyshire, P., Waldron, K. and Bevan, M.W. (2007) Signaling from an altered cell wall to the nucleus mediates sugar-responsive growth and development in *Arabidopsis thaliana*. *Plant Cell* **19**, 2500–2515.

Liang, Y., Basu, D., Pattathil, S., Xu, W., Venetos, A., Martin, S.L., Faik, A., Hahn, M.G. and Showalter, A.M. (2013) Biochemical and physiological characterization of *fut4* and *fut6* mutants defective in arabinogalactan-protein fucosylation in Arabidopsis. *J. Exp. Bot.* **64**, 5537–5551.

Liu, X.-L., Liu, L., Niu, Q.-K., Xia, C., Yang, K.Z., Li, R., Chen, L.Q., Zhang, X.Q., Zhou, Y. and Ye, D. (2011) Male gametophyte defective 4 encodes a rhamnogalacturonan II xylosyltransferase and is important for growth of pollen tubes and roots in Arabidopsis. *Plant J.* **65**, 647–660.

Matsunaga, T., Ishii, T., Matsumoto, S., Higuchi, M., Darvill, A., Albersheim, P. and O'Neill, M.A. (2004) Occurrence of the primary cell wall polysaccharide rhamnogalacturonan II in pteridophytes, lycophytes, and bryophytes. Implications for the evolution of vascular plants. *Plant Physiol.* **134**, 339–351.

Nakamura, A., Furuta, H., Maeda, H., Nagamatsu, Y. and Yoshimoto, A. (2001) Analysis of structural components and molecular construction of soybean soluble polysaccharides by stepwise enzymatic degradation. *Biosci. Biotechnol. Biochem.* **65**, 2249–2258.

Okeley, N.M., Alley, S.C., Anderson, M.E. *et al.* (2013) Development of orally active inhibitors of protein and cellular fucosylation. *Proc. Natl. Acad. Sci. U. S. A.* **110**, 5404–5409.

O'Neill, M.A., Warrenfeltz, D., Kates, K., Pellerin, P., Doco, T., Darvill, A.G. and Albersheim, P. (1996) Rhamnogalacturonan-II, a pectic polysaccharide in the walls of growing plant cell, forms a dimer that is covalently cross-linked by a borate ester. *In vitro* conditions for the formation and hydrolysis of the dimer. *J. Biol. Chem.* **271**, 22923–22930.

O'Neill, M.A., Eberhard, S., Albersheim, P. and Darvill, A.G. (2001) Requirement of borate cross-linking of cell wall rhamnogalacturonan II for Arabidopsis growth. *Science*, **294**, 846–849.

O'Neill, M.A., Ishii, T., Albersheim, P. and Darvill, A.G. (2004) Rhamnogalacturonan II: structure and function of a borate cross-linked cell wall pectic polysaccharide. *Annu. Rev. Plant Biol.* **55**, 109–139.

Pabst, M., Fischl, R.M., Brecker, L., Morelle, W., Fauland, A., Köfeler, H., Altmann, F. and Léonard, R. (2013) Rhamnogalacturonan II structure shows variation in the side chains monosaccharide composition and methylation status within and across different plant species. *Plant J.* **76**, 61–72.

Perrin, R.M., DeRocher, A.E., Bar-Peled, M., Zeng, W., Norambuena, L., Orellana, A., Raikhel, N.V. and Keegstra, K. (1999) Xyloglucan fucosyltransferase, an enzyme involved in plant cell wall biosynthesis. *Science*, **284**, 1976–1979.

Perrin, R.M., Jia, Z., Wagner, T.A., O'Neill, M.A., Sarria, R., York, W.S., Raikhel, N.V. and Keegstra, K. (2003) Analysis of xyloglucan fucosylation in Arabidopsis. *Plant Physiol.* **132**, 768–778.

Rayon, C., Lerouge, P. and Faye, L. (1998) The protein N-glycosylation in plants. *J. Exp. Bot.* **49**, 1463–1472.

Rayon, C., Cabanes-Macheteau, M., Loutelier-Bourhis, C., Salliot-Maire, I., Lemoine, J., Reiter, W.-D., Lerouge, P. and Faye, L. (1999) Characterization of *N*-glycans from Arabidopsis. Application to a fucose-deficient mutant. *Plant Physiol.* **119**, 725–734.

Reuhs, B.L., Glenn, J., Stephens, S.B., Kim, J.S., Christie, D.B., Glushka, J.G., Zablackis, E., Albersheim, P., Darvill, A.G. and O'Neill, M.A. (2004) L-Galactose replaces L-fucose in the pectic polysaccharide rhamnogalacturonan II synthesized by the L-fucose-deficient mur1 Arabidopsis mutant. *Planta*, **219**, 147–157.

Rillahan, C.D., Antonopoulos, A., Lefort, C.T., Sonon, R., Azadi, P., Ley, K., Dell, A., Haslam, S.M. and Paulson, J.C. (2012) Global metabolic inhibitors of sialyl- and fucosyltransferases remodel the glycome. *Nat. Chem. Biol.* **8**, 661–668.

von Schaewen, A., Sturm, A., O'Neill, J. and Chrispeels, M.J. (1993) Isolation of a mutant *Arabidopsis* plant that lacks *N*-acetyl glucosaminyl transferase I and is unable to synthesize Golgi-modified complex *N*-linked glycans. *Plant Physiol.* **102**, 1109–1118.

Schwarz, R.T. and Datema, R. (1980) Inhibitors of protein glycosylation. *Trends Biochem. Sci.* **5**, 65–67.

Smyth, K.M., Mikolajek, H., Werner, J.M. and Marchant, A. (2013) 2β-deoxy-Kdo is an inhibitor of the *Arabidopsis thaliana* CMP-2-Keto-3-deoxy-manno-octulosonic acid synthetase, the enzyme required for activation of Kdo prior to incorporation into rhamnogalacturonan II. *Mol. Plant* **6**, 981–984.

Som, P., Atkins, H.L., Bandoypadhyay, D. *et al.* (1980) A fluorinated glucose analog, 2-fluoro-2-deoxy-D-glucose (F-18): nontoxic tracer for rapid tumor detection. *J. Nucl. Med.* **21**, 670–675.

Strasser, R., Altmann, F., Mach, L., Glössl, J. and Steinkellner, H. (2004) Generation of *Arabidopsis thaliana* plants with complex *N*-glycans lacking β1,2-linked xylose and core α1,3-linked fucose. *FEBS Lett.* **561**, 132–136.

Tryfona, T., Liang, H.-C., Kotake, T., Tsumuraya, Y., Stephens, E. and Dupree, P. (2012) Structural characterization of Arabidopsis leaf arabinogalactan polysaccharides. *Plant Physiol.* **160**, 653–666.

Vanzin, G.F., Madson, M., Carpita, N.C., Raikhel, N.V., Keegstra, K. and Reiter, W.-D. (2002) The *mur2* mutant of *Arabidopsis thaliana* lacks fucosylated xyloglucan because of a lesion in fucosyltransferase AtFUT1. *Proc. Natl. Acad. Sci. U. S. A.* **99**, 3340–3345.

Villalobos, J.A., Yi, B.R. and Wallace, I.S. (2015) 2-fluoro-L-fucose is a metabolically incorporated inhibitor of plant cell wall polysaccharide fucosylation. *PLoS ONE*, **10**, doi: 10.1371/journal.pone.0139091.

Voxeur, A. and Fry, S.C. (2014) Glycosylinositol phosphorylceramides from *Rosa* cell cultures are boron-bridged in the plasma membrane and form complexes with rhamnogalacturonan II. *Plant J.* **79**, 139–149.

Voxeur, A., Gilbert, L., Rihouey, C., Driouich, A., Rothan, C., Baldet, P. and Lerouge, P. (2011) Silencing of the GDP-D-mannose 3,5-epimerase affects the structure and cross-linking of the pectic polysaccharide rhamnogalacturonan II and plant growth in tomato. *J. Biol. Chem.* **286**, 8014–8020.

Voxeur, A., André, A., Breton, C. and Lerouge, P. (2012) Identification of putative rhamnogalacturonan-II specific glycosyltransferases in Arabidopsis using a combination of bioinformatics approaches. *PLoS ONE*, **7**, e51129.

Wimmer, M.A., Lochnit, G., Bassil, E., Mühling, K.H. and Goldbach, H.E. (2009) Membrane-associated, boron-interacting proteins isolated by boronate affinity chromatography. *Plant Cell Physiol.* **50**, 1292–1304.

Wolf, S., Mouille, G. and Pelloux, J. (2009) Homogalacturonan methyl-esterification and plant development. *Mol. Plant* **2**, 851–860.

York, W.S., Kumar Kolli, V.S., Orlando, R., Albersheim, P. and Darvill, A.G. (1996) The structures of arabinoxyloglucans produced by solanaceous plants. *Carbohydr. Res.* **285**, 99–128.

Zablackis, E., Huang, J., Müller, B., Darvill, A.G. and Albersheim, P. (1995) Characterization of the cell-wall polysaccharides of *Arabidopsis thaliana* leaves. *Plant Physiol.* **107**, 1129–1138.

Zablackis, E., York, W.S., Pauly, M., Hantus, S., Reiter, W.D., Chapple, C.C., Albersheim, P. and Darvill, A. (1996) Substitution of L-fucose by L-galactose in cell walls of Arabidopsis mur1. *Science*, **272**, 1808–1810.

Supporting Information

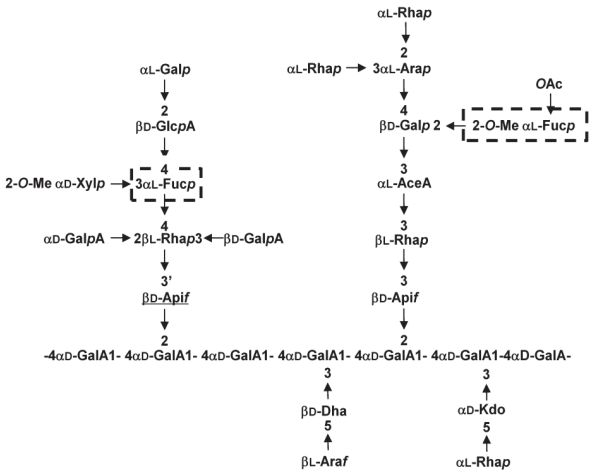

Figure S1. Structure of rhamnogalacturonan II (RG-II).

Fucose residues are indicated in dashed squares. Underlined apiose residue is involved in the borate cross-linking of RG-II.

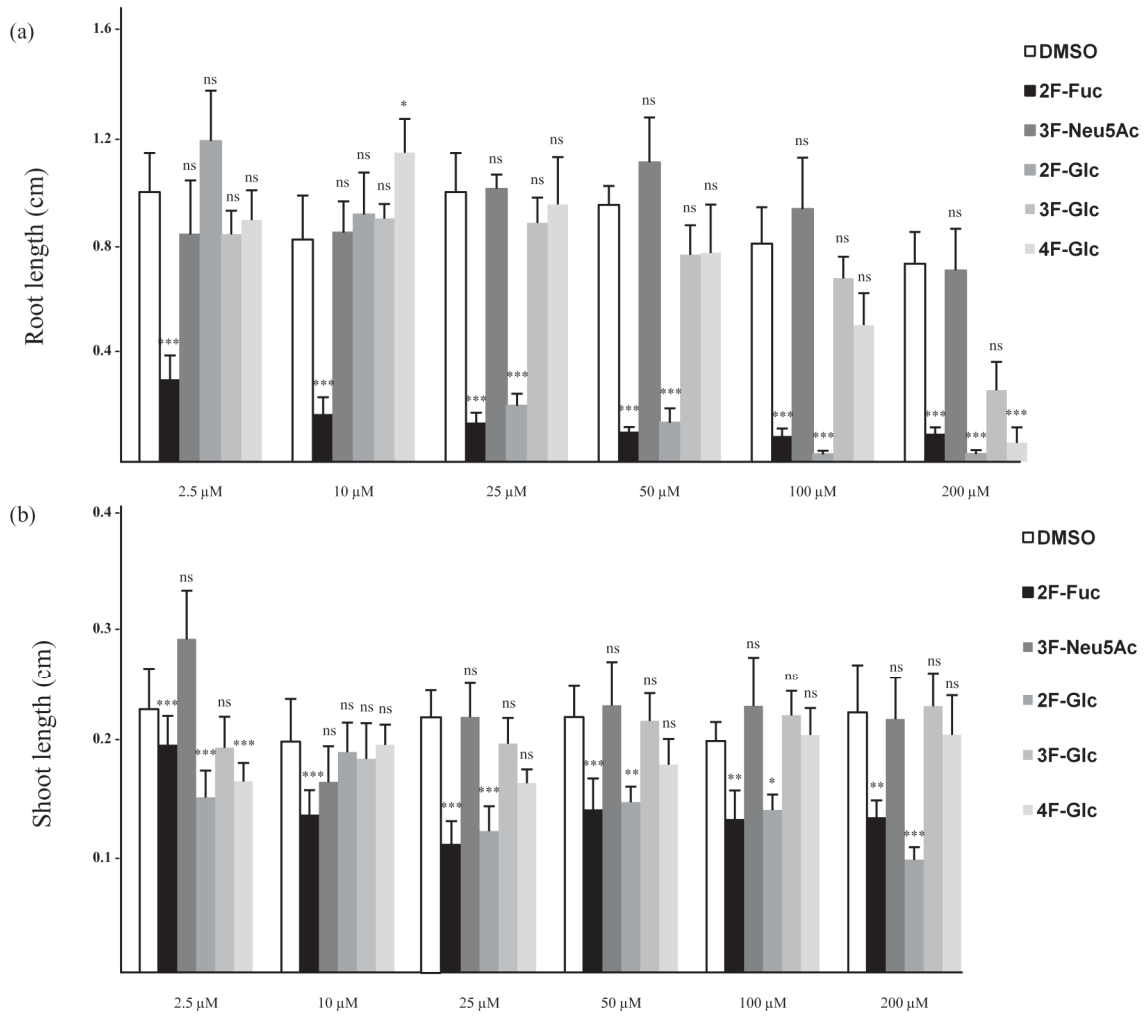

Figure S2. Effects of fluoro monosaccharide analogues on plant growth.

Root (a) and shoot (b) length of 4-day-old Arabidopsis seedlings grown on medium supplemented with peracetylated 2F-Fuc, 5F-Neu5Ac, 2F-Glc, 3F-Glc or 4F-Glc at 2.5 µM, 10 µM, 25 µM, 50 µM, 100 µM and 200 µM. DMSO were tested at the same dilution as the control. The results are given as mean ± SEM (n>10 seedlings). Dunn's multiple comparisons test, ns, not significant, * $p<0.05$, ** $p<0.01$, *** $p<0.001$.

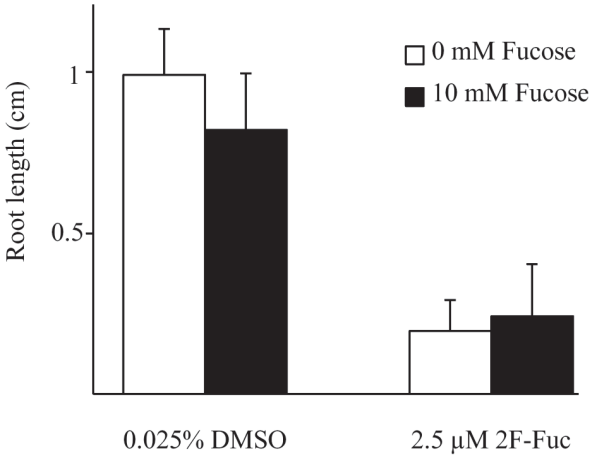

Figure S3. Excess of fucose did not restore the inhibitory effect of 2F-Fuc.

Root length of 4-day-old Arabidopsis seedlings treated with 2.5 µM 2F-Fuc, 10 mM fucose or both. DMSO: negative control. Data are mean ± SEM (n>25 seedlings). No significant difference was observed between conditions with or without 10 mM fucose. Mann-Whitney test.

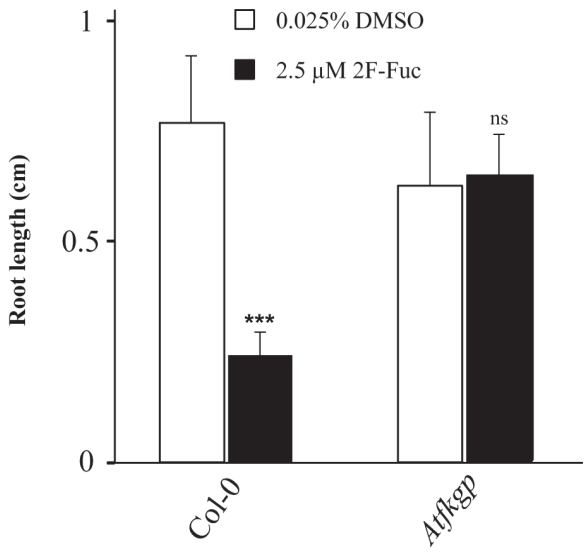

Figure S4. Cytosolic L-fucokinase and GDP-L-fucose pyrophosphorylase activities are not affected by 2F-Fuc. Root length of 4-day-old Arabidopsis Col-0 and *Atfkgp* seedlings grown on media supplemented with DMSO or with 2.5 µM 2F-Fuc. The results are given as mean ± SEM (n>50 seedlings). * indicates significant difference with the negative control (0.025% DMSO), Mann-Whitney test, $p<0.001$.

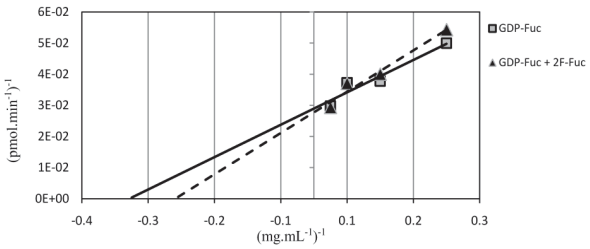

Kinetics parameters of AtFUT1	GDP-Fuc (control)	GDP-Fuc + 2F-Fuc
Km value for XyG ($mg.mL^{-1}$)	0.409	0.544
Ki value (mM)	-	3

Figure S5. Inhibition of AtFUT1 fucosyltransferase activity by 2F-Fuc.

AtFUT1 activity toward tamarind xyloglucan was evaluated using 30 µM GDP-[^{14}C]fucose. Affinity of AtFUT1 toward xyloglucan decreased (- 33%) in presence of 1 mM 2F-Fuc and a Ki value of 3 mM was calculated for inhibition of AtFUT1 activity by 2F-Fuc.

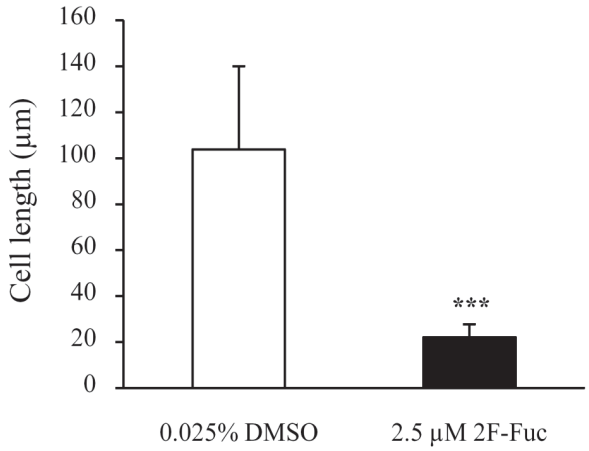

Figure S6. Effect of 2F-Fuc on cell elongation.

Length of the cells in the elongation zone of 4-day-old Arabidopsis seedlings treated with 2.5 µM 2F-Fuc or not (0.025% DMSO). Values are mean ± SEM (n> 70 cells from at least 12 roots). Unpaired t-test, *** $p<0.001$.

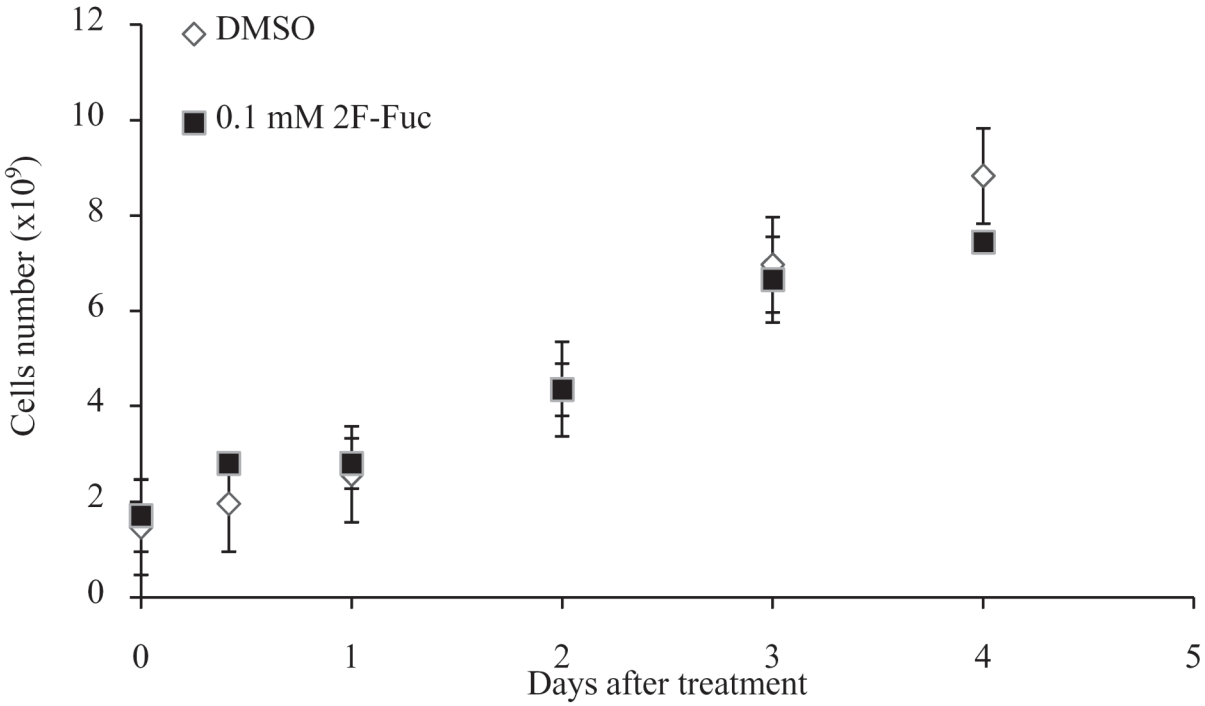

Figure S7. Effect of 2F-Fuc on BY-2 cell division.

Tobacco BY-2 suspension-cultured cells were incubated with 0.1 mM 2F-Fuc or 1% DMSO (control) 4 days after subculture. No significant difference was found between treatments (Mann-Whitney, $p > 0.05$). Data are mean ± SEM of three measurements ($n > 500$ cells).

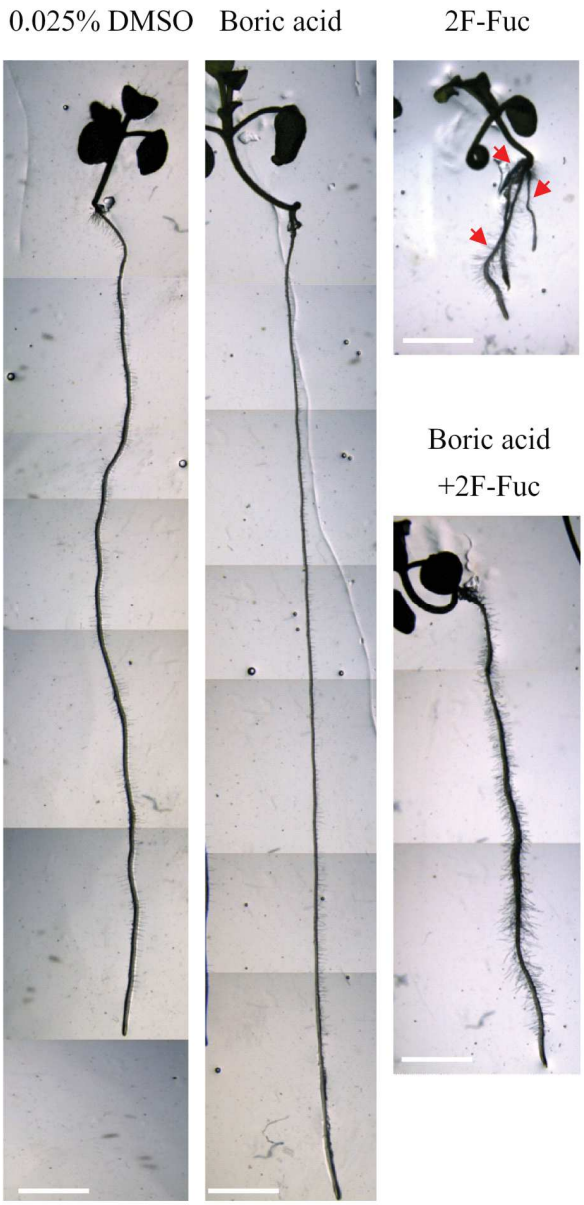

Figure S8. Emergence of adventitious roots in 14-day-old Arabidopsis treated seedlings. Fourteen-day-old Arabidopsis seedlings were grown on control medium (0.025% DMSO) or 0.75 mM boric acid with or without 2.5 μM of 2F-Fuc. Images were assembled using Microsoft Office Powerpoint. Data are mean ± SEM. (n>24 roots). Red arrows indicate adventitious roots. Scale bars 3 mm.